Analytical Framework for the Performance Evaluation of Cooperative and Cognitive Radio Systems With Practical Considerations

Thesis by

Fahd Ahmed Khan

In Partial Fulfillment of the Requirements

For the Degree of

Doctor of Philosophy

(*Electrical Engineering*)

King Abdullah University of Science and Technology (KAUST),

Thuwal, Makkah Province,

Kingdom of Saudi Arabia

August, 2013

The thesis of Fahd Ahmed Khan is approved by the examination committee

Committee Chairperson: Dr. Mohamed-Slim Alouini

Committee Member: Dr. Marc Genton

Committee Member: Dr. Taous-Meriem Laleg

Committee Member: Dr. Hong-Chuan Yang

ABSTRACT

Cooperative and cognitive radio systems have been proposed as a solution to improve the quality-of-service (QoS) and spectrum efficiency of existing communication systems. The objective of this dissertation is to propose and analyse schemes for cooperative and cognitive radio systems considering real world scenarios and to make these technologies implementable.

In most of the research on cooperative relaying, it has been assumed that the communicating nodes have perfect channel state information (CSI). However, in reality, this is not the case and the nodes may only have an estimate of the CSI or partial knowledge of the CSI. Thus, in this dissertation, depending on the amount of CSI available, novel receivers are proposed to improve the performance of amplify-and-forward relaying. Specifically, new coherent receivers are derived which do not perform channel estimation at the destination by using the received pilot signals directly for decoding. The derived receivers are based on new metrics that use distribution of the channels and the noise to achieve improved symbol-error-rate (SER) performance. The SER performance of the derived receivers is further improved by utilizing the decision history in the receivers. In cases where receivers with low complexity are desired, novel non-coherent receiver which detects the signal without knowledge of CSI is proposed. In addition, new receivers are proposed for the situation when only partial CSI is available at the destination i.e. channel knowledge of either the source-relay link or the relay-destination link but not both, is available. These receivers are

termed as 'half-coherent receivers' since they have channel-state-information of only one of the two links in the system.

In practical systems, the CSI at the communicating terminals becomes outdated due to the time varying nature of the channel and results in system performance degradation. In this dissertation, the impact of using outdated CSI for relay selection on the performance of a network where two sources communicate with each other via fixed-gain amplify-and-forward relays is studied and for a Rayleigh faded channel, closed-form expressions for the outage probability (OP), moment generating function (MGF) and SER are derived. Relay location is also taken into consideration and it is shown that the performance can be improved by placing the relay closer to the source whose channel is more outdated.

Some practical issues encountered in cognitive radio systems (CRS) are also investigated. The QoS of CRS can be improved through spatial diversity which can be achieved by either using multiple antennas or exploiting the independent channels of each user in a multi-user network. In this dissertation, both approaches are examined and in multi-antenna CRS, transmit antenna selection (TAS) is proposed where as in a multi-user CRS, user selection is proposed to achieve performance gains. TAS reduces the implementation cost and complexity and thus makes CRS more feasible. Additionally, unlike previous works, in accordance with real world systems, the transmitter is assumed to have limited peak transmit power. For both these schemes, considering practical channel models, closed-form expression for the OP performance, SER performance and ergodic capacity (EC) are obtained and the performance in the asymptotic regimes is also studied. Furthermore, the OP performance is also analyzed taking into account the interference from the primary network on the cognitive network.

TABLE OF CONTENTS

ACRONYMS

Symbol	Meaning
16-QAM	16-Quadrature-Amplitude-Modulation
AF	Amplify-and-Forward
AS	Antenna Selection
AWGN	Additive White Gaussian Noise
BPSK	Binary Phase-Shift-Keying
CCE	Cascaded Channel Estimation
CDF	Cumulative Density Function
CRS	Cognitive Radio Systems
CSI	Channel State Information
DCE	Disintegrated Channel Estimation
DF	Decode-and-Forward
DSTBC	Distributed Space Time Block Code
E2E	End-to-End
E2E-SNR	End-to-End SNR
EC	Ergodic Capacity
EGC	Equal Gain Combining
FG	Fixed Gain
i.i.d	independent and identically distributed
i.n.i.d	independent but not identical
LMMSE	Linear-Minimum-Mean-Squared-Error
MAL	Maximum Averaged Likelihood
MCS	MIMO Cognitive System
MGF	Moment Generating Function
MIMO	Multiple-Input Multiple-Output
ML	Maximum-Likelihood
MRC	Maximum Ratio Combining
MRS	Max-min RS

Symbol	**Meaning**
OC	Outdated CSI
OP	Outage Probability
OTN	Opportunistic Two-way relaying Network
PDF	Probability Distribution Function
PU	Primary User
PU-Rx	Primary User Receiver
PU-Tx	Primary User Transmitter
QoS	Quality of Service
RF	Radio Frequency
RS	Relay Selection
SC	Selection Combining
SER	Symbol-Error-Rate
SNR	Signal-to-Noise Ratio
STBC	Space Time Block Code
SU	Secondary User
SU-Rx	Secondary User Receiver
SU-Tx	Secondary User Transmitter
TAS	Transmit Antenna Selection
TWR	Two-Way Relaying
TWRN	Two-Way Relaying Network

LIST OF FIGURES

Chapter 1

Introduction

Recent advances in wireless communication technology have led to huge demand for the deployment of new wireless services and applications requiring good quality-of-service (QoS). Achieving good QoS through a wireless channel has its own challenges, the most important of which is overcoming the detrimental effect of fading. When a signal is transmitted via a wireless channel, multiple copies of the signal are received at the destination due to reflection and scattering. These multiple copies add constructively or destructively to cause abrupt variation in signal power. This rapid fluctuation of the signal power in a wireless channel is termed as fading [1]. Fading significantly degrades the performance of the wireless communication systems. For example, in an additive white Gaussian noise (AWGN) channel for binary phase shift keying (BPSK), the error probability decreases exponentially with increasing transmit power. However, in the case of Rayleigh fading, the error rate performance of BPSK decreases only linearly [1] [1]. On the other hand, the increasing number of wireless services require more wireless spectrum. However, the wireless spectrum is a scarce resource as it has already been allocated for various services and there is very limited

[1] Fading is a random phenomena and various random distributions have been proposed to model the effect of fading [2]. For example, in a multiple scattering environment, the fading envelop is modeled using Rayleigh distribution. If there exist a line of sight path from the transmitter to the receiver, Rician distribution is used to model fading. Various other distributions used for modeling fading are discussed in [2].

additional spectrum to accommodate the new emerging wireless services and applications [3]. Different solutions have been proposed to overcome both these issues. One of the solutions proposed to improve the QoS is through cooperative communication where as cognitive radio has been proposed to tackle the issue of spectrum scarcity.

1.1 Cooperative Communications to Improve QoS

Overcoming the detrimental effect of fading is the means to get improved QoS. Few basic techniques to mitigate fading are briefly discussed below as well as the idea of cooperative communication to counter the issue fading is introduced.

1.1.1 Fading Mitigation Techniques

An approach to overcome the severe effect of fading is to send multiple copies of the signal over the wireless channel such that each copy of the signal experiences independent fading and it is improbable that multiple independent paths experience deep fades at the same time. This technique is called diversity. Diversity can be achieved by multiple ways [1].

- Time Diversity: As the wireless channel is time varying, a simple technique to achieve diversity is to transmit the signal over multiple time slots where each time slot experiences independent fading i.e. the signal is transmitted in time slots separated by time greater than the coherence time of the channel.

- Frequency Diversity: Diversity can also be achieved by transmitting the same signal over different carrier frequencies that are separated by more than the coherence bandwidth of the channel and thus experience independent fading. This is termed as frequency diversity.

- Space Diversity: Diversity can also be achieved in space by transmitting the multiple copies of the signal using multiple antennas where each antenna experiences independent fading.

1.1.2 Multiple-Input Multiple-Output Systems and Space Time Coding

Spatial diversity can be achieved by multiple input multiple output (MIMO) systems in which the communicating terminals have multiple antennas. These multiple antennas are utilized to improve the error-rate performance of the system by transmitting and receiving multiple copies of the signal, each of which experiences an independent fading realization. The received signals are combined using the well known combining techniques to obtain a diversity gain and thus, improved error-rate performance [1].

The multiple antennas can also be utilized to improve the throughput of the system by transmitting a different signal from each antenna. This is known as spatial multiplexing. However, in this case the error-rate performance is degraded. Thus, there exists a trade-off between error-rate performance and throughput of a MIMO system known as the diversity multiplexing tradeoff [4].

Space-time coding, i.e. encoding data in both space and time, can be used to achieve improved error-rate performance as well as increased throughput. Space time block codes are an example of space-time codes using which good diversity as well as good throughput can be achieved. The main aim of space time block code (STBC) design is to achieve maximum diversity gain along with highest possible transmission rate and to minimize the decoding complexity [5].

In [6], Alamouti proposed a STBC for a system with 2 transmit antennas and 1 receive antenna, that was able to extract diversity or order 2 with only linear

processing complexity at the receiver. After Alamouti's work a lot of research has been done in the design of STBCs. Many different types of space time block codes such as orthogonal STBCs, quasi-orthogonal STBCs and algebraic STBCs have been proposed. For more details on STBC design one can refer to [7].

In the case of multiple antenna receivers, a copy of the signal is received at each receive antenna. In order to decode the received signal the receiver needs to combine the copies received at each antenna. Some well known signal combining techniques are [2]

- Maximum Ratio Combining (MRC): The received signals are combined after weighting the received copies proportional to the amplitude of the fading realization of the channel and compensating the phase.
- Equal Gain Combining (EGC): The received signals are combined after giving all the received copies equal weight and compensating the phase.
- Selection Combining (SC): The signal with the maximum channel fading amplitude is selected.

1.1.3 Cooperative Communications Using Relays

As has been discussed, fading has detrimental effect on the performance of the communication systems and one approach to overcome fading is by spatial diversity. For spatial diversity, the terminal needs to have multiple antennas. However, in practice incorporating multiple antennas in small mobile devices is complex. Increasing the number of antennas is only possible by increasing the number of radio frequency (RF) chains which increases the cost. Furthermore, for the antennas to experience independent fading, they must be separated by approximately one half-wavelength.

Thus, this results in an increase in the size of the device and thus reduces mobility [8].

One solution for getting improved performance by spatial diversity without adding antennas is that multiple single antenna devices cooperate with each other to improve the performance of the network. This technique in which multiple single antenna nodes cooperate is called cooperative communications. These nodes can be base stations, mobiles or any other communication device.

Relays can also be employed to gain diversity benefits by cooperation. Relays are devices that receive the signal from the transmitter and retransmit to the destination after some amplification. Relays can be utilized in many different scenarios. They can be utilized to increase the coverage area [9]. Relays can also help extend the battery life of the network by reducing the transmit powers of the nodes in the network. In addition, the performance of the network can be improved with the aid of cooperating relays that form a distributed multiple-input multiple-output system [9, 10, 11].

Two types of relays have been proposed in literature:

- Amplify-and-Forward (AF) Relays: Relays that simply transmit an amplified version of the received signal.
- Decode-and-Forward (DF) Relays: Relays that decode the received signal and then transmit the amplified version of the decoded signal.

Amplify and forward is one of the most used relay protocol in the literature and is currently employed in signal repeaters and other terrestrial communications [12] due to its low complexity.

Using multiple relays, data can be encoded in both space and time in a distributed fashion to achieve diversity and multiplexing gain. This is called distributed space time coding. Several distributed STBC (DSTBC) have been proposed and analyzed

for amplify-and-forward relaying. One can refer to [10, 13] and the references therein for more details.

Cooperative relaying helps mitigate the fading and achieve spatial diversity gains. However, a drawback of employing relays is the loss of throughput/spectral-efficiency due to orthogonal signaling [14]. Two-way relaying (or Bidirectional relaying), where two users exchange information via common intermediate relays, has been proposed to improve the throughput compared to traditional one-way relaying while maintaining its diversity benefits [15]. Unlike one-way relaying, two-way relaying (TWR) requires only two time slots to communicate data between two sources, where as one way relaying requires more time slots.

1.2 Tackling Spectrum Scarcity Through Cogntive Radio

Recent measurement studies have shown that the wireless spectrum is greatly under-utilized [3]. By utilizing the spectrum efficiently, it is possible to fulfill the demand for the increasing number of wireless services. As a consequence, cognitive radio has been proposed to improve the utilization of the spectrum [16, 17]. Cognitive radio is a more general concept i.e. it is smart a communication device that is aware of its surrounding and can adapt accordingly to give improved performance. Improving spectrum utilization through spectrum sharing is just one of its operation.

The idea of spectrum sharing is that the cognitive/secondary network transmits using the spectrum already allocated to some primary network [16, 17]. Various protocols have been proposed for spectrum sharing. One such protocol is where the secondary network uses the spectrum only when the primary network is not using

the spectrum [18]. This approach requires robust spectrum sensing algorithms which sense the spectrum perfectly [19, 20, 21]. However, ideal spectrum sensing cannot be achieved in practice and in case of miss-detection, the primary network experiences severe interference. Another approach of spectrum sharing is the underlay approach in which the secondary network is allowed to transmit concurrently with primary network using the spectrum of the primary network if it does not cause harmful interference to the primary receiver i.e. the peak interference to the primary network should be below a predefined threshold [18]. Thus, by limiting the interference from the secondary network, an acceptable level of performance of the primary network can be guaranteed and the secondary network can also communicate and improve the utilization of the spectrum. In this dissertation, only the underlay setup is considered.

1.3 Practical Issues in Cooperative and Cognitive Radio Networks

In this dissertation, various practical issues faced in current cooperative and cognitive radio systems are discussed and addressed. A brief outline of the addressed issues is mentioned below.

Cooperative Communication With Imperfect Channel State Information

- For good performance the communicating nodes need to possess the knowledge of channel state information (CSI). However in practical systems CSI is not available at the communicating nodes and needs to be estimated. This estimation is not perfect and results in imperfect CSI at the nodes. This results in degradation in system performance. In this dissertation, we look into the aspect of receiver design for cooperative relay networks when the nodes possess

imperfect CSI.

- Due to time varying nature of the channel, the CSI knowledge at the communication nodes can become outdated which results in performance degradation of a two-way relay network (TWRN) where a single relay is selected for transmission based on outdated CSI.

Achieving Spatial Diversity in Practical Cognitive Radio Systems

- As mentioned previously, spatial diversity can be achieved by increasing the number of antennas on the terminals. However, adding multiple antennas at the terminals comes at a cost. For each additional antenna element, a new radio-frequency chain is also needed and thus, the cost as well as complexity of the terminal is increased. One of the approaches to get the benefits of multiple antennas at lower complexity is antenna selection (AS) [8, 22]. The complexity of AS is lower because the terminal where AS is done, the number of RF chains required is equal to the number of antennas selected for communication. Even with lower complexity, AS gives full diversity [8, 22]. Transmit antenna selection (TAS) is a form of AS where the antenna selection is performed at the transmitter [23]. TAS can be a suitable choice to achieve spatial diversity for practical cognitive radio systems. Thus, in this dissertation, the performance of a *power limited* MIMO cognitive network employing TAS is analyzed. The term power limited is emphasized, because usually in literature, for tractable analysis, the transmit power is assumed to be unlimited which is unrealistic for practical cognitive radio systems.

- In a multi-user network, another approach to achieve spatial diversity is by exploiting the best channels which become available when there are more users

or mobility [24]. By selecting the user that has the best channel gives rise to a multiuser diversity effect which results in improved QoS and an increase in the overall capacity of the network [25, 26, 27]. Applying this concept of multi-user diversity to a multi-user cognitive network, the QoS can be improved by selecting the user with the best channel. In realistic scenarios, the users are located randomly w.r.t to the base station and thus they experience independent and non-identical channels. The analysis in this dissertation takes this practical aspect into account and the performance of the multi-user network is analyzed considering a generic independent and non-identical Nakagmi-m fading model. This channel fading model includes the Rayleigh and Rician channel fading models as its sub-cases. In addition, in accordance with practical constraints, the peak transmit power of each user is assumed to be limited.

After giving a brief overview of the topics addressed in this dissertation, a literature review along with the main contributions are elaborated henceforth.

1.4 Cooperative Communication with Imperfect CSI

1.4.1 Receiver Design for Relay Networks

The objective of the receiver is to decide what data was transmitted based on the received signal. The optimal receiver is one that results in minimum probability of error. The receivers can mainly be divided into two types [5]:

- Coherent Receivers: Receivers which have knowledge of phase and amplitude of the channel fading realization.

- Non-Coherent Receivers: Receivers which do not have knowledge of phase nor amplitude of the channel fading realization.

Due to the knowledge of the CSI the coherent receivers perform better than the non-coherent receivers. However, the non-coherent receivers have lower complexity. The optimal receiver in either case is the receiver based on the maximum a posteriori (MAP) rule [5]. If the transmitted symbols are equiprobable then the optimal receiver is the maximum-likelihood (ML) receiver [5]. The optimal receiver design might be complicated and involve significant processing. In this case several sub-optimal receivers with lower complexity can be designed which give performance close to that of the optimal receiver.

In real world systems, the receiver does not have knowledge of phase nor amplitude of the channel gain and thus has to estimate it. This estimation leads to imperfect CSI. In the case of imperfect CSI, the receiver not only needs to obtain the best estimate of the CSI but also has to process the received signal with the estimated CSI in the best way to improve the robustness to the channel estimation error. For point-to-point links, various receiver designs, for the case of imperfect CSI have been proposed in the literature [2, 28, 29, 30, 31].

In most studies related to relay networks, it has been assumed that the destination in the network has either complete CSI or no CSI of the links in the system. For example, in [32], maximum likelihood based coherent receiver with perfect CSI was proposed for both DF relaying as well as AF relaying. When the destination has no CSI, non-coherent receivers can be employed that offer a low complexity of implementation at the cost of some degradation in performance. They have been extensively studied in the literature [32, 33, 34, 35, 36, 37, 38, 39]. In [32], the authors also proposed a non-coherent receiver for DF relaying. However, for AF relaying it

was shown that the optimal non-coherent receiver resulted in an intractable integral and no closed form exists. Thus, a suboptimal non-coherent receiver was proposed. In [33], a non-coherent maximum likelihood receiver was designed for the distributed space-time block-coded system with an AF relay. Bounds on the performance of on-off keying and binary frequency shift keying using optimum non-coherent receiver for AF relaying were derived in [34]. Approximate non-coherent detectors for AF relaying in Rayleigh fading channels were proposed in [35] and [36]. A non-coherent receiver for AF cooperative systems with lower complexity was proposed in [37]. A non-coherent generalized-likelihood-ratio-test based receiver for AF relaying has also been proposed [38]. The performance analysis of the non-coherent envelop detector for frequency-shift-keying was done in [39].

For a cooperative relay network, coherent receiver design with imperfect CSI was initially studied in [40] and [35], where reference [40] studied the performance of coherent detection for AF relaying using linear-minimum-mean-squared-error (LMMSE) channel estimate and reference [35] studied the performance of the mismatched coherent receiver for the case of DSTBC. The performance of the mismatched coherent receivers for orthogonal and non-orthogonal AF protocols was studied in [41]. A slightly less complex receiver with partial CSI (only the phase information of the cascaded channel), was also proposed in [41]. In [42], two sub-optimum detection rules were proposed namely the enhanced Gaussian based detection rule and the unconditional PDF based detection rule. The former rule performed close to optimal when the noise at the receiver is dominantly Gaussian, whereas the latter rule gave better performance if the noise at the receiver was non-Gaussian. A hybrid of both schemes was also proposed. In [35, 40, 41], the channel estimation is performed once at the destination for the cascaded source-relay and relay-destination channel. This is called cascaded channel estimation (CCE). In [43] and [44], disintegrated channel

estimation (DCE) was also considered where estimation of the source-relay channel was done at the relay and estimation of the relay-destination channel was done at the destination, separately.

Our Contribution:

Novel Receivers For AF Relaying With Distributed STBC Using Cascaded and Disintegrated Channel Estimation

Coherent receiver design in the aforementioned works consider the simple Euclidean distance metric in the receivers. In Chapter 2, it is demonstrated that symbol-error-rate (SER) performances of these receivers can be further improved by designing better metrics which use additional information of the channel and noise. Specifically, novel pilot-symbol-aided coherent receivers using CCE and DCE for DSTBC system with AF relaying are derived by using the maximum averaged likelihood (MAL) methods [28, 31]. The new receivers do not require channel estimation in certain parts of communications by using the received pilot signals directly for decoding to save processing complexity and power. To achieve this, the distribution of the channel and the noise is utilized to outperform the conventional Euclidean distance metric receivers.

Furthermore, the decision history is utilized in the derived receivers to give further performance gain without increasing the number of pilots or the transmit power of pilots. We also propose the use of decision history in the simple Euclidean distance metric to improve the SER performance. The effect of decision history on the performance of the new receivers is examined for different weighting schemes. Numerical results show that the new receivers have significant performance gains over the conventional receivers. In some cases, the performance gain can be as large as 2.5 dB in effective signal-to-noise ratio for both CCE and DCE in 16-quadrature-amplitude-

modulation (16-QAM) with Rayleigh fading. The effect of the quantization error that occurs when the relay forwards the quantized estimate of the source-relay channel to the destination for DCE on the receiver performances is also shown by simulation.

The new contributions in Chapter 2 that are different from existing works can be summarized as follows:

- New receiver metrics that utilize the distribution of the channels and the noise are derived with better SER performances.
- The decision history is incorporated in the newly derived metrics as well as the existing Euclidean distance metric to achieve performance gains.
- The effect of the decision history on the performances of the receivers is studied for different weighting schemes.
- The effect of quantization on the performance of the derived receivers for DCE is examined.

Novel Non-Coherent and Half-Coherent Receivers for Amplify-and-Forward Relaying

As mentioned previously, in most studies related to relay networks, it has been assumed that the destination in the network has either complete CSI or no CSI of the links in the system. Furthermore, in all the aforementioned works related to receiver design, the channel was assumed to have Rayleigh fading. When the channel has Rician fading, the non-coherent receiver designs proposed in these previous works are sub-optimal. Thus, in Chapter 3, we derive the optimal non-coherent receiver for Rician fading channels. To reduce the implementation complexity, we also propose a sub-optimal non-coherent receiver with lower complexity but similar performance to that of the optimal non-coherent receiver.

In addition, considering Rician faded environment, we also derive new detectors for the case in which the receiver has the CSI of only one of the two links in the relaying system, i.e. the receiver only has the CSI of either the source-relay link or the relay-destination link. These receivers are termed as 'half-coherent receivers' and are useful in scenarios where either the relay is fixed so that it can afford higher complexity by estimating and forwarding the source-relay CSI to the destination node that is unable to estimate the channel or when the destination can afford complexity by estimating the relay-destination link for an ad-hoc relay that has to keep low complexity due to the complexity limitations. The analytical expressions for the symbol-error-rate performances of the proposed receivers for M-ary frequency-shift-keying are derived. These new receivers provide an alternative to the coherent and non-coherent receivers in the literature; they outperform the non-coherent receivers while they are less complicated than the coherent receivers. In cases when only the relay or destination can afford additional complexity caused by channel estimation, they are also indispensable. As will be shown later, our proposed receivers perform better than the conventional non-coherent energy detector receiver, especially at low signal-to-noise ratio (SNR).

1.4.2 Opportunistic Bidirectional Relaying With Outdated CSI

As was discussed previously, a drawback of employing relays is the loss of throughput due to orthogonal signaling [14]. Two-way-relaying is one option to improve the throughput. However, even with TWR as the number of relays increases, spectral efficiency is reduced. This loss in spectral-efficiency can be compensated by employing relay selection (RS) where a single relay is opportunistically selected for transmission

and thus, the throughput is improved compared to the system where all the relays participate. It has also been shown that RS also preserves the same spatial diversity [45, 46, 47]. Many works have analyzed the performance of relay selection in context of two-way relaying eg. see [48, 49, 50, 51] and references therein. In [48],the performance of the max-min RS technique and the max-sum RS technique was analyzed and a hybrid RS scheme was proposed. It was shown that max-min RS scheme extracts the full diversity gain and is suitable at high SNR. Performance of various full diversity achieving schemes based on joint network coding and opportunistic relaying have been analyzed in [52] and [53]. For bidirectional amplify-and-forward relaying, the performance of opportunistic RS based on the max-min criteria was analyzed in terms of outage probability and SER in [49, 50, 51] and it was shown that this scheme achieves full diversity.

All these previous works assumed that the channel remains the same during the RS phase and the data transmission phase. Due to time varying nature of the channel, this assumption is not always true and it is possible that due to feedback delay or scheduling delay, an outdated channel is used for RS. This impacts the performance of the system significantly and for traditional one-way relay networks, it is shown that RS using outdated CSI (OC) results in diversity loss eg. see [54, 55, 56, 57, 58]. This loss in performance and diversity also occurs for an opportunistic two-way relaying network (OTN) with OC based RS [59, 60]. The performance of an OTN with max-min RS (MRS) scheme based on OC was analyzed in [59] and the lower and upper bounds on the outage performance and SER performance were derived. It was also shown that the diversity is lost due to OC. The authors in [60] also considered an OTN with max-min RS and OC (OTN-MRS-OC), and obtained closed-form expressions for outage probability and SER. In both these works, variable gain AF relays were assumed i.e. the relays possessed the CSI of the links.

Our Contribution:

In Chapter 4, we analyze the performance of OTN-MRS-OC with fixed gain (FG) AF relays. Furthermore, for FG relays, the statistics of the end-to-end SNR (E2E-SNR) are different from the ones obtained for variable gain relays in [59] and [60]. Thus, in Chapter 4, we obtain the closed-form expressions for the outage performance, moment-generating-function of the E2E-SNR and the SER performance for both coherent and non-coherent one-dimensional modulation schemes. Numerical simulation results are also presented to validate the derived analytical results. In addition, unlike previous works considering RS based on OC, the impact of relay location is also studied and it is shown that the performance of the OTN-MRS-OC can be improved by moving the relay closer to the source whose channel is more outdated.

1.5 Achieving Spatial Diversity in Practical Cognitive Radio Systems

1.5.1 Power Limited Cognitive Network with TAS/MRC

For standard point-to-point links, it has been shown that even with lower complexity, AS achieves full diversity [8, 22]. Furthermore, it has also been proved that for MIMO point-to-point links TAS with MRC at the receiver achieves an order of diversity equal to the product of the number of transmit and receive antennas [23, 61]. Various other studies have also been done to analyze the performance of point-to-point TAS/MRC system for different fading conditions eg. see [62, 63, 64, 65, 66] and references therein.

In the context of cognitive radio, it is well known that the secondary link capacity can be enhanced by means of spatial diversity which can be achieved by increasing the number of antennas on the terminals in the cognitive network [67, 68, 69, 70, 71, 72].

The capacity of the secondary link, where the secondary user receiver (SU-Rx) has n_R antennas and employs MRC was initially investigated in [68]. In [69], the authors studied the effect on capacity of the secondary link when the SU-Tx does not have perfect channel information of the interference link (i.e. link between SU-Tx and primary user receiver (PU-Rx)). In both these works the authors considered only the average interference power constraint. In [70], a peak transmit power constraint in addition to peak interference power constraint was considered and it was shown that the secondary link capacity scales as $\ln(n_R)$ and this system achieves a diversity order of n_R. The capacity of the secondary link with n_R receive antennas and employing MRC when the channel has Nakagami-m fading was recently studied in [71]. The ergodic capacity and outage capacity of a MIMO secondary link, where SU-Tx has n_T antennas and the SU-Rx has n_R antennas, was recently studied in [72].

As discussed previously, TAS can be employed to reduce the complexity at the SU-Tx. TAS in a spectrum sharing setting was initially analyzed in [73] where the PU-Rx was assumed to have a single antenna. It was shown that capacity is determined by a geographical relationship expressed as a ratio of the SU-Tx-to-SU-Rx distance and the SU-Tx-to-PU-Rx distance. The performance of transmit antenna selection, when the PU-Rx has n_R antennas and employs MRC, was recently analyzed in [74]. The authors obtained closed form expression for the outage probability and the ergodic capacity of the secondary link, considering only a peak interference power constraint. In [72], the authors also considered a cognitive system with TAS/MRC, however, the study was simulation based and no analysis was presented.

Our Contribution:

In all the previous works discussing TAS/MRC in a cognitive setting, no detailed performance analysis was presented for a more practical scenario i.e. when the SU-

Tx has a limited peak transmit power. Generally, in the underlay setting, the transmit power of the SU-Tx is inversely proportional to the channel power of the interference link. If the SU-Tx is not assumed to have limited peak power, then the SU-Tx will quickly drain out its battery by transmitting with very high power if the interference link is very poor. Therefore, it is essential that the SU-Tx has limit on the peak transmit power. In addition, these previous works ignored the interference from the primary network on the secondary network and thus, the analysis does not depict a realistic scenario.

In Chapter 5, a MIMO cognitive system (MCS) employing TAS at the SU-Tx and MRC at the SU-Rx is considered. The performance of this system is analyzed for a more realistic scenario where the SU-Tx has a limited peak transmit power in addition to the peak interference power constraint. Additionally, the interference from the primary network on the secondary network is also considered. Specifically, two scenarios are considered; 1) the MIMO cognitive system with TAS/MRC (MCS-TM) does not experience interference from the primary network (denote by MCS-TM-NI), and 2) MCS-TM does experience interference from the primary network (denote by MCS-TM-WI). The performance of both these scenarios is analyzed and exact closed-form expressions for the outage probability are obtained. A new and simple expression of the cumulative density function (CDF) of the output SNR for the MCS-TM-NI is also derived. Using this new expression of the CDF, exact closed-form expressions are obtained for the probability distribution function (PDF) and the q-th moment of the output SNR, the moment generating function (MGF), the SER performance and the ergodic capacity. In addition, a precise lower bound on the ergodic capacity at high SNR is also derived. Numerical simulations results are also presented and they match well with the derived results. Furthermore, asymptotic performance results for MCS-TM-NI are also derived and it is shown that the generalized diversity gain for

this scheme is equal to the product of the number of transmit and receive antennas.

1.5.2 Opportunistic Multi-user Cognitive Network With Limited Transmit Power

In a spectrum sharing setting, multi-user diversity can be exploited but it is different from the traditional multi-user case because of the interference power constraints imposed on the secondary user (SU). Thus, in this case, the selected SU needs to have jointly a good transmission link and a poor interference link. The effect of multi-user diversity in an underlay network with independent and identically distributed (i.i.d) Rayleigh fading was initially studied in [75] where the SU having the best SNR was selected for transmission. It was shown in [75] that at sufficiently high transmit power, the selection of the user is more influenced by the interference link and the multi-user diversity gain in terms of capacity scales similar to the scaling law of the non-spectrum sharing system. The ergodic capacity of the multi-user underlay system was derived for a more generic hyper-Nakagami-m fading channel in [76]. In both these works, the capacity was given in terms of a single integral expression which can be evaluated using the well known numerical integration techniques. The outage capacity as well as the effective capacity for an opportunistic cognitive broadcast channel having i.i.d Rayleigh fading was also analyzed in [77]. Multi-user interference diversity which takes into account the interference from the primary network was studied in [78], However, no performance analysis was presented. In [79], a new scheduling scheme was proposed and analyzed where the user is selected from a subset of users who's interference powers are below a certain threshold. A drawback of this scheme is that it is possible that sometimes the initial subset is empty and thus no SU is selected for transmission. This will cause a reduction in throughput of the secondary network.

In [80], a broadcast cognitive channel was considered where the secondary user first selects a spectrum from a number of available spectra. The spectrum which causes the least interference to the primary users (PUs) is selected for transmission. Then using this spectrum the signal is transmitted to the user with the best channel. A similar setup was considered in [81] and it was shown that the throughput scales double-logarithmically with the number of users and linearly with the number of available bands. This system setup requires continuous monitoring of all the available spectra and thus increases the complexity of the band manager.

Our Contribution:

The performance of a multi-user underlay cognitive network is studied where the secondary user having the highest post-scheduling/output SNR is scheduled for transmission. The SUs are not selected based on thresholding, as in [79]. Thus, a SU is always selected for transmission and there is no loss in throughput. The channel is assumed to have independent but not identical (i.n.i.d) Nakagami-m fading. Note that this channel fading model is more generic and includes the channel fading models considered in [75, 77] as its sub-cases. Considering an interference power constraint and a maximum transmit power constraint on the SU, a power allocation scheme at the SUs is derived. For this policy the SU transmitter (SU-Tx) requires the instantaneous CSI of the link between the SU-Tx and the PU-Rx. The advantage of this scheme is that the interference constraint is never violated and thus, the primary network does not experience interference greater than the allowed peak interference level. After the power allocation, the SU having the best SNR is selected for transmission.

Moreover, effect of interference from the PU on the SU is also considered and the performance of the opportunistic multi-user underlay cognitive network (OMU-CN) is analyzed for two scenarios; 1) OMU-CN does not experience interference from the

PU (denote by OMU-CN-NI) and 2) OMU-CN experiences interference from the PU (denote by OMU-CN-WI). For both scenarios, exact closed-form expressions are obtained for the CDF of the output SNR which is then utilized to analyze the outage performance. An alternate new and simple expression for the CDF of the output SNR for the OMU-CN-NI is also derived. Using this new expression of the CDF, exact closed-form expressions are derived for the moment generating function of the output SNR, the SER performance and the ergodic capacity. Additionally, the performance of the OMU-CN-NI is analyzed in the asymptotic regimes and the generalized diversity order of the multi-user scheduling scheme is obtained. It is shown that when the interference link is very poor and there is no limit on the transmit power, this scheduling scheme achieves full diversity. Furthermore, it is shown that when there is no interference from the PU the performance of this multi-user scheduling scheme saturates due to limited peak transmit power or limited peak interference power. Numerical simulations are also presented to corroborate the derived analytical results. It is also shown that the scheduling scheme considered in this chapter achieves higher capacity compared to the hybrid scheduling scheme in [79].

Chapter 2

Novel Receivers For AF Relaying With Distributed STBC Using Cascaded and Disintegrated Channel Estimation

2.1 Introduction

In this chapter, novel pilot-symbol-aided coherent receivers using CCE and DCE are derived for a DSTBC system with AF relaying. The receiver are derived based on the distribution of the channel and the noise. These new receivers use the received pilot signal to decode the incoming signal and thus save the processing complexity and power required to estimate the channel. Furthermore, decision based receivers are obtained by incorporating the decision history in the derived receivers. These decision based receivers give improved performance without increasing the number of pilots or the transmit power of pilots. Decision history is also incorporated in the conventional Euclidean distance based receivers to give improved performance. The

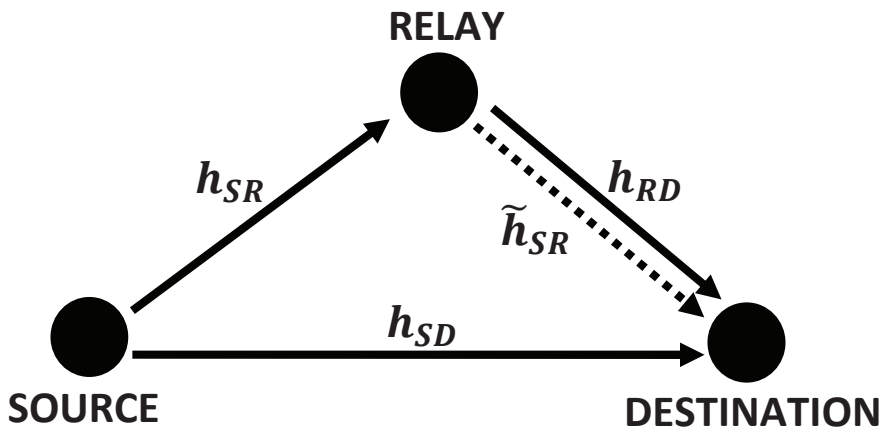

Figure 2.1: Diagram of a wireless relay system.

effect of decision history on the performance of the new receivers is examined for different weighting schemes. The performances of the new receivers are shown using numerical simulations.

2.2 System Model

Consider a system in which transmission is carried out from the source to the destination via a relay as shown in Fig. 2.1. All the nodes are assumed to have single antenna. The transmission is completed in two time slots [82, 33, 83, 84, 85]. During the first time slot, the source transmits the signal to the relay. In the second time slot, both the relay and the source transmit the signal to the destination. This system can be considered as a distributed space-time coded system with 2 transmit antennas and 1 receive antenna. Note that the destination could also listen during the first time slot [35, 41, 86, 82, 84]. This requires a more complicated space-time code [35, 41, 86]. For example, the code used in [86] is $\bar{\mathbf{X}} = \begin{bmatrix} 0 & x_1 & 0 & {x_2}^* \\ x_1 & x_2 & -x_2^* & x_1^* \end{bmatrix}^{\mathsf{T}}$. The dimensionality of this code is high and thus, it costs extra memory and processing power at the

destination. The derivation in this chapter can be easily extended to this case.

The transmission is assumed to occur in blocks of length $N + M$, where N is the number of data symbols and M is the number of pilot symbols. The data and pilots are encoded using the Alamouti code [6]. The pilots are sent at the beginning of each block. The channel gains of all the links are assumed to be constant during the block transmission. The channel gains for the source-relay channel, the relay-destination channel and the source-destination channel are denoted by h_{SR}, h_{RD} and h_{SD}, respectively, and are assumed to be independent zero mean complex Gaussian (ZMCG) random variables each with variance 0.5 per dimension. $\tilde{h}_{SR}$ denotes the quantized estimate of h_{SR}[1].

The received data vector at the destination is expressed as

$$\mathbf{y} = \mathbf{X}\mathbf{h}_C + \mathbf{n} \tag{2.1}$$

where $\mathbf{y} = [\mathbf{y}_1{}^\mathsf{T}\ \mathbf{y}_2{}^\mathsf{T} \dots \mathbf{y}_{\frac{N}{2}}{}^\mathsf{T}]^\mathsf{T}$, $\mathbf{X} = [\mathbf{X}_1^\mathsf{T}\ \mathbf{X}_2^\mathsf{T} \dots \mathbf{X}_{\frac{N}{2}}^\mathsf{T}]^\mathsf{T}$ is the transmitted data matrix, $\mathbf{h}_C = [\sqrt{\frac{E_{RD}E_{SR}}{E_{SR}+N_o}}h_{SR}h_{RD}\ \sqrt{E_{SD}}h_{SD}]^\mathsf{T}$ denotes the cascaded channel gain and the channel gain in the direct link, $\mathbf{n} = [\mathbf{n}_1^\mathsf{T}\ \mathbf{n}_2^\mathsf{T} \dots \mathbf{n}_{\frac{N}{2}}{}^\mathsf{T}]^\mathsf{T}$ is the noise vector, and

$$\mathbf{y}_i = \mathbf{X}_i\mathbf{h}_C + \mathbf{n}_i \tag{2.2}$$

with $\mathbf{y}_i = [y_{2i-1}\ y_{2i}]^\mathsf{T}$, $\mathbf{X}_i = \begin{bmatrix} x_{2i-1} & x_{2i} \\ -x_{2i}^* & x_{2i-1}^* \end{bmatrix}$ and $\mathbf{n}_i = [\eta_{2i-1}\ \eta_{2i}]^\mathsf{T}$. The index in (2.2) varies from 1 to $N/2$, assuming that $N/2$ is an integer. In (2.2), y_{2i-1} is the received

[1]It will be discussed later that, in the case of disintegrated channel estimation, $\tilde{h}_{SR}$ is forwarded by the relay to the destination.

signal after the $2(2i-1)$th time slot and is expressed as [2]

$$y_{2i-1} = \sqrt{\frac{E_{RD}E_{SR}}{E_{SR}+N_o}} h_{SR}h_{RD}x_{2i-1} + \sqrt{E_{SD}}h_{SD}x_{2i} + \eta_{2i-1}$$

where $\eta_{2i-1} = \sqrt{\frac{E_{RD}}{E_{SR}+N_o}} h_{RD}n_{R,2i-1} + n_{D,2i-1}$ is the collective noise at the destination and y_{2i} is the received signal after the $2(2i)$th time slot and is given by

$$y_{2i} = \sqrt{\frac{E_{RD}E_{SR}}{E_{SR}+N_o}} h_{SR}h_{RD}(-x_{2i}^*) + \sqrt{E_{SD}}h_{SD}x_{2i-1}^* + \eta_{2i}$$

where $\eta_{2i} = \sqrt{\frac{E_{RD}}{E_{SR}+N_o}} h_{RD}n_{R,2i} + n_{D,2i}$ is the collective noise at the destination, x_{2i-1} and x_{2i} are the transmitted data symbols, $n_{R,k}$ is the noise at the relay during time slot k and $n_{D,k}$ is the noise at the destination during time slot k, $k = 2i, 2i-1$. The noise terms $n_{R,k}$ and $n_{D,k}$ are ZMCG with variance $\frac{N_o}{2}$ per dimension. It is noted that η_{2i-1} and η_{2i} are not complex Gaussian. However, the closed form expression for the exact PDF of the collective noise does not exist and therefore, the analysis using the exact system model would lead to intractable results. Thus, in order to obtain tractable results, assume η_{2i-1} and η_{2i} to be complex Gaussian as in [33, 83, 87, 40, 88, 85]. It will be shown, that the receivers derived using this approximation still provide performance gains. The variances of η_{2i-1} and η_{2i} are $\mathbb{E}[\eta_{2i-1}^2] = \mathbb{E}[\eta_{2i}^2] = \sigma_\eta^2 = \left(1 + \frac{E_{RD}}{E_{SR}+N_o}\right) N_o$, where E_{SR}, E_{RD} and E_{SD} are the source-relay, relay-destination and source-destination transmitted energies, respectively.

The ideal receiver, denoted as the genie receiver, assumes perfect channel knowledge. The metric for the genie receiver is

$$\hat{\mathbf{X}} = \arg\min_{\mathbf{X}} \ \|\mathbf{y} - \mathbf{X}\mathbf{h}_C\|^2. \tag{2.3}$$

In reality, the receiver does not have perfect CSI and the CSI is estimated using the pilot symbols. The channel estimate is then used in the metric in (2.3) to decode

[2]The signal at the relay is normalized by a fixed gain $\sqrt{\mathbb{E}[y_R^2]} = \sqrt{E_{SR}+N_o}$ [33], where $\mathbb{E}[\cdot]$ denotes the expectation operator. Thus, the multiplying factor at the relay does not depend on h_{SR}.

the received signal. This minimum Euclidean distance receiver is also called the mismatched receiver in [28] and is expressed as

$$\hat{\mathbf{X}} = \arg\min_{\mathbf{X}} \ \|\mathbf{y} - \mathbf{X}\hat{\mathbf{h}}\|^2 \tag{2.4}$$

where $\hat{\mathbf{h}}$ can be the ML estimate of the cascaded source-relay-destination channel (in the case of CCE) or the product of the ML estimates of the source-relay channel and the relay-destination channel (in the case of DCE).

2.3 Channel Estimation

2.3.1 Cascaded Channel Estimation

In the case of CCE, the channel is estimated at the destination using the received pilot vector $\mathbf{z}$ which can be expressed similar to (2.1) as

$$\mathbf{z} = \mathbf{P}\mathbf{h}_C + \mathbf{n}_\mathbf{P} \tag{2.5}$$

where $\mathbf{z} = [z_1 \ z_2 \dots z_M]^\mathsf{T}$ is the received pilot vector, $\mathbf{P} = [\mathbf{P}_1^\mathsf{T} \ \mathbf{P}_2^\mathsf{T} \dots \mathbf{P}_{\frac{M}{2}}^\mathsf{T}]^\mathsf{T}$ is the transmitted pilot block, $\mathbf{P}_i = \begin{bmatrix} p_{2i-1} & p_{2i} \\ -p_{2i}^* & p_{2i-1}^* \end{bmatrix}$, and $\mathbf{n}_\mathbf{P} = [\eta_{p1} \ \eta_{p2} \dots \eta_{pM}]^\mathsf{T}$ is the ZMCG noise with variance σ_η^2 that is added to the received pilot signal at the destination.

2.3.2 Disintegrated Channel Estimation

In the case of DCE, the relay estimates the source-relay channel using the pilots sent by the source. It then replaces the pilots from the source with the new pilots

and sends them to the destination to estimate the relay-destination channel. It also forwards the quantized estimate of the source-relay channel, obtained at the relay, to the destination [43, 44]. The received pilot vector at the relay can be expressed as

$$\mathbf{z}_{SR} = \mathbf{p}_1\sqrt{E_{SR}}h_{SR} + \mathbf{n}_R \tag{2.6}$$

where $\mathbf{z}_{SR} = [z_{SR,1}\ z_{SR,2} \dots z_{SR,M}]^{\mathsf{T}}$ is the received pilot vector at the relay, $\mathbf{p}_1$ denotes the first column of the pilot matrix $\mathbf{P}$ and $\mathbf{n}_R = [n_{R,1}\ n_{R,3} \dots n_{R,2M-1}]^{\mathsf{T}}$ is the ZMCG noise added at the relay. The relay replaces the received pilot vector with new pilots and thus, the received pilot vector at the destination can be expressed as

$$\mathbf{z}_D = \mathbf{P}\mathbf{h}_D + \mathbf{n}_D \tag{2.7}$$

where $\mathbf{z}_D = [z_{D,1}\ z_{D,2} \dots z_{D,M}]^{\mathsf{T}}$ is the received pilot vector, $\mathbf{h}_D = [\sqrt{E_{RD}}h_{RD}\ \sqrt{E_{SD}}h_{SD}]^{\mathsf{T}}$ is the destination channel vector and $\mathbf{n}_D = [n_{D,2}\ n_{D,4} \dots n_{D,2M}]$ is the ZMCG noise that is added to the received pilot signals at the destination.

The ML estimate in (2.4) is calculated as [89]

$$\hat{\mathbf{h}} = (\mathbf{U}^{\mathsf{H}}\mathbf{U})^{-1}\mathbf{U}^{\mathsf{H}}\mathbf{w} \tag{2.8}$$

where $(\cdot)^{\mathsf{H}}$ denotes the Hermitian operator,$\mathbf{w}$ is the received pilot vector and $\mathbf{U}$ is the matrix of transmitted pilots. The error in the ML estimate is $\mathbf{e} = (\mathbf{U}^{\mathsf{H}}\mathbf{U})^{-1}\mathbf{U}^{\mathsf{H}}\mathbf{n}$ [89], where $\mathbf{n}$ is the noise in the received pilot vector.Note that the symbols $\mathbf{U}$, $\mathbf{w}$ and $\mathbf{n}$ in (2.8), can be replaced by $\mathbf{P}$, $\mathbf{z}$ and $\mathbf{n}_{\mathbf{P}}$ in (2.5), $\mathbf{p}_1$, $\mathbf{z}_{SR}$ and $\mathbf{n}_R$ in (2.6) or $\mathbf{P}$, $\mathbf{z}_D$ and $\mathbf{n}_D$ in (2.7) to obtain the ML channel estimate in each case. Note also that the receiver in (2.4) has been proved the best among all existing receivers in [32, 33, 35, 40, 43, 44]. Thus, in the following, we only compare our new receivers

with (2.4).

2.4 Minimum Euclidean Distance Receiver With Decision History

The performance of the conventional receiver in (2.4) can be improved by incorporating the decision history, similar to [31], which results in a better estimate of the CSI. In the derivation, we assume that the decoding is done for the N data symbols in each block based on $\mathbf{X}_i$, $i = 1, \ldots N/2$, as this reduces the decoding complexity. For the ith decoding block, the channel estimate is improved by incorporating the decision history as

$$\hat{\mathbf{h}}_{DH} = \left(\mathbf{P}^{\mathsf{H}}\mathbf{P} + \sum_{k=0}^{i-1} \hat{\mathbf{X}}_k^{\mathsf{H}} \hat{\mathbf{X}}_k \right)^{-1} \left(\mathbf{P}^{\mathsf{H}}\mathbf{z} + \sum_{k=0}^{i-1} \hat{\mathbf{X}}_k^{\mathsf{H}} \mathbf{y}_k \right) \tag{2.9}$$

where $\hat{\mathbf{X}}_k$ is the data decision of $\mathbf{X}_k$ and $\mathbf{y}_k$ is the received signal of $\mathbf{X}_k$. If the previous decisions are correct, they have the same effect as the pilots. If the previous decisions are incorrect, they will lead to an unreliable estimate. Therefore, to reduce the detrimental effect of the decision errors, the previous decisions can be weighted according to the noise statistics as

$$\hat{\mathbf{h}}_{WDH} = \left(\mathbf{P}^{\mathsf{H}}\mathbf{P} + \frac{1}{\sigma_\eta^2} \sum_{k=0}^{i-1} \hat{\mathbf{X}}_k^{\mathsf{H}} \hat{\mathbf{X}}_k \right)^{-1} \left(\mathbf{P}^{\mathsf{H}}\mathbf{z} + \frac{1}{\sigma_\eta^2} \sum_{k=0}^{i-1} \hat{\mathbf{X}}_k^{\mathsf{H}} \mathbf{y}_k \right). \tag{2.10}$$

In this case, if the noise is strong, it is more likely that the decision error is high. Then, the effect of the decision errors on the channel estimate is reduced by using a smaller weighting factor.

Since the decoding is based on blocks, the channel estimate can also be improved

by giving less weights on the older decisions of the block and giving more weights on the newest decisions. Then, after every iteration, the quality of the channel estimate is improved, and the probability of error is reduced. Thus, one has

$$\hat{\mathbf{h}}_{IDH} = \left(\mathbf{P}^{\mathsf{H}}\mathbf{P} + \lambda_i\right)^{-1}\left(\mathbf{P}^{\mathsf{H}}\mathbf{z} + \xi_i\right) \tag{2.11}$$

where $\lambda_i = \hat{\mathbf{X}}_{i-1}^{\mathsf{H}}\hat{\mathbf{X}}_{i-1} + \frac{\lambda_{i-1}}{\sigma_\eta^2}$ and $\xi_i = \hat{\mathbf{X}}_{i-1}^{\mathsf{H}}\mathbf{y}_{i-1} + \frac{\xi_{i-1}}{\sigma_\eta^2}$. Finally, one can combine (2.10) and (2.11) to obtain the channel estimate used in our new receiver as

$$\hat{\mathbf{h}}_{WIDH} = \left(\mathbf{P}^{\mathsf{H}}\mathbf{P} + \Lambda_i\right)^{-1}\left(\mathbf{P}^{\mathsf{H}}\mathbf{z} + \Xi_i\right) \tag{2.12}$$

where $\Lambda_i = \frac{1}{\sigma_\eta^2}\hat{\mathbf{X}}_{i-1}^{\mathsf{H}}\hat{\mathbf{X}}_{i-1} + \frac{\Lambda_{i-1}}{\sigma_\eta^2}$ and $\Xi_i = \frac{1}{\sigma_\eta^2}\hat{\mathbf{X}}_{i-1}^{\mathsf{H}}\mathbf{y}_{i-1} + \frac{\Xi_{i-1}}{\sigma_\eta^2}$ with $\Lambda_0 = \Xi_0 = 0$, $\hat{\mathbf{X}}_0^{\mathsf{H}}\hat{\mathbf{X}}_0 = 0$ and $\hat{\mathbf{X}}_0^{\mathsf{H}}\mathbf{y}_0 = 0$. Note that [31] proposed the idea of decision history but did not consider the Euclidean distance receiver or weighting. Therefore, (2.9)-(2.12) are our new results.

2.4.1 Minimum Euclidean Distance Receiver With Decision History For CCE (MEDDH-CCE)

One can improve the conventional mismatched receivers in (2.4) by using $\hat{\mathbf{h}}_{WIDH}$ from (2.12). Using (2.12), the improved mismatched receiver using cascaded channel estimation based on the Euclidean distance metric can expressed as

$$\hat{\mathbf{X}}_{MEDDH-CCE} = \arg\min_{\mathbf{X}} \ \left\|\mathbf{y} - \mathbf{X}\left(\mathbf{P}^{\mathsf{H}}\mathbf{P} + \Lambda_i\right)^{-1}\left(\mathbf{P}^{\mathsf{H}}\mathbf{z} + \Xi_i\right)\right\|^2 \tag{2.13}$$

where Λ_i and Ξ_i are defined as before. It can be shown that (2.12) performs better than (2.9)-(2.11).

2.4.2 Minimum Euclidean Distance Receiver With Decision History For DCE (MEDDH-DCE)

In the case of DCE, the ML estimate for the channel is expressed as

$$\hat{\mathbf{h}}_C = (\mathbf{P}^{\mathsf{H}}\mathbf{P})^{-1}(\mathbf{M}\mathbf{P}^{\mathsf{H}}\mathbf{z}) \tag{2.14}$$

where $\mathbf{M} = \begin{bmatrix} \frac{\tilde{h}_{SR}}{\sqrt{E_{SR}+N_o}} & 0 \\ 0 & 1 \end{bmatrix}$ and $\tilde{h}_{SR}$ is the quantized value of the ML estimate $\hat{h}_{SR}$ of the source-relay channel given by

$$\hat{h}_{SR} = (\mathbf{p}_1{}^{\mathsf{H}}\mathbf{p}_1)^{-1}\mathbf{p}_1{}^{\mathsf{H}}\mathbf{z}_{SR}. \tag{2.15}$$

Similarly, the improved mismatched receiver using disintegrated channel estimation based on the Euclidean distance metric can be derived as

$$\hat{\mathbf{X}}_{MEDDH-DCE} = \arg\min_{\mathbf{X}} \ \|\mathbf{y} - \mathbf{X}\left(\mathbf{P}^{\mathsf{H}}\mathbf{P} + \Lambda_i\right)^{-1}\left(\mathbf{M}\mathbf{P}^{\mathsf{H}}\mathbf{z} + \Xi_i\right)\|^2 \tag{2.16}$$

The receiver in (2.16) uses the matrix $\mathbf{M}$, which has to be multiplied with the ML estimate due to the DCE. This matrix does not appear in (2.13) for CCE. Using (2.13) and (2.16), the performances of the improved mismatched receivers using the simple Euclidean distance metric with decision history can be examined.

2.5 Maximum Averaged Likelihood Receivers

The Euclidean distance metric in (2.4) does not use any information about the channel and noise statistics, such as fading distribution and the noise power and thus, better metrics can be derived by taking them into account [28, 31]. In this section, we

derive the new receiver metrics, for both CCE and DCE, that outperform the existing Euclidean distance metric. Again, we assume that the decoding is done for the N data symbols in each block based on $\mathbf{X}_i$, $i = 1, \ldots N/2$, as this reduces the decoding complexity.

2.5.1 Maximum Averaged Likelihood Receivers For CCE

Maximum Averaged Likelihood Receiver Without Channel Distribution (MALnCS-CCE)

In [31], the receiver metric was derived that used the received pilot information directly and did not require explicit channel estimation as

$$\hat{\mathbf{X}} = \arg\max_{\mathbf{X}} \left\{ \int f_{\mathbf{y}/\mathbf{h}_C,\mathbf{X}}(\mathbf{y}) \cdot f_{\mathbf{z}/\mathbf{h}_C,\mathbf{P}}(\mathbf{z}) \, \mathtt{d}\mathbf{h}_C \right\}. \tag{2.17}$$

The expression in (2.17) is similar to the expression of the MAP detector except that it includes the conditional PDF of the received pilot signal in addition to the conditional PDF of the received data signal. In (2.17), it effectively assumes that no prior information about the channel is available such that the averaging is done over a uniform distribution. However, when the distribution of the channel is available, averaging over the actual distribution results in an improved receiver, as will be shown later. The conditional probability density function (PDF) of the received signal $\mathbf{y}_i$ is [89, eq.(15.17)]

$$f_{\mathbf{y}_i/\mathbf{h}_C,\mathbf{X}_i}(\mathbf{y}_i) = \frac{\exp\left(-(\mathbf{y}_i - \mathbf{X}_i\mathbf{h}_C)^{\mathsf{H}}\mathbf{C}_{n_i}^{-1}(\mathbf{y}_i - \mathbf{X}_i\mathbf{h}_C)\right)}{\pi^2 \det(\mathbf{C}_{\mathbf{n}_i})} \tag{2.18}$$

where $\mathbf{C}_{\mathbf{n}_i} = \left(1 + \frac{E_{RD}}{E_{SR}+N_o}\right) N_o \cdot \mathbb{I}_2$ is the noise covariance matrix, $\det(\cdot)$ is the determinant operator and $\mathbb{I}_k$ denotes the identity matrix of order $k \times k$. The conditional

PDF of the received pilot signal $\mathbf{z}$ is

$$f_{\mathbf{z}/\mathbf{h}_C,\mathbf{P}}(\mathbf{z}) = \frac{\exp\left(-(\mathbf{z}-\mathbf{P}\mathbf{h}_C)^{\mathsf{H}}\mathbf{C}_{\mathbf{z}}^{-1}(\mathbf{z}-\mathbf{P}\mathbf{h}_C)\right)}{\pi^M \det(\mathbf{C}_{\mathbf{z}})} \tag{2.19}$$

where $\mathbf{C}_{\mathbf{z}} = \left(1+\frac{E_{RD}}{E_{SR}+N_o}\right) N_o \cdot \mathbb{I}_M$ is the noise covariance matrix. Substituting (2.18) and (2.19) in (2.17), solving the resulting integral using the fact that, for Alamouti code, $\mathbf{X}_i^{\mathsf{H}}\mathbf{X}_i = c \cdot \mathbb{I}_2$ and $\mathbf{P}^{\mathsf{H}}\mathbf{P} = d \cdot \mathbb{I}_2$, where c and d are constants, and simplifying the result one obtains

$$\hat{\mathbf{X}}_{i,MALnCSnDH-CCE} = \arg\max_{\mathbf{X}_i} \left\{ -\ln(\det(\mathbf{A}_{\mathbf{X_i}})) + \frac{(\mathbf{\Gamma}_{\mathbf{X_i}})(\mathbf{A}_{\mathbf{X_i}})^{-1}(\mathbf{\Gamma}_{\mathbf{X_i}})^{\mathsf{H}}}{\sigma_\eta^2} \right\} \tag{2.20}$$

where $\mathbf{A}_{\mathbf{X_i}} = \mathbf{X}_i^{\mathsf{H}}\mathbf{X}_i + \mathbf{P}^{\mathsf{H}}\mathbf{P}$, $\mathbf{\Gamma}_{\mathbf{X_i}} = \mathbf{y}_i^{\mathsf{H}}\mathbf{X}_i + \mathbf{z}^{\mathsf{H}}\mathbf{P}$, $\sigma_\eta^2 = \left(1+\frac{E_{RD}}{E_{SR}+N_o}\right) N_o$ and $\ln(\cdot)$ denotes the natural logarithm. The derived new metric in (2.20) involves only the statistics of the collective noise at the destination. It can be noted that the receiver given by (2.20) is more complicated than the receiver in (2.4), although the receiver in (2.20) saves the cost of channel estimation. In particular, (2.20) requires about $36M^2$ real multiplications while (2.4) requires $24M^2$ real multiplications, where M denotes the constellation size. Thus, the overall complexity of (2.20) is higher than that of (2.4) and the receiver in (2.20) is more useful in applications where performance is more important.

The receiver in (2.20) does not use any decision history. Similar to the case of the conventional coherent receiver, decision history can be utilized to improve the performance of the derived new receiver metric. The history parameters Υ_i and Λ_i

are added to the new receiver metric in (2.20) and one obtains

$$\hat{\mathbf{X}}_{i,MALnCSDH-CCE} = \arg\max_{\mathbf{X}_i} \left\{ -\ln\left(\det(\mathbf{A}_{\mathbf{X_i}} + \Lambda_i)\right) + \frac{(\mathbf{\Gamma}_{\mathbf{X_i}} + \Upsilon_i)(\mathbf{A}_{\mathbf{X_i}} + \Lambda_i)^{-1}(\mathbf{\Gamma}_{\mathbf{X_i}} + \Upsilon_i)^{\mathsf{H}}}{\sigma_\eta^2} \right\} \tag{2.21}$$

where Λ_i is as before and $\Upsilon_i = \frac{1}{\sigma_\eta^2}\mathbf{y}_{i-1}^{\mathsf{H}}\hat{\mathbf{X}}_{i-1} + \frac{\Upsilon_{i-1}}{\sigma_\eta^2}$ with $\Upsilon_0 = 0$. Note that the receiver in (2.21) uses the decision history in (2.12). One may also use (2.9)-(2.11), but they do not offer better performances.

Maximum Averaged Likelihood Receiver With Channel Distribution (MALCS-CCE)

As mentioned previously, using the distribution of the channel in (2.17) can result in an improved metric. The resulting metric uses additional information of the channel distribution and can be derived as [28, 31]

$$\hat{\mathbf{X}} = \arg\max_{\mathbf{X}} \left\{ \int f_{\mathbf{y}/\mathbf{h}_C,\mathbf{X}}(\mathbf{y}) \cdot f_{\mathbf{z}/\mathbf{h}_C,\mathbf{P}}(\mathbf{z}) \cdot f_{\mathbf{h}_C}(\mathbf{h})\ \mathrm{d}\mathbf{h}_C \right\}. \tag{2.22}$$

From (2.1), $\mathbf{h}_C = [h_1\ h_2]^T = [\sqrt{\frac{E_{RD}E_{SR}}{E_{SR}+N_o}}h_{SR}h_{RD}\ \sqrt{E_{SD}}h_{SD}]^T$. In this case it can be observed that h_2 is ZMCG with variance $\sigma_{h_2}^2 = E_{SD}$. The exact PDF of h_1 is given in [36] but it does not lead to tractable derivation. We therefore use the approximation, $f_{h_1}(x) \approx f_{h_{1,r}}(x) \cdot f_{h_{1,i}}(x)$, i.e. the real and imaginary parts of the product of complex Gaussian random variables are independent. From [36]

$$f_{h_{1,r}}(x) = f_{h_{1,i}}(x) = \frac{1}{\sigma_1\sigma_2} \cdot \exp\left(-\frac{2}{\sigma_1\sigma_2} \cdot |x|\right) \tag{2.23}$$

where, $h_{1,r}$ and $h_{1,i}$ are the real and imaginary parts of h_1 and $\sigma_1^2 = \sigma_2^2 = \sqrt{\frac{E_{RD}E_{SR}}{E_{SR}+N_o}}$.

Using the above results, (2.22) can be solved to obtain

$$\hat{\mathbf{X}}_{i,MALCSnDH-CCE} = \arg\max_{X_i} \left\{ -\ln \Delta_{\mathbf{X_i}} - \ln\left(\Delta_{\mathbf{X_i}} + \frac{1}{\sigma_{h_2}^2}\right) + \frac{\Gamma_{\mathbf{x_{i,2}}}{}^{H}\Gamma_{\mathbf{x_{i,2}}}}{\Delta_{\mathbf{X_i}} + \frac{1}{\sigma_{h_2}^2}} + \right.$$
$$\ln\left(\text{experfc}\left(\frac{(\zeta - \Re(\Gamma_{\mathbf{x_{i,1}}}))^2}{\Delta_{\mathbf{X_i}}}\right) + \text{experfc}\left(\frac{(\zeta + \Re(\Gamma_{\mathbf{x_{i,1}}}))^2}{\Delta_{\mathbf{X_i}}}\right)\right) + \quad (2.24)$$
$$\left. \ln\left(\text{experfc}\left(\frac{(\zeta - \Im(\Gamma_{\mathbf{x_{i,1}}}))^2}{\Delta_{\mathbf{X_i}}}\right) + \text{experfc}\left(\frac{(\zeta + \Im(\Gamma_{\mathbf{x_{i,1}}}))^2}{\Delta_{\mathbf{X_i}}}\right)\right)\right\}$$

where $\Gamma_{\mathbf{x_{i,1}}} = \mathbf{y}_i^{\mathsf{H}}\mathbf{x}_{i,1} + \mathbf{z}^{\mathsf{H}}\mathbf{p}_1$, $\Gamma_{\mathbf{x_{i,2}}} = \mathbf{y}_i^{\mathsf{H}}\mathbf{x}_{i,2} + \mathbf{z}^{\mathsf{H}}\mathbf{p}_2$, $\zeta = \frac{1}{\sigma_1\sigma_2}$ and $\Delta_{\mathbf{X_i}} = \frac{\sqrt{\det(\mathbf{A}_{\mathbf{X_i}})}}{\sigma_\eta^2}$, $\mathbf{x}_{i,1}$ and $\mathbf{x}_{i,2}$ denote the first and second column of $\mathbf{X}_i$, $\mathbf{p}_1$ and $\mathbf{p}_2$ denote the first and second column of $\mathbf{P}$, respectively, $\Re(\cdot)$ and $\Im(\cdot)$ denote the real and imaginary parts of the argument and $\text{experfc}(x) = \exp(x) \cdot \text{erfc}(\sqrt{x})$ and $\text{erfc}(\cdot)$ denotes the complementary error function. We denote the derived metric in (2.24) as MALCS-CCE and the metric in (2.20) as MALnCS-CCE. Also, the metric given by (2.24) is more complex than (2.20), as it requires evaluation of the exponential and erfc functions.

Similarly, the performance of the derived new receiver in (2.24) can be improved by incorporating the decision history, giving

$$\hat{\mathbf{X}}_{i,MALCSDH-CCE} =$$
$$\arg\max_{X_i} \left\{ -\ln \Sigma_{\mathbf{X_i}} - \ln\left(\Sigma_{\mathbf{X_i}} + \frac{1}{\sigma_{h_2}^2}\right) + \frac{(\Gamma_{\mathbf{x_{i,2}}} + \Theta_{2,i})^{\mathsf{H}}(\Gamma_{\mathbf{x_{i,2}}} + \Theta_{2,i})}{\Sigma_{\mathbf{X_i}} + \frac{1}{\sigma_{h_2}^2}} + \right.$$
$$\ln\left(\text{experfc}\left(\frac{(\zeta - \Re(\Gamma_{\mathbf{x_{i,1}}} + \Theta_{1,i}))^2}{\Sigma_{\mathbf{X_i}}}\right) + \text{experfc}\left(\frac{(\zeta + \Re(\Gamma_{\mathbf{x_{i,1}}} + \Theta_{1,i}))^2}{\Sigma_{\mathbf{X_i}}}\right)\right) +$$
$$\left. \ln\left(\text{experfc}\left(\frac{(\zeta - \Im(\Gamma_{\mathbf{x_{i,1}}} + \Theta_{1,i}))^2}{\Sigma_{\mathbf{X_i}}}\right) + \text{experfc}\left(\frac{(\zeta + \Im(\Gamma_{\mathbf{x_{i,1}}} + \Theta_{1,i}))^2}{\Sigma_{\mathbf{X_i}}}\right)\right)\right\} \quad (2.25)$$

where $\Theta_{1,i} = \frac{1}{\sigma_\eta^2}\mathbf{y}_{i-1}^{\mathsf{H}}\hat{\mathbf{x}}_{i-1,1} + \frac{\Theta_{1,i-1}}{\sigma_\eta^2}$ with $\mathbf{y}_0^{\mathsf{H}}\hat{\mathbf{x}}_{0,1} = 0$ and $\Theta_{1,0} = 0$, $\Theta_{2,i} = \frac{1}{\sigma_\eta^2}\mathbf{y}_{i-1}^{\mathsf{H}}\hat{\mathbf{x}}_{i-1,2} +$

$\frac{\Theta_{2,i-1}}{\sigma_\eta^2}$ with $\mathbf{y}_0^{\mathsf{H}}\hat{\mathbf{x}}_{0,2}=0$ and $\Theta_{2,0}=0$, $\Sigma_{\mathbf{X_i}}=\frac{\sqrt{\det(\mathbf{A}_{\mathbf{X_i}}+\Lambda_i)}}{\sigma_\eta^2}$ and $\Lambda_i=\frac{1}{\sigma_\eta^2}\hat{\mathbf{X}}_{i-1}^{\mathsf{H}}\hat{\mathbf{X}}_{i-1}+\frac{\Lambda_{i-1}}{\sigma_\eta^2}$ with $\Lambda_0=0$ and $\hat{\mathbf{X}}_0^{\mathsf{H}}\hat{\mathbf{X}}_0=0$, $\hat{\mathbf{x}}_{i,1}$ and $\hat{\mathbf{x}}_{i,2}$ denote the first and second column of $\hat{\mathbf{X}}_i$, as the data decisions, respectively.

2.5.2 Maximum Averaged Likelihood Receivers For DCE

In the case of DCE, the source-relay channel is estimated at the relay by the ML estimator given in (2.15). This source-relay channel estimate is quantized and forwarded to the destination via the feed forward channel as $\tilde{h}_{SR}$ [44].

Maximum Averaged Likelihood Receiver Without Channel Distribution (MALnCS-DCE)

The receiver metric for the destination can be derived by using the received pilot information directly without channel estimation as [31]

$$\hat{\mathbf{X}}=\arg\max_{\mathbf{X}}\left\{\int f_{\mathbf{y}/\mathbf{h}_C,\mathbf{X}}(\mathbf{y})\cdot f_{\mathbf{z}_D/\mathbf{h}_D,\mathbf{P}}(\mathbf{z})\,\mathrm{d}\mathbf{h}_D\Big|_{h_{SR}=\tilde{h}_{SR}}\right\}. \tag{2.26}$$

It can be noted that the metric in (2.26) is slightly modified by not integrating over the source-relay channel. Instead, we substitute it for the value of the quantized estimate of the source-relay channel that has been forwarded by the relay.

The conditional PDF of the received signal $\mathbf{y}_i$ is given by (2.18) with $\mathbf{C}_{\mathbf{n}_i}=\left(1+\frac{E_{RD}}{E_{SR}+N_o}\right)N_o\cdot\mathbb{I}_2$. The conditional PDF of the received pilot signal $\mathbf{z}_D$ is expressed as

$$f_{\mathbf{z}_D/\mathbf{h}_D,\mathbf{P}}(\mathbf{z})=\frac{\exp\left(-(\mathbf{z}-\mathbf{P}\mathbf{h}_D)^{\mathsf{H}}\mathbf{C}_{\mathbf{z}}^{-1}(\mathbf{z}-\mathbf{P}\mathbf{h}_D)\right)}{\pi^M\det(\mathbf{C}_{\mathbf{z}})} \tag{2.27}$$

where $\mathbf{C}_{\mathbf{z}}=N_o\cdot\mathbb{I}_M$ is the noise covariance matrix.

Substituting (2.18) and (2.27) in (2.26) and solving the resulting integral, one has

$$\hat{\mathbf{X}}_{i,MALnCSnDH-DCE} = \arg\max_{\mathbf{X}_i} \Big\{ -\ln\left(\mathbf{\Omega}_{\mathbf{X_i}}\right) + \left(\mathbf{\Psi}_{\mathbf{x_{i,1}}}\right)\left(\mathbf{\Omega}_{\mathbf{X_i}}\right)^{-1}\left(\mathbf{\Psi}_{\mathbf{x_{i,1}}}\right)^{\mathsf{H}} - \ln\left(\mathbf{\Phi}_{\mathbf{X_i}}\right) + \left(\mathbf{\Psi}_{\mathbf{x_{i,2}}}\right)\left(\mathbf{\Phi}_{\mathbf{X_i}}\right)^{-1}\left(\mathbf{\Psi}_{\mathbf{x_{i,2}}}\right)^{\mathsf{H}} \Big\} \tag{2.28}$$

where, $\mathbf{\Omega}_{\mathbf{X_i}} = \frac{\sqrt{\det\left(\mathbf{X}_i^{\mathsf{H}}\mathbf{X}_i\right)}\cdot\tilde{h}_{SR}^{H}\tilde{h}_{SR}}{\sigma_\eta^2(E_{SR}+N_o)} + \frac{\sqrt{\det\left(\mathbf{P}^{\mathsf{H}}\mathbf{P}\right)}}{\sigma_z^2}$, $\mathbf{\Phi}_{\mathbf{X_i}} = \frac{\sqrt{\det\left(\mathbf{X}_i^{\mathsf{H}}\mathbf{X}_i\right)}}{\sigma_\eta^2} + \frac{\sqrt{\det\left(\mathbf{P}^{\mathsf{H}}\mathbf{P}\right)}}{\sigma_z^2}$, $\mathbf{\Psi}_{\mathbf{x_{i,1}}} = \frac{\mathbf{y}_i^{\mathsf{H}}\mathbf{x}_{i,1}\cdot\tilde{h}_{SR}}{\sigma_\eta^2\sqrt{E_{SR}+N_o}} + \frac{\mathbf{z}^{\mathsf{H}}\mathbf{p}_1}{\sigma_z^2}$, $\mathbf{\Psi}_{\mathbf{x_{i,2}}} = \frac{\mathbf{y}_i^{\mathsf{H}}\mathbf{x}_{i,2}}{\sigma_\eta^2} + \frac{\mathbf{z}^{\mathsf{H}}\mathbf{p}_2}{\sigma_z^2}$, $\sigma_\eta^2 = \left(1 + \frac{E_{RD}}{E_{SR}+N_o}\right)N_o$ and $\sigma_z^2 = N_o$. The above metric uses the quantized ML estimate of the source-relay channel. It can also be noted that the derived metric in (2.28) uses the information of the noise variance. Again, this receiver does not perform channel estimation for the source-destination and the relay-destination channels. But it does for the source-relay channel.

By incorporating the decision history into the metric, its performance can be improved and one obtains

$$\hat{\mathbf{X}}_{i,MALnCSDH-DCE} = \arg\max_{\mathbf{X}_i} \Big\{ -\ln\left(\mathbf{\Omega}_{\mathbf{X_i}} + \Lambda_{A,i}\right) + \left(\mathbf{\Psi}_{\mathbf{x_{i,1}}} + \Xi_{A,i}\right)\left(\mathbf{\Omega}_{\mathbf{X_i}} + \Lambda_{A,i}\right)^{-1}\left(\mathbf{\Psi}_{\mathbf{x_{i,1}}} + \Xi_{A,i}\right)^{\mathsf{H}} - \ln\left(\mathbf{\Phi}_{\mathbf{X_i}} + \Lambda_{B,i}\right) + \left(\mathbf{\Psi}_{\mathbf{x_{i,2}}} + \Xi_{B,i}\right)\left(\mathbf{\Phi}_{\mathbf{X_i}} + \Lambda_{B,i}\right)^{-1}\left(\mathbf{\Psi}_{\mathbf{x_{i,2}}} + \Xi_{B,i}\right)^{\mathsf{H}} \Big\} \tag{2.29}$$

where, $\Xi_{A,i} = \frac{\Xi_{A,i-1}}{\sigma_\eta^2} + \frac{\mathbf{y}_{i-1}^{\mathsf{H}}\hat{\mathbf{x}}_{i-1,1}\cdot\tilde{h}_{SR}}{\sigma_\eta^2\sqrt{E_{SR}+N_o}}$ with $\mathbf{y}_0^{\mathsf{H}}\hat{\mathbf{x}}_{0,1} = 0$ and $\Xi_{A,0} = 0$, $\Xi_{B,i} = \frac{\Xi_{B,i-1}}{\sigma_\eta^2} + \frac{\mathbf{y}_{i-1}^{\mathsf{H}}\hat{\mathbf{x}}_{i-1,2}}{\sigma_\eta^2}$ with $\mathbf{y}_0^{\mathsf{H}}\hat{\mathbf{x}}_{0,2} = 0$ and $\Xi_{B,0} = 0$, $\Lambda_{A,i} = \frac{\Lambda_{A,i-1}}{\sigma_\eta^2} + \frac{\sqrt{\det\left(\hat{\mathbf{X}}_{i-1}^{\mathsf{H}}\hat{\mathbf{X}}_{i-1}\right)}\cdot\tilde{h}_{SR}^{\mathsf{H}}\tilde{h}_{SR}}{\sigma_\eta^2(E_{SR}+N_o)}$ with $\Lambda_{A,0} = 0$, $\Lambda_{B,i} = \frac{\Lambda_{B,i-1}}{\sigma_\eta^2} + \frac{\sqrt{\det\left(\hat{\mathbf{X}}_{i-1}^{\mathsf{H}}\hat{\mathbf{X}}_{i-1}\right)}}{\sigma_\eta^2}$ with $\Lambda_{B,0} = 0$.

Maximum Averaged Likelihood Receiver With Channel Distribution (MALCS-DCE)

Using the channel distribution, the new metric is obtained by solving the following integral

$$\hat{\mathbf{X}} = \arg\max_{\mathbf{X}} \left\{ \int f_{\mathbf{y}/\mathbf{h}_C,\mathbf{X}}(\mathbf{y}) \cdot f_{\mathbf{z}_D/\mathbf{h}_D,\mathbf{P}}(\mathbf{z}) \cdot f_{\mathbf{h}_D}(\mathbf{h})\ \mathrm{d}\mathbf{h}_D \Big|_{h_{SR}=\tilde{h}_{SR}} \right\}. \tag{2.30}$$

From (2.7), $\mathbf{h}_D = [\sqrt{E_{RD}}h_{RD}\ \sqrt{E_{SD}}h_{SD}]^{\mathsf{T}} = [h_1\ h_2]^T$. In this case, it can be observed that both h_1 and h_2 are complex Gaussian with zero mean and variance $\sigma_{RD}^2 = E_{RD}$ and $\sigma_{SD}^2 = E_{SD}$ respectively. Thus the joint PDF of both the channels is complex Gaussian.

Substituting (2.18) and (2.27) in (2.30) and solving the resulting integral, one has

$$\begin{aligned}\hat{\mathbf{X}}_{i,MALCSnDH-DCE} = \\ \arg\max_{\mathbf{X}_i} \Big\{ &- \ln\left(\mathbf{\Omega}_{\mathbf{X_i}} + \frac{1}{\sigma_{RD}^2}\right) - \ln\left(\mathbf{\Phi}_{\mathbf{X_i}} + \frac{1}{\sigma_{SD}^2}\right) + \\ &(\mathbf{\Psi}_{\mathbf{x_{i,1}}})(\mathbf{\Omega}_{\mathbf{X_i}} + \frac{1}{\sigma_{RD}^2})^{-1}(\mathbf{\Psi}_{\mathbf{x_{i,1}}})^{\mathsf{H}} + (\mathbf{\Psi}_{\mathbf{x_{i,2}}})(\mathbf{\Phi}_{\mathbf{X_i}} + \frac{1}{\sigma_{SD}^2})^{-1}(\mathbf{\Psi}_{\mathbf{x_{i,2}}})^{\mathsf{H}} \Big\}.\end{aligned} \tag{2.31}$$

The values of $\mathbf{\Omega}_{\mathbf{X_i}}$, $\mathbf{\Phi}_{\mathbf{X_i}}$, $\mathbf{\Psi}_{\mathbf{x_{i,1}}}$, $\mathbf{\Psi}_{\mathbf{x_{i,2}}}$, σ_η^2, σ_z^2, $\mathbf{x}_{i,1}$, $\mathbf{x}_{i,2}$, $\mathbf{p}_1$ and $\mathbf{p}_2$ are the same as those in (2.28). If the ML estimate of the source-relay channel is replaced by its original value, the metric given by (2.31) is the optimal metric.

Again, the performance of the derived receiver in (2.31) can be improved by in-

corporating the decision history and one obtains

$$\hat{\mathbf{X}}_{i,MALCSDH-DCE} = \arg\max_{\mathbf{X}_i} \Big\{ -\ln\left(\mathbf{\Omega}_{\mathbf{X_i}} + \frac{1}{\sigma_{RD}^2} + \Lambda_{A,i}\right) - \ln\left(\mathbf{\Phi}_{\mathbf{X_i}} + \frac{1}{\sigma_{SD}^2} + \Lambda_{B,i}\right) + (\mathbf{\Psi}_{\mathbf{x_{i,1}}} + \Xi_{A,i})(\mathbf{\Omega}_{\mathbf{X_i}} + \frac{1}{\sigma_{RD}^2} + \Lambda_{A,i})^{-1}(\mathbf{\Psi}_{\mathbf{x_{i,1}}} + \Xi_{A,i})^{\mathsf{H}} + (\mathbf{\Psi}_{\mathbf{x_{i,2}}} + \Xi_{B,i})(\mathbf{\Phi}_{\mathbf{X_i}} + \frac{1}{\sigma_{SD}^2} + \Lambda_{B,i})^{-1}(\mathbf{\Psi}_{\mathbf{x_{i,2}}} + \Xi_{B,i})^{\mathsf{H}} \Big\}. \tag{2.32}$$

The history parameters $\Xi_{A,i}$, $\Xi_{B,i}$, $\Lambda_{A,i}$ and $\Lambda_{B,i}$ are defined as before. Note that all the proposed new receivers require knowledge of the noise variance. This can be accurately estimated by using estimators in [90] and [91]. The estimate is often χ^2-distributed with its variance decreasing with the sample size. Since the noise variance changes little during communication, one can use a large sample size to make the estimation error negligible offline.

2.6 Numerical Results and Discussion

In this section, the symbol-error-rate (SER) performances of the newly derived receivers are evaluated by simulation. Consider 16-QAM as an example. Other modulation schemes can also be examined in a similar way. The number of pilots in the simulation is chosen to be 2 and each pilot is chosen from the inner constellation point of the 16-QAM constellation and has the same phase. It can be shown that having different phases does not affect the performance. This does not mean that the pilot has much less energy than the data, because the data from the same inner point has the same energy. For DCE, assume that the channel estimate sent by the relay is quantized with infinite bits unless stated otherwise. The block size is chosen to be 80. The performances of the new receivers are compared with the

conventional mismatched ML receiver in (2.4), denoted by MEDnDH-CCE for CCE, and MEDnDH-DCE for DCE. The genie receiver is used as a benchmark. For the remaining receivers we use the notations defined previously.

Fig. 2.2 and Fig. 2.3 compare the MEDDH receivers using different forms of decision history for CCE and DCE, respectively. Equation (2.4) gives the conventional mismatched receiver without decision history and is denoted as MEDnDH. It can be observed from Fig. 2.2 that, for CCE, the MEDDH receiver using (2.12) performs about 1 dB better than the MEDDH receiver using (2.9) and approximately 2.5 dB better than the conventional MEDnDH-CCE receiver. For DCE, the MEDDH receiver using (2.12) also performs 2.5 dB better than the conventional MEDnDH-DCE receiver, as can be seen in Fig. 2.3. The MEDDH receiver using (2.11) performs the second best and the MEDDH receiver using (2.9) gives the least performance gain. Thus, significant gains can be achieved by incorporating the decision history in the receiver metric. It can also be shown that this performance gain increases by increasing the block length. In the following all the MEDDH receivers use (2.12).

In deriving the MALCSnDH-CCE receiver, we assumed that the real and imaginary parts were independent in order to get tractable results. This assumption can be justified as follows. It can be easily shown that the correlation between the real and imaginary parts of the product of complex Gaussian is zero as the joint PDF is an even function. Additionally, Fig. 2.4 compares the exact metric, i.e. the integral in (2.22), with the approximation in (2.24), for a system without the direct link. The assumption of simulating (2.22) and (2.24) without the direct link does not affect the analysis because the source-destination channel and the source-relay-destination channel are independent and one can obtain the exact metric for the source-destination link. One can observe from Fig. 2.4 that the receiver in (2.22) performs almost the same as the receiver in (2.24). Thus, the approximation error caused by this assumption is

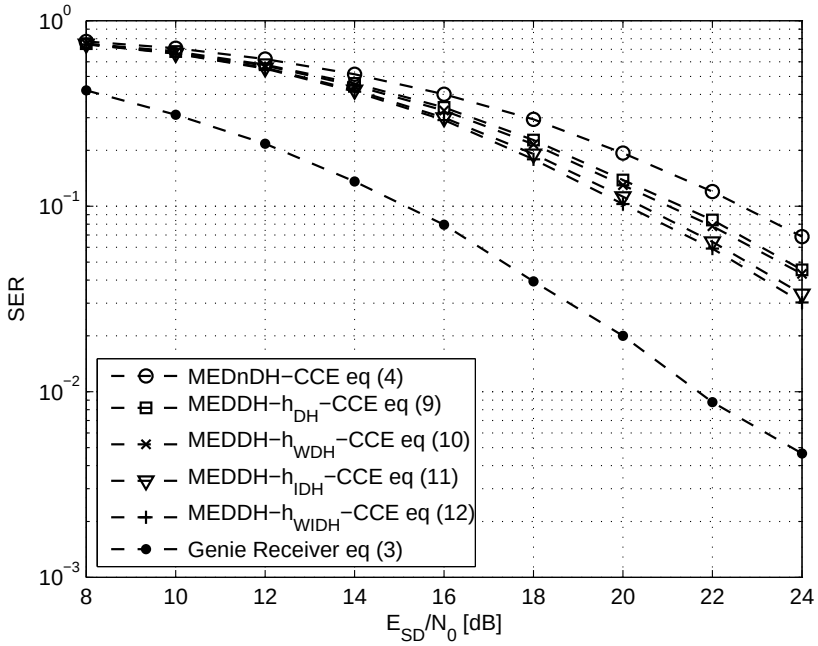

Figure 2.2: SER performance comparison of the MEDDH receivers using different forms of decision history for CCE.

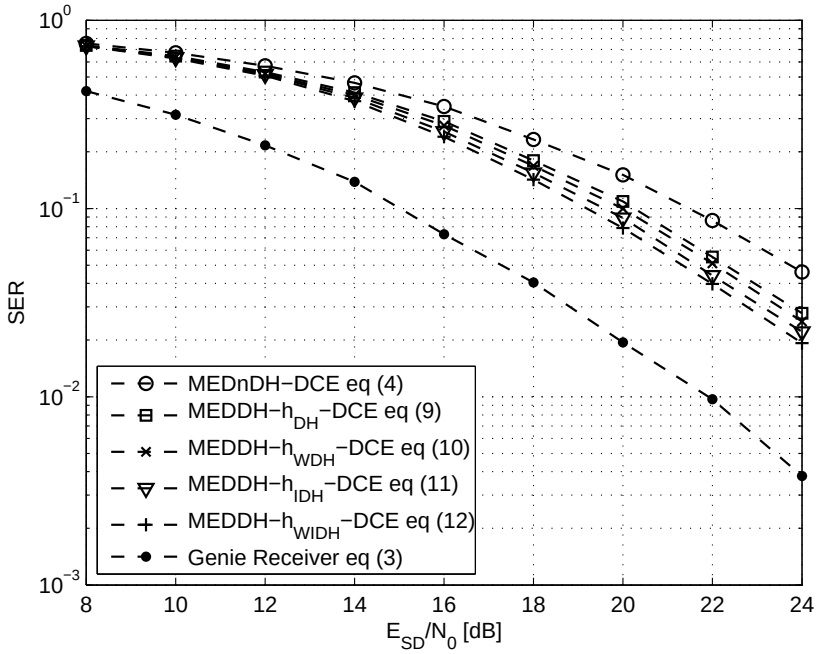

Figure 2.3: SER performance comparison of the MEDDH receivers using different forms of decision history for DCE.

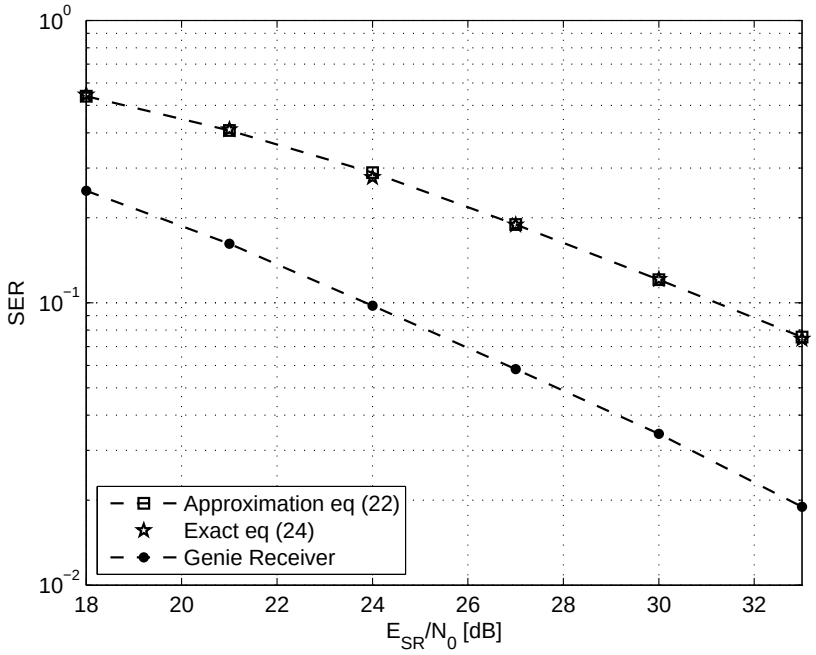

Figure 2.4: SER performance comparison of the exact metric and the approximate metric for the MALCSnDH-CCE receiver.

negligible.

Fig. 2.5 and Fig. 2.6 compare the performances of the new receivers using CCE and DCE, respectively, when $E_{SR} = E_{RD} = E_{SD}$. For CCE, it can be observed from Fig. 2.5 that the decision history always gives a gain of approximately 2.5 dB over the receivers without decision history at high E_{SD}/N_o for all the receiver metrics used. Also, at high E_{SD}/N_o, all the receivers without decision history have similar performances and all the receivers with decision history perform similarly. At low E_{SD}/N_o, the MALCSDH receiver performs slightly better than the other receivers, as its metric in (2.25) utilizes information of the channel distribution. Similar observations in the case of DCE can be made from Fig. 2.6. Comparing Fig. 2.5 and Fig. 2.6 it can be observed that the receivers for DCE perform approximately 1 dB better than the corresponding receivers for CCE, as better estimates of all the links are obtained due to lower pilot noise at the relay and destination.

Next, consider two cases of unbalanced links. Fig. 2.7 and Fig. 2.8 show the first case where the source-relay channel power is set to 50 dB, i.e., a very good source-relay channel is assumed such that a very good source-relay channel estimate is obtained in the case of DCE. Assume, $E_{RD} = E_{SD}$. It can be observed from Fig. 2.7 that the overall performances of all the receivers using CCE are improved compared with Fig. 2.5. The MALCSDH receiver performs slightly better than the other receivers and the performance gain is more noticeable at low $\frac{E_{SD}}{N_o}$. The performance gains of the new receivers over the MEDnDH receiver is reduced to approximately 1.7 dB as compared with Fig. 2.5. For the receivers using DCE, in Fig. 2.8, the performances are better than those in Fig. 2.6. The MALCSnDH receiver performs approximately 0.5 dB better than the MEDnDH receiver at high $\frac{E_{SD}}{N_o}$. This is due to the fact that $\tilde{h}_{SR} \approx h_{SR}$ and the derived MALCSnDH receiver metric becomes close to the optimal metric. It can also be noted that the MALnCSDH and the MALCSDH receivers perform the same at high $\frac{E_{SD}}{N_o}$, as $\frac{1}{\sigma^2_{SD}} = \frac{1}{\sigma^2_{RD}} \approx 0$ in this case and the MALnCSDH and MALCSDH metrics are almost the same. The receivers using the decision history perform about 2.2 dB better than the MEDnDH receiver. The MALnCSDH and the MALCSDH receivers perform approximately 0.8 dB better than the MEDDH receiver. Comparing Fig. 2.8 with Fig. 2.7, the receivers using DCE performs approximately 1.2 dB better than the corresponding receivers using CCE.

Fig. 2.9 and Fig. 2.10 show the second case, where the destination links have high power i.e. $E_{SD} = E_{RD} = 50$ dB or $E_{SD} = 35$ dB. The receivers with CCE and with DCE perform better than the corresponding receivers in balanced links in Fig. 2.5 and Fig. 2.6, respectively, as the destination links are very good. In the case when $E_{SD} = 35$ dB, at low E_{SR}/N_0, the performance of the receivers is much better compared to the case when $E_{SD} = E_{RD} = 50$ because the noise at the destination due

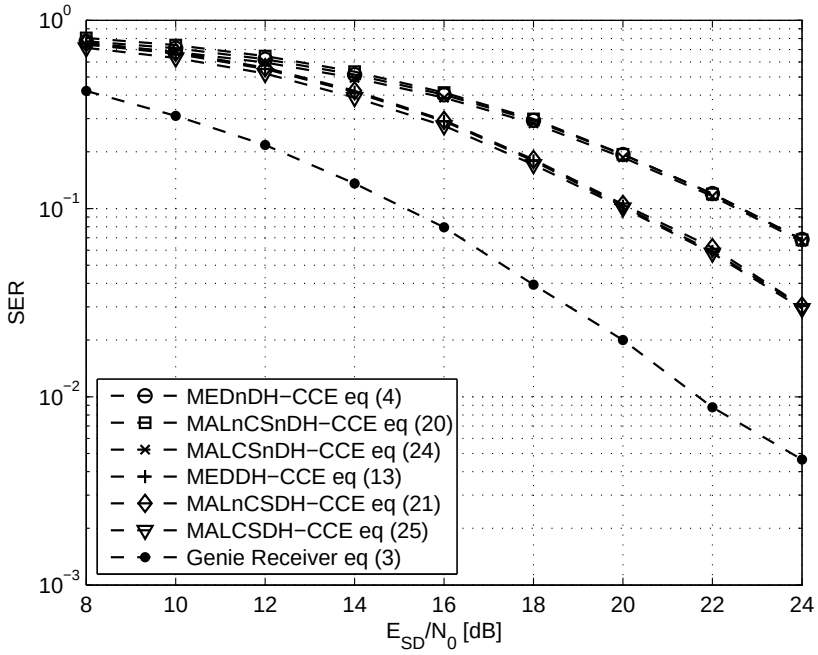

Figure 2.5: SER performance comparison of different new receivers using CCE in balanced links.

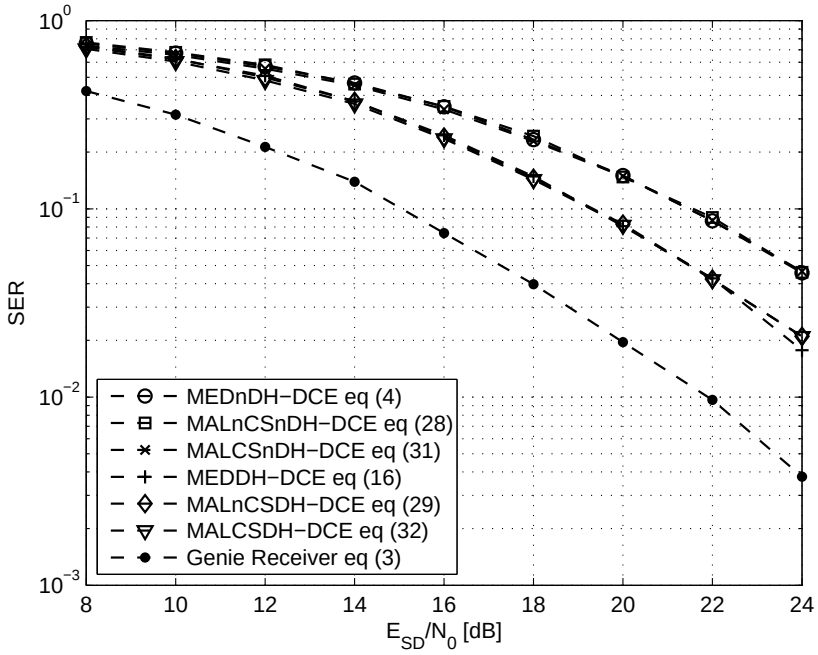

Figure 2.6: SER performance comparison of different new receivers using DCE in balanced links.

to the relay is lower. However, at high E_{SR}/N_0, the performance of the receivers with $E_{SD} = E_{RD} = 50$ is better. Note that, for low values of $E_{SR} = E_{RD}$ and $E_{SD} = 35$ dB, the system can be considered as a system without a relay. As $E_{SR} = E_{RD}$ is increased the relay link helps improve the performance of the system as can be observed in Fig. 2.9 and Fig. 2.10. In Fig. 2.9, for the receivers using CCE when $E_{SD} = E_{RD} = 50$, it can be observed that the MEDDH receiver with weights according to (2.9) performs better than the MEDDH receiver given by (2.13). This happens because if the destination links re very good, then the noise component from the relay received at the destination is also increased. Thus, the effective noise is increased and the effect of decision history on the metric is reduced and that the MEDDH receiver becomes the same as the MEDnDH receiver (i.e. without decision history). For the case when $E_{SD} = 35$, as the relay noise component at the destination is not increased so the MEDDH receiver given by (2.13) gives better performance. Thus, finding optimal weights is an important factor in obtaining good performance gains. In the case of receivers using DCE, when $E_{SD} = E_{RD} = 50$ dB,the performances of the MEDnDH, MALnCSnDH, MALCSnDH, MEDDH, MALnCSDH and MALCSDH receivers are graphically identical, as shown in Fig. 2.10. The estimates of the source-destination and the relay-destination channel are very good in all the receivers and the performance in this case is limited by the accuracy of the estimate of the source-relay destination channel and thus, the effect of improper weights cannot be observed in this case. Due to similar reasoning as before, when $E_{SD} = 35$ dB, at low E_{SR}/N_0 the performance of the receivers is better compared to the receivers with $E_{SD} = E_{RD} = 50$.

Fig. 2.11 and Fig. 2.12 show the effect of finite quantization of the source-relay channel estimate on the receiver performances in balanced links. The max-Lloyd quantizer is used for quantizing the estimates at the relay. Comparing Fig. 2.11

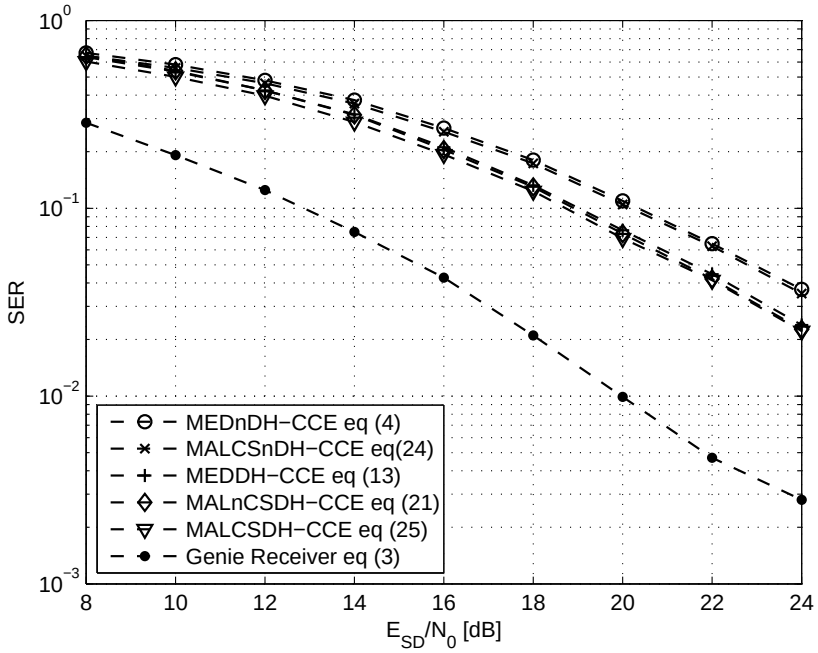

Figure 2.7: SER performance comparison of the different new receivers using CCE in unbalanced links when the source-relay channel power is 50dB.

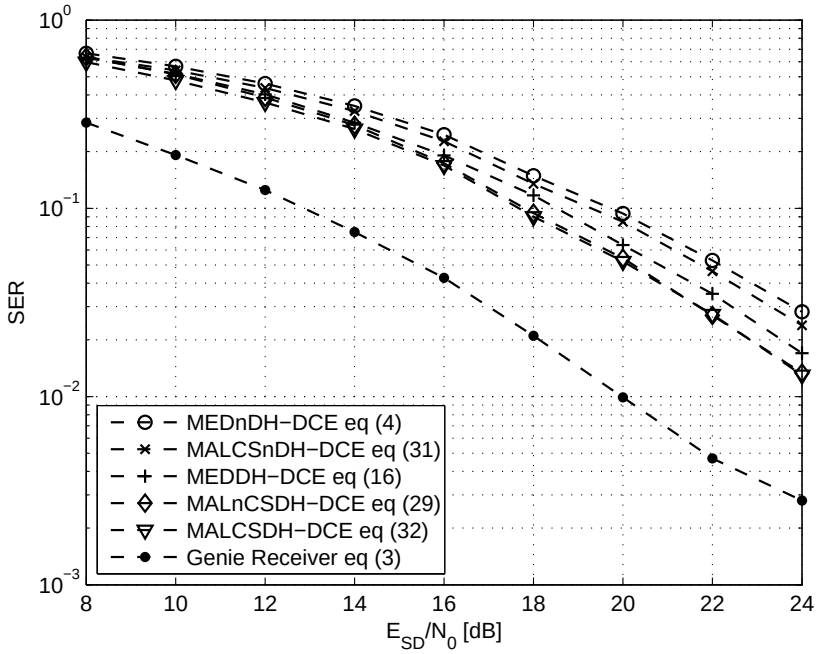

Figure 2.8: SER performance comparison of the different new receivers using DCE in unbalanced links when the source-relay channel power is 50dB.

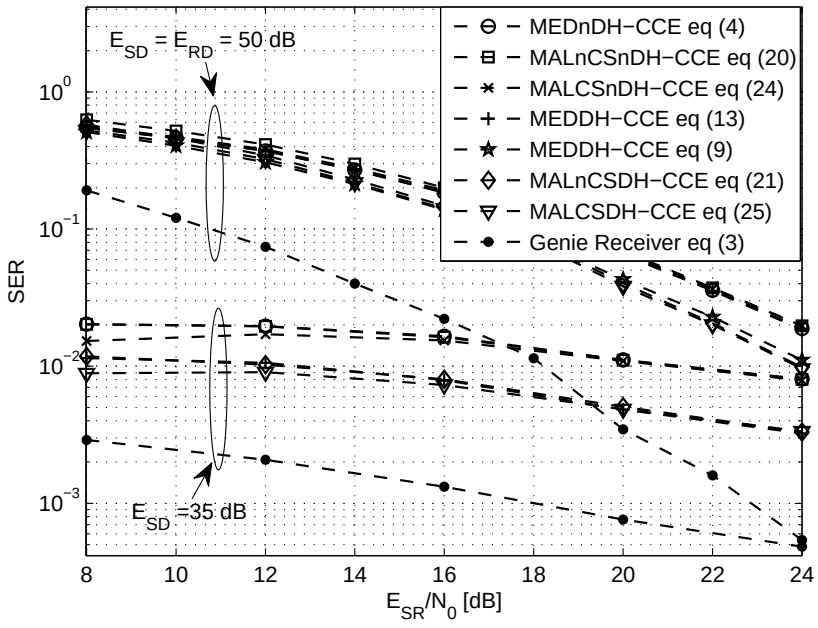

Figure 2.9: SER performance comparison of different new receivers for CCE in unbalanced links with different destination channel powers.

with previous figures using infinite number of bits, one sees that, as the number of quantization bits is decreased, the performances of the receivers is degraded. At high $\frac{E_{SD}}{N_o}$, there is an error floor. A number of quantization bits equal to 4 is enough to achieve nearly the same performance as the performance with infinite bit quantization, as can be observed in Fig. 2.12, which agrees with the result in [44].

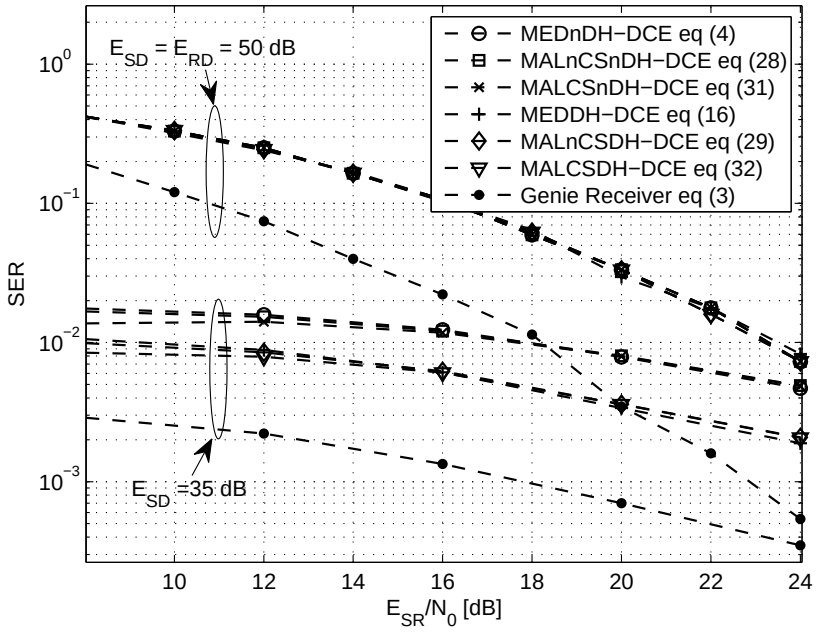

Figure 2.10: SER performance comparison of different new receivers for DCE in unbalanced links with different destination channel powers.

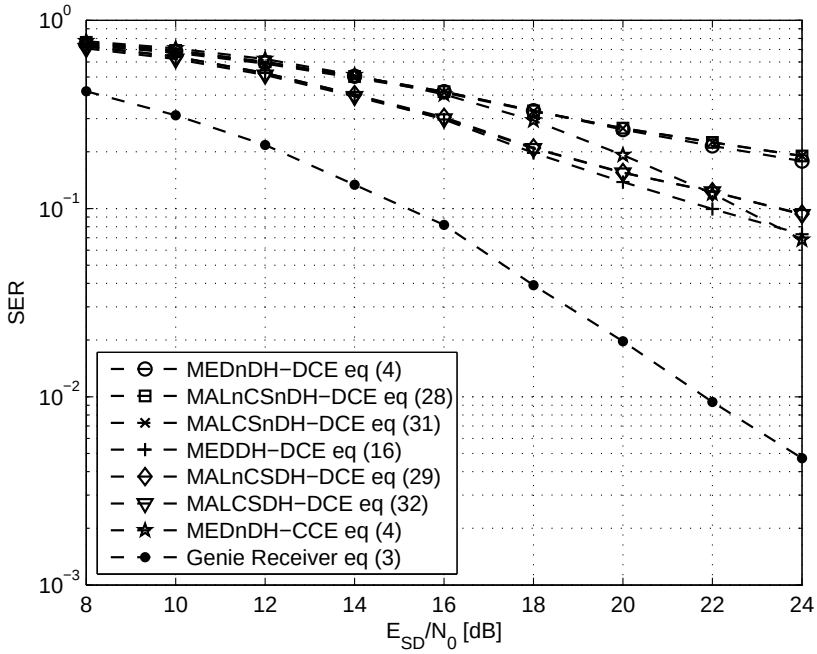

Figure 2.11: SER performance comparison of different new receivers using DCE with 2-bit quantized source-relay channel estimate forwarded from the relay to destination.

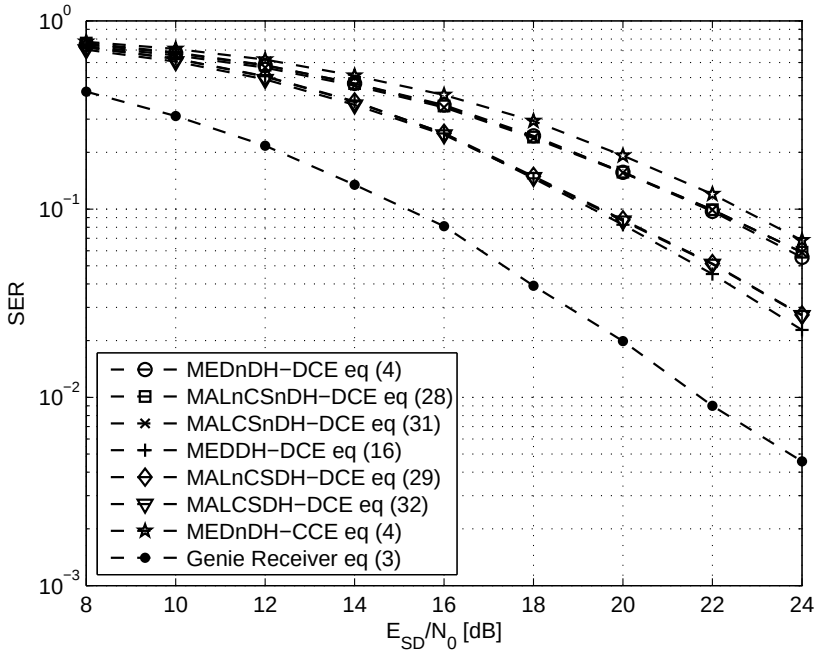

Figure 2.12: SER performance comparison of different new receivers using DCE with 4-bit quantized source-relay channel estimate forwarded from the relay to destination.

Chapter 3

Novel Non-Coherent and Half-Coherent Receivers for AF Relaying

In the previous chapter, fully coherent receivers were derived for AF relaying that processed the received data using some information of the cascaded source-relay-destination channel which was extracted using the pilots. In this chapter, alternate receivers for AF relaying are derived that either utilize only partial CSI knowledge or do not require any knowledge of CSI. Specifically, considering a Rician faded channel, an optimal non-coherent receiver for AF relaying is derived. Furthermore, a sub-optimal non-coherent receiver with lower complexity but similar performance to that of the optimal non-coherent receiver is also proposed. In addition, receivers for the case when the destination possesses CSI of either the source-relay channel or the relay-destination channel are also derived. The former case corresponds to the scenario when the relay is fixed, and has the ability/complexity to estimate and forwards the source-relay channel information to the destination. Where as, the destination has low complexity and does not have the channel estimation module and thus, is

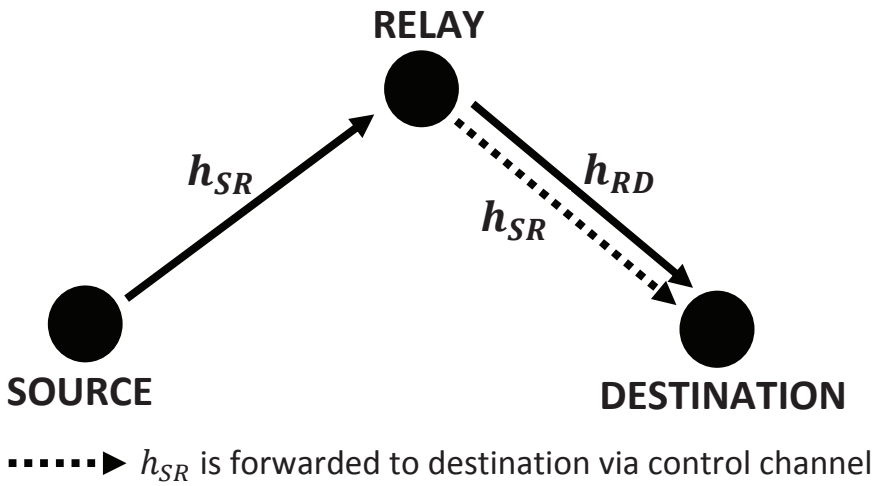

Figure 3.1: System Model.

unable to estimate the relay-destination link. The later case corresponds to the reversed scenario where the destination has the ability/complexity to estimate the relay-destination link only and the relay is without the channel estimation module. In this case, the destination estimates the relay destination channel using the pilot signal transmitted by the relay. These receivers are termed as 'half-coherent receivers' as they have CSI of only one of the two links. In this chapter, the analytical expressions for the symbol-error-rate (SER) performances of the proposed receivers as well as the energy detector receiver are also derived considering M-ary frequency-shift-keying. The performances of the proposed receivers are depicted using numerical simulations.

3.1 System Model

Consider a system as shown in Fig. 3.1 where data is transmitted from the source to the destination via a single relay. All the nodes are assumed to have single antenna. During time slot one, the source transmits to the relay and during time slot two, the relay transmits to the destination. The signal at the relay is normalized by a fixed

gain and then forwarded to the destination.

The source-relay and relay-destination channels are denoted by h_{SR} and h_{RD}, respectively. The channels are assumed to be independent and experience flat Rician fading. Thus, h_{SR} is assumed to be $\mathcal{CN}(\mu_{SR}, \sigma^2_{SR})$ and h_{RD} is assumed to be $\mathcal{CN}(\mu_{RD}, \sigma^2_{RD})$, where $\mathcal{CN}(a, b)$ denotes a complex Gaussian random variable with mean a and variance b. The modulation scheme is M-ary frequency-shift-keying (M-FSK). The transmitted signal is chosen from alphabet $\chi \in \{\exp(j2\pi f_1 t), \exp(j2\pi f_2 t) \ldots \exp(j2\pi f_M t)\}$, where $j = \sqrt{-1}$, t denotes time and $f_1, f_2 \ldots f_M$ are M orthogonal frequencies.

Given that frequency f_i is transmitted, after matched-filtering, the decision statistics can be expressed as

$$\begin{aligned} \mathbf{y}_i &= \sqrt{\frac{E_{SR}E_{RD}}{\bar{E}_{SR}+N_0}}h_{SR}h_{RD} + \sqrt{\frac{E_{RD}}{\bar{E}_{SR}+N_0}}h_{RD}\mathbf{n}_{R,i} + \mathbf{n}_{D,i}, \\ \mathbf{y}_k &= \sqrt{\frac{E_{RD}}{\bar{E}_{SR}+N_0}}h_{RD}\mathbf{n}_{R,k} + \mathbf{n}_{D,k}, \quad \forall k \in \{1, 2 \ldots M\} \;\; \& \;\; k \neq i, \end{aligned} \tag{3.1}$$

where $\sqrt{\frac{1}{\bar{E}_{SR}+N_0}}$ is the fixed normalizing gain at the relay, E_{SR} and E_{RD} are the desired signal powers' at the relay and destination, respectively and $\bar{E}_{SR} = E_{SR}\sigma^2_{SR}$. In (3.1), $\mathbf{n}_{R,i}$ and $\mathbf{n}_{D,i}$ denote the complex additive white Gaussian noise at the receiver and the destination for the ith frequency, respectively and are assumed to be $\mathcal{CN}(0, N_0)$, $\mathbf{y}_i$ and $\mathbf{y}_k$ denote the outputs of the matched-filter matched to frequency f_i and f_k, respectively.

3.2 Novel Non-Coherent Receivers

The optimal non-coherent receiver can be derived by using the maximum likelihood principle. As the transmitted symbols are equiprobable, the log-likelihood ratio in

the case of binary frequency-shift-keying (BFSK) for $M = 2$ can be expressed as

$$\log\left(\frac{f_{\mathbf{y}_1,\mathbf{y}_2|f_1}(y_1,y_2)}{f_{\mathbf{y}_1,\mathbf{y}_2|f_2}(y_1,y_2)}\right) \gtrless_{f_2}^{f_1} 0. \tag{3.2}$$

From (3.1) it can be observed that $\mathbf{y}_1$ and $\mathbf{y}_2$ are not independent. However, conditioned on h_{RD}, $\mathbf{y}_1$ and $\mathbf{y}_2$ are independent and the likelihood ratio can be expressed as

$$\Gamma_{NC} = \log\left(\frac{\int f_{\mathbf{y}_1|h_{RD},f_1}(y_1)\cdot f_{\mathbf{y}_2|h_{RD},f_1}(y_2) f_{h_{RD}}(h_{RD})\mathsf{d}h_{RD}}{\int f_{\mathbf{y}_1|h_{RD},f_2}(y_1)\cdot f_{\mathbf{y}_2|h_{RD},f_2}(y_2) f_{h_{RD}}(h_{RD})\mathsf{d}h_{RD}}\right) = \log\left(\frac{I_N}{I_D}\right) \gtrless_{f_2}^{f_1} 0, \tag{3.3}$$

where $f_{h_{RD}}(h_{RD}) = \exp\left(-|h_{RD}-\mu_{RD}|^2/\sigma_{RD}^2\right)/\pi\sigma_{RD}^2$ is the PDF of the complex relay-destination channel, $f_{\mathbf{y}_i|h_{RD},f_k}$ is $\mathcal{CN}\left(0, \frac{E_{RD}}{\bar{E}_{SR}+N_0}N_0|h_{RD}|^2+N_0\right)$ and $f_{\mathbf{y}_i|h_{RD},f_i}$ is $\mathcal{CN}\left(\sqrt{\frac{E_{SR}E_{RD}}{\bar{E}_{SR}+N_0}}\mu_{SR}h_{RD}, \frac{E_{SR}E_{RD}}{\bar{E}_{SR}+N_0}\sigma_{SR}^2|h_{RD}|^2+\frac{E_{RD}}{\bar{E}_{SR}+N_0}N_0|h_{RD}|^2+N_0\right)$, respectively, for $i,k\in\{1,\dots M\}$ & $i\neq k$. After substituting the values, the numerator in the argument of log function in (3.3) can be expressed as

$$\begin{aligned} I_N = \int f_{\mathbf{y}_1|h_{RD},f_1}(y_1)\cdot f_{\mathbf{y}_2|h_{RD},f_1}(y_2) f_{h_{RD}}(h_{RD})\mathsf{d}h_{RD} = \\ \int \frac{\exp\left(-\frac{|y_1-\sqrt{\frac{E_{SR}E_{RD}}{\bar{E}_{SR}+N_0}}\mu_{SR}h_{RD}|^2}{\left(\frac{E_{SR}E_{RD}}{\bar{E}_{SR}+N_0}\sigma_{SR}^2|h_{RD}|^2+\frac{E_{RD}}{\bar{E}_{SR}+N_0}N_0|h_{RD}|^2+N_0\right)}\right)}{\pi\left(\frac{E_{SR}E_{RD}}{\bar{E}_{SR}+N_0}\sigma_{SR}^2|h_{RD}|^2+\frac{E_{RD}}{\bar{E}_{SR}+N_0}N_0|h_{RD}|^2+N_0\right)} \\ \times \frac{\exp\left(-\frac{|y_2|^2}{\left(\frac{E_{RD}}{\bar{E}_{SR}+N_0}N_0|h_{RD}|^2+N_0\right)}\right)}{\pi\left(\frac{E_{RD}}{\bar{E}_{SR}+N_0}N_0|h_{RD}|^2+N_0\right)}\frac{\exp\left(-\frac{|h_{RD}-\mu_{RD}|^2}{\sigma_{RD}^2}\right)}{\pi\sigma_{RD}^2}\mathsf{d}h_{RD} \end{aligned} \tag{3.4}$$

Applying polar transformation I_N is given as

$$I_N = \int_0^{\infty} \frac{x \exp\left(-\frac{|y_1|^2 + \frac{E_{SR}E_{RD}}{E_{SR}+N_0}|\mu_{SR}|^2x^2}{\left(\left(\frac{E_{SR}E_{RD}}{E_{SR}+N_0}\sigma_{SR}^2 + \frac{E_{RD}}{E_{SR}+N_0}N_0\right)x^2+N_0\right)}\right)}{\pi\left(\left(\frac{E_{SR}E_{RD}}{E_{SR}+N_0}\sigma_{SR}^2 + \frac{E_{RD}}{E_{SR}+N_0}N_0\right)x^2 + N_0\right)} \frac{\exp\left(-\frac{|y_2|^2}{\left(\frac{E_{RD}}{E_{SR}+N_0}N_0x^2+N_0\right)}\right)}{\pi\left(\frac{E_{RD}}{E_{SR}+N_0}N_0x^2 + N_0\right)} \frac{\exp\left(-\frac{x^2+|\mu_{RD}|^2}{\sigma_{RD}^2}\right)}{\pi\sigma_{RD}^2} \times$$
$$\int_0^{2\pi} \exp\left(\frac{2\sqrt{\frac{E_{SR}E_{RD}}{E_{SR}+N_0}}x\mathcal{R}\{y_1^H\mu_{SR}e^{j\theta_{RD}}\}}{\left(\left(\frac{E_{SR}E_{RD}}{E_{SR}+N_0}\sigma_{SR}^2 + \frac{E_{RD}}{E_{SR}+N_0}N_0\right)x^2 + N_0\right)}\right) \exp\left(\frac{2x\mathcal{R}\{e^{-j\theta_{RD}}\mu_{RD}\}}{\sigma_{RD}^2}\right) \mathrm{d}\theta_{RD}\mathrm{d}x \tag{3.5}$$

where θ_{RD} is the phase of h_{RD}. After integrating w.r.t θ_{RD}, I_N is expressed as

$$I_N = \frac{2\exp\left(-\frac{|\mu_{RD}|^2}{\sigma_{RD}^2}\right)}{\sigma_{RD}^2} \int_0^{\infty} \frac{x\exp\left(-\frac{\frac{E_{SR}E_{RD}}{E_{SR}+N_0}|\mu_{SR}|^2x^2}{(c_1+c_2)x^2+c_3)} - \frac{x^2}{\sigma_{RD}^2}\right)}{\pi\left(\left(c_1+c_2\right)x^2+c_3\right)} \frac{\exp\left(-\frac{|y_1|^2}{((c_1+c_2)x^2+c_3)} - \frac{|y_2|^2}{(c_2x^2+c_3)}\right)}{\pi\left(c_2x^2+c_3\right)} \times$$
$$I_0\left(2x\sqrt{\left(\frac{\sqrt{\frac{E_{SR}E_{RD}}{E_{SR}+N_0}}\mathcal{R}\{y_1^H\mu_{SR}\}}{\left(\left(c_1+c_2\right)x^2+c_3\right)} + \frac{\mathcal{R}\{\mu_{RD}\}}{\sigma_{RD}^2}\right)^2 + \left(\frac{\sqrt{\frac{E_{SR}E_{RD}}{E_{SR}+N_0}}\mathcal{I}\{y_1^H\mu_{SR}\}}{\left(\left(c_1+c_2\right)x^2+c_3\right)} - \frac{\mathcal{I}\{\mu_{RD}\}}{\sigma_{RD}^2}\right)^2}\right) \mathrm{d}x \tag{3.6}$$

where $c_1 = \frac{E_{SR}E_{RD}}{E_{SR}+N_0}\sigma_{SR}^2$, $c_2 = \frac{E_{RD}}{E_{SR}+N_0}N_0$ and $c_3 = N_0$. Similarly, the expression for the denominator in the argument of log function in (3.3) can be obtained by interchanging y_1 and y_2 in (3.6) as

$$I_D = \frac{2\exp\left(-\frac{|\mu_{RD}|^2}{\sigma_{RD}^2}\right)}{\sigma_{RD}^2} \int_0^{\infty} \frac{x\exp\left(-\frac{\frac{E_{SR}E_{RD}}{E_{SR}+N_0}|\mu_{SR}|^2x^2}{((c_1+c_2)x^2+c_3)} - \frac{x^2}{\sigma_{RD}^2}\right)}{\pi\left(\left(c_1+c_2\right)x^2+c_3\right)} \frac{\exp\left(-\frac{|y_2|^2}{((c_1+c_2)x^2+c_3)} - \frac{|y_1|^2}{(c_2x^2+c_3)}\right)}{\pi\left(c_2x^2+c_3\right)} \times$$
$$I_0\left(2x\sqrt{\left(\frac{\sqrt{\frac{E_{SR}E_{RD}}{E_{SR}+N_0}}\mathcal{R}\{y_2^H\mu_{SR}\}}{\left(\left(c_1+c_2\right)x^2+c_3\right)} + \frac{\mathcal{R}\{\mu_{RD}\}}{\sigma_{RD}^2}\right)^2 + \left(\frac{\sqrt{\frac{E_{SR}E_{RD}}{E_{SR}+N_0}}\mathcal{I}\{y_2^H\mu_{SR}\}}{\left(\left(c_1+c_2\right)x^2+c_3\right)} - \frac{\mathcal{I}\{\mu_{RD}\}}{\sigma_{RD}^2}\right)^2}\right) \mathrm{d}x \tag{3.7}$$

Substituting the expressions of I_N and I_D in (3.3), the optimal non-coherent detector for BFSK is obtained. In the case of M-FSK, the detected frequency is

$$\hat{f}_{\Xi,NC} \,:\, \Xi = \arg\max_{l} \left\{ \log \left(\int_0^{\infty} \frac{x \exp\left(-\frac{\frac{E_{SR}E_{RD}}{E_{SR}+N_0}|\mu_{SR}|^2 x^2}{((c_1+c_2)x^2+c_3)} - \frac{x^2}{\sigma_{RD}^2} \right)}{\pi\left((c_1+c_2)\,x^2+c_3\right)} \exp\left(-\frac{|y_l|^2}{((c_1+c_2)\,x^2+c_3)} \right) \prod_{\substack{k=1 \\ k\neq l}}^{M} \frac{\exp\left(-\frac{|y_k|^2}{(c_2x^2+c_3)} \right)}{\pi\left(c_2x^2+c_3\right)} \right.$$
$$\left. \times I_0\left(2x \sqrt{ \left(\frac{\sqrt{\frac{E_{SR}E_{RD}}{E_{SR}+N_0}}\mathcal{R}\{y_l^H \mu_{SR}\}}{((c_1+c_2)\,x^2+c_3)} + \frac{\mathcal{R}\{\mu_{RD}\}}{\sigma_{RD}^2} \right)^2 + \left(\frac{\sqrt{\frac{E_{SR}E_{RD}}{E_{SR}+N_0}}\mathcal{I}\{y_l^H \mu_{SR}\}}{((c_1+c_2)\,x^2+c_3)} - \frac{\mathcal{I}\{\mu_{RD}\}}{\sigma_{RD}^2} \right)^2 } \right) \mathrm{d}x \right) \right\}. \tag{3.8}$$

No closed-form solution is available for the integrals in (3.6), (3.7) and (3.8). However, the optimum noncoherent detectors in (3.3) and (3.8) can provide a very useful benchmark on the detection performance.

In order to reduce the complexity at the receiver, the integrals in (3.6), (3.7) and (3.8) can be approximated using the Gauss-Laguerre formula [92]. The integrals in (3.6) and (3.7) can be approximated as

$$I_q \approx \sum_{i_0=1}^{N_1} w_\gamma(x_{i_0}) \exp(x_{i_0}) \frac{x_{i_0} \exp\left(-\frac{\frac{E_{SR}E_{RD}}{E_{SR}+N_0}|\mu_{SR}|^2 x_{i_0}^2}{\left((c_1+c_2)x_{i_0}^2+c_3\right)} - \frac{x_{i_0}^2}{\sigma_{RD}^2} \right)}{\pi\left((c_1+c_2)\,x_{i_0}^2+c_3\right)} \frac{\exp\left(-\frac{|y_i|^2}{\left((c_1+c_2)x_{i_0}^2+c_3\right)} - \frac{|y_k|^2}{\left(c_2x_{i_0}^2+c_3\right)} \right)}{\pi\left(c_2x_{i_0}^2+c_3\right)} \times$$
$$I_0\left(2x_{i_0} \sqrt{ \left(\frac{\sqrt{\frac{E_{SR}E_{RD}}{E_{SR}+N_0}}\mathcal{R}\{y_i^H \mu_{SR}\}}{\left((c_1+c_2)\,x_{i_0}^2+c_3\right)} + \frac{\mathcal{R}\{\mu_{RD}\}}{\sigma_{RD}^2} \right)^2 + \left(\frac{\sqrt{\frac{E_{SR}E_{RD}}{E_{SR}+N_0}}\mathcal{I}\{y_i^H \mu_{SR}\}}{\left((c_1+c_2)\,x_{i_0}^2+c_3\right)} - \frac{\mathcal{I}\{\mu_{RD}\}}{\sigma_{RD}^2} \right)^2 } \right), \tag{3.9}$$

where, $q \in \{N, D\}$, if $q = N$ then $(i,k) = (1,2)$, if $q = D$ then $(i,k) = (2,1)$, $w_\gamma(x_k) = \frac{x_k}{(N_2+1)^2 L_{N_2+1}(x_k^2)}$, x_k is the kth zero of the Laguerre polynomial $L_n(x)$ [92] and N_1 is the number of points chosen for the Gauss-Laguerre rule. Substituting this approximate expression in (3.3), a sub-optimal non-coherent receiver for BFSK

is obtained. Similarly, in the case of M-FSK the detected frequency is

$$\hat{f}_{\Xi,S-NC} \; : \; \Xi = \arg\max_{l} \left\{ \log \left(\sum_{i_0=1}^{N_1} \frac{x_{i_0} \exp\left(- \frac{\frac{E_{SR}E_{RD}}{E_{SR}+N_0}|\mu_{SR}|^2 x_{i_0}^2}{\left((c_1+c_2)x_{i_0}^2+c_3\right)} - \frac{x_{i_0}^2}{\sigma_{RD}^2} - \frac{|y_l|^2}{\left((c_1+c_2)x_{i_0}^2+c_3\right)} \right)}{(w_\gamma(x_{i_0}))^{-1} \exp(-x_{i_0})\pi \left((c_1+c_2)\, x_{i_0}^2 + c_3\right)} \prod_{\substack{k=1 \\ k\neq l}}^{M} \frac{\exp\left(- \frac{|y_k|^2}{\left(c_2 x_{i_0}^2+c_3\right)} \right)}{\pi \left(c_2 x_{i_0}^2 + c_3\right)} \right.$$
$$\left. \times I_0 \left(2x_{i_0} \sqrt{ \left(\frac{\sqrt{\frac{E_{SR}E_{RD}}{E_{SR}+N_0}} \mathcal{R}\{y_l^H \mu_{SR}\}}{\left((c_1+c_2)\, x_{i_0}^2 + c_3\right)} + \frac{\mathcal{R}\{\mu_{RD}\}}{\sigma_{RD}^2} \right)^2 + \left(\frac{\sqrt{\frac{E_{SR}E_{RD}}{E_{SR}+N_0}} \mathcal{I}\{y_l^H \mu_{SR}\}}{\left((c_1+c_2)\, x_{i_0}^2 + c_3\right)} - \frac{\mathcal{I}\{\mu_{RD}\}}{\sigma_{RD}^2} \right)^2 } \right) \right) \right\}. \tag{3.10}$$

In general, the Gauss-Laguerre quadrature method is a numerical approach to solve the integrals and its accuracy depends on the number of terms used. However, in our case, only one or two terms are required to give significant performance gain, as will be shown in the numerical results section (see Fig. 3.2). This one/two point approximation significantly reduces the complexity at the receiver and thus, this suboptimal detector in (3.10) is useful for the applications considered in this chapter.

3.3 Novel Half-Coherent Receivers

In this section, the new receivers are derived for both cases, i.e. at the receiver either 1) CSI of only the source-relay link is available or 2) CSI of only the relay-destination link is available. For the first case, it is assumed that the transmitter sends pilots to the relay based on which the relay estimates the source-relay channel. The CSI estimate is quantized and forwarded to the destination via a control channel [43, 44, 93]. In this case, the quantization errors are ignored and it is assumed that the receiver receives the channel estimate perfectly. For the second case, it is assumed that the relay sends a pilot signal to the destination, based on which the relay-destination channel is estimated at the destination [43, 44, 93].

3.3.1 Only CSI of the Source-Relay Link is Available

The optimal receiver which has perfect source-relay CSI can be derived by using the maximum likelihood principle. As the transmitted symbols are equiprobable, the log-likelihood ratio in the case of binary frequency-shift-keying (BFSK) for $M = 2$ can be expressed as

$$\log\left(\frac{f_{\mathbf{y}_1,\mathbf{y}_2|h_{SR},f_1}(y_1,y_2)}{f_{\mathbf{y}_1,\mathbf{y}_2|h_{SR},f_2}(y_1,y_2)}\right) \gtrless_{f_2}^{f_1} 0. \tag{3.11}$$

Using (3.1), for this case, the log-likelihood ratio can be further derived as

$$\Gamma_{SR} = \log\left(\frac{\int f_{\mathbf{y}_1|h_{SR},h_{RD},f_1}(y_1)\cdot f_{\mathbf{y}_2|h_{SR},h_{RD},f_1}(y_2) f_{h_{RD}}(h_{RD})\mathsf{d}h_{RD}}{\int f_{\mathbf{y}_1|h_{SR},h_{RD},f_2}(y_1)\cdot f_{\mathbf{y}_2|h_{SR},h_{RD},f_2}(y_2) f_{h_{RD}}(h_{RD})\mathsf{d}h_{RD}}\right) \gtrless_{f_2}^{f_1} 0. \tag{3.12}$$

Thus, $f_{\mathbf{y}_i|h_{SR},h_{RD},f_i}(y_i)$ and $f_{\mathbf{y}_i|h_{SR},h_{RD},f_k}(y_i)$ are $\mathcal{CN}(\sqrt{\frac{E_{SR}E_{RD}}{E_{SR}+N_0}}h_{SR}h_{RD}, \frac{E_{RD}N_0}{E_{SR}+N_0}|h_{RD}|^2 + N_0)$ and $\mathcal{CN}(0, \frac{E_{RD}}{E_{SR}+N_0}|h_{RD}|^2 N_0 + N_0)$, respectively, for $i,k \in \{1,\dots M\}$ & $i \neq k$. Compared with (3.2) one sees that the likelihood functions in (3.11) and (3.12) have knowledge of h_{SR} while (3.2) does not.

In the case of M-FSK, the detected frequency is

$$\hat{f}_{\Xi,SR} \;:\; \Xi = \arg\max_{l}\left\{\log\left(\int f_{\mathbf{y}_l|h_{SR},h_{RD},f_1}(y_l)\cdot\prod_{\substack{k=1\\k\neq l}}^{M} f_{\mathbf{y}_k|h_{SR},h_{RD},f_1}(y_k) f_{h_{RD}}(h_{RD})\mathsf{d}h_{RD}\right)\right\}. \tag{3.13}$$

In order to derive an approximate sub-optimal detector in closed-form, assume that the collective noise at the receiver is complex Gaussian as in [33, 42, 87, 88]. It will be later shown that this approximation is good and gives us gains, although one does expect to lose some performance due to approximation error. Given that

frequency f_1 is transmitted, the decision statistics can be expressed as

$$\mathbf{y}_i = \sqrt{\frac{E_{SR}E_{RD}}{\bar{E}_{SR}+N_0}}h_{SR}h_{RD} + \eta_i,, \tag{3.14}$$
$$\mathbf{y}_k = \eta_k, \quad \forall k \in \{1, 2 \dots M\} \;\; \& \;\; k \neq i,$$

where $\eta_i = \sqrt{\frac{E_{RD}}{\bar{E}_{SR}+N_0}}h_{RD}\mathbf{n}_{R,i} + \mathbf{n}_{D,i}$ denotes the collective noise at the destination for ith frequency. The collective noise is assumed to be $\mathcal{CN}(0, \frac{E_{RD}}{\bar{E}_{SR}+N_0}\left(\sigma_{RD}^2 + \mu_{RD}^2\right)N_0 + N_0)$.

In the case of BFSK, from (3.14), $\mathbf{y}_1$ and $\mathbf{y}_2$ are $\mathcal{CN}(\hat{\mu}_{RD}h_{SR},\, \hat{\sigma}_{RD}^2|h_{SR}|^2 + \sigma_\eta^2)$ and $\mathcal{CN}(0, \sigma_\eta^2)$, respectively, where $\hat{\mu}_{RD} = \sqrt{\frac{E_{SR}E_{RD}}{\bar{E}_{SR}+N_0}}\mu_{RD}$, $\hat{\sigma}_{RD}^2 = \frac{E_{SR}E_{RD}}{\bar{E}_{SR}+N_0}\sigma_{RD}^2$ and $\sigma_\eta^2 = \frac{E_{RD}}{\bar{E}_{SR}+N_0}\left(\sigma_{RD}^2 + \mu_{RD}^2\right)N_0 + N_0$. Substituting the values in (3.11) and simplifying the result, the log-likelihood ratio becomes

$$\log\left(\frac{\exp\left(-\frac{|y_1-\hat{\mu}_{RD}h_{SR}|^2}{\hat{\sigma}_{RD}^2|h_{SR}|^2+\sigma_\eta^2} + \frac{|y_1|^2}{\sigma_\eta^2}\right)}{\exp\left(-\frac{|y_2-\hat{\mu}_{RD}h_{SR}|^2}{\hat{\sigma}_{RD}^2|h_{SR}|^2+\sigma_\eta^2} + \frac{|y_2|^2}{\sigma_\eta^2}\right)}\right) \gtrless_{f_2}^{f_1} 0.$$

After some algebraic manipulation, one has

$$|y_1|^2 + \frac{2\Re\{y_1^{\mathsf{H}}\hat{\mu}_{RD}h_{SR}\}}{\hat{\sigma}_{RD}^2|h_{SR}|^2}\sigma_\eta^2 \gtrless_{f_2}^{f_1} |y_2|^2 + \frac{2\Re\{y_2^{\mathsf{H}}\hat{\mu}_{RD}h_{SR}\}}{\hat{\sigma}_{RD}^2|h_{SR}|^2}\sigma_\eta^2. \tag{3.15}$$

By adding $|\hat{\mu}_{RD}h_{SR}|^2\frac{\sigma_\eta^4}{\hat{\sigma}_{RD}^4|h_{SR}|^4}$ on both sides, the log-likelihood ratio can be expressed as

$$\Gamma_{SR,G} = \frac{\left|y_1 + \hat{\mu}_{RD}h_{SR}\frac{\sigma_\eta^2}{\hat{\sigma}_{RD}^2|h_{SR}|^2}\right|^2}{\left|y_2 + \hat{\mu}_{RD}h_{SR}\frac{\sigma_\eta^2}{\hat{\sigma}_{RD}^2|h_{SR}|^2}\right|^2} \gtrless_{f_2}^{f_1} 1. \tag{3.16}$$

In the case of M-FSK, the detected frequency is

$$\hat{f}_{\Xi,SR,G} \;:\; \Xi = \arg\max_l \left\{\left|y_l + \hat{\mu}_{RD}h_{SR}\frac{\sigma_\eta^2}{\hat{\sigma}_{RD}^2|h_{SR}|^2}\right|^2\right\}. \tag{3.17}$$

Substituting values in (3.17), one has

$$\hat{f}_{\Xi,SR,G} \ : \ \Xi = \arg\max_{l} \left\{ \left| y_l + \mu_{RD} h_{SR} \frac{\frac{E_{RD}}{\bar{E}_{SR}+N_0} \left(\sigma_{RD}^2 + \mu_{RD}^2\right) N_0 + N_0}{\sqrt{\frac{E_{SR}E_{RD}}{\bar{E}_{SR}+N_0}} \sigma_{RD}^2 |h_{SR}|^2} \right|^2 \right\}.$$

For balanced links with $E_{RD} = E_{SR}$ and high values of E_{RD}, the detected frequency can be approximated as

$$\hat{f}_{\Xi,SR,G,HighSNR} \ : \ \Xi = \arg\max_{l} \left\{ \left| y_l + \frac{1}{\sqrt{E_{RD}}} \frac{\mu_{RD} h_{SR} ((\sigma_{RD}^2 + \mu_{RD}^2) N_0 + N_0)}{\sigma_{RD}^2 |h_{SR}|^2} \right|^2 \right\}. \tag{3.18}$$

Thus, from (3.18) it can be observed that, at high E_{RD} with balanced links, the term $\Delta = \frac{1}{\sqrt{E_{RD}}} \frac{\mu_{RD} h_{SR} \left(\left(\sigma_{RD}^2 + \mu_{RD}^2\right) N_0 + N_0 \right)}{\sigma_{RD}^2 |h_{SR}|^2}$ goes to zero and the detector becomes the same as the energy detector. Otherwise, the new detector is different due to the bias term Δ and as will be shown later, performs better than the conventional non-coherent energy detector.

In the above derivation, it has been assumed that the receiver has perfect source-relay CSI. In reality, the receiver only has an estimate of the source-relay channel. Mismatched receivers can be obtianed by replacing h_{SR} with its estimate $\bar{h}_{SR}$ in (3.13) and (3.17) [29, 35].

3.3.2 Only CSI of the Relay-Destination Link is Available

In this case, the log-likelihood ratio for BFSK is expressed as

$$\log \left(\frac{f_{\mathbf{y}_1|h_{RD},f_1}(y_1) \cdot f_{\mathbf{y}_2|h_{RD},f_1}(y_2)}{f_{\mathbf{y}_1|h_{RD},f_2}(y_1) \cdot f_{\mathbf{y}_2|h_{RD},f_2}(y_2)} \right) \gtrless_{f_2}^{f_1} 0. \tag{3.19}$$

From (3.1), given that frequency f_1 is transmitted, conditioned on the relay-destination channel $\mathbf{y}_1$ and $\mathbf{y}_2$ are $\mathcal{CN}(\hat{\mu}_{SR} h_{RD}, \hat{\sigma}_{SR}^2 |h_{RD}|^2 + \sigma_{\eta RD}^2)$ and $\mathcal{CN}(0, \sigma_{\eta RD}^2)$, respectively, where $\hat{\mu}_{SR} = \sqrt{\frac{E_{SR}E_{RD}}{\bar{E}_{SR}+N_0}} \mu_{SR}$, $\sigma_{\eta RD}^2 = \frac{E_{RD}}{\bar{E}_{SR}+N_0} |h_{RD}|^2 N_0 + N_0$ and $\hat{\sigma}_{SR}^2 = \frac{E_{SR}E_{RD}}{\bar{E}_{SR}+N_0} \sigma_{SR}^2$.

Similar to the previous case, after substituting the values in (3.19) and simplifying the result, the log-likelihood ratio for BFSK is obtained as

$$\Gamma_{RD} = \frac{\left| y_1 + \hat{\mu}_{SR} h_{RD} \frac{\sigma^2_{\eta RD}}{\hat{\sigma}^2_{SR}|h_{RD}|^2} \right|^2}{\left| y_2 + \hat{\mu}_{SR} h_{RD} \frac{\sigma^2_{\eta RD}}{\hat{\sigma}^2_{SR}|h_{RD}|^2} \right|^2} \gtrless_{f_2}^{f_1} 1. \tag{3.20}$$

In the case of M-FSK, the detected frequency is

$$\hat{f}_{\Xi,RD} \ : \ \Xi = \arg\max_l \left\{ \left| y_l + \hat{\mu}_{SR} h_{RD} \frac{\sigma^2_{\eta RD}}{\hat{\sigma}^2_{SR}|h_{RD}|^2} \right|^2 \right\}. \tag{3.21}$$

Note that the detectors in (3.20) and (3.21) are optimal detectors. Similarly, in the case of balanced links it can be shown that at high E_{SR}, this detector also becomes the energy detector.

By assuming the collective noise to be complex Gaussian, an approximate sub-optimal detector can be derived for this case as well. By substituting the conditional PDF from (3.14) in (3.19), the log-likelihood ratio is obtained as

$$\Gamma_{RD,G} = \frac{\left| y_1 + \hat{\mu}_{SR} h_{RD} \frac{\sigma^2_{\eta}}{\hat{\sigma}^2_{SR}|h_{RD}|^2} \right|^2}{\left| y_2 + \hat{\mu}_{SR} h_{RD} \frac{\sigma^2_{\eta}}{\hat{\sigma}^2_{SR}|h_{RD}|^2} \right|^2} \gtrless_{f_2}^{f_1} 1. \tag{3.22}$$

In the case of M-FSK, the detected frequency is

$$\hat{f}_{\Xi,RD,G} \ : \ \Xi = \arg\max_l \left\{ \left| y_l + \hat{\mu}_{SR} h_{RD} \frac{\sigma^2_{\eta}}{\hat{\sigma}^2_{SR}|h_{RD}|^2} \right|^2 \right\}. \tag{3.23}$$

Comparing (3.22) to (3.20), one notes that the only difference is that in $\sigma^2_{\eta RD}$, $|h_{RD}|^2$ is replaced with $(\sigma^2_{RD} + \mu^2_{RD})$. Furthermore, the metrics in (3.22) and (3.16) are very similar, and one can easily obtain one from the other by interchanging h_{SR} with h_{RD}, μ_{SR} with μ_{RD} and σ^2_{SR} with σ^2_{RD}, respectively. Similar to (3.18), for the case of

balanced links it can be shown that at high E_{RD} (or E_{SR}), this detector also becomes the energy detector.

For the case of Rayleigh fading channel, the new detectors can be derived by setting $\mu_{SR} = \mu_{RD} = 0$. In this case, the proposed half-coherent receivers degenerate to the energy detector, i.e.

$$\hat{f}_{\Xi,NC} \ : \ \Xi = \arg\max_{l} |y_l|^2. \tag{3.24}$$

Thus, for a Rayleigh fading channel, an interesting observation is that having CSI of either the source-relay link or the relay-destination link is effectively the same as having no CSI at all. In fact, if the link whose CSI is unknown at the receiver experiences Rayleigh fading then the half-coherent receiver becomes the same as the energy detector.

3.4 Performance Analysis of the New Receivers

In this section, the analytical expressions for the SER of our newly proposed half-coherent receivers are derived. In the derivation, the estimation errors are not taken into account and it is assumed that the receiver has perfect CSI.

3.4.1 Only CSI of the Source-Relay Link is Available

From the M-FSK detector in (3.17), let $z_{SR,l} = y_l + \hat{\mu}_{RD} h_{SR} \frac{\sigma_\eta^2}{\tilde{\sigma}_{RD}^2 |h_{SR}|^2}$. Thus, the detector can also be expressed as $\hat{\mathbf{x}}_{SR,G} = \max_l\{\gamma_{SR,l}\}$, where $\gamma_{SR,l} = |z_{SR,l}|$ [1]. Given that f_i is transmitted, the probability that f_i is received is $P_c = Pr\{\max_k\{\gamma_{SR,k}\} < \gamma_{SR,i}\}$, $\forall k \ \& \ k \neq i$. Conditioned on h_{SR} and h_{RD}, $z_{SR,i}$ is $\mathcal{CN}(\sqrt{\frac{E_{SR}E_{RD}}{E_{SR}+N_0}} h_{SR} h_{RD} +$

[1] Note that, $\hat{\mathbf{x}}_{SR,G} = \max_l\{|z_{SR,l}|\}$ is the same as $\hat{\mathbf{x}}_{SR,G} = \max_l\{|z_{SR,l}|^2\}$.

$\hat{\mu}_{RD}h_{SR}\frac{\sigma_\eta^2}{\hat{\sigma}_{RD}^2|h_{SR}|^2}, \sigma_{\eta RD}^2)$ and $z_{SR,k}$ is $\mathcal{CN}(\hat{\mu}_{RD}h_{SR}\frac{\sigma_\eta^2}{\hat{\sigma}_{RD}^2|h_{SR}|^2}, \sigma_{\eta RD}^2)$ and thus, $\gamma_{SR,i}$ and $\gamma_{SR,k}$ are Rician random variables (RV)[2]. Also conditioned on h_{SR}, h_{RD} and $\gamma_{SR,i}$, $\gamma_{SR,k}$ are independent and identically distributed (i.i.d) for all values of k. Thus, the conditional symbol error probability for M-FSK can be expressed as

$$Pe_{SR,G,MFSK|h_{SR},h_{RD},z_{SR,i}} = 1 - Pr\{\gamma_{SR,k} < \gamma_{SR,i}|h_{SR}, h_{RD}, \gamma_{SR,i} = \gamma\}^{M-1}, \quad (3.25)$$

where $Pr\{\gamma_{SR,k} < \gamma_{SR,i}|h_{SR}, h_{RD}, \gamma_{SR,i} = \gamma\}$ is the conditional CDF of $\gamma_{SR,k}$ and is given as $1 - Q\left(\frac{\sqrt{2}|\nu_{SR}|}{\sigma_{\eta RD}}, \frac{\sqrt{2}\gamma}{\sigma_{\eta RD}}\right)$ with $Q(\cdot,\cdot)$ being the first order Marcum-Q function and $\nu_{SR} = \hat{\mu}_{RD}\frac{\sigma_\eta^2}{\hat{\sigma}_{RD}^2|h_{SR}|}$ [94]. Thus, the conditional symbol error probability can be expressed as

$$Pe_{SR,G,MFSK|h_{SR},h_{RD},z_{SR,i}} = 1 - \left(1 - Q\left(\frac{\sqrt{2}|\nu_{SR}|}{\sigma_{\eta RD}}, \frac{\sqrt{2}\gamma}{\sigma_{\eta RD}}\right)\right)^{M-1}. \quad (3.26)$$

The unconditional symbol error probability can be obtained from (3.26) as

$$Pe_{SR,G,MFSK} = 1 - \int\int\int\int \left(1 - Q\left(\frac{\sqrt{2}|\hat{\mu}_{RD}|\sigma_\eta^2}{\hat{\sigma}_{RD}^2\kappa_{SR}\sqrt{\varepsilon\kappa_{RD}^2 + N_0}}, \frac{\sqrt{2}\gamma}{\sqrt{\varepsilon\kappa_{RD}^2 + N_0}}\right)\right)^{M-1}$$
$$\times f_{\gamma_{SR,i}}(\gamma, \kappa_{SR}, \kappa_{RD}, \theta_{RD}) f_{\kappa_{SR}}(\kappa_{SR}) f_{h_{RD}}(\kappa_{RD}, \theta_{RD}) \mathsf{d}\gamma \ \mathsf{d}\kappa_{SR} \ \mathsf{d}\kappa_{RD} \ \mathsf{d}\theta_{RD}, \quad (3.27)$$

where $h_{SR} = \kappa_{SR}e^{j\theta_{SR}}$ and $h_{RD} = \kappa_{RD}e^{j\theta_{RD}}$, $f_{h_{RD}}(\kappa_{RD}, \theta_{RD}) = \frac{\kappa_{RD}}{\pi\sigma_{RD}^2}\exp\left(-\frac{\kappa_{RD}^2+|\mu_{RD}|^2}{\sigma_{RD}^2}\right)$ $\times\exp\left(\frac{2\kappa_{RD}\Re\{e^{-j\theta_{RD}}\mu_{RD})\}}{\sigma_{RD}^2}\right)$ denotes the joint amplitude-phase PDF of the relay-destination link, $f_{\kappa_{SR}}(\kappa_{SR}) = \frac{2\kappa_{SR}}{\sigma_{SR}^2}\exp\left(-\frac{\kappa_{SR}^2+|\mu_{SR}|^2}{\sigma_{SR}^2}\right)\mathbf{I}_0\left(\frac{2\kappa_{SR}|\mu_{SR}|}{\sigma_{SR}^2}\right)$ denotes the PDF of the amplitude of the source-relay link, $f_{\gamma_{SR,i}}(\gamma, \kappa_{SR}, \kappa_{RD}, \theta_{RD}) = \frac{2\gamma}{\varepsilon\kappa_{RD}^2+N_0} \times$

[2]Note that, while finding the statistics of $z_{SR,i}$, we do not assume the collective noise in the received signal y_i to be complex Gaussian. Thus, the performance analysis expressions derived in this section give exact performance.

$\exp\left(-\frac{\gamma^2+\varsigma^2\kappa_{SR}^2\left|\kappa_{RD}e^{j\theta_{RD}}+\hat{\mu}_{RD}\frac{\sigma_\eta^2}{\varsigma\hat{\sigma}_{RD}^2\kappa_{SR}^2}\right|^2}{\varepsilon\kappa_{RD}^2+N_0}\right)\mathbf{I}_0\left(\frac{2\gamma\varsigma\kappa_{SR}\left|\kappa_{RD}\exp(j\theta_{RD})+\hat{\mu}_{RD}\frac{\sigma_\eta^2}{\varsigma\hat{\sigma}_{RD}^2\kappa_{SR}^2}\right|}{\varepsilon\kappa_{RD}^2+N_0}\right)$ denotes the PDF of γ, $\mathbf{I}_0(.)$ is the modified Bessel function of the first kind of order zero, $\varepsilon=\frac{E_{RD}}{\bar{E}_{SR}+N_0}N_0$, and $\varsigma=\sqrt{\frac{E_{SR}E_{RD}}{\bar{E}_{SR}+N_0}}$.

For further simplification, one can approximate the integral in (3.27), w.r.t. γ using the Gauss-Laguerre formula [92] yielding

$$Pe_{SR,G,MFSK}=$$
$$1-\sum_{i_1=1}^{N_2}w_\gamma(x_{i_1})\exp(x_{i_1})\int\int\int\left(1-Q\left(\frac{\sqrt{2}\hat{\mu}_{RD}\sigma_\eta^2}{\hat{\sigma}_{RD}^2\kappa_{SR}\sqrt{\varepsilon\kappa_{RD}^2+N_0}},\frac{\sqrt{2}x_{i_1}}{\sqrt{\varepsilon\kappa_{RD}^2+N_0}}\right)\right)^{M-1}$$
$$\times f_{\gamma_{SR,i}}(x_{i_1},\kappa_{SR},\kappa_{RD},\theta_{RD})\times f_{\kappa_{SR}}(\kappa_{SR})\times f_{h_{RD}}(\kappa_{RD},\theta_{RD})\ \mathsf{d}\kappa_{SR}\ \mathsf{d}\kappa_{RD}\mathsf{d}\theta_{RD}, \tag{3.28}$$

where, $w_\gamma(x_k)=\frac{x_k}{(N_2+1)^2L_{N_2+1}(x_k^2)}$, x_k is the kth zero of the Laguerre polynomial $L_n(x)$ [92] and N_2 is the number of points chosen for the Gauss-laguerre rule. Then, (3.28) can be evaluated numerically using standard mathematical packages such as MATHEMATICA®.

In the case of BFSK, a different approach is employed to obtain a slightly simplified performance expression compared with (3.27). The log-likelihood ratio in (3.16) can be rewritten as

$$\left|y_1+\hat{\mu}_{RD}h_{SR}\frac{\sigma_\eta^2}{\hat{\sigma}_{RD}^2|h_{SR}|^2}\right|^2\gtrless_{f_2}^{f_1}\left|y_2+\hat{\mu}_{RD}h_{SR}\frac{\sigma_\eta^2}{\hat{\sigma}_{RD}^2|h_{SR}|^2}\right|^2. \tag{3.29}$$

Let $z_{SR,1}=y_1+\hat{\mu}_{RD}h_{SR}\frac{\sigma_\eta^2}{\hat{\sigma}_{RD}^2|h_{SR}|^2}$ and $z_{SR,2}=y_2+\hat{\mu}_{RD}h_{SR}\frac{\sigma_\eta^2}{\hat{\sigma}_{RD}^2|h_{SR}|^2}$. Thus, (3.29) can be expressed as

$$\gamma_{SR,G,BFSK}=\left(|z_{SR,1}|^2-|z_{SR,2}|^2\right)\gtrless_{f_2}^{f_1}0.$$

Conditioned on h_{SR} and h_{RD}, $z_{SR,1}$ and $z_{SR,2}$ are $\mathcal{CN}(\sqrt{\frac{E_{SR}E_{RD}}{\bar{E}_{SR}+N_0}}h_{RD}h_{SR}+\hat{\mu}_{RD}h_{SR}\frac{\sigma_\eta^2}{\hat{\sigma}_{RD}^2|h_{SR}|^2}$,

$\sigma^2_{\eta RD})$ and $\mathcal{CN}(\hat{\mu}_{RD}h_{SR}\frac{\sigma^2_\eta}{\hat{\sigma}^2_{RD}|h_{SR}|^2}, \sigma^2_{\eta RD})$, respectively. Thus, $\gamma_{SR,G,BFSK}$, conditioned on h_{SR} and h_{RD}, is the difference of two independent chi-square random variables. The conditional symbol error probability is $Pe_{SR,G,BFSK|h_{SR},h_{RD}} = Pr\{\gamma_{SR,G,BFSK|h_{SR},h_{RD}} < 0\}$, which can be evaluated using [95] as

$$Pe_{SR,G,BFSK|h_{SR},h_{RD}} = \frac{1}{2} - \frac{1}{2\pi j}\int_{-\infty}^{\infty} \frac{\phi_{\gamma_{SR,G,BFSK|h_{SR},h_{RD}}}(\omega)}{\omega}\mathsf{d}\omega, \tag{3.30}$$

where $\phi_{\gamma_{SR,G,BFSK|h_{SR},h_{RD}}}(\omega) = \mathbb{E}[\exp\left(j\omega\gamma_{SR,G,BFSK|h_{SR},h_{RD}}\right)]$ is the characteristic function of $\gamma_{SR,G,BFSK|h_{SR},h_{RD}}$. Substituting the characteristic function from [**?**] in (3.30), one obtains

$$Pe_{SR,G,BFSK|h_{SR},h_{RD}} = \frac{1}{2} - \frac{1}{2\pi j}\int_{-\infty}^{\infty} \frac{\exp\left(\frac{j\omega(|u_1(h_{SR},h_{RD})|^2 - |u_2(h_{SR})|^2) - \omega^2\sigma(h_{RD})(|u_1(h_{SR},h_{RD})|^2 + |u_2(h_{SR})|^2)}{(1+\omega^2\sigma(h_{RD})^2)}\right)}{\omega(1+\omega^2\sigma(h_{RD})^2)}\mathsf{d}\omega, \tag{3.31}$$

where $u_1(h_{SR}, h_{RD}) = \sqrt{\frac{E_{SR}E_{RD}}{E_{SR}+N_0}}h_{RD}h_{SR} + \hat{\mu}_{RD}h_{SR}\frac{\sigma^2_\eta}{\hat{\sigma}^2_{RD}|h_{SR}|^2}$, $u_2(h_{SR}) = \hat{\mu}_{RD}h_{SR}\frac{\sigma^2_\eta}{\hat{\sigma}^2_{RD}|h_{SR}|^2}$ and $\sigma(h_{RD}) = \frac{E_{RD}}{E_{SR}+N_0}|h_{RD}|^2N_0 + N_0$. Then, $Pe_{SR,G,BFSK}$ can be obtained by averaging $Pe_{SR,G,BFSK|h_{SR},h_{RD}}$ to give

$$Pe_{SR,G,BFSK} = \int\int\int Pe_{SR,G|h_{SR},h_{RD}}(\kappa_{SR}, \kappa_{RD}, \theta_{RD}) f_{\kappa_{SR}}(\kappa_{SR}) f_{h_{RD}}(\kappa_{RD}, \theta_{RD}) \mathsf{d}\kappa_{SR}\ \mathsf{d}\kappa_{RD}\ \mathsf{d}\theta_{RD}. \tag{3.32}$$

After integrating w.r.t θ_{RD} and κ_{SR}, the expression obtained for $Pe_{SR,G,BFSK}$ is

$$
\begin{aligned}
&Pe_{SR,G,BFSK} = \\
&\sum_{k=0}^{\infty} \int_{0}^{\infty} \int_{-\infty}^{\infty} \psi(k) \left(\frac{\varsigma^2 \omega^2 g_1(\kappa_{RD})}{\left(\omega^2 \left(g_1(\kappa_{RD})\right)^2 + 1\right) - \varsigma^2 \left(j\omega - \omega^2 g_1(\kappa_{RD})\right) \kappa_{RD}^2 \sigma_{SR}^2} \right)^{\frac{k+1}{2}} \\
&\quad \times \exp\left(-\frac{\kappa_{RD}^2}{\sigma_{RD}^2}\right) \mathbf{I}_0 \left(2\kappa_{RD} \left(\frac{|\mu_{RD}| \varrho \varsigma^2 \left(j\omega - \omega^2 g_1(\kappa_{RD})\right)}{\left(\omega^2 \left(g_1(\kappa_{RD})\right)^2 + 1\right)} + \frac{|\mu_{RD}|}{\sigma_{RD}^2} \right) \right) \\
&\quad \times \mathbf{K}_{k+1} \left(\sqrt{ \frac{8\varrho^2 |\mu_{RD}|^2 \varsigma^2 \omega^2 g_1(\kappa_{RD})}{\left(\omega^2 \left(g_1(\kappa_{RD})\right)^2 + 1\right)} \left(\frac{1}{\sigma_{SR}^2} - \frac{\varsigma^2 \left(j\omega - \omega^2 g_1(\kappa_{RD})\right)}{\left(\omega^2 \left(g_1(\kappa_{RD})\right)^2 + 1\right)} \right) } \right) \mathsf{d}\kappa_{RD} \mathsf{d}\omega,
\end{aligned}
\tag{3.33}
$$

where $g_1(s) = \varepsilon s^2 + N_0$, $\psi(k) = \frac{4\sqrt{2}\varrho |\mu_{RD}||\mu_{SR}|^{2k}}{\sigma_{RD}^2 (\sigma_{SR}^2)^{\frac{1}{2}(3k+1)} (k!)^2} \exp\left(-\frac{|\mu_{RD}|^2}{\sigma_{RD}^2} - \frac{|\mu_{SR}|^2}{\sigma_{SR}^2}\right)$, $\varrho = \frac{\sigma_\eta^2}{\hat{\sigma}_{RD}^2}$, and $\mathbf{K}_p(.)$ is the pth order modified Bessel function of the second kind. The expression in (3.33) cannot be obtained in closed-form but can be evaluated numerically using standard mathematical packages such as MATHEMATICA®.

3.4.2 Only CSI of the Relay-Destination Link is Available

The SER expression for the detector in (3.23) is considered first. Let $z_{RD,l} = y_l + \hat{\mu}_{SR} h_{RD} \frac{\sigma_\eta^2}{\hat{\sigma}_{SR}^2 |h_{RD}|^2}$. Similar to the case in the previous subsection, the detector in this case can also be expressed as $\hat{\mathbf{x}}_{RD,G} = \max_l\{\gamma_{RD,l}\}$, where $\gamma_{RD,l} = |z_{RD,l}|$. Given that f_i is transmitted, the probability that f_i is received is $P_c = Pr\{\max_k\{\gamma_{RD,k}\} < \gamma_{RD,i}\}$, $\forall k \ \& \ k \neq i$. Conditioned on h_{RD}, $z_{RD,i}$ and $z_{RD,k}$ are $\mathcal{CN}(\hat{\mu}_{SR} h_{RD} + \hat{\mu}_{SR} h_{RD} \frac{\sigma_\eta^2}{\hat{\sigma}_{SR}^2 |h_{RD}|^2}, \hat{\sigma}_{SR}^2 |h_{RD}|^2 + \sigma_{\eta RD}^2)$ and $\mathcal{CN}(\hat{\mu}_{SR} h_{RD} \frac{\sigma_\eta^2}{\hat{\sigma}_{SR}^2 |h_{RD}|^2}, \sigma_{\eta RD}^2)$, respectively. Therefore, conditioned on h_{RD}, $\gamma_{RD,i}$ and $\gamma_{RD,k}$ are Rician RVs. Now, assuming that $\gamma_{RD,i}$ is known, then $\gamma_{RD,k}$ are i.i.d for all values of k. Thus, the

conditional symbol error probability for M-FSK can be expressed as

$$Pe_{RD,G,MFSK|h_{RD},\gamma_{RD,i}} = 1 - Pr\{\gamma_{RD,k} < \gamma_{RD,i}|h_{RD}, \gamma_{RD,i} = \gamma\}^{M-1}, \tag{3.34}$$

where $Pr\{\gamma_{RD,k} < \gamma_{RD,i}|h_{RD}, \gamma_{RD,i} = \gamma\} = 1 - Q\left(\frac{\sqrt{2}|\nu_{RD}|}{\sigma_{\eta RD}}, \frac{\sqrt{2}\gamma}{\sigma_{\eta RD}}\right)$ is the conditional CDF of $\gamma_{RD,k}$ and $\nu_{RD} = \hat{\mu}_{SR}\frac{\sigma_\eta^2}{\hat{\sigma}_{SR}^2|h_{RD}|}$ [94]. Applying this result, the conditional symbol error probability can be expressed as

$$Pe_{RD,G,MFSK|h_{SR},h_{RD},\gamma_{RD,i}} = 1 - \left(1 - Q\left(\frac{\sqrt{2}|\nu_{RD}|}{\sigma_{\eta RD}}, \frac{\sqrt{2}\gamma}{\sigma_{\eta RD}}\right)\right)^{M-1}. \tag{3.35}$$

The unconditional symbol error probability can be obtained as

$$Pe_{RD,G,MFSK} = 1 - \int\int \left(1 - Q\left(\frac{\sqrt{2}|\hat{\mu}_{SR}|\sigma_\eta^2}{\hat{\sigma}_{SR}^2\kappa_{RD}\sqrt{\varepsilon\kappa_{RD}^2 + N_0}}, \frac{\sqrt{2}\gamma}{\sqrt{\varepsilon\kappa_{RD}^2 + N_0}}\right)\right)^{M-1} \times f_{\gamma_{RD,i}}(\gamma, \kappa_{RD}) f_{\kappa_{RD}}(\kappa_{RD}) \mathsf{d}\gamma \ \mathsf{d}\kappa_{RD}, \tag{3.36}$$

where $f_{\gamma_{RD,i}}(\gamma, \kappa_{RD}) = \frac{2\gamma}{\hat{\sigma}_{SR}^2\kappa_{RD}^2 + \varepsilon\kappa_{RD}^2 + N_0} \exp\left(-\frac{\gamma^2 + \kappa_{RD}^2|\hat{\mu}_{SR}|^2\left|1 + \frac{\sigma_\eta^2}{\hat{\sigma}_{SR}^2\kappa_{RD}^2}\right|^2}{\hat{\sigma}_{SR}^2\kappa_{RD}^2 + \varepsilon\kappa_{RD}^2 + N_0}\right) \times \mathbf{I}_0\left(\frac{2\gamma\kappa_{RD}|\hat{\mu}_{SR}|\left|1 + \frac{\sigma_\eta^2}{\hat{\sigma}_{SR}^2\kappa_{RD}^2}\right|}{\hat{\sigma}_{SR}^2\kappa_{RD}^2 + \varepsilon\kappa_{RD}^2 + N_0}\right)$ denotes the PDF of $\gamma_{RD,i}$ and $f_{\kappa_{RD}}(\kappa_{RD}) = \frac{2\kappa_{RD}}{\sigma_{RD}^2} \times \exp\left(-\frac{\kappa_{RD}^2 + |\mu_{RD}|^2}{\sigma_{RD}^2}\right) \mathbf{I}_0\left(\frac{2\kappa_{RD}|\mu_{RD}|}{\sigma_{RD}^2}\right)$ denotes the PDF of the amplitude of the relay-destination link.

By replacing σ_η with $\sigma_{\eta RD} = \sqrt{\varepsilon\kappa_{RD}^2 + N_0}$ in (3.36), one obtains the symbol error

rate expression for the metric in (3.21) as

$$Pe_{RD,MFSK} = 1- \int \left(1 - Q\left(\frac{\sqrt{2}\hat{\mu}_{SR}(\varepsilon\kappa_{RD}^2 + N_0)}{\hat{\sigma}_{SR}^2\kappa_{RD}\sqrt{\varepsilon\kappa_{RD}^2 + N_0}}, \frac{\sqrt{2}\gamma}{\sqrt{\varepsilon\kappa_{RD}^2 + N_0}}\right)\right)^{M-1} \bar{f}_{\gamma_{RD,i}}(\gamma, \kappa_{RD}) f_{\kappa_{RD}}(\kappa_{RD}) \mathsf{d}\gamma \ \mathsf{d}\kappa_{RD}, \tag{3.37}$$

where

$$\bar{f}_{\gamma_{RD,i}}(\gamma, \kappa_{RD}) = \frac{2\gamma}{\hat{\sigma}_{SR}^2\kappa_{RD}^2 + \varepsilon\kappa_{RD}^2 + N_0} \exp\left(-\frac{\gamma^2 + \kappa_{RD}^2|\hat{\mu}_{SR}|^2|1 + \frac{(\varepsilon\kappa_{RD}^2 + N_0)}{\hat{\sigma}_{SR}^2\kappa_{RD}^2}|^2}{\hat{\sigma}_{SR}^2\kappa_{RD}^2 + \varepsilon\kappa_{RD}^2 + N_0}\right) \mathbf{I}_0\left(\frac{2\gamma\kappa_{RD}|\hat{\mu}_{SR}||1 + \frac{(\varepsilon\kappa_{RD}^2 + N_0)}{\hat{\sigma}_{SR}^2\kappa_{RD}^2}|}{\hat{\sigma}_{SR}^2\kappa_{RD}^2 + \varepsilon\kappa_{RD}^2 + N_0}\right).$$

The integrals in (3.36) and (3.37) cannot be obtained in closed form but can be evaluated using the available mathematical packages such as MATHEMATICA®.

In the case of BFSK, simplified performance expressions can be obtained. For the detector in (3.22), let $z_{RD,1} = y_1 + \hat{\mu}_{SR}h_{RD}\frac{\sigma_\eta^2}{\hat{\sigma}_{SR}^2|h_{RD}|^2}$ and $z_{RD,2} = y_2 + \hat{\mu}_{SR}h_{RD}\frac{\sigma_\eta^2}{\hat{\sigma}_{SR}^2|h_{RD}|^2}$. The log-likelihood ratio in (3.22) can be expressed as

$$\gamma_{RD,G,BFSK} = \frac{|z_{RD,1}|}{|z_{RD,2}|} \gtrless_{f_2}^{f_1} 1. \tag{3.38}$$

Conditioned on h_{RD}, $z_{RD,1}$ and $z_{RD,2}$ are $\mathcal{CN}(\hat{\mu}_{SR}h_{RD} + \hat{\mu}_{SR}h_{RD}\frac{\sigma_\eta^2}{\hat{\sigma}_{SR}^2|h_{RD}|^2}, \hat{\sigma}_{SR}^2|h_{RD}|^2 + \sigma_{\eta RD}^2)$ and $\mathcal{CN}(\hat{\mu}_{SR}h_{RD}\frac{\sigma_\eta^2}{\hat{\sigma}_{SR}^2|h_{RD}|^2}, \sigma_{\eta RD}^2)$, respectively. Thus, $\gamma_{RD,G,BFSK|h_{RD}}$ is a ratio of two independent Rician random variables. The conditional symbol error probability is $Pe_{RD,G,BFSK|h_{RD}} =$
$Pr\{\ \gamma_{RD,G,BFSK|h_{RD}} < 1\} = F_{\gamma_{RD,G|h_{RD}}}(1)$, where $F_{\gamma_{RD,G,BFSK|h_{RD}}}(\gamma)$ denotes the conditional CDF of $\gamma_{RD,G,BFSK|h_{RD}}$. Using the CDF of the ratio of Rician random variables given in [94] and averaging $F_{\gamma_{RD,G,BFSK|h_{RD}}}(1)$ over the complex relay-destination

channel, h_{RD}, the symbol error probability is

$$Pe_{RD,G,BFSK} = \int_0^\infty Q\left(\alpha(\kappa_{RD}), \beta(\kappa_{RD})\right) f_{\kappa_{RD}}(\kappa_{RD}) \mathsf{d}\kappa_{RD} - \int_0^\infty \zeta(\kappa_{RD}) \exp\left(-\frac{\alpha^2(\kappa_{RD}) + \beta^2(\kappa_{RD})}{2}\right) \mathbf{I}_0\left(\alpha(\kappa_{RD})\beta(\kappa_{RD})\right) f_{\kappa_{RD}}(\kappa_{RD}) \mathsf{d}\kappa_{RD}, \tag{3.39}$$

where $\alpha(\kappa_{RD}) = \sqrt{\frac{2|\hat{\mu}_{SR}|^2\left(\frac{\sigma_\eta^2}{\hat{\sigma}_{SR}^2\kappa_{RD}}\right)^2}{\hat{\sigma}_{SR}^2\kappa_{RD}^2+2\left(\varepsilon\kappa_{RD}^2+N_0\right)}}$, $\beta(\kappa_{RD}) = \sqrt{\frac{2|\hat{\mu}_{SR}|^2\left(\kappa_{RD}+\frac{\sigma_\eta^2}{\hat{\sigma}_{SR}^2\kappa_{RD}}\right)^2}{\hat{\sigma}_{SR}^2\kappa_{RD}^2+2\left(\varepsilon\kappa_{RD}^2+N_0\right)}}$ and $\zeta(\kappa_{RD}) = \frac{\hat{\sigma}_{SR}^2\kappa_{RD}^2+\varepsilon\kappa_{RD}^2+N_0}{\hat{\sigma}_{SR}^2\kappa_{RD}^2+2\left(\varepsilon\kappa_{RD}^2+N_0\right)}$. For the detector in (3.20), the probability of symbol error can be easily obtained by replacing σ_η^2 with $\sigma_{\eta RD}^2 = \varepsilon\kappa_{RD}^2 + N_0$ in (3.39). Thus, one has

$$Pe_{RD,BFSK} = \int_0^\infty Q\left(\bar{\alpha}(\kappa_{RD}), \bar{\beta}(\kappa_{RD})\right) f_{\kappa_{RD}}(\kappa_{RD}) \mathsf{d}\kappa_{RD} - \int_0^\infty \zeta(\kappa_{RD}) \exp\left(-\frac{\bar{\alpha}^2(\kappa_{RD}) + \bar{\beta}^2(\kappa_{RD})}{2}\right) \mathbf{I}_0\left(\bar{\alpha}(\kappa_{RD})\bar{\beta}(\kappa_{RD})\right) f_{\kappa_{RD}}(\kappa_{RD}) \mathsf{d}\kappa_{RD}, \tag{3.40}$$

where $\bar{\alpha}(\kappa_{RD}) = \sqrt{\frac{2|\hat{\mu}_{SR}|^2\left(\frac{\varepsilon\kappa_{RD}^2+N_0}{\hat{\sigma}_{SR}^2\kappa_{RD}}\right)^2}{\hat{\sigma}_{SR}^2\kappa_{RD}^2+2\left(\varepsilon\kappa_{RD}^2+N_0\right)}}$ and $\bar{\beta}(\kappa_{RD}) = \sqrt{\frac{2|\hat{\mu}_{SR}|^2\left(\kappa_{RD}+\frac{\varepsilon\kappa_{RD}^2+N_0}{\hat{\sigma}_{SR}^2\kappa_{RD}}\right)^2}{\hat{\sigma}_{SR}^2\kappa_{RD}^2+2\left(\varepsilon\kappa_{RD}^2+N_0\right)}}$ Note that the single integral expressions in (3.39) and (3.40) are simpler compared to (3.36) and (3.37) and can be evaluated numerically using standard mathematical packages such as MATHEMATICA®. One may also use (3.36) and (3.37) to evaluate the error rate of BFSK with higher computational complexity.

3.4.3 Performance Analysis of the Conventional Non-Coherent Energy Detector

The performance of all the proposed receivers is upper bounded by the performance of the conventional non-coherent energy detector. Thus, in this section, we analyse

the SER performance of the energy detector. Given that frequency f_1 is transmitted, the probability that f_1 is detected using the energy detector in case of MFSK can be expressed as

$$P_{c,\mathcal{ED}} = Pr\{|\mathbf{y}_1|^2 > \max_k |\mathbf{y}_k|^2\} \tag{3.41}$$

Conditioned on h_{RD} and $\mathbf{y}_1$, the probabilty of correct decision can be expressed as

$$P_{c,\mathcal{ED}|h_{RD},y_1} = Pr\{z_{ED} < |\mathbf{y}_1|\} = F_{z_{ED}}(|\mathbf{y}_1|) \tag{3.42}$$

where $z_{ED} = \max_k |\mathbf{y}_k|$ and $F_{z_{ED}}(\cdot)$ denotes the CDF of z_{ED}. Since z_{ED} is the maximum of $M-1$ i.i.d. Rayleigh random variables, the conditional probability of correct decision can be expressed as

$$\begin{aligned} P_{c,\mathcal{ED}|h_{RD},\mathbf{y}_1} &= \left(1 - \exp\left(-\frac{|y_1|^2}{\left(\frac{E_{RD}}{E_{SR}+N_0}N_0|h_{RD}|^2 + N_0\right)}\right)\right)^{M-1} \\ &= \sum_{k=0}^{M-1}\binom{M-1}{k}(-1)^k \exp\left(-\frac{k}{\left(\frac{E_{RD}}{E_{SR}+N_0}N_0|h_{RD}|^2 + N_0\right)}|y_1|^2\right) \end{aligned} \tag{3.43}$$

Thus, $P_{c,\mathcal{ED}|h_{RD}}$ can be obtained by averaging over the PDF of $\mathbf{y}_1$ as

$$\begin{aligned} &P_{c,\mathcal{ED}|h_{RD}} = \\ &\int \sum_{k=0}^{M-1}\binom{M-1}{k}(-1)^k \exp\left(-\frac{k}{\left(\frac{E_{RD}}{E_{SR}+N_0}N_0|h_{RD}|^2 + N_0\right)}|y_1|^2\right) f_{|\mathbf{y}_1|}(|y_1|)\mathsf{d}|y_1| \end{aligned} \tag{3.44}$$

where $f_{|\mathbf{y}_1|}(\cdot)$ denotes the PDF of $|\mathbf{y}_1|$. Substituting the PDF in (3.44) gives

$$P_{c,\mathcal{ED}|h_{RD}} = \sum_{k=0}^{M-1}\binom{M-1}{k}(-1)^k \int \exp\left(-\frac{k}{\sigma_z^2}|y_1|^2\right)\frac{1}{\pi\sigma_{y_1}^2}\exp\left(-\frac{|y_1-\mu_{y_1}|^2}{\sigma_{y_1}^2}\right)\mathsf{d}|y_1| \tag{3.45}$$

where $\mu_{y_1} = \sqrt{\frac{E_{SR}E_{RD}}{\bar{E}_{SR}+N_0}}\mu_{SR}h_{RD}$, $\sigma^2_{y_1} = \frac{E_{SR}E_{RD}}{\bar{E}_{SR}+N_0}\sigma^2_{SR}|h_{RD}|^2 + \frac{E_{RD}}{\bar{E}_{SR}+N_0}N_0|h_{RD}|^2 + N_0$ and $\sigma^2_z = \left(\frac{E_{RD}}{\bar{E}_{SR}+N_0}N_0|h_{RD}|^2 + N_0\right)$. Applying polar transformation $P_{c,\mathcal{ED}|h_{RD}}$ can be expressed as

$$P_{c,\mathcal{ED}|h_{RD}} = \sum_{k=0}^{M-1}\binom{M-1}{k}\frac{(-1)^k}{\pi\sigma^2_{y_1}}\exp\left(-\frac{|\mu_{y_1}|^2}{\sigma^2_{y_1}}\right)\times \int_0^\infty x\exp\left(-\left(\frac{1}{\sigma^2_{y_1}}+\frac{k}{\sigma^2_z}\right)x^2\right)\int_0^{2\pi}\exp\left(\frac{2x\mathcal{R}\{e^{-j\theta_y}\mu_{y_1}\}}{\sigma^2_{y_1}}\right)d\theta_y \mathsf{d}x \tag{3.46}$$

Integrating w.r.t. θ_y one obtains

$$P_{c,\mathcal{ED}|h_{RD}} = \sum_{k=0}^{M-1}\binom{M-1}{k}(-1)^k\frac{2x}{\sigma^2_{y_1}}\exp\left(-\frac{|\mu_{y_1}|^2}{\sigma^2_{y_1}}\right)\int_0^\infty\exp\left(-\left(\frac{1}{\sigma^2_{y_1}}+\frac{k}{\sigma^2_z}\right)x^2\right)I_0\left(\frac{2x|\mu_{y_1}|}{\sigma^2_{y_1}}\right)\mathsf{d}x \tag{3.47}$$

Integrating w.r.t x and after some algebraic manipulations $P_{c,\mathcal{ED}|h_{RD}}$ can be expressed as

$$P_{c,\mathcal{ED}|h_{RD}} = \sum_{k=0}^{M-1}\binom{M-1}{k}(-1)^k\frac{1}{\left(1+\frac{\sigma^2_{y_1}}{\sigma^2_z}k\right)}\exp\left(-\frac{k|\mu_{y_1}|^2}{\sigma^2_z+\sigma^2_{y_1}k}\right) \tag{3.48}$$

The unconditioned probability of correct decision, $P_{c,\mathcal{ED}}$ is given by

$$P_{c,\mathcal{ED}} = \sum_{k=0}^{M-1}\binom{M-1}{k}(-1)^k\int\frac{1}{\left(1+\frac{\sigma^2_{y_1}}{\sigma^2_z}k\right)}\exp\left(-\frac{k|\mu_{y_1}|^2}{\sigma^2_z+\sigma^2_{y_1}k}\right)f_{h_{RD}}(h_{RD})\mathsf{d}h_{RD} \tag{3.49}$$

Substituing the PDF of h_{RD} and applying polar transformation one gets

$$P_{c,\mathcal{ED}} = \sum_{k=0}^{M-1} \binom{M-1}{k} \frac{(-1)^k}{\pi\sigma_{RD}^2} \int_0^\infty \frac{x \exp\left(-\frac{x^2+|\mu_{RD}|^2}{\sigma_{RD}^2}\right)}{\left(1 + \frac{\left(\left(\frac{E_{SR}E_{RD}}{E_{SR}+N_0}\sigma_{SR}^2 + \frac{E_{RD}}{E_{SR}+N_0}N_0\right)x^2+N_0\right)}{\left(\frac{E_{RD}}{E_{SR}+N_0}N_0x^2+N_0\right)}k\right)} \times$$
$$\exp\left(-\frac{k\frac{E_{SR}E_{RD}}{E_{SR}+N_0}|\mu_{SR}|^2x^2}{\left(\frac{E_{RD}}{E_{SR}+N_0}N_0x^2+N_0\right)+\left(\left(\frac{E_{SR}E_{RD}}{E_{SR}+N_0}\sigma_{SR}^2+\frac{E_{RD}}{E_{SR}+N_0}N_0\right)x^2+N_0\right)k}\right) \int_0^{2\pi} \exp\left(\frac{2x\mathcal{R}\{e^{-j\theta_{RD}}\mu_{RD}\}}{\sigma_{RD}^2}\right) \mathsf{d}\theta_{RD}\mathsf{d}x \tag{3.50}$$

Integrating w.r.t. θ_{RD}, $P_{c,\mathcal{ED}}$ is obtained as

$$P_{c,\mathcal{ED}} = \sum_{k=0}^{M-1} \binom{M-1}{k} \frac{(-1)^k}{\sigma_{RD}^2} \exp\left(-\frac{|\mu_{RD}|^2}{\sigma_{RD}^2}\right) \int_0^\infty \frac{2x}{\left(1 + \frac{\left(\left(\frac{E_{SR}E_{RD}}{E_{SR}+N_0}\sigma_{SR}^2 + \frac{E_{RD}}{E_{SR}+N_0}N_0\right)x^2+N_0\right)}{\left(\frac{E_{RD}}{E_{SR}+N_0}N_0x^2+N_0\right)}k\right)} \times$$
$$\exp\left(-\frac{k\frac{E_{SR}E_{RD}}{E_{SR}+N_0}|\mu_{SR}|^2x^2}{\left(\frac{E_{RD}}{E_{SR}+N_0}N_0x^2+N_0\right)+\left(\left(\frac{E_{SR}E_{RD}}{E_{SR}+N_0}\sigma_{SR}^2+\frac{E_{RD}}{E_{SR}+N_0}N_0\right)x^2+N_0\right)k} - \frac{x^2}{\sigma_{RD}^2}\right) I_0\left(\frac{2|\mu_{RD}|}{\sigma_{RD}^2}x\right) \mathsf{d}x \tag{3.51}$$

The integral in (3.51) is not available in closed form but can be evaluated numerically using standard mathematical packages such as MATHEMATICA®. The probability of error can be found using (3.51) as

$$P_{e,\mathcal{ED}} = 1 - P_{c,\mathcal{ED}}. \tag{3.52}$$

3.5 Numerical Results and Discussion

In this section, the SER performances of the derived receivers are shown by numerical results. The modulation scheme is BFSK and 8-FSK. The performances of the derived receivers are compared to the genie receiver (i.e. receiver has perfect CSI of both links), and the conventional non-coherent energy detector receiver. The SER performances of the genie receiver and the non-coherent receivers are obtained by computer simulation. For the newly-proposed half-coherent receivers, the SER performances

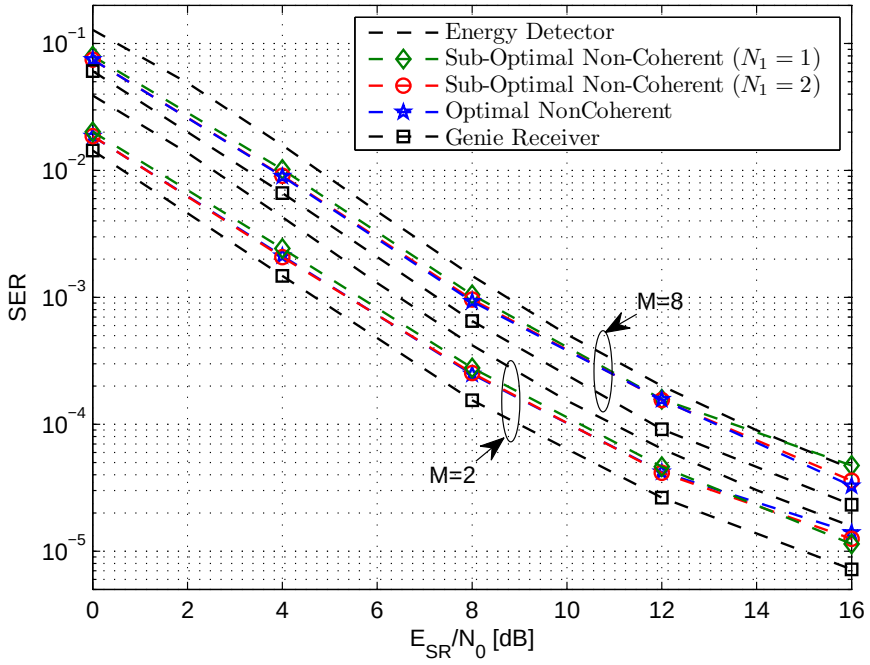

Figure 3.2: Symbol error rate (SER) performance comparison of optimal and sub-optimal non-coherent receivers in balanced links when $\mu_{RD} = \mu_{SR} = 2(1 + j)$.

given by (3.28), (3.33), (3.36), (3.37), (3.39) and (3.40) are verified by simulation. Furthermore, the SER performance of the conventional non-coherent detector given in (3.52) is also verified by simulation.

The SER performances of the non-coherent receivers for both BFSK and 8-FSK are shown in Fig. 3.2 when $E_{SR} = E_{RD}$ and $\mu_{SR} = \mu_{RD} = 2(1 + j)$. It can be observed that at low E_{SR}/N_0, the proposed non-coherent receivers perform better than the non-coherent energy detector. In fact, at a SER of 10^{-3}, a gain of approximately 1 dB can be obtained in the case of BFSK. It can also be observed that the proposed approximation to the optimal non-coherent receiver gives close to optimal SER performance. Even with $N_1 = 2$, the performance of the sub-optimal non-coherent receiver matches closely with that of the optimal non-coherent receiver. Furthermore, if lower complexity is desired the sub-optimal receiver with $N_1 = 1$ can be used which

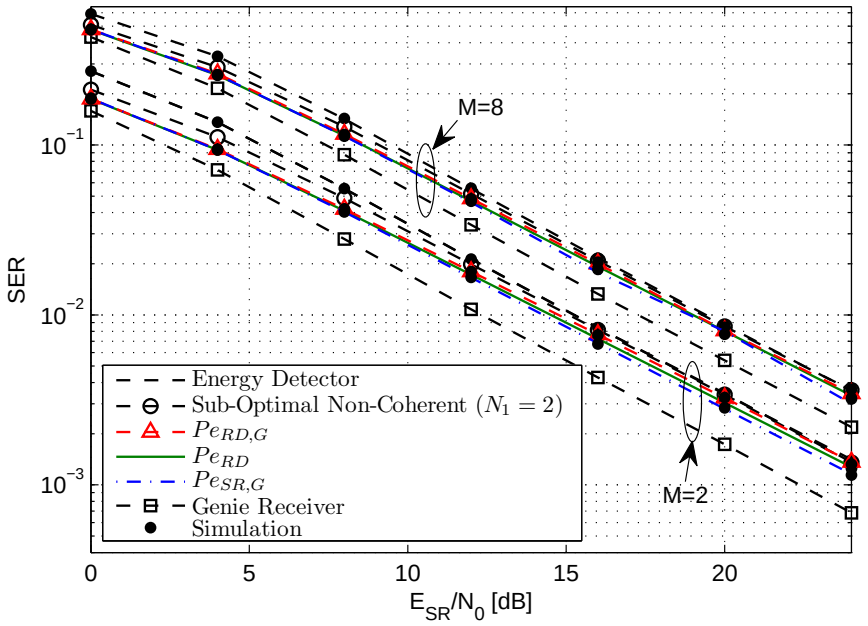

Figure 3.3: Symbol error rate (SER) performance in balanced links when $\mu_{RD} = \mu_{SR} = 1 + j$.

also achieves considerable performance gain over the conventional receiver.

Fig. 3.3 and Fig. 3.4 show the performance of the half-coherent receiver for both BFSK and 8-FSK under balanced links, i.e. $E_{SR} = E_{RD}$, with $\mu_{SR} = \mu_{RD} = 1 + j$ and $\mu_{SR} = \mu_{RD} = 2(1 + j)$, respectively. The SER performance is compared to the conventional non-coherent energy detector and the proposed sub-optimal non-coherent receiver with $N_1 = 2$. In both figures, it can be observed that at low E_{SR}/N_0, the half-coherent receiver performs better than the non-coherent receivers. In fact a performance gain of about 1.2 dB can be obtained at BER of 10^{-3} using these receivers as compared to the conventional non-coherent energy detector based receiver for BFSK with $\mu_{SR} = \mu_{RD} = 2(1 + j)$. Compared to the proposed non-coherent receiver, a slight performance gain is obtained for the half-coherent receivers and this performance gain increases as μ_{SR} decreases.

Furthermore, as E_{SR}/N_0 increases, it can be observed that the performance gain

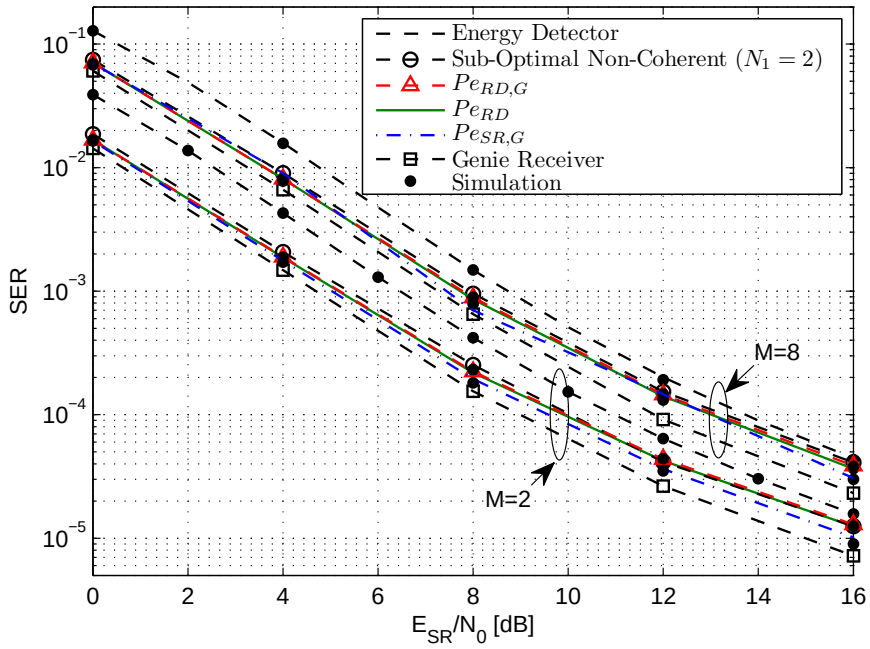

Figure 3.4: Symbol error rate (SER) performance in balanced links when $\mu_{RD} = \mu_{SR} = 2(1 + j)$.

of the half-coherent receiver decreases as was explained in (3.18). The SER performance gain of all the receivers, including the newly proposed receivers, increases as M decreases. Comparing Fig. 3.3 with Fig. 3.4, it can be observed that the performances of all the receivers improve as μ_{RD} and μ_{SR} increase. Note also that from Fig. 3.4, the performances of the receiver conditioned on the source-relay channel is better than the performances of the receivers conditioned on the relay-destination channel. This implies that having knowledge of h_{SR} is better as it gives better performance. It can also be observed that this performance gain is increased if μ_{RD} and μ_{SR} are increased. At low values of μ_{RD} and μ_{SR}, the receivers essentially perform the same. Furthermore, it can be observed in Fig. 3.3 that for lower values of μ_{RD} and μ_{SR}, there is not much difference in the performance between the receivers with Gaussian approximation and without Gaussian approximation. From Fig. 3.3 and Fig. 3.4,

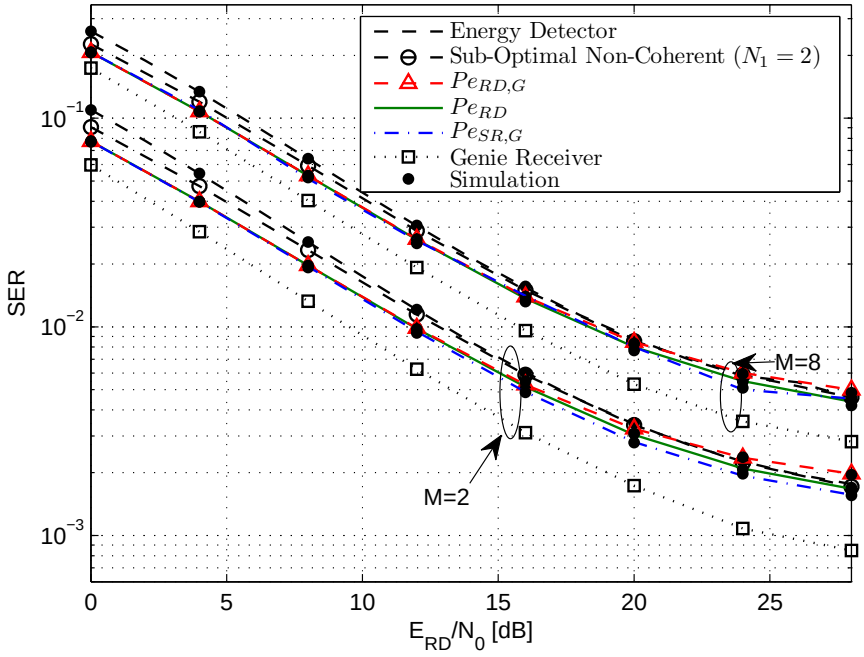

Figure 3.5: Symbol error rate (SER) performance in unbalanced links when $E_{SR}/N_0 = 20$ dB and $\mu_{RD} = \mu_{SR} = 1 + j$.

it can be observed that the simulation results (denoted by black dots) match closely with the analytical results given by (3.28), (3.33), (3.36), (3.37), (3.39), (3.40) and (3.52).

Fig. 3.5 shows the performance of the proposed receivers under unbalanced links in which $E_{SR}/N_0 = 20$ dB and $\mu_{SR} = \mu_{RD} = 1 + j$. Again, at low E_{RD}/N_0, the proposed non-coherent receiver and the half-coherent receivers performs better as compared to the conventional energy detector based receiver and the half-coherent receiver performs slightly better compared to the proposed non-coherent receiver. As E_{RD}/N_0 is increased, the performance gain of the proposed receivers is reduced. At high E_{RD}/N_0, an error floor is obtained because the end-to-end signal-to-noise ratio approaches a constant value [39]. In this case, it can be observed that the receivers with Gaussian approximation and without Gaussian approximation perform the same

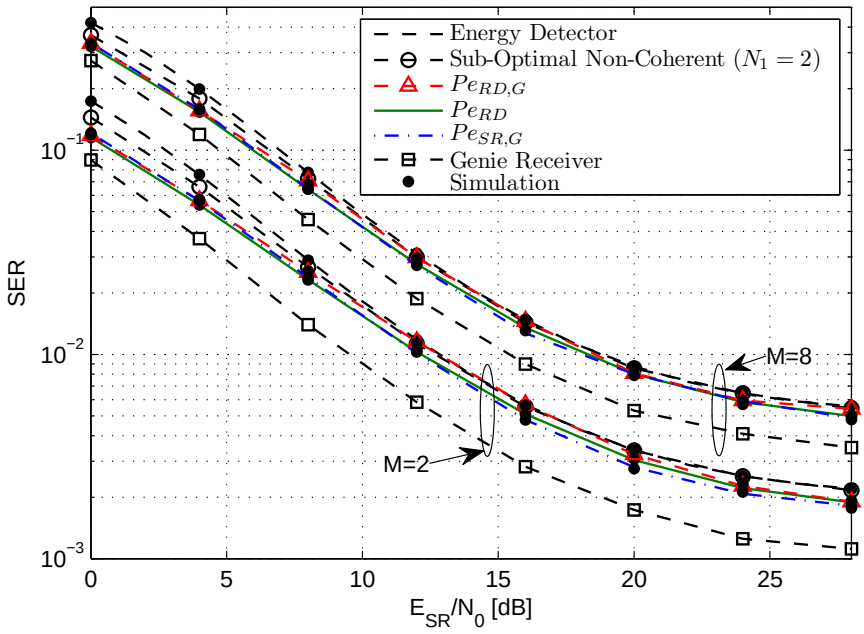

Figure 3.6: Symbol error rate (SER) performance in unbalanced links when $E_{RD}/N_0 = 20$ dB and $\mu_{RD} = \mu_{SR} = 1 + j$.

at low E_{RD}/N_0. However, at high E_{RD}/N_0, the performance of the receiver with CSI relay-destination link and Gaussian approximation degrades. As we assumed the value of E_{RD} to be high, the noise at the destination is affected more by the noise from the relay. The noise from the relay is not complex Gaussian and thus the difference in performance is notable. Furthermore, the performance gain of the new receivers decreases with increasing M.

Fig. 3.6 shows the performance of the proposed receivers under unbalanced links in which $E_{RD}/N_0 = 20$ dB and $\mu_{SR} = \mu_{RD} = 1 + j$. Again, at low E_{RD}/N_0, the proposed non-coherent receiver and the half-coherent receivers performs better as compared to the conventional energy detector based receiver and the half-coherent receiver performs slightly better compared to the proposed non-coherent receiver. Furthermore, similar to the previous cases, the performance of the proposed receivers approaches the performance of the non-coherent receiver at high E_{SR}/N_0. Moreover,

in this case, there is a slight difference in the performance of the receivers with and without the Gaussian approximation because E_{RD} is high and thus, the collective noise is not well approximated as complex Gaussian. At high E_{SR}/N_0, the first term on the right hand side of (3.1) becomes $\sqrt{\frac{E_{SR}E_{RD}}{E_{SR}+N_0}}h_{SR}h_{RD} \approx \sqrt{E_{RD}}h_{SR}h_{RD}$ resulting in a constant end-to-end SNR and an error floor occurs. Furthermore, it can be observed that the receiver conditioned on h_{SR} performs better than the receivers conditioned on h_{RD}. Again in this case, the performance gain of the new receivers decreases with increasing M. From Fig. 3.5 and Fig. 3.6, it can be observed that the simulation results match closely with the analytical results.

Chapter 4

Performance of Opportunistic Bidirectional Relaying With Outdated CSI

4.1 Introduction

The imperfect CSI, considered in previous chapters, exists due to noise that is added to the pilot signal. Another type of imperfect CSI which arises in communication systems is outdated CSI. This occurs due to the time varying nature of the channel. In this chapter, the impact of outdated CSI on cooperative relaying network is analyzed. Specifically, an opportunistic TWR network is considered in which a single relay is selected for transmission. The relay selection (RS) is done based on outdated CSI. The RS criteria considered is max-min RS. In this chapter, the performance of this system is analyzed and closed-form expressions for the outage performance, moment-generating-function of the E2E-SNR and the SER performance are obtained. The derived analytical results are corroborated by numerical simulations. Furthermore, the impact of relay location is also studied.

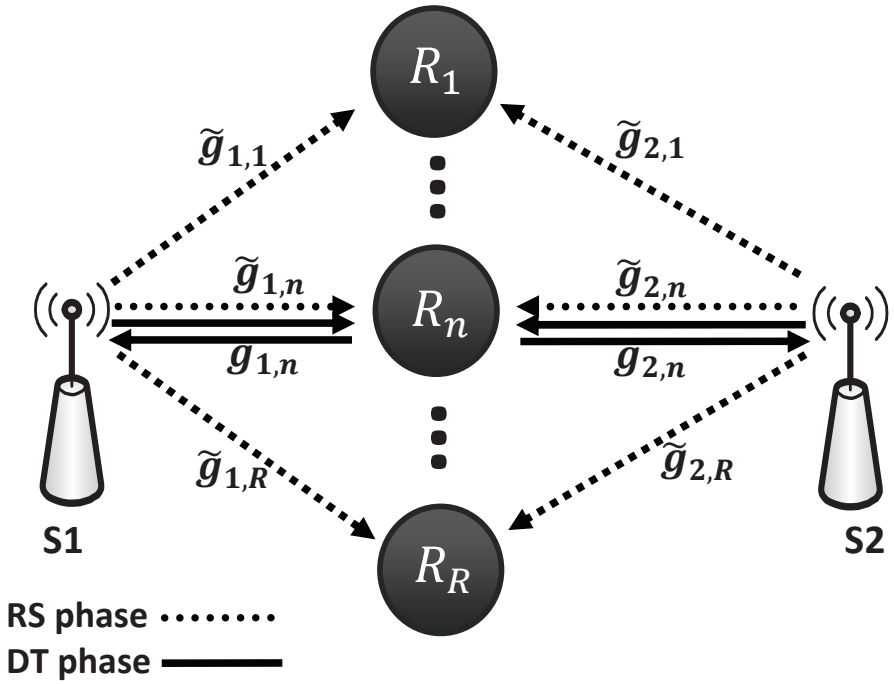

Figure 4.1: System Model.

4.2 System Model

Consider a system shown in Fig. 4.1 where two sources, denoted by S1 and S2, communicate with each other via R two-way AF relays. The direct link between both the sources is assumed to be deeply faded. A single relay is opportunistically selected for transmission and data transmission occurs after the relay selection. Data transmission in a two-way relaying network is carried out in two phases (i) multiple access phase and (ii) broadcast phase. In the multiple access phase both the sources transmit simultaneously to the relay where as in the broadcast phase the relay transmits to both the sources.

We consider a realistic scenario, where there is a delay between the RS phase and data transmission. Due to this delay, the channel becomes outdated i.e. the channel conditions during the data transmission are different from those during the RS phase.

During the RS phase (past realizations), $\tilde{g}_{1,n}$ and $\tilde{g}_{2,n}$ are used to denote the channel gains, between S1 and the n-th relay and between S2 and the n-th relay, respectively. Similarly, $g_{1,n}$ and $g_{2,n}$ are the channel gains during the data transmission (recent realizations). The channel is assumed to be independent and identically distributed (i.i.d) and have Rayleigh fading.

For a Rayleigh fading channel, the past and current realizations of the channel gains are related with each other as

$$g_{1,n} = \rho_1 \tilde{g}_{1,n} + \sqrt{1-\rho_1^2} v_n, \;\; g_{2,n} = \rho_2 \tilde{g}_{2,n} + \sqrt{1-\rho_2^2} w_n, \tag{4.1}$$

where $\rho_1 = J_0\left(2\pi f_{D,1} T\right)$ and $\rho_2 = J_0\left(2\pi f_{D,2} T\right)$ are the correlation coefficients, T denotes the time delay between the RS phase and the data transmission, $f_{D,1}$ is the maximum Doppler frequency shift of the channel between S1 and the relays, $f_{D,2}$ is the maximum Doppler frequency shift of the channel between the relays and S2, $J_0(\cdot)$ denotes the zero-order Bessel function of the first kind. $\tilde{g}_{1,n}$ and v_n are both zero mean complex Gaussian (ZMCG) random variables (RVs) with variance σ_1. Similarly, $\tilde{g}_{2,n}$ and w_n are both ZMCG RVs with variance σ_2.

Given that the n-th relay is selected for transmission, the end-to-end SNR (E2E-SNR), after removing the self interference, at S2 can be expressed as $\Upsilon_n = \frac{P_S G^2 |g_{2,n}|^2 |g_{1,n}|^2}{G^2 |g_{2,n}|^2 N_0 + N_0}$ $= \frac{P_S |g_{2,n}|^2 |g_{1,n}|^2}{|g_{2,n}|^2 N_0 + \frac{N_0}{G^2}}$ where P_S is the transmit power of the sources, P_R is the transmit power of the relays, N_0 is the variance of the additive ZMCG noise at the sources and the relays, and G denotes the amplification gain at the relays. For fixed gain relays, $G = \sqrt{\frac{P_R}{P_S \mathbf{E}\left[|\tilde{g}_{1,n}|^2\right] + P_S \mathbf{E}\left[|\tilde{g}_{2,n}|^2\right] + N_0}}$, therefore the end-to-end SNR from S1 to S2 can be expressed as $\Upsilon_n = \frac{\eta_1 \eta_2 \gamma_{1,n} \gamma_{2,n}}{\eta_2 \gamma_{2,n} + \bar{C}}$ where $\gamma_{1,n} = |g_{1,n}|^2$, $\gamma_{2,n} = |g_{2,n}|^2$, $\eta_1 = \frac{P_S}{N_0}$, $\eta_2 = \frac{P_R}{N_0}$, $\bar{C} = \left(\eta_1 \left(\mathbf{E}\left[|\tilde{g}_{1,n}|^2\right] + \mathbf{E}\left[|\tilde{g}_{2,n}|^2\right]\right) + 1\right)$ and $\mathbf{E}[\cdot]$ denotes the expectation operator. Note that $\tilde{\gamma}_{1,n} = |\tilde{g}_{1,n}|^2$ and $\tilde{\gamma}_{2,n} = |\tilde{g}_{2,n}|^2$ are the corresponding channel power gains during the RS phase. For an i.i.d Rayleigh fading channel, $\tilde{\gamma}_{1,n}$ and $\tilde{\gamma}_{2,n}$ are i.i.d

exponential RVs with mean σ_1 and σ_2, respectively, $\forall\, n$. The PDF and CDF of an exponential RV X with mean μ is given as $f_X(x) = \frac{1}{\mu} e^{-\frac{x}{\mu}}$ and $F_X(x) = \left(1 - e^{-\frac{x}{\mu}}\right)$, respectively. Furthermore, following (4.1), it can be shown that $\tilde{\gamma}_{i,n}$ and $\gamma_{i,n}$ are two correlated exponential RVs and their joint PDF is given as [54]

$$f_{\tilde{\gamma}_{i,n},\gamma_{i,n}}(y,x) = \frac{1}{(1-\rho_i^2)\sigma_i^2} e^{-\frac{x+y}{(1-\rho_i^2)\sigma_i}} I_0\left(\frac{2\sqrt{\rho_i^2 x\, y}}{(1-\rho_i^2)\,\sigma_i}\right), \tag{4.2}$$

where, $i = 1$ denotes the S1 to relay link, $i = 2$ denotes the S2 to relay link and σ_i is the mean power of the source-i to relay link.

For opportunistic relaying, the E2E-SNR is given as

$$\Upsilon_{\mathcal{F}} = \frac{\eta_1 \eta_2 \gamma_{1,eq} \gamma_{2,eq}}{\eta_2 \gamma_{2,eq} + C} \tag{4.3}$$

where $C = (\eta_1 (\mathbf{E}[\tilde{\gamma}_{1,eq}] + \mathbf{E}[\tilde{\gamma}_{2,eq}]) + 1)$, $\gamma_{1,eq}$ is the effective instantaneous channel power gain of the S1 to relay link and $\gamma_{2,eq}$ is the effective instantaneous channel power gain of the S2 to relay link[1]. Both $\gamma_{1,eq}$ and $\gamma_{2,eq}$ depends on the RS criteria. In this chapter, the RS is done based on the Max-Min criteria where the selected relay is $k = \arg\max_i \{\min\{\tilde{\gamma}_{1,i}, \tilde{\gamma}_{2,i}\}\} = \arg\max_i \{\Lambda_i\}$. It can be noted that the RS criteria uses the past realization of the channel power gain.

4.3 Performance Analysis

In order to analyze the performance of the OTWRN-OC, the statistic (CDF and PDF) of $\Upsilon_{\mathcal{F}}$ are required[2].

[1] Without loss of generality, similar to (4.3), the E2E-SNR at S1 can be obtained by interchanging the indices 1 and 2. In this sequel, we present the performance analysis based on the E2E-SNR at S2. The performance at S1 can be obtained by interchanging the indices 1 and 2.

[2] Detailed derivations are available at http://arxiv.org/abs/1305.5913.

4.3.1 CDF and PDF of $\Upsilon_{\mathcal{F}}$

As $\Upsilon_{\mathcal{F}}$ depends on recent realizations $\gamma_{1,eq}$ and $\gamma_{2,eq}$ which are correlated with their past realization $\tilde{\gamma}_{1,eq}$ and $\tilde{\gamma}_{2,eq}$, therefore, first the CDF and PDF of $\tilde{\gamma}_{1,eq}$ and $\tilde{\gamma}_{2,eq}$ are derived. Following the steps given in Appendix 4.5.1, the CDF and the PDF of $\tilde{\gamma}_{1,eq}$ and $\tilde{\gamma}_{2,eq}$ can be obtained. Using the derived PDFs and CDFs in (4.12) and (4.13), and following the procedure in Appendix 4.5.2, the PDFs and CDFs of the equivalent channel power gain during the data transmission phase ($\gamma_{1,eq}$ and $\gamma_{2,eq}$) are obtained in (4.17) and (4.18). Using (4.3), the CDF of $\Upsilon_{\mathcal{F}}(\Phi) = \Pr\{\Upsilon_{\mathcal{F}} < \Phi\}$ is given by

$$F_{\Upsilon_{\mathcal{F}}}(\Phi) = \Pr\left\{\frac{\eta_1\eta_2\gamma_{1,eq}\gamma_{2,eq}}{\eta_2\gamma_{2,eq}+C} < \Phi\right\} = \Pr\left\{\gamma_{1,eq} < \frac{\Phi(\eta_2\gamma_{2,eq}+C)}{\eta_1\eta_2\gamma_{2,eq}}\right\}, \tag{4.4}$$

which can be evaluated by conditioning on $\gamma_{2,eq}$ and then averaging using the PDF of $\gamma_{2,eq}$ as

$$F_{\Upsilon_{\mathcal{F}}}(\Phi) = \int_0^\infty F_{\gamma_{1,eq}}\left(\frac{\Phi(\eta_2\gamma+C)}{\eta_1\eta_2\gamma}\right) f_{\gamma_{2,eq}}(\gamma)\, d\gamma. \tag{4.5}$$

Substituting the CDF of $\gamma_{1,eq}$ and PDF of $\gamma_{2,eq}$ into (4.5) and doing some algebraic manipulations one gets

$$F_{\Upsilon_{\mathcal{F}}}(\Phi) = \sum_{\mathcal{F}} \mathcal{X}_{\mathcal{F}}\left(1 - \Theta_2 e^{-\Theta_1\frac{\Phi}{\eta_1}}\int_0^\infty e^{-\Theta_2\gamma-\Theta_1\frac{\Phi C}{\eta_1\eta_2\gamma}} d\gamma\right), \tag{4.6}$$

where $\Theta_1 = \frac{\beta_{1,j_1,i_1}}{\left(\bar{v}_1\beta_{1,j_1,i_1}+\rho_1^2\right)}$, $\Theta_2 = \frac{\beta_{2,j_2,i_2}}{\left(\bar{v}_2\beta_{2,j_2,i_2}+\rho_2^2\right)}$, $\bar{v}_1 = (1-\rho_1^2)\sigma_1$, $\bar{v}_2 = (1-\rho_2^2)\sigma_2$, $\mathcal{X}_{\mathcal{F}} = R^2\binom{R-1}{i_1}\binom{R-1}{i_2}(-1)^{i_1+i_2}\alpha_{1,j_1,i_1}\alpha_{2,j_2,i_2}$ and $\sum_{i_1=0}^{R-1}\sum_{j_1=2}^{3}\sum_{i_2=0}^{R-1}\sum_{j_2=2}^{3}$ is represented using shorthand notation $\sum_{\mathcal{F}}$. Solving the integration using [96, Eq. (3.478.4)], yields

$$F_{\Upsilon_{\mathcal{F}}}(\Phi) = \sum_{\mathcal{F}} \mathcal{X}_{\mathcal{F}}\left(1 - 2e^{-\Theta_1\frac{\Phi}{\eta_1}}\sqrt{\frac{\Theta_1\Theta_2 C}{\eta_1\eta_2}}\Phi K_1\left(2\sqrt{\frac{\Theta_1\Theta_2 C}{\eta_1\eta_2}}\Phi\right)\right), \tag{4.7}$$

The PDF of $\Upsilon_{\mathcal{F}}$ can be obtained by taking the derivative of the CDF in (4.7). Using (4.7), various performance metric such as the MGF, outage probability, and SER can be derived.

4.3.2 Outage Probability:

Using the CDF in (4.7), the outage performance of the OTWRN-OC can be obtained as

$$\mathcal{O}(\Psi) = F_{\Upsilon_{\mathcal{F}}}(\Psi) \tag{4.8}$$

where $\Psi = 2^{\mathcal{R}} - 1$ and $\mathcal{R}$ is the transmission rate.

4.3.3 MGF and Symbol Error Rate Performance:

The MGF and the SER can be obtained using the CDF of the E2E-SNR [97]. We define function $S(\cdot,\cdot,\cdot)$ as

$$S(c_1, c_2, c_3) = c_1 \int_0^{\infty} x^{c_2} e^{-c_3 x} F_{\Upsilon_{\mathcal{F}}}(x) dx. \tag{4.9}$$

The MGF and the SER can be expressed in terms of $S(\cdot,\cdot,\cdot)$ i.e. MGF is give by $\mathcal{M}_{\Upsilon_{\mathcal{F}}}(s) = \mathcal{S}(s, 0, s)$, SER for non-coherent modulations is obtained as $\mathcal{P}_{e,\mathcal{NC}} = \mathcal{S}(a\,b, 0, b)$ and SER for coherent modulations is obtained as $\mathcal{P}_{e,\mathcal{C}} = \mathcal{S}\left(\frac{a}{2}\sqrt{\frac{b}{2\pi}}, -\frac{1}{2}, \frac{b}{2}\right)$. a and b are modulation-specific constants eg. for non-coherent modulations, $(a, b) = (0.5, 1)$ for DBPSK and $(a, b) = (0.5, 0.5)$ for NCBFSK, and for coherent modulations, $(a, b) = (1, 2)$ for BPSK, $(a, b) = (1, 1)$ for BFSK, $(a, b) = \left(2\frac{M-1}{M}, 6\frac{\log_2(M)}{M^2-1}\right)$ for M-PAM. The closed-form solution of $S(\cdot,\cdot,\cdot)$ is derived in Appendix 4.5.3. The solution in (4.20) involves a Gamma function and a Meijer-G function which are available in well known mathematical packages and thus, the SER performance can be easily and accurately evaluated.

4.4 Numerical Results and Discussion

In this section, some selected numerical results as well as Monte-Carlo based simulation results are presented to verify the derived analytical results. In obtaining

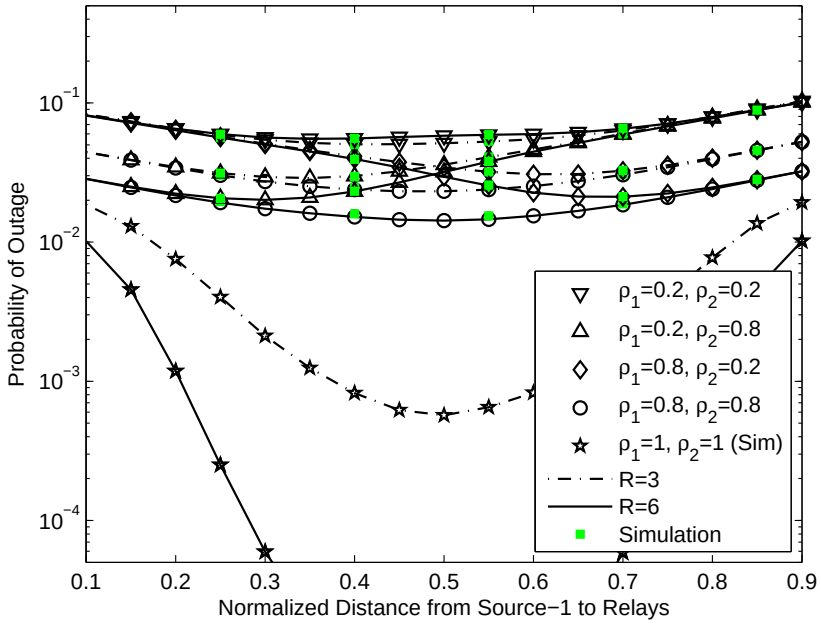

Figure 4.2: Probability of outage performance as a function of relay location where $\eta_1 = 15$ dB and $\upsilon = 3$.

these numerical results, $\mathcal{R} = 1$, $N_0 = 1$, $\eta_1 = \eta_2$. These parameters are fixed in the simulation unless stated. The effect of path-loss is captured by taking $\sigma_1 = d_1^{-\upsilon}$ and $\sigma_2 = d_2^{-\upsilon} = (1 - d_1)^{-\upsilon}$, where d_i is the distance of source-i from the relays and υ is the path-loss exponent. Note that the distances d_i are normalized w.r.t. the distance between both sources.

Fig. 5.2 shows the effect of varying the relay location on the outage probability performance of the . It can be observed that the performance degrades as the correlation, ρ_i, reduces. For the case when $\rho_1 = \rho_2 = 1$, the best performance is achieved when $d_1 = 0.5$, i.e. the relay is in the middle of both sources. If $\rho_1 < \rho_2$ or $\rho_1 > \rho_2$, $d_1 = 0.5$ does not give best outage performance. For $\rho_1 < \rho_2$, the outage probability can be lowered by reducing d_1 and vice-verse. Furthermore, it can be observed that increasing the number of relays improves the outage performance only if the correlation is sufficiently high. If the correlation is very low then, adding relays has no

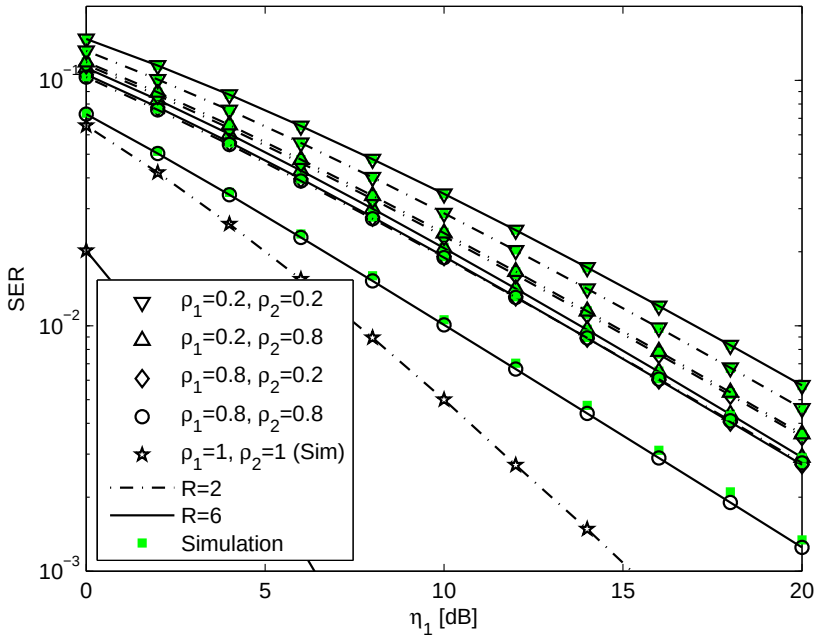

Figure 4.3: Symbol error rate performance of BPSK modulation where $d_1 = 0.5$ and $\upsilon = 3$.

benefit as can be observed for the case when $\rho_1 = \rho_2 = 0.2$.

Fig. 4.3 shows the SER of BPSK modulation scheme as a function of η_1 when the relays are in the middle of the sources i.e. $(d_1 = 0.5)$. It can be observed that when $\rho_i < 1$, the performance degrades severely and diversity is lost. Furthermore, SER increases as correlation decreases. Again it can be noticed that increasing the number of relays improves the performance only if the correlation is sufficiently high. When correlation is very less, adding relays can even degrade performance as can be observed for $\rho_1 = \rho_2 = 0.2$. The SER performance however, can be improved by varying d_1 and finding the optimal relay position. Note that, in both figures, the simulation results match well with the analytical results.

4.5 Appendix

4.5.1 CDF and PDF of $\tilde{\gamma}_{1,eq}$ and $\tilde{\gamma}_{2,eq}$

The CDF of $\tilde{\gamma}_{1,eq}$ can be obtained as

$$F_{\tilde{\gamma}_{1,eq}}(\Phi) = R\left(\Pr\left(\tilde{\gamma}_{1,n} < \Phi \bigcap \tilde{\gamma}_{1,n} > \tilde{\gamma}_{2,n} \bigcap n = k\right) + \Pr\left(\tilde{\gamma}_{1,n} < \Phi \bigcap \tilde{\gamma}_{1,n} < \tilde{\gamma}_{2,n} \bigcap n = k\right)\right). \tag{4.10}$$

Note that $n = k$ denotes that relay k is selected for transmission. $F_{\tilde{\gamma}_{1,eq}}(\cdot)$ can be expressed as

$$F_{\tilde{\gamma}_{1,eq}}(\Phi) = R\left(\int_0^{\Phi} f_{\tilde{\gamma}_{1,n}}(x) \int_0^{x} f_{\tilde{\gamma}_{2,n}}(y) \prod_{i\neq n} F_{\Lambda_i}(x)\, dydx + \int_0^{\Phi} f_{\tilde{\gamma}_{1,n}}(x) \prod_{i\neq n} F_{\Lambda_i}(x) \int_x^{\infty} f_{\tilde{\gamma}_{2,n}}(y)\, dydx\right) \tag{4.11}$$

where $f_{\tilde{\gamma}_{1,n}}(\cdot)$ and $f_{\tilde{\gamma}_{2,n}}(\cdot)$ denote the PDF of $\tilde{\gamma}_{1,n}$and $\tilde{\gamma}_{2,n}$, respectively and $F_{\Lambda_i}(x) = 1 - e^{-\left(\frac{1}{\sigma_1}+\frac{1}{\sigma_2}\right)x}$ denotes the CDF of Λ_i. Substituting the PDF and CDF in (4.11), using binomial expansion, integrating w.r.t y and x and doing some algebraic manipulations yields $F_{\tilde{\gamma}_{1,eq}}(\Phi)$ as

$$F_{\tilde{\gamma}_{1,eq}}(\Phi) = R\sum_{i=0}^{R-1}\sum_{j=1}^{3}\binom{R-1}{i}(-1)^i\,\alpha_{1,j,i}e^{-\beta_{1,j,i}\Phi} \tag{4.12}$$

where $\beta_{1,1,i} = 0$, $\beta_{1,2,i} = \frac{1}{\sigma_1}$, $\beta_{1,3,i} = \chi_i$, $\alpha_{1,1,i} = (\kappa_{1,1,i} - \kappa_{1,2,i})$, $\alpha_{1,2,i} = -\kappa_{1,1,i}$, $\alpha_{1,3,i} = \kappa_{1,2,i}$, $\kappa_{1,1,i} = \left(\sigma_2\left(\chi_i - \frac{1}{\sigma_1}\right)\right)^{-1}$, $\kappa_{1,2,i} = \left(\left(\sigma_1\sigma_2\left(\chi_i - \frac{1}{\sigma_1}\right)\chi_i\right)^{-1} - (\sigma_1\chi_i)^{-1}\right)$ and $\chi_i = \left(\frac{i+1}{\sigma_1} + \frac{i+1}{\sigma_2}\right)$. Taking the derivative of the CDF in (4.12) yields the PDF of $\tilde{\gamma}_{1,eq}$ as

$$f_{\tilde{\gamma}_{1,eq}}(\Phi) = R\sum_{i=0}^{R-1}\sum_{j=2}^{3}\binom{R-1}{i}(-1)^{i+1}\,\alpha_{1,j,i}\beta_{1,j,i}e^{-\beta_{1,j,i}\Phi}, \tag{4.13}$$

Similarly the expression for $F_{\tilde{\gamma}_{2,eq}}(\cdot)$ and $f_{\tilde{\gamma}_{2,eq}}(\cdot)$ can be obtained by interchanging indices 1 and 2. The mean of $\tilde{\gamma}_{q,eq}$, where $q \in \{1,2\}$, is given as

$$\mathbf{E}\left[\tilde{\gamma}_{q,eq}\right] = R\sum_{i=0}^{R-1}\sum_{j=2}^{3}\binom{R-1}{i}(-1)^{i+1}\,\frac{\alpha_{q,j,i}}{\beta_{q,j,i}} \tag{4.14}$$

4.5.2 CDF and PDF of $\gamma_{1,eq}$ and $\gamma_{2,eq}$

The PDF of $\gamma_{1,eq}$, $f_{\gamma_{1,eq}}(\cdot)$, can be obtained as

$$f_{\gamma_{1,eq}}(x) = \int_0^\infty f_{\tilde{\gamma}_{1,eq},\gamma_{1,eq}}(y,x)\,dy \tag{4.15}$$

where $f_{\tilde{\gamma}_{1,eq},\gamma_{1,eq}}(\cdot,\cdot)$ is the joint PDF of $\gamma_{1,eq}$ and $\tilde{\gamma}_{1,eq}$

$$\begin{aligned} f_{\tilde{\gamma}_{1,eq},\gamma_{1,eq}}(y,x) = R\sum_{i=0}^{R-1}\sum_{j=2}^{3}\binom{R-1}{i}(-1)^{i+1}\nu_1 \times \\ \alpha_{1,j,i}\beta_{1,j,i}e^{-\nu_1 x-\left(\beta_{1,j,i}+\rho_1^2\nu_1\right)y} I_0\left(2\sqrt{\rho_1^2\nu_1^2 x\,y}\right) \end{aligned} \tag{4.16}$$

where $\nu_1 = \frac{1}{(1-\rho_1^2)\sigma_1}$. Substituting the joint PDF from (4.16) into (4.15) and solving the resulting integration using [96]

$$f_{\gamma_{1,eq}}(x) = R\sum_{i=0}^{R-1}\sum_{j=2}^{3}\binom{R-1}{i}(-1)^{i+1}\frac{\nu_1\alpha_{1,j,i}\beta_{1,j,i}}{(\beta_{1,j,i}+\rho_1^2\nu_1)}e^{-\frac{\nu_1\beta_{1,j,i}}{\left(\beta_{1,j,i}+\rho_1^2\nu_1\right)}x} \tag{4.17}$$

Integrating $f_{\gamma_{1,eq}}(\cdot)$ yields CDF, $F_{\gamma_{1,eq}}(\cdot)$, as

$$F_{\gamma_{1,eq}}(x) = R\sum_{i=0}^{R-1}\sum_{j=2}^{3}\binom{R-1}{i}(-1)^{i+1}\alpha_{1,j,i}\left(1-e^{-\frac{\nu_1\beta_{1,j,i}}{\left(\beta_{1,j,i}+\rho_1^2\nu_1\right)}x}\right) \tag{4.18}$$

The CDF and PDF of $\gamma_{2,eq}$ can be obtained by interchanging indices 1 and 2.

4.5.3 Closed Form Solution of $S(c_1, c_2, c_3)$

$S(\cdot,\cdot,\cdot)$ is defined as

$$S(c_1,c_2,c_3) = c_1\int_0^\infty x^{c_2}e^{-c_3 x}F_{\Upsilon_{\mathcal{F}}}(x)dx \tag{4.19}$$

Substituting the CDF from (4.7) into (4.19), representing $K_1(\cdot)$in terms of Meijer-G function [98, Eq. (03.04.26.0008.01)], solving the integration using [96, Eq. (7.813.1)] and applying the scaling property yields

$$\begin{aligned} \mathcal{S}(c_1,c_2,c_3) = c_1\sum_{\mathcal{F}}\mathcal{X}_{\mathcal{F}}\left(c_3^{-1-c_2}\Gamma(1+c_2) - \right. \\ \left.\left(\frac{\Theta_1\Theta_2 C}{\eta_1\eta_2}\right)^{-c_2-1} G_{1,2}^{2,1}\left(\left(c_3+\frac{\Theta_1}{\eta_1}\right)^{-1}\frac{\Theta_1\Theta_2 C}{\eta_1\eta_2}\middle| \begin{matrix} 1,- \\ c_2+2, c_2+1 \end{matrix}\right)\right) \end{aligned} \tag{4.20}$$

where $G_{p,q}^{m,n}(\cdot)$ is the Meijer-G function defined in [96, Eq. (9.301)].

Chapter 5

Performance of Power Limited Cognitive Network with TAS/MRC

5.1 Introduction

Similar to point-to-point communication systems, the performance of cognitive radio networks can be improved by spatial diversity. In this chapter, a MIMO cognitive system (MCS) in an underlay setting is considered. The SU-Rx is assumed to combine the received signals using MRC. The performance of the MCS is studied when the SU-Tx has limited peak transmit power and employs AS. Interference from the primary network to the secondary network is also taken into account and two scenarios are considered; 1) the MIMO cognitive system with TAS/MRC (MCS-TM) does not experience interference from the primary network (denote by MCS-TM-NI), and 2) MCS-TM does experience interference from the primary network (denote by MCS-TM-WI). For both these systems, exact closed-form expressions for the outage probability are derived. A new and simple expression of the CDF of the output SNR

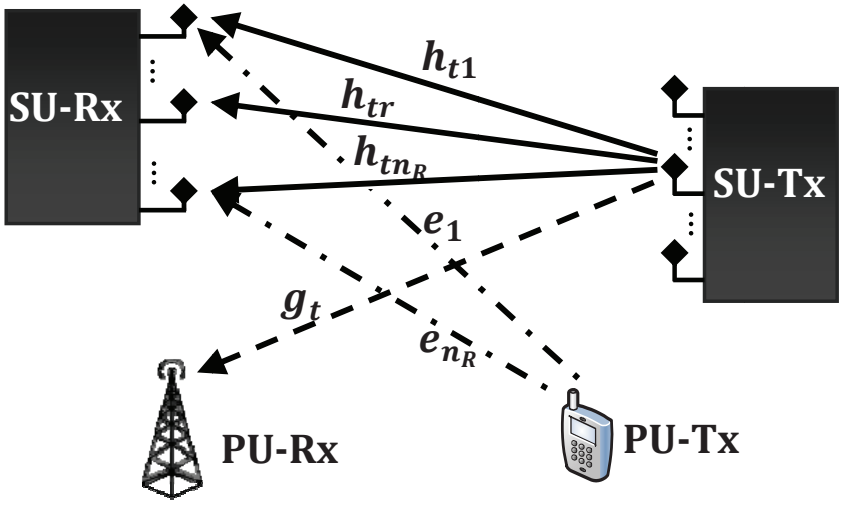

Figure 5.1: System Model.

for the MCS-TM-NI is also obtained. Using this CDF expression, closed-form expressions are obtained for the PDF, the q-th moment and the MGF of the output SNR. Additionally, exact closed-form expressions characterizing the SER performance and the ergodic capacity are also obtained. Furthermore, a precise lower bound on the ergodic capacity at high SNR is also derived. Furthermore, the performance of the MCS-TM-NI is analyzed in the asymptotic regimes. Numerical simulation results which verify the analytical results are also presented.

5.2 System Model

Consider an underlay secondary network with one transmitter and one receiver which are operating in the presence of a primary network with a single primary transmitter (PU-Tx) and a single primary receiver (PU-Rx) as shown in Fig. 5.1. The SU-Tx is equipped with n_T antennas and the SU-Rx is equipped with n_R antennas. However, both the PU-Tx and the PU-Rx are assumed to have a single antenna. The channel is assumed to have independent and identically distributed (i.i.d.) Rayleigh

fading. The channel power gain between the t-th antenna of the SU-Tx and the r-th antenna of the SU-Rx is denoted by h_{tr}. Similarly, the channel power gain between the antenna of the PU-Tx and the r-th antenna of the SU-Rx is denoted by e_r and the channel power gain between the t-th antenna of the SU-Tx and the antenna of the PU-Rx is denoted by g_t. In case of Rayleigh channel, h_{tr}, e_r and g_t are exponential random variables with means λ_t, ν and μ_t, respectively. The PDF and CDF of an exponential random variable X with mean ω can be expressed as $f_X(x) = \frac{1}{\omega} e^{-\frac{x}{\omega}} U(x)$ and $F_X(x) = \left(1 - e^{-\frac{x}{\omega}}\right) U(x)$, respectively, where $f_X(\cdot)$ denotes the PDF of X, $F_X(\cdot)$ denotes the CDF of X and $U(x)$ denotes the unit step function.

5.2.1 Power Allocation

The primary network requires that the interference caused by the secondary network is below a threshold Q. Moreover, the SU-Tx cannot transmit using a power greater than P_{max}. Thus, the power allocation policy for the t-th antenna at the SU-Tx can be expressed as

$$P_T(t) = \min\left\{P_{max}, \frac{Q}{g_t}\right\}. \tag{5.1}$$

5.2.2 Antenna Selection & Output SNR

In the TAS/MRC scheme, the signal is transmitted by the SU-Tx using a single antenna where the antenna selection is done based on the output SNR and the signals received at the SU-Rx antennas are combined using MRC. Thus, in this case, the output SNR for the t-th antenna can be expressed as

$$\gamma_T(t) = \min\left\{P_{max}, \frac{Q}{g_t}\right\} \frac{1}{N_0} \sum_{r=1}^{n_R} |h_{tr}|^2 = \min\left\{P_{max}, \frac{Q}{g_t}\right\} \frac{\eta_t}{N_0}. \tag{5.2}$$

η_t is a sum of i.i.d exponential random variables, thus, its PDF is

$$f_{\eta_t}(x) = \frac{1}{\lambda_t^{n_R}\Gamma(n_R)} x^{n_R-1} e^{-\frac{x}{\lambda_t}} U(x), \tag{5.3}$$

where $\Gamma(\cdot)$ is the Gamma function [96, Eq. (8.310.1)]. The selected antenna $\bar{t}$, can be obtained from $\gamma_T(t)$ as

$$\bar{t}_T = \arg\max_t \left\{ \min\left\{ P_{max}, \frac{Q}{g_t} \right\} \frac{\eta_t}{N_0} \right\}, \tag{5.4}$$

and the output SNR for the MCS can be expressed as

$$\gamma_\epsilon = \max_t \left\{ \min\left\{ P_{max}, \frac{Q}{g_t} \right\} \frac{\eta_t}{N_0} \right\}. \tag{5.5}$$

Note that the antenna selection is done on the basis of output SNR and it does not take into account the interference from the PU-Tx and is thus, a sub-optimal selection scheme. However, this selection scheme has lower complexity as it does not require the CSI of the interference link from the PU-Tx, resulting in a lower overhead/feedback.

In the following sections the performance analysis of the MCS-TM-NI and MCS-TM-WI employing antenna selection according to (5.4) is presented.

5.3 MIMO Secondary Network without Interference

For the MCS-TM-NI where the SU-RX does not experience interference from the PU-Tx, the output SNR is given by γ_ϵ in (5.5). In order to analyze the performance of this system, the statistics (PDF and the CDF) of γ_ϵ are required.

5.3.1 Statistics of the Output SNR

In order to obtain the CDF expression of γ_ϵ, the CDF expression of the output SNR for the t-th antenna, $F_{\gamma_T(t)}(\cdot)$, is required and is given by following remark.

Remark 1. *The CDF of the output SNR for the t-th antenna for the MCS-TM-NI is given as*

$$F_{\gamma_T(t)}(x) = 1 - e^{-\frac{N_0}{\lambda_t P_{max}}x} \sum_{m=0}^{n_R-1} \frac{\left(\frac{N_0}{\lambda_t}\right)^m x^m}{m! P_{max}^m} \left(1 - \left(\frac{N_0}{\lambda_t Q}\right)^{n_R-m} e^{-\frac{Q}{\mu_t P_{max}}} \frac{x^{n_R-m}}{\left(\frac{1}{\mu_t} + \frac{N_0}{Q\lambda_t}x\right)^{n_R-m}}\right). \tag{5.6}$$

Proof. See Appendix 5.6.1. □

An expression for the CDF of $\gamma_T(t)$ has been derived previously [74, Eq. (5)]. However, the CDF expression derived in [74, Eq. (5)] is different from the one obtained in (5.6). As we will see in what follows, Eq. (5.6) can be used to derive an alternate representation of the CDF of the output SNR for the MCS-TM-NI which leads to a tractable performance analysis. For an i.i.d channel, the CDF of the output SNR for the MCS-TM-NI can be obtained from $F_{\gamma_T(t)}(\cdot)$ and is given as.

$$F_{\gamma_\epsilon}(x) = \left(1 - e^{-\frac{N_0}{\lambda_t P_{max}}x} \sum_{m=0}^{n_R-1} \frac{\left(\frac{N_0}{\lambda_t}\right)^m}{m! P_{max}^m} x^m \left(1 - \left(\frac{N_0}{\lambda_t Q}\right)^{n_R-m} e^{-\frac{Q}{\mu_t P_{max}}} \frac{x^{n_R-m}}{\left(\frac{1}{\mu_t} + \frac{N_0}{Q\lambda_t}x\right)^{n_R-m}}\right)\right)^{n_T}. \tag{5.7}$$

For the case of limited transmit power, no expression for the CDF of γ_ϵ was derived in [74]. Therefore, for the limited transmit power case, we derive an alternate expression

for the CDF of γ_ϵ in (5.7) which leads to a tractable performance analysis of the MCS-TM-NI and is given by Remark 2.

Remark 2. *For a MCS-TM-NI having limited transmit power, an alternate expression of the CDF of the output SNR in* (5.7)*, which is helpful in obtaining the exact closed form expressions for the MGF, SER and ergodic capacity, is given as*

$$F_{\gamma_\epsilon}(x) = 1 + \sum_{\mathcal{F}} \Delta_{\mathcal{F}} \frac{x^{\Xi_A} e^{-\Xi_B x}}{(x+\xi)^{\Xi_C}}. \tag{5.8}$$

where $\Xi_A = \sum_{l=1}^{k} m_l + (n_R - m_l)w_l$, $\Xi_B = \frac{N_0}{\lambda_t P_{max}} k$, $\xi = \frac{Q\lambda_t}{N_0 \mu_t}$, $\Xi_C = \sum_{l=1}^{k}(n_R - m_l)w_l$, $\Delta_{\mathcal{F}} = \kappa_k^A \kappa_{k,m}^B \kappa_{w,m,k}^C$, $\kappa_k^A = \binom{n_T}{k}(-1)^k$, $\kappa_{k,m}^B = \prod_{l=1}^{k} \frac{\left(\frac{N_0}{\lambda_t}\right)^{m_l}}{m_l! P_{max}^{m_l}}$, $\kappa_{w,m,k}^C = \prod_{l=1}^{k}(-1)^{w_l} e^{-\frac{Q}{\mu_t P_{max}} w_l}$, $\sum_{\mathcal{F}}$ *is short hand notation for* $\sum_{k=1}^{n_T} \sum_{\mathbf{m}} \sum_{\boldsymbol{w} \in \theta_k}$, θ_k *is the set of all possible* k *bit binary numbers and* w_l *is the* l*th bit of the binary number* $\mathbf{w} \in \theta_k$ *and* $\sum_{\mathbf{m}}$ *is shorthand notation of* $\sum_{m_1=0}^{n_R-1} \sum_{m_2=0}^{n_R-1} \cdots \sum_{m_k=0}^{n_R-1}$.

Proof. See Appendix 5.6.2. □

Using (5.8) the outage performance of the MCS-TM-NI can be obtained. Indeed, as we will see in what follows, using the CDF expression in (5.8), we derive various performance measures in the next section.

Remark 3. *For a MCS-TM-NI having limited transmit power, an alternate expression of the PDF of the output SNR is given as*

$$f_{\gamma_\epsilon}(x) = \sum_{\mathcal{F}} \Delta_{\mathcal{F}} \left(\Xi_A \frac{x^{\Xi_A - 1} e^{-\Xi_B x}}{(x+\xi)^{\Xi_C}} - \Xi_B \frac{x^{\Xi_A} e^{-\Xi_B x}}{(x+\xi)^{\Xi_C}} - \Xi_C \frac{x^{\Xi_A} e^{-\Xi_B x}}{(x+\xi)^{\Xi_C + 1}} \right). \tag{5.9}$$

Proof. $f_{\gamma_\epsilon}(x)$ is obtained by taking derivative of $F_{\gamma_\epsilon}(x)$ in (5.8). □

It follows that the PDF in (5.9) can be used to obtain the moments of the output SNR.

Remark 4. *For a MCS-TM-NI with limited transmit power, the q-th moment of the output SNR is given by*

$$\begin{aligned}\varphi_q = \sum_{\mathcal{F}} \Delta_{\mathcal{F}} \left(\Xi_A \mathcal{I}(\Xi_A - 1 + q, \Xi_C, \Xi_B, \xi)\right. \\ \left. -\Xi_B \mathcal{I}(\Xi_A + q, \Xi_C, \Xi_B, \xi) - \Xi_C \mathcal{I}(\Xi_A + q, \Xi_C + 1, \Xi_B, \xi)\right),\end{aligned} \tag{5.10}$$

where $q > 0$ and $\mathcal{I}(\alpha_1, \alpha_2, \alpha_3, \xi)$ is given in (5.63) *derived in Appendix 5.6.4.*

Proof. The q-th moment is obtained using

$$\varphi_q = \mathbf{E}\left[\gamma_\epsilon^q\right] = \int_0^\infty x^q f_{\gamma_\epsilon}(x) dx. \tag{5.11}$$

Substituting the PDF from (5.9) into (5.11) and after doing some algebraic manipulations yields

$$\begin{aligned}\varphi_q = \sum_{\mathcal{F}} \Delta_{\mathcal{F}} \left(\Xi_A \int_0^\infty \frac{x^{\Xi_A - 1 + q} e^{-\Xi_B x}}{(x+\xi)^{\Xi_C}} dx \right. \\ \left. -\Xi_B \int_0^\infty \frac{x^{\Xi_A + q} e^{-\Xi_B x}}{(x+\xi)^{\Xi_C}} dx - \Xi_C \int_0^\infty \frac{x^{\Xi_A + q} e^{-\Xi_B x}}{(x+\xi)^{\Xi_C + 1}} dx\right).\end{aligned} \tag{5.12}$$

Eq. (5.12) can be represented in form of (5.10), where $\mathcal{I}(\alpha_1, \alpha_2, \alpha_3, \xi) = \int_0^\infty \frac{x^{\alpha_1} e^{-\alpha_3 x}}{(x+\xi)^{\alpha_2}} dx$, with $\alpha_1 > -1$ and $\alpha_3 > 0$. □

Eq. (5.10) can also be used to calculate the zeroth moment. Note that $\mathcal{I}(\alpha_1, \alpha_2, \alpha_3, \xi)$ is only defined for $\alpha_1 > -1$. In (5.10), $\alpha_1 = -1$ only occurs for the term $\mathcal{I}(\Xi_A - 1 + q, \Xi_C, \Xi_B, \xi)$ when $\Xi_A = 0$ and $q = 0$. In this case the term $\mathcal{I}(\Xi_A - 1 + q, \Xi_C, \Xi_B, \xi)$ is being multiplied with Ξ_A which results in a zero. Therefore, (5.10) can be accurately evaluated for $q = 0$ by replacing $\mathcal{I}(\Xi_A - 1 + q, \Xi_C, \Xi_B, \xi)$ with any constant c, when $\Xi_A = 0$.

5.3.2 Performance Analysis Measures

Moment Generating Function

The MGF of the output SNR can be obtained using the CDF as [99, Eq. (18)]

$$\mathcal{M}(s) = s \int_0^\infty e^{-sx} F_{\gamma_\epsilon}(x) dx. \tag{5.13}$$

Substituting the CDF from (5.8) into (5.13), it gives

$$\mathcal{M}(s) = s \int_0^\infty e^{-sx} dx + s \int_0^\infty \sum_{\mathcal{F}} \Delta_{\mathcal{F}} \frac{x^{\Xi_A} e^{-(\Xi_B+s)x}}{(x+\xi)^{\Xi_C}} dx. \tag{5.14}$$

Substituting $z = x + \xi$ in the second term on the right hand side of (5.14) and using binomial expansion with some algebraic manipulations yields

$$\mathcal{M}(s) = s \int_0^\infty e^{-sx} dx + \sum_{\mathcal{F}} \Delta_{\mathcal{F}} s \int_\xi^\infty \frac{1}{z^{\Xi_C}} \sum_{n=0}^{\Xi_A} \binom{\Xi_A}{n} z^n (-\xi)^{\Xi_A - n} e^{-(\Xi_B+s)(z-\xi)} dz. \tag{5.15}$$

By solving the integral, the closed form MGF of the output SNR of the MCS-TM-NI can be obtained as

$$\begin{aligned} \mathcal{M}(s) = 1 + \sum_{\mathcal{F}} \sum_{n=0}^{\Xi_A} \binom{\Xi_A}{n} (-\xi)^{\Xi_A - n} \Delta_{\mathcal{F}} \times \\ s\, e^{(\Xi_B+s)\xi} \left(\Xi_B + s\right)^{-1+\Xi_C-n} \Gamma\left(1 - \Xi_C + n, \left(\Xi_B + s\right)\xi\right). \end{aligned} \tag{5.16}$$

The MGF in (5.16) involves an exponential function and a Gamma function which are available in well known mathematical packages and thus, it can be easily evaluated. The MGF in (5.16) can be used to obtain moments of the output SNR and can also

be used to derive different performance measures such as the SER [2].

Symbol Error Rate Performance

The average symbol error rate can be obtained using the CDF of output SNR as [97]

$$\mathcal{P}_e = -\int_0^\infty \bar{P}'_e(x) F_{\gamma_\epsilon}(x) dx, \tag{5.17}$$

where $\mathcal{P}_e$ is the average symbol error rate, $\bar{P}'_e(x) = \frac{\partial P_e(\cdot)}{\partial x}$ is the derivative of the conditional error probability (CEP) $P_e(\cdot)$ and $F_{\gamma_\epsilon}(\cdot)$ denotes the CDF of the output SNR (γ_ϵ). The SER performance of the MCS-TM-NI can be derived for various modulation formats depending on its CEP form [97].

Coherent Binary Modulations and M-PAM Modulation: The conditional error probability (CEP) for coherent binary phase-shift-keying (BPSK), coherent binary frequency-shift-keying (BFSK) and M-ary pulse amplitude modulation (M-PAM) can be represented as

$$P_{e,\mathcal{C}}(x) = aQ(\sqrt{bx}), \tag{5.18}$$

where $(a, b) = (1, 2)$ for BPSK, $(a, b) = (1, 1)$ for BFSK, $(a, b) = \left(2\frac{M-1}{M}, 6\frac{\log_2(M)}{M^2-1}\right)$ for M-PAM and $Q(\cdot)$ denotes the Gaussian Q-function [94].

The unconditional SER for these modulation schemes can be found as

$$\mathcal{P}_{e,\mathcal{C}} = \frac{a}{2}\sqrt{\frac{b}{2\pi}} \int_0^\infty \frac{1}{\sqrt{x}} e^{-\frac{b}{2}x} F_{\gamma_\epsilon}(x) dx. \tag{5.19}$$

Substituting the CDF from (5.8) into (5.19), $P_{e,C}$ can be given by

$$\mathcal{P}_{e,\mathcal{C}} = \frac{a}{2}\sqrt{\frac{b}{2\pi}} \int_0^\infty \frac{1}{\sqrt{x}} e^{-\frac{b}{2}x} dx + \frac{a}{2}\sqrt{\frac{b}{2\pi}} \int_0^\infty \frac{1}{\sqrt{x}} e^{-\frac{b}{2}x} \sum_{\mathcal{F}} \Delta_{\mathcal{F}} \frac{x^{\Xi_A} e^{-\Xi_B x}}{(x+\xi)^{\Xi_C}} dx. \tag{5.20}$$

Substituting $z = x + \xi$ in the second integral term in (5.20) yields

$$\mathcal{P}_{e,\mathcal{C}} = \frac{a}{2} + \frac{a}{2}\sqrt{\frac{b}{2\pi}} \sum_{\mathcal{F}} \Delta_{\mathcal{F}} e^{\left(\Xi_B + \frac{b}{2}\right)\xi} \int_{\xi}^{\infty} z^{-\Xi_C} \left(z - \xi\right)^{\Xi_A - \frac{1}{2}} e^{-\left(\Xi_B + \frac{b}{2}\right)z}. \tag{5.21}$$

Using [96, Eq. (3.383.4)] the integral in (5.21) can be solved to give

$$\begin{aligned} \mathcal{P}_{e,\mathcal{C}} = \frac{a}{2} + \frac{a}{2}\sqrt{\frac{b}{2\pi}} \sum_{\mathcal{F}} \Delta_{\mathcal{F}} \Gamma\left(\Xi_A + \frac{1}{2}\right) \left(\Xi_B + \frac{b}{2}\right)^{-\frac{1}{2}\left(\Xi_A - \Xi_C + \frac{3}{2}\right)} \times \\ \xi^{\frac{1}{2}\left(\Xi_A - \Xi_C - \frac{1}{2}\right)} e^{\frac{\xi}{2}\left(\Xi_B + \frac{b}{2}\right)} W_{\vartheta_1, \vartheta_2}\left(\left(\Xi_B + \frac{b}{2}\right)\xi\right), \end{aligned} \tag{5.22}$$

where $\vartheta_1 = \frac{1}{2}\left(-\Xi_C - \Xi_A + \frac{1}{2}\right)$, $\vartheta_2 = \frac{1}{2}\left(-\Xi_A + \Xi_C - \frac{1}{2}\right)$, $W_{\lambda,\mu}(z)$ is the WhittakerW function defined in [96, Eq. (9.220.4)]. Eq. (5.22) gives a closed form expression involving an exponential function, Gamma function and a WhittakerW function which are available in well known mathematical packages and thus, it can be used evaluate the performance of coherent binary modulations as well as M-PAM modulation schemes for a MCS-TM-NI.

Non-Coherent Modulations: The conditional error probability (CEP) for differential binary phase-shift-keying (DBPSK) and non-coherent binary frequency-shift-keying (NCBFSK) can be represented as

$$P_{e,\mathcal{NC}}(x) = ae^{-bx}, \tag{5.23}$$

where $(a, b) = (0.5, 1)$ for DBPSK and $(a, b) = (0.5, 0.5)$ for NCBFSK. The SER for non-coherent modulations can be obtained using

$$\mathcal{P}_{e,\mathcal{NC}} = a\,b \int_0^{\infty} e^{-bx} F_{\gamma_\epsilon}(x) dx = a\,b \frac{\mathcal{M}(s)}{s}\bigg|_{s=b}. \tag{5.24}$$

Subsituting the MGF from (5.16) into (5.24) yields

$$\mathcal{P}_{e,\mathcal{NC}} = a\left(1+\sum_{\mathcal{F}}\sum_{n=0}^{\Xi_A}\binom{\Xi_A}{n}(-\xi)^{\Xi_A-n}\Delta_{\mathcal{F}}\times \right. \\ \left. e^{(\Xi_B+b)\xi}b\left(\Xi_B+b\right)^{-1+\Xi_C-n}\Gamma\left(1-\Xi_C+n,\left(\Xi_B+b\right)\xi\right)\right). \tag{5.25}$$

Eq. (5.25) involves an exponential function and a Gamma function which are available in well known mathematical packages and thus, it can be easily evaluated. Thus, Eq. (5.25) gives a closed form expression to evaluate the performance of various non-coherent modulation schemes for a MCS-TM-NI. For example setting $(a,b)=(0.5,1)$, the SER performance of DBPSK modulation scheme is obtained.

Ergodic Capacity

The ergodic capacity of a MCS-TM-NI can be derived using the CDF of γ_ϵ as [100]

$$C = \frac{\log_2(e)}{B}\int_0^\infty \ln\left(1+x\right) f_{\gamma_\epsilon}(x)dx = \frac{\log_2(e)}{B}\int_0^\infty \frac{1-F_{\gamma_\epsilon(x)}}{(x+1)}dx. \tag{5.26}$$

After substituting the CDF from (5.8) into (5.26) and solving the resulting expression, the ergodic capacity is given in Remark 3.

Remark 5. *For a MCS-TM-NI having limited transmit power, the ergodic capacity, is given as*

$$C = -\frac{\log_2(e)}{B}\sum_{\mathcal{F}}\sum_{v_1=1}^{v}\sum_{v_2=1}^{\delta_{v_1}}\Delta_{\mathcal{F}}\kappa^D_{v_1,v_2}\bar{\zeta}_{v_1}^{\Xi_A-v_2+1}\frac{1}{\Gamma\left(v_2\right)}G^{2,1}_{1,2}\left(\Xi_B\bar{\zeta}_{v_1}\middle|\begin{matrix}-\Xi_A\\ -\Xi_A+v_2-1,0\end{matrix}\right), \tag{5.27}$$

where $\kappa^D_{v_1,v_2}$ *can be obtained recursively using* (5.68) *and* $G^{m,n}_{p,q}(\cdot)$ *is the Meijer-G function defined in [96, Eq. (9.301)].*

Proof. See Appendix 5.6.4. □

Eq. (5.27) involves a Gamma function and a Meijer-G function which are available in well known mathematical packages and thus, it can be easily evaluated to yield the ergodic capacity of a MCS-TM-NI.

5.3.3 Asymptotic Performance Analysis

The exact closed-form expressions for the outage performance, SER, and the ergodic capacity obtained in the previous section do not yield much insight about the performance with varying system parameters. Thus, in this section, the outage and SER performance of the MCS-TM-NI is analyzed for asymptotic regimes.

Asymptotic Outage Performance

- $P_{max} \to \infty$

  As $P_{max} \to \infty$, it can be shown that the CDF in (5.7) can be expressed as

$$F_{\gamma_\epsilon}^{floor}(x) = \left(1 - \left(1 - \left(\frac{N_0}{\lambda_t Q}\right)^{n_R} \frac{x^{n_R}}{\left(\frac{1}{\mu_t} + \frac{N_0}{Q\lambda_t}x\right)^{n_R}}\right)\right)^{n_T}, \tag{5.28}$$

  which can be simplified to give

$$F_{\gamma_\epsilon}^{floor}(x) = \left(1 + \frac{Q}{N_0}\frac{\lambda_t}{\mu_t}\frac{1}{x}\right)^{-n_R n_T}. \tag{5.29}$$

  Therefore, for fixed x as $P_{max} \to \infty$, the probability that a MCS-TM-NI is in outage becomes constant and is given by (5.29). Note that the value of the floor depends on the product $n_T n_R$. Therefore a system with $(n_T, n_R) = (x, y)$ and $(n_T, n_R) = (y, x)$ will have the same floor.

- $P_{max} \to \infty$ & $\frac{\lambda_t}{\mu_t} \to \infty$

  If the interference link is very poor and the secondary link is very good i.e. $\frac{\lambda_t}{\mu_t} \to \infty$, the probability of outage is can be derived from (5.29) as

$$F_{\gamma_\epsilon}^{\infty}(x) = x^{n_R n_T} \left(\frac{Q}{N_0}\right)^{-n_R n_T} \left(\frac{\lambda_t}{\mu_t}\right)^{-n_R n_T}. \tag{5.30}$$

  It can be noted from (5.30) that the outage probability reduces with increasing $\frac{\lambda_t}{\mu_t}$ with a slope of $n_T n_R$ in the log scale.

- *Generalized Diversity Gain*

  Using the concept of generalized diversity gain, which was introduced in [101], the diversity of the secondary link can be obtained. The generalized diversity gain is defined as

$$d = \lim_{\mu_t \to 0} \frac{\log\left(F_{\gamma_\epsilon}^{\infty}(x)\right)}{\log\left(\mu_t\right)}. \tag{5.31}$$

  Substituting (5.30) into (6.18), it can be concluded that the diversity gain for a MCS-TM-NI in the asymptotic regime is $n_T n_R$. This implies that, when the total number of antennas is fixed i.e. $n_R + n_T = \bar{\varphi}$, where $\bar{\varphi}$ is some constant, the number of antennas should be divided equally over the transmitter and receiver, i.e. $n_T = n_R$, to get the highest diversity gain.

Asymptotic SER Performance

Coherent Binary Modulations and M-PAM Modulation:

- $P_{max} \to \infty$

  The SER for coherent modulation schemes as $P_{max} \to \infty$ can be obtained using

$F_{\gamma_\epsilon}^{floor}(\cdot)$ as

$$\mathcal{P}_{e,\mathcal{C}}^{floor} = \frac{a}{2}\sqrt{\frac{b}{2\pi}}\int_0^\infty \frac{1}{\sqrt{x}} e^{-\frac{b}{2}x} F_{\gamma_\epsilon}^{floor}(x)dx. \tag{5.32}$$

Substituting the CDF from (5.29) into (5.32), making transformation of variable $z = x + \xi$, and solving the resulting integral using [96, Eq. (3.383.4)], the asymptotic SER performance for coherent binary and M-PAM modulation schemes is given as

$$\mathcal{P}_{e,\mathcal{C}}^{floor} = \frac{a e^{\frac{b}{4}\xi}}{2\sqrt{\pi}} \left(\frac{b}{2}\xi\right)^{-\frac{1}{4}} \Gamma\left(n_R n_T + \frac{1}{2}\right) W_{-n_R n_T + \frac{1}{4}, -\frac{1}{4}}\left(\frac{b}{2}\xi\right). \tag{5.33}$$

Therefore, as $P_{max} \to \infty$, the probability of error for a MCS-TM-NI becomes constant and is given by (5.33).

- $P_{max} \to \infty$ & $\frac{\lambda_t}{\mu_t} \to \infty$

  If the interference link is very poor and the secondary link is very good i.e. $\frac{\lambda_t}{\mu_t} \to \infty$, the probability of error for coherent modulations is given as

$$\mathcal{P}_{e,\mathcal{C}}^{\infty} = \frac{a}{2}\sqrt{\frac{b}{2\pi}}\int_0^\infty \frac{1}{\sqrt{x}} e^{-\frac{b}{2}x} F_{\gamma_\epsilon}^{\infty}(x)dx. \tag{5.34}$$

Substituting the CDF from (5.30) into (5.34), and solving the resulting integral using [96, Eq. (3.381.4)], yields

$$\mathcal{P}_{e,\mathcal{C}}^{\infty} = \frac{a\left(\frac{b}{2}\right)^{-n_R n_T}\Gamma\left(n_R n_T + \frac{1}{2}\right)}{2\sqrt{\pi}} \left(\frac{Q}{N_0}\right)^{-n_R n_T} \left(\frac{\lambda_t}{\mu_t}\right)^{-n_R n_T}. \tag{5.35}$$

It can be noted from (5.35) that the SER reduces with increasing $\frac{\lambda_t}{\mu_t}$ with a slope of $n_T n_R$ in the log scale. Thus, similar to the outage probability, for a fixed number of antennas, the number of antennas should be divided equally over the transmitter and receiver, i.e. $n_T = n_R$, to get the best performance in

the asymptotic regime.

Non-Coherent Modulations:

- $P_{max} \to \infty$

  Following a similar approach, the SER for non-coherent modulation schemes as $P_{max} \to \infty$ is given as

$$\mathcal{P}_{e,\mathcal{NC}}^{floor} = a\Gamma\left(n_R n_T + 1\right) e^{\frac{\xi}{2}b} W_{-n_R n_T, -\frac{1}{2}}\left(b\xi\right). \tag{5.36}$$

  Therefore, as $P_{max} \to \infty$, the probability of error for a MCS-TM-NI becomes constant and is given by (5.36).

- $P_{max} \to \infty$ & $\frac{\lambda_t}{\mu_t} \to \infty$

  Similarly, when the secondary to primary interference link is very poor and the secondary link is very good i.e. $\frac{\lambda_t}{\mu_t} \to \infty$, the probability of error for non-coherent schemes is given as

$$\mathcal{P}_{e,\mathcal{NC}}^{\infty} = a\, b^{-n_R n_T} \Gamma\left(n_R n_T + 1\right) \left(\frac{Q}{N_0}\right)^{-n_R n_T} \left(\frac{\lambda_t}{\mu_t}\right)^{-n_R n_T}. \tag{5.37}$$

  Similar to (5.37), it can be noted from (5.35) that the SER reduces with increasing $\frac{\lambda_t}{\mu_t}$ with a slope of $n_T n_R$ in the log scale.

Lower Bound on Ergodic Capacity

A precise lower bound on the ergodic capacity at high SNRs can be obtained using the moments obtained from (5.10), as [102, Eq. (8)]

$$\bar{C}\left(\bar{\gamma}_\epsilon\right) = \aleph\left(\log\left(\bar{\gamma}_\epsilon\right) + \mu\right) = \aleph\left(\log\left(\bar{\gamma}_\epsilon\right) + \frac{\partial}{\partial n} A F^{(q)}\Big|_{q=0}\right), \tag{5.38}$$

where $\bar{C}\left(\bar{\gamma}_{\epsilon}\right)$ denotes the lower bound on ergodic capacity, $\aleph = \frac{\log_2(e)}{B}$ and $AF^{(q)} = \frac{\varphi_q}{(\varphi_1)^q} - 1$ is the q-th order amount of fading. Substituting the expression of $AF^{(q)}$ into (5.38), taking the derivative and doing some algebraic manipulations the lower bound is obtained as

$$\bar{C}\left(\bar{\gamma}_{\epsilon}\right) = \aleph \left(\frac{\partial}{\partial q} \varphi_q \Big|_{q=0} \right) \tag{5.39}$$

Substituting the q-th moment expression from (5.10) into (5.39), yields

$$\begin{aligned} \bar{C}\left(\bar{\gamma}_{\epsilon}\right) = \aleph \sum_{\mathcal{F}} \Delta_{\mathcal{F}} \frac{\partial}{\partial q} \left(\Xi_A \mathcal{I}(\Xi_A - 1 + q, \Xi_C, \Xi_B, \xi) - \right. \\ \left. \Xi_B \mathcal{I}(\Xi_A + q, \Xi_C, \Xi_B, \xi) - \Xi_C \mathcal{I}(\Xi_A + q, \Xi_C + 1, \Xi_B, \xi) \right)\big|_{q=0}, \end{aligned} \tag{5.40}$$

which can be finally expressed as

$$\begin{aligned} \bar{C}\left(\bar{\gamma}_{end}\right) = \aleph \sum_{\mathcal{F}} \Delta_{\mathcal{F}} \left(\Xi_A \mathcal{D}_{\mathcal{I}}(\Xi_A - 1, \Xi_C, \Xi_B, \xi) - \right. \\ \left. \Xi_B \mathcal{D}_{\mathcal{I}}(\Xi_A, \Xi_C, \Xi_B, \xi) - \Xi_C \mathcal{D}_{\mathcal{I}}(\Xi_A, \Xi_C + 1, \Xi_B, \xi) \right), \end{aligned} \tag{5.41}$$

where $\mathcal{D}_{\mathcal{I}}(\bar{\alpha}_1, \alpha_2, \alpha_3, \xi) = \frac{\partial}{\partial q} \mathcal{I}(\bar{\alpha}_1 + q, \alpha_2, \alpha_3, \xi)\Big|_{q=0}$. After some steps outlined in Appendix 5.6.5, $\mathcal{D}_{\mathcal{I}}(\bar{\alpha}_1, \alpha_2, \alpha_3, \xi)$ can be represented in closed-form as

$$\begin{aligned} \mathcal{D}_{\mathcal{I}}(\bar{\alpha}_1, \alpha_2, \alpha_3, \xi) = \alpha_3^{-1-\bar{\alpha}_1+\alpha_2} \Gamma\left(1 + \bar{\alpha}_1\right) \left(-\log\left(\alpha_3\right) U(\alpha_2, \alpha_2 - \bar{\alpha}_1, \alpha_3 \xi) + \right. \\ \left. \psi^{(0)}\left(1 + \bar{\alpha}_1\right) U(\alpha_2, \alpha_2 - \bar{\alpha}_1, \alpha_3 \xi) - U^{(0,1,0)}(\alpha_2, \alpha_2 - \bar{\alpha}_1, \alpha_3 \xi) \right), \end{aligned} \tag{5.42}$$

where $U^{(0,1,0)}(a, b, z) = \frac{\partial}{\partial b} U(a, b, z)$.

Similar to (5.10), $\mathcal{D}_{\mathcal{I}}(\bar{\alpha}_1, \alpha_2, \alpha_3, \xi)$ is only defined for $\bar{\alpha}_1 > -1$ and $\bar{\alpha}_1 = -1$ only occurs for the term $\mathcal{D}_{\mathcal{I}}(\Xi_A - 1, \Xi_C, \Xi_B, \xi)$ when $\Xi_A = 0$. Again, in this case the term $\mathcal{D}_{\mathcal{I}}(\Xi_A - 1, \Xi_C, \Xi_B, \xi)$ is being multiplied with Ξ_A which makes the product zero. Therefore, (5.41) can be evaluated correctly by replacing $\mathcal{D}_{\mathcal{I}}(\Xi_A - 1, \Xi_C, \Xi_B, \xi)$ with

any constant c, when $\Xi_A = 0$. Note that (5.41) gives a very tight lower bound on the ergodic capacity at high SNRs as will be shown in the next section.

5.4 MIMO Secondary Network with Interference

In the case when the SU-Rx experiences interference from the PU-Tx, the end-to-end (E2E) signal-to-noise plus interference ratio (SINR) can be expressed in terms of the output SNR γ_ϵ as

$$\gamma_{\mathcal{I}} = \frac{\gamma_\epsilon}{\frac{P_P}{N_0}\daleth + 1} \tag{5.43}$$

where $\daleth = \sum_{r=1}^{n_R} |e_r|^2$ denotes the interference from the PU-Tx and P_P denotes the transmit power of the PU-Tx. In reality, when MRC is performed, only the desired signal power is aggregated according to (5.2) where as the interference power is not aggregated as $\daleth = \sum_{r=1}^{n_R} |e_r|^2$. Thus, the model considered here corresponds to the worst case scenario and gives the maximum possible interference.

5.4.1 Statistics of the Output SINR

The CDF expression of $\gamma_{\mathcal{I}}$ is given by following remark.

Remark 6. *The CDF of the output SINR for a MCS-TM-WI is given as*

$$F_{\gamma_{\mathcal{I}}}(\Phi) =$$
$$1 + \sum_{\mathcal{F}} \sum_{i_1=0}^{\Xi_A} \sum_{i_2=0}^{n_R-1} \binom{\Xi_A}{i_1} \binom{n_R-1}{i_2} \frac{\Delta_{\mathcal{F}} (-1)^{\Xi_A - i_1 - i_2 + n_R - 1}}{\Gamma(n_R) \xi^{-\Xi_A + i_1}} \left(\frac{N_0}{P_P \nu}\right)^{n_R} \Phi^{i_1 - \Xi_C} e^{-\Xi_B \Phi} \times$$
$$e^{\left(1+\frac{\xi}{\Phi}\right)\left(\frac{N_0}{P_P \nu} + \Xi_B \Phi\right)} \left(1 + \frac{\xi}{\Phi}\right)^{n_R - 1 - i_2} \left(\frac{N_0}{P_P \nu} + \Xi_B \Phi\right)^{-\varpi} \Gamma\left(\varpi, \left(\frac{N_0}{P_P \nu} + \Xi_B \Phi\right)\left(1 + \frac{\xi}{\Phi}\right)\right) \tag{5.44}$$

where $\varpi = i_1 + i_2 - \Xi_C + 1$.

Proof. See Appendix 5.6.6. □

Using (6.49) the outage performance of the MCS-TM-WI with interference can be obtained.

5.4.2 Performance Analysis Measures

Similar to the analysis in the previous section, the expressions for the MGF and the SER can be obtained by substituting the CDF in (6.49), into (5.13) and (5.19), respectively, and solving the resulting integrals. However, to the best of authors knowledge closed-form solution to the resulting integrals does not exist and one has to resort to numerical integration techniques to evaluate the expressions.

5.5 Numerical Results and Discussion

In this section, some selected numerical results as well as Monte-Carlo based simulation results are presented to verify the derived analytical results. In obtaining these numerical results, $R = 2$, $N_0 = 1$, $\lambda_t = 1$ dB, $\mu_t = 1$ dB, $\bar{\gamma} = \frac{P_{max}}{N_0}$ and $B = 1$. These parameters are fixed in the simulation unless stated. The outage performance of a MCS-TM-NI is shown in Fig. 5.2. The curves for probability of outage are generated using (5.8), where $x = 2^R - 1$. The asymptotic floor is plotted using (5.29). It can be observed that as $\bar{\gamma}$ increases, the probability of outage decreases until it becomes constant due to the fixed Q. As the interference constraint is relaxed, i.e. Q increases, the outage probability decreases which is obvious. Furthermore, for a higher value of Q, the SU-Tx can transmit using a higher power and thus, the outage performance saturates at a lower value. In addition, it can be observed that as the number of antennas increases, the outage probability decreases. Moreover, the performance gain by increasing the number of receive antennas is greater compared to only increasing

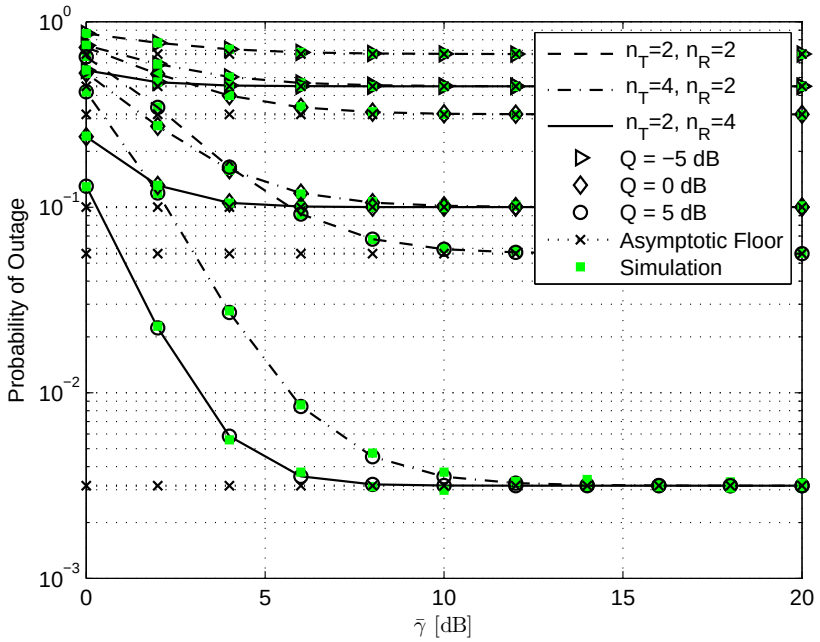

Figure 5.2: Probability of outage performance of a MIMO-CS with TAS/MRC.

the transmit antenna. It was mentioned previously when discussing (5.29) that the floor depends on the product $n_R n_T$, therefore, one can observe in Fig. 5.2 that the system with $(n_T, n_R) = (4, 2)$ and $(n_T, n_R) = (2, 4)$ have the same floor. However, the system with $(n_T, n_R) = (2, 4)$ performs better due to higher array gain.

The SER performance of coherent modulation schemes and non-coherent modulation schemes for the MCS-TM-NI is shown in Fig. 5.3 and Fig. 5.4, respectively. The modulation scheme considered in Fig. 5.3 is BPSK $(a, b) = (1, 2)$ and the curves are generated using (5.22). The asymptotic floor is plotted using (5.33). The modulation scheme considered in Fig. 5.4 is DBPSK $(a, b) = (0.5, 1)$ and the curves are generated using (5.25). It can be observed that as $\bar{\gamma}$ increases the SER decreases. Again, as Q is fixed the SER saturates at high $\bar{\gamma}$. Similar to the outage performance, as the interference constraint is relaxed, the saturation occurs at a lower value. Again in this case, increasing the number of antennas decreases the SER. Similar to the outage

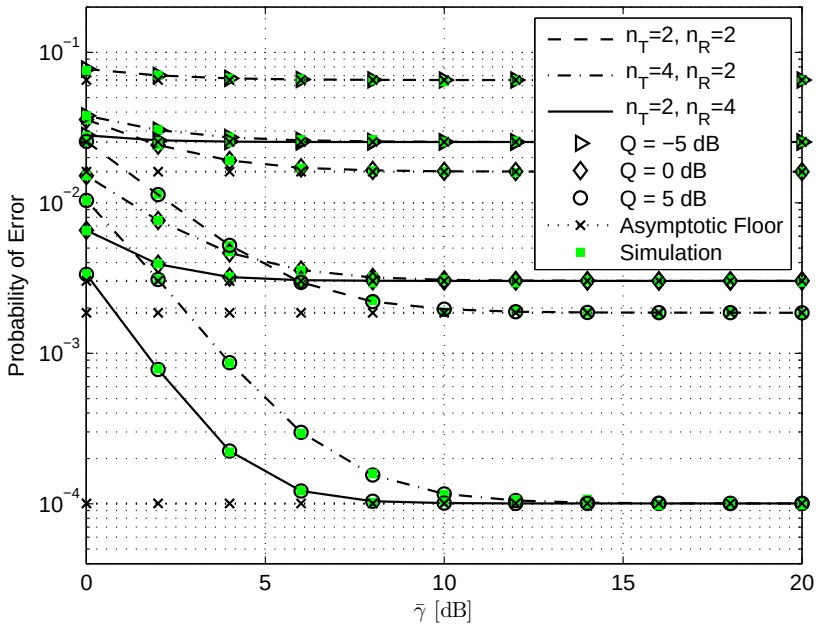

Figure 5.3: Symbol error rate performance of a MIMO-CS with TAS/MRC with coherent BPSK modulation.

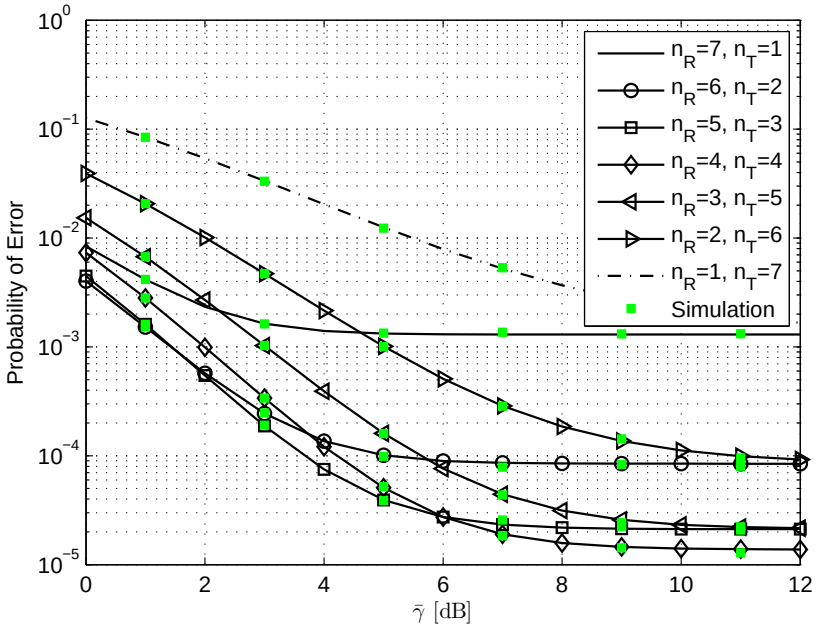

Figure 5.4: Symbol error rate performance of a MIMO-CS with TAS/MRC with non-coherent BDPSK modulation.

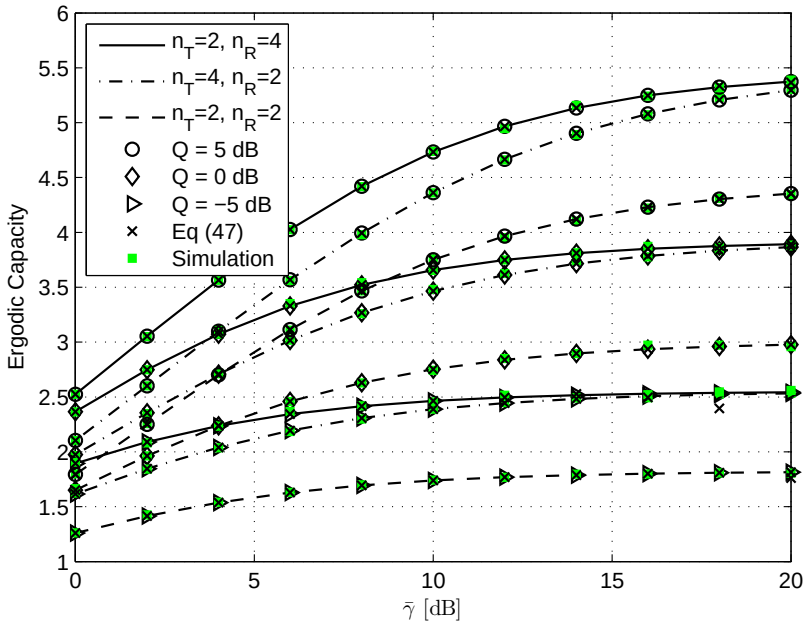

Figure 5.5: Ergodic capacity of a MIMO-CS with TAS/MRC.

floor, the floor in this case depends on the product $n_R n_T$ and one can observe that the system with $(n_T, n_R) = (4, 2)$ and $(n_T, n_R) = (2, 4)$ have the same floor which can be deduced from (5.33) and (5.36). Furthermore, in Fig. 5.4, the SER performance is compared for various antenna configurations when the total number of antennas is fixed i.e. $n_R + n_T = 8$. The highest diversity gain can be obtained by dividing the antennas equally over the transmitter and receiver. In addition, it can be observed, system with $(n_T, n_R) = (\alpha, \beta)$, where $\beta > \alpha$, always performs better compared to the system with $(n_T, n_R) = (\beta, \alpha)$, although both have the same generalized diversity gain of $\alpha\beta$. This is due to the fact that having more number of receive antennas results in higher array gain. In add all the figures, it can be noted that the simulation results match well with the analytical results.

The ergodic capacity of a MCS-TM-NI is shown in Fig. 5.5. The curves are generated using (5.64). In addition, we have also shown the results using the derived closed

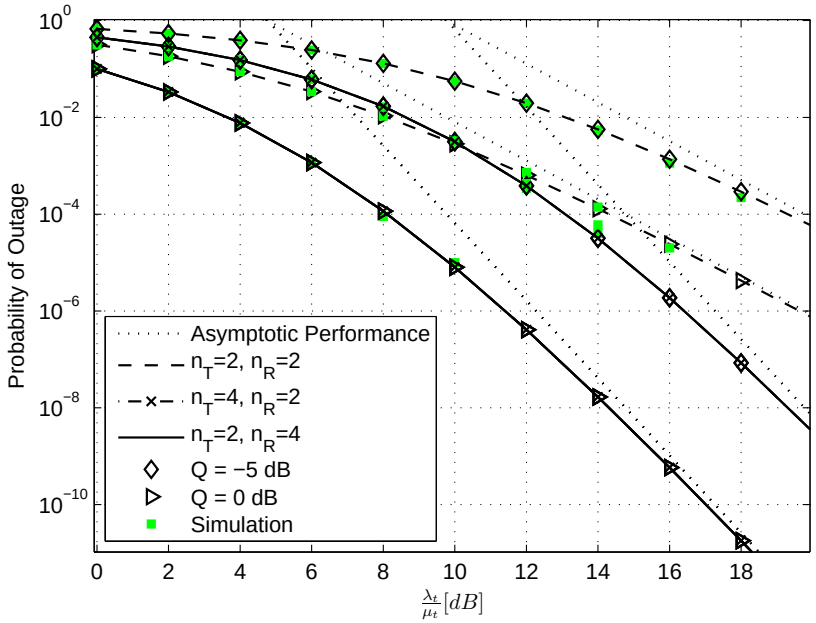

Figure 5.6: Probability of outage of a MIMO-CS with TAS/MRC in the asymptotic regime i.e. $\bar{\gamma} \to \infty$.

form expression for capacity given by (5.27) and are denoted by the 'x' marker in Fig. 5.5. The expressions were evaluated using MATLAB® and MATHEMATICA®. It can be observed that the results using the closed form expression in (5.27) match well with the results from (5.64). However, at high $\bar{\gamma}$, due to numerical computational issues (5.27) gives incorrect results. From Fig. 5.5, it can be observed that the ergodic capacity increases with increasing $\bar{\gamma}$ or increasing Q. Again, at high $\bar{\gamma}$, the capacity saturates due to fixed Q. Furthermore, increasing the number of antenna improves the capacity. In addition, it can be observed that in the low SNR regime, i.e. $\bar{\gamma}$ is low, increasing the number of receive antennas is more benificial compared to increasing the number of transmit antennas, as the capacity gain is higher. However, in the high SNR regime, i.e. $\bar{\gamma} \to \infty$, the ergodic capacity depends only on the product $n_T n_R$, so same performance gain can be achieved by adding more antennas on any of the terminals.

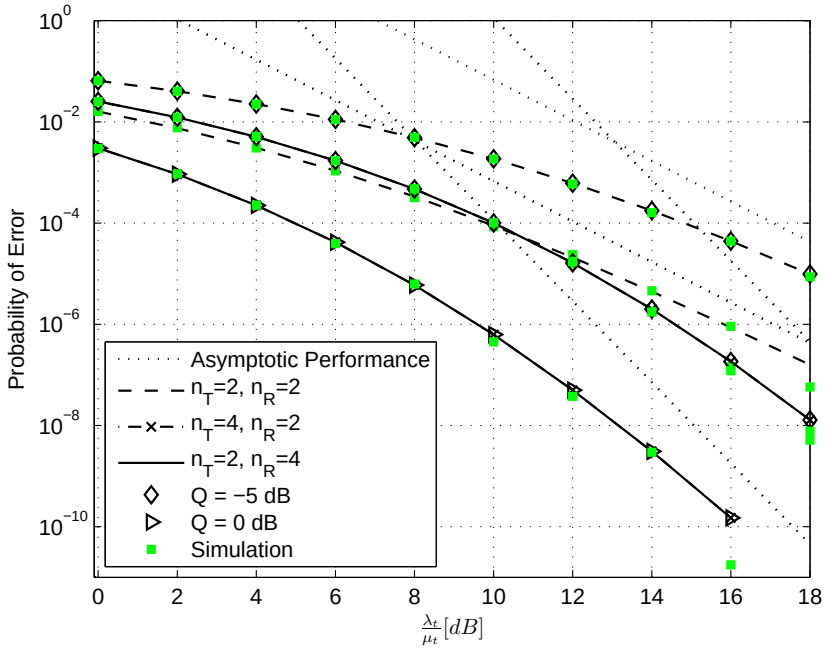

Figure 5.7: Symbol error rate performance of a MIMO-CS with TAS/MRC in the asymptotic regime, i.e. $\bar{\gamma} \to \infty$, for BPSK modulation.

Fig. 6.5 shows the outage performance a function of ratio of channel parameters λ_t and μ_t at high $\bar{\gamma}$. Similarly, Fig. 6.6 shows the SER performance of BPSK modulation as a function of ratio of channel parameters λ_t and μ_t at high $\bar{\gamma}$. It can be observed that as $\frac{\lambda_t}{\mu_t}$ increases the outage probability and SER reduces. Similarly, the outage probability and SER reduce with increasing Q. Furthermore, as the number of antennas increase the performance improves. Similar to previous figures, the performance of the system with $(n_T, n_R) = (4, 2)$ matches the performance of the system with $(n_T, n_R) = (2, 4)$ at high $\bar{\gamma}$. In addition, the asymptotic outage and SER performance obtained using (5.30) and (5.35) is also shown. It can be observed that the system with $(n_T, n_R) = (2, 2)$ has a lower generalized diversity gain compared to the system with $(n_T, n_R) = (2, 4)$ and $(n_T, n_R) = (4, 2)$ (both of which have the same generalized diversity gain).

The ergodic capacity of a MCS-TM-NI is shown in Fig. 5.8. The curve depicting

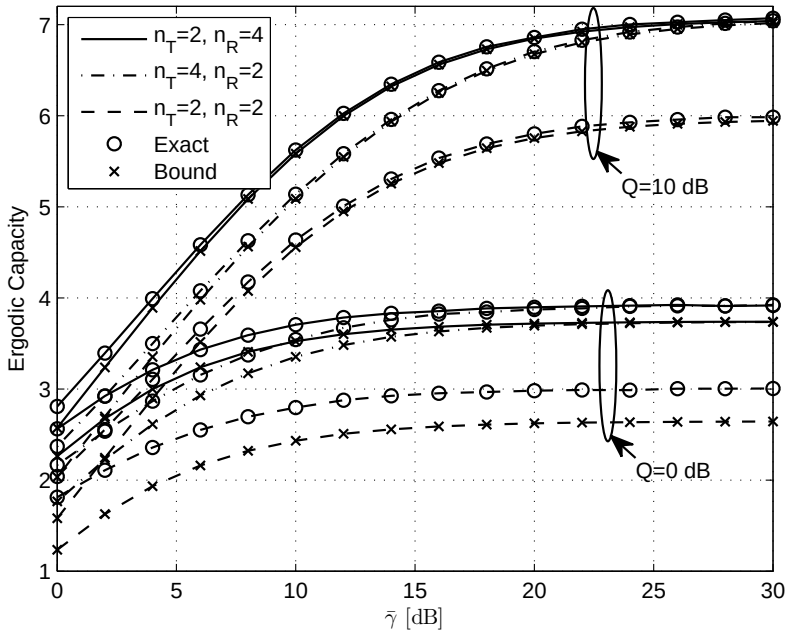

Figure 5.8: Lower bound on ergodic capacity of a MIMO-CS with TAS/MRC.

the lower bound is generated using (5.41). The expressions were evaluated using MATLAB® and MATHEMATICA®. It can be observed that the bound is tight for high $\bar{\gamma}$ and high Q. Moreover, the bound becomes tighter as $\bar{\gamma}$, Q, n_T or n_R increase. As was shown in Fig. 5.5, at high $\bar{\gamma}$, due to numerical computational issues (5.27) gives incorrect results. In such situations, Eq. (5.41) can be used to obtain accurate lower bound on the ergodic capacity.

The outage performance of a MCS-TM-WI is shown in Fig. 5.9. The curves for probability of outage are generated using (6.49), where $x = 2^R - 1$. In the simulations, we have considered the case where the PU-Tx transmits with the maximum available power i.e. P_{max} i.e. $P_P = P_{max}$. It can be observed that interference from the primary network results in severe degradation in performance of the secondary network and that the outage probability of the MCS-TM-WI increases as the interference power from the PU-Tx increases. It can also be observed that increasing $\bar{\gamma}$ does

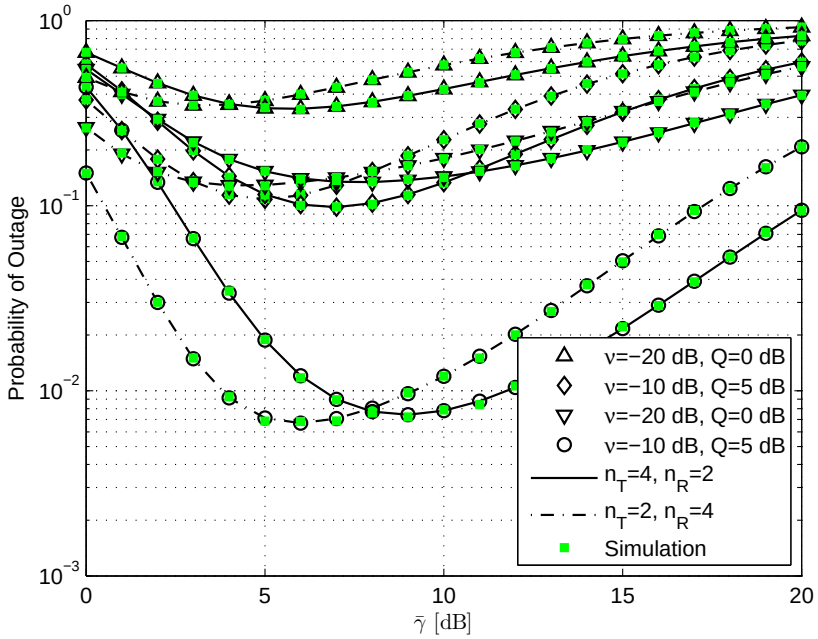

Figure 5.9: Probability of outage performance of a MIMO-CS with interference.

not always improve the secondary network performance. This happens because the PU-Rx interference constraint limits the transmit power of the SU-Tx, where as the interference power from the PU-Tx increases with increasing P_{max}. However, when the PU-Rx interference constraint is relaxed (Q is large), increasing P_{max} improves the outage performance. In addition, it can be observed that at low $\bar{\gamma}$, as the number of antennas increases, the outage probability decreases and that the MCS-TM-WI with greater number of receive antennas performs better. However, at high $\bar{\gamma}$, it can be observed that the MCS-TM-WI with higher receive antennas performs worse as it accumulates more interference from the PU-Tx.

5.6 Appendix

5.6.1 CDF of Output SNR for the t-th Transmit Antenna

From (5.2), the end-to-end SNR for the t-th antenna can be expressed as

$$\gamma_T(t) = \begin{cases} \frac{P_{max}}{N_0}\eta_t & , \ g_t < \frac{Q}{P_{max}} \\ \frac{Q}{N_0 g_t}\eta_t & , \ g_t > \frac{Q}{P_{max}} \end{cases} . \tag{5.45}$$

Conditioned on g_t, the PDF of $\gamma_T(t)$ can be expressed as

$$f_{\gamma_T(t)|g_t}(y) = \begin{cases} \frac{N_0^{n_R}}{\lambda_t^{n_R} P_{max}^{n_R} \Gamma(n_R)} y^{n_R-1} e^{-\frac{yN_0}{\lambda_t P_{max}}} & , \ g_t < \frac{Q}{P_{max}} \\ \frac{N_0^{R}}{\lambda_t^{n_R} Q^{n_R} \Gamma(n_R)} y^{n_R-1} g_t^{n_R} e^{-\frac{yN_0}{\lambda_t Q} g_t} & , \ g_t > \frac{Q}{P_{max}} \end{cases} \tag{5.46}$$

The PDF of $\gamma_T(t)$ can be obtained by averaging $f_{\gamma_T(t)|g_t}(\cdot)$ using the PDF of g_t as

$$\begin{aligned} f_{\gamma_T(t)}(y) = &\int_0^{\frac{Q}{P_{max}}} \frac{N_0^{n_R}}{\lambda_t^{n_R} P_{max}^{n_R} \Gamma(n_R)} y^{n_R-1} e^{-\frac{yN_0}{\lambda_t P_{max}}} \frac{1}{\mu_t} e^{-\frac{g}{\mu_t}} dg \\ &+ \int_{\frac{Q}{P_{max}}}^{\infty} \frac{N_0^{n_R}}{\lambda_t^{n_R} Q^{n_R} \Gamma(n_R)} y^{n_R-1} g^{n_R} e^{-\frac{yN_0}{\lambda_t Q} g} \frac{1}{\mu_t} e^{-\frac{g}{\mu_t}} dg. \end{aligned} \tag{5.47}$$

After some algebraic manipulations $f_{\gamma_T(t)}(y)$ can be expressed as

$$\begin{aligned} f_{\gamma_T(t)}(y) = &\frac{N_0^{n_R}}{\lambda_t^{n_R} P_{max}^{n_R} \Gamma(n_R)} y^{n_R-1} e^{-\frac{yN_0}{\lambda_t P_{max}}} F_{g_t}\left(\frac{Q}{P_{max}}\right) \\ &+ \frac{N_0^{n_R}}{\lambda_t^{n_R} Q^{n_R} \Gamma(n_R)} \frac{1}{\mu_t} y^{n_R-1} \int_{\frac{Q}{P_{max}}}^{\infty} g^{n_R} e^{-\left(\frac{yN_0}{\lambda_t Q} + \frac{1}{\mu_t}\right) g} dg. \end{aligned} \tag{5.48}$$

The CDF of $\gamma_T(t)$ can be obtained by integrating the PDF as

$$\begin{aligned} F_{\gamma_T(t)}(x) = &\frac{F_{g_t}\left(\frac{Q}{P_{max}}\right) N_0^{n_R}}{\lambda_t^{n_R} P_{max}^{n_R} \Gamma(n_R)} \int_0^x y^{n_R-1} e^{-\frac{yN_0}{\lambda_t P_{max}}} dy \\ &+ \int_0^x \frac{N_0^{n_R}}{\lambda_t^{n_R} Q^{n_R} \Gamma(n_R)} \frac{1}{\mu_t} y^{n_R-1} \int_{\frac{Q}{P_{max}}}^{\infty} g^{n_R} e^{-\left(\frac{yN_0}{\lambda_t Q}+\frac{1}{\mu_t}\right)g} dg dy. \end{aligned} \tag{5.49}$$

Integrating w.r.t. y first, $F_{\gamma_T(t)}(x)$ is obtained as

$$\begin{aligned} F_{\gamma_T(t)}(x) = &\frac{F_{g_t}\left(\frac{Q}{P_{max}}\right)}{\Gamma(n_R)} \left(\Gamma\left(n_R\right) - \Gamma\left(n_R, \frac{N_0 x}{\lambda_t P_{max}}\right)\right) + \frac{N_0^{n_R} Q^{-n_R}}{\lambda_t^{n_R} \Gamma(n_R)} \\ &\times \frac{1}{\mu_t} \int_{\frac{Q}{P_{max}}}^{\infty} g^{n_R} e^{-\left(\frac{1}{\mu_t}\right)g} \left(\frac{gN_0}{\lambda_t Q}\right)^{-n_R} \left(\Gamma\left(n_R\right) - \Gamma\left(n_R, \frac{gN_0}{\lambda_t Q} x\right)\right) dg, \end{aligned} \tag{5.50}$$

where $\Gamma(\cdot,\cdot)$ denotes the upper incomplete Gamma function [96, Eq. (8.350.2)]. After some algebraic manipulations, (5.50) can be expressed as

$$\begin{aligned} F_{\gamma_T(t)}(x) = &\frac{F_{g_t}\left(\frac{Q}{P_{max}}\right)}{\Gamma(n_R)} \left(\Gamma\left(n_R\right) - \Gamma\left(n_R, \frac{N_0 x}{\lambda_t P_{max}}\right)\right) \\ &+ \int_{\frac{Q}{P_{max}}}^{\infty} \frac{e^{-\left(\frac{1}{\mu_t}\right)g}}{\mu_t} dg - \frac{1}{\mu_t} \int_{\frac{Q}{P_{max}}}^{\infty} e^{-\left(\frac{1}{\mu_t}\right)g} \Gamma\left(n_R, \frac{gN_0}{\lambda_t Q} x\right) dg. \end{aligned} \tag{5.51}$$

Solving the integral in (5.51) and simplifying one obtains

$$\begin{aligned} F_{\gamma_T(t)}(x) = &\frac{F_{g_t}\left(\frac{Q}{P_{max}}\right)}{\Gamma(n_R)} \left(\Gamma\left(n_R\right) - \Gamma\left(n_R, \frac{N_0 x}{\lambda_t P_{max}}\right)\right) \\ &+ e^{-\frac{Q}{\mu_t P_{max}}} - \frac{1}{\Gamma(n_R)} \left(e^{-\frac{1}{\mu_t}\frac{Q}{P_{max}}} \Gamma\left(n_R, \frac{N_0}{\lambda_t P_{max}} x\right)\right. \\ &\left. - \left(\frac{N_0}{\lambda_t Q}\right)^{n_R} \left(\frac{x}{\frac{1}{\mu_t} + \frac{xN_0}{\lambda_t Q}}\right)^{n_R} \Gamma\left(n_R, \left(\frac{1}{\mu_t} + \frac{xN_0}{\lambda_t Q}\right) \frac{Q}{P_{max}}\right)\right). \end{aligned} \tag{5.52}$$

After some algebraic manipulations $F_{\gamma_A(t)}(x)$ can be expressed as

$$F_{\gamma_T(t)}(x) = 1 - \frac{1}{\Gamma(n_R)}\Gamma\left(n_R, \frac{N_0}{\lambda_t P_{max}}x\right) + \frac{\left(\frac{N_0}{\lambda_t Q}\right)^{n_R}}{\Gamma(n_R)}\left(\frac{x}{\frac{1}{\mu_t}+\frac{xN_0}{\lambda_t Q}}\right)^{n_R}\Gamma\left(n_R, \left(\frac{Q}{\mu_t P_{max}}+\frac{N_0}{\lambda_t P_{max}}x\right)\right). \tag{5.53}$$

As n_R is integer, using [96, Eq. (8.352.2)], $F_{\gamma_A(t)}(x)$ can be expressed as

$$F_{\gamma_T(t)}(x) = 1 - \frac{1}{\Gamma(n_R)}(n_R-1)!e^{-\frac{N_0}{\lambda_t P_{max}}x}\sum_{m=0}^{n_R-1}\frac{\left(\frac{N_0}{\lambda_t P_{max}}x\right)^m}{m!} + \frac{\left(\frac{N_0}{\lambda_t Q}\right)^{n_R}}{\Gamma(n_R)}\left(\frac{x}{\frac{1}{\mu_t}+\frac{xN_0}{\lambda_t Q}}\right)^{n_R}(n_R-1)!e^{-\left(\frac{Q}{\mu_t P_{max}}+\frac{N_0}{\lambda_t P_{max}}x\right)}\sum_{m=0}^{n_R-1}\frac{\left(\frac{Q}{\mu_t P_{max}}+\frac{N_0}{\lambda_t P_{max}}x\right)^m}{m!}. \tag{5.54}$$

After some algebraic manipulations $F_{\gamma_A(t)}(x)$ can finally be expressed as (5.6).

5.6.2 CDF of Output SNR for MCS-TM-NI

Applying the binomial expansion to (5.7) and doing some algebraic manipulations yields,

$$F_{\gamma_\epsilon}(x) = 1 + \sum_{k=1}^{n_T}\binom{n_T}{k}(-1)^k e^{-\frac{N_0}{\lambda_t P_{max}}kx}\times \left(\sum_{m=0}^{n_R-1}\frac{\left(\frac{N_0}{\lambda_t}\right)^m x^m}{m!P_{max}^m}\left(1-\left(\frac{N_0}{\lambda_t Q}\right)^{n_R-m}\frac{x^{n_R-m}e^{-\frac{Q}{\mu_t P_{max}}}}{\left(\frac{1}{\mu_t}+\frac{N_0}{Q\lambda_t}x\right)^{n_R-m}}\right)\right)^k. \tag{5.55}$$

Expressing the product of sum as the sum of products one gets

$$F_{\gamma_\epsilon}(x) = 1 + \sum_{k=1}^{n_T} \binom{n_T}{k} (-1)^k e^{-\frac{N_0}{\lambda_t P_{max}} kx} \times \left(\sum_{m_1=0}^{n_R-1} \sum_{m_2=0}^{n_R-1} \cdots \sum_{m_k=0}^{n_R-1} \prod_{l=1}^{k} \frac{\left(\frac{N_0}{\lambda_t}\right)^{m_l}}{m_l! P_{max}^{m_l}} x^{m_l} \left(1 - \left(\frac{N_0}{\lambda_t Q} \right)^{n_R - m_l} e^{-\frac{Q}{\mu_t P_{max}}} \frac{x^{n_R-m_l}}{\left(\frac{1}{\mu_t} + \frac{N_0}{Q\lambda_t} x \right)^{n_R-m_l}} \right) \right), \tag{5.56}$$

which can be further expressed as

$$F_{\gamma_\epsilon}(x) = 1 + \sum_{k=1}^{n_T} \kappa_k^A e^{-\frac{N_0}{\lambda_t P_{max}} kx} \times \left(\sum_{\mathbf{m}} \kappa_{k,m}^B x^{\sum_{l=1}^{k} m_l} \prod_{l=1}^{k} \left(1 - \left(\frac{N_0}{\lambda_t Q} \right)^{n_R - m_l} \frac{x^{n_R-m_l} e^{-\frac{Q}{\mu_t P_{max}}}}{\left(\frac{1}{\mu_t} + \frac{N_0}{Q\lambda_t} x \right)^{n_R-m_l}} \right) \right), \tag{5.57}$$

where $\sum_{\mathbf{m}}$ is shorthand notation of $\sum_{m_1=0}^{n_R-1} \sum_{m_2=0}^{n_R-1} \cdots \sum_{m_k=0}^{n_R-1}$, $\kappa_k^A = \binom{n_T}{k}(-1)^k$ and $\kappa_{k,m}^B = \prod_{l=1}^{k} \frac{\left(\frac{N_0}{\lambda_t}\right)^{m_l}}{m_l! P_{max}^{m_l}}$. Using [99, Eq. (9)] (5.57) can be expressed as

$$F_{\gamma_\epsilon}(x) = 1 + \sum_{k=1}^{n_T} \kappa_k^A e^{-\frac{N_0}{\lambda_t P_{max}} kx} \times \left(\sum_{\mathbf{m}} \kappa_{k,m}^B x^{\sum_{l=1}^{k} m_l} \sum_{\mathbf{w} \in \theta_k} \prod_{l=1}^{k} (-1)^{w_l} \left(\left(\frac{N_0}{\lambda_t Q} \right)^{n_R - m_l} e^{-\frac{Q}{\mu_t P_{max}}} \frac{x^{n_R-m_l}}{\left(\frac{1}{\mu_t} + \frac{N_0}{Q\lambda_t} x \right)^{n_R-m_l}} \right)^{w_l} \right), \tag{5.58}$$

where θ_k is the set of all possible k bit binary numbers and w_l is the lth bit of the binary number $\mathbf{w} \in \theta_k$. After some algebraic manipulations one gets

$$F_{\gamma_\epsilon}(x) = 1 + \sum_{k=1}^{n_T} \sum_{\mathbf{m}} \sum_{\boldsymbol{w} \in \theta_k} \kappa_k^A \kappa_{k,m}^B \kappa_{w,m,k}^C \frac{x^{\sum_{l=1}^{k} m_l + \sum_{l=1}^{k} (n_R - m_l) w_l} e^{-\frac{N_0}{\lambda_t P_{max}} kx}}{\left(x + \frac{Q\lambda_t}{N_0 \mu_t} \right)^{\sum_{l=1}^{k} (n_R - m_l) w_l}}, \tag{5.59}$$

where $\kappa^C_{w,m,k} = \prod_{l=1}^{k}(-1)^{w_l} e^{-\frac{Q}{\mu_t P_{max}} w_l}$. Let $\sum_{\mathcal{F}}$ is short hand notation for $\sum_{k=1}^{n_T} \sum_{\mathbf{m}} \sum_{\boldsymbol{w}\in\theta_k}$, $\Delta_{\mathcal{F}} = \kappa^A_k \kappa^B_{k,m} \kappa^C_{w,m,k}$, $\Xi_A = \sum_{l=1}^{k} m_l + (n_R - m_l) w_l$, $\Xi_B = \frac{N_0}{\lambda_t P_{max}} k$, $\xi = \frac{Q\lambda_t}{N_0 \mu_t}$ and $\Xi_C = \sum_{l=1}^{k} (n_R - m_l) w_l$. The CDF of end-to-end SNR can finally be expressed as (5.8).

5.6.3 Closed-form Representation of $\mathcal{I}(\alpha_1, \alpha_2, \alpha_3, \xi)$

$$\mathcal{I}(\alpha_1, \alpha_2, \alpha_3, \xi) = \int_0^{\infty} \frac{x^{\alpha_1} e^{-\alpha_3 x}}{(x+\xi)^{\alpha_2}} dx, \tag{5.60}$$

where $\alpha_1 > -1$ and $\alpha_3 > 0$. Substitute $z = x + \xi$ and solving the integral using [96, Eq. (3.383.4)] yields

$$\mathcal{I}(\alpha_1, \alpha_2, \alpha_3, \xi) = \alpha_3^{-\frac{\alpha_1 - \alpha_2 + 2}{2}} \xi^{\frac{\alpha_1 - \alpha_2}{2}} \Gamma(\alpha_1 + 1)\, e^{\frac{\xi}{2}\alpha_3} W_{\frac{-\alpha_2 - \alpha_1}{2}, \frac{-\alpha_1 + \alpha_2 - 1}{2}}(\alpha_3 \xi), \tag{5.61}$$

where $W_{\lambda,\mu}(z)$ is the WhittakerW function defined in [96, Eq. (9.220.4)]. Using [98, Eq. (07.45.26.0005.01)], (5.61) can be represented in terms of Meijer-G function yielding

$$\mathcal{I}(\alpha_1, \alpha_2, \alpha_3, \xi) = \frac{\alpha_3^{-1-\alpha_1+\alpha_2}}{\Gamma(\alpha_2)} G^{2,1}_{1,2}\left(\alpha_3 \xi \,\middle|\, \begin{matrix} 1 - \alpha_2 \\ 0, 1 + \alpha_1 - \alpha_2 \end{matrix} \right), \tag{5.62}$$

where $G^{m,n}_{p,q}(\cdot)$ is the Meijer-G function defined in [96, Eq. (9.301)]. Using [98, Eq. (07.34.03.0719.01)], (5.62) can be represented as

$$\mathcal{I}(\alpha_1, \alpha_2, \alpha_3, \xi) = \alpha_3^{-1-\alpha_1+\alpha_2} \Gamma(1 + \alpha_1)\, U(\alpha_2, \alpha_2 - \alpha_1, \alpha_3 \xi), \tag{5.63}$$

where $U(a, b, z)$ denotes the Tricomi confluent hypergeometric function defined in [98, Eq. (07.33.07.0001.01)].

5.6.4 Ergodic Capacity of MCS-TM-NI

Substituting the CDF from (5.8) into (5.26) yields

$$C = -\frac{\log_2(e)}{B} \int_0^{\infty} \sum_{\mathcal{F}} \Delta_{\mathcal{F}} x^{\Xi_A} e^{-\Xi_B x} (1+x)^{-1} (x+\xi)^{-\Xi_C} \, dx, \tag{5.64}$$

which can be expressed as

$$C = -\frac{\log_2(e)}{B} \sum_{\mathcal{F}} \Delta_{\mathcal{F}} \int_0^{\infty} x^{\Xi_A} e^{-\Xi_B x} \prod_{q=1}^{2} (x-\zeta_q)^{-\tau_q} \, dx, \tag{5.65}$$

where $\zeta_1 = 1$, $\zeta_2 = \xi$, $\tau_1 = 1$ and $\tau_2 = \Xi_C$. It is possible that $\zeta_1 = \zeta_2$, so one can express (5.65) as

$$C = -\frac{\log_2(e)}{B} \sum_{\mathcal{F}} \Delta_{\mathcal{F}} \int_0^{\infty} x^{\Xi_A} e^{-\Xi_B x} \prod_{q=1}^{\upsilon} \left(x+\bar{\zeta}_q\right)^{-\delta_q} \, dx, \tag{5.66}$$

where υ denotes the number of distinct roots of $\prod_{q=1}^{2} (x+\zeta_q)^{-\tau_q}$, $\bar{\zeta}_q$ denotes the q-th distinct root of $\prod_{q=1}^{2} (x+\zeta_q)^{-\tau_q}$, $\delta_q = \sum_{o=1,\zeta_o==\zeta_q}^{2} \tau_o$ denotes the multiplicity of root $\bar{\zeta}_q$. Eq. (5.66) can be expressed using partial fractions as [103, Eq. (2)]

$$C = -\frac{\log_2(e)}{B} \sum_{\mathcal{F}} \Delta_{\mathcal{F}} \int_0^{\infty} x^{\Xi_A} e^{-\Xi_B x} \sum_{v_1=1}^{\upsilon} \sum_{v_2=1}^{\delta_{v_1}} \kappa_{v_1,v_2}^{D} \left(x+\bar{\zeta}_{v_1}\right)^{-v_2} \, dx, \tag{5.67}$$

where κ_{v_1,v_2}^{D} can be obtained recursively as

$$\kappa_{v_1,v_2}^{D} = \begin{cases} \prod_{q=1,q\neq v_1}^{\upsilon} \left(\bar{\zeta}_{v_1} - \bar{\zeta}_q\right)^{-\delta_q} & ,v_2 = \delta_i \\ \sum_{q=1}^{\delta_{v_1}-v_2} \frac{\kappa_{v_1,v_2+q}^{D}(-1)^q}{\delta_{v_1}-v_2} \times & \\ \sum_{p=1,p\neq v_1}^{\upsilon} \frac{\delta_p}{\left(\bar{\zeta}_{v_1}-\bar{\zeta}_p\right)^{-q}} & ,v_2 = \delta_{v_1}-1,\ldots 1. \end{cases} \tag{5.68}$$

After rearranging the terms and substituting $z = x + \bar{\zeta}_{v_1}$ in (5.67) gives

$$C = -\frac{\log_2(e)}{B} \sum_{\mathcal{F}} \sum_{v_1=1}^{v} \sum_{v_2=1}^{\delta_{v_1}} \Delta_{\mathcal{F}} \kappa^{D}_{v_1,v_2} \int_{\bar{\zeta}_{v_1}}^{\infty} \left(z - \bar{\zeta}_{v_1}\right)^{\Xi_A} e^{-\Xi_B\left(z-\bar{\zeta}_{v_1}\right)} z^{-v_2} dz. \tag{5.69}$$

Using [96, Eq. (3.383.4)], the integral in (5.69) can be solved to give (5.70),

$$C = -\frac{\log_2(e)}{B} \sum_{\mathcal{F}} \sum_{v_1=1}^{v} \sum_{v_2=1}^{\delta_{v_1}} \Delta_{\mathcal{F}} \kappa^{D}_{v_1,v_2} \Xi_B^{-\frac{\Xi_A - v_2 + 2}{2}} \bar{\zeta}_{v_1}^{\frac{\Xi_A - v_2}{2}} \Gamma\left(\Xi_A + 1\right) e^{\frac{\Xi_B \bar{\zeta}_{v_1}}{2}} W_{\varsigma_1,\varsigma_2}\left(\Xi_B \bar{\zeta}_{v_1}\right), \tag{5.70}$$

where $\varsigma_1 = \frac{-v_2 - \Xi_A}{2}$ and $\varsigma_2 = \frac{-\Xi_A + v_2 - 1}{2}$. Using the relation between the WhittakerW function and the Meijer-G function [98, Eq. (07.45.26.0005.01)] and after some algebraic manipulation, the expression of capacity in (5.70) can be expressed as (5.27).

5.6.5 Derivation of $\mathcal{D}_{\mathcal{I}}(\bar{\alpha}_1, \alpha_2, \alpha_3, \xi)$:

Using (5.63), $\frac{\partial}{\partial q}\mathcal{I}(\bar{\alpha}_1 + q, \alpha_2, \alpha_3, \xi)$ is given as

$$\frac{\partial}{\partial q}\mathcal{I}(\bar{\alpha}_1 + q, \alpha_2, \alpha_3, \xi) = \alpha_3^{-1-\bar{\alpha}_1+\alpha_2} \left(\frac{\partial}{\partial q} \alpha_3^{-q} \Gamma\left(1 + \bar{\alpha}_1 + q\right) U(\alpha_2, \alpha_2 - \bar{\alpha}_1 - q, \alpha_3 \xi) \right) \tag{5.71}$$

Taking the derivative yields

$$\begin{aligned} &\frac{\partial}{\partial q}\mathcal{I}(\bar{\alpha}_1 + q, \alpha_2, \alpha_3, \xi) = \alpha_3^{-1-\bar{\alpha}_1+\alpha_2} \Gamma\left(1 + \bar{\alpha}_1 + q\right) \alpha_3^{-q} \times \\ &\big(-\log\left(\alpha_3\right) U(\alpha_2, \alpha_2 - \bar{\alpha}_1 - q, \alpha_3 \xi) + U^{(0,1,0)}(\alpha_2, \alpha_2 - \bar{\alpha}_1 - q, \alpha_3 \xi) \\ &\qquad + \psi^{(0)}\left(1 + \bar{\alpha}_1 + q\right) U(\alpha_2, \alpha_2 - \bar{\alpha}_1 - q, \alpha_3 \xi) \big) \end{aligned} \tag{5.72}$$

where $U^{(0,1,0)}(a, b, z) = \frac{\partial}{\partial b} U(a, b, z)$. Substituting $q = 0$ in (5.72), yields (5.42).

5.6.6 CDF of Output SINR

The CDF of $\gamma_{\mathcal{I}}$ is given as

$$F_{\gamma_{\mathcal{I}}}(\Phi) = \Pr\{\gamma_{\mathcal{I}} < \Phi\} = \Pr\left\{\frac{\gamma_\epsilon}{\frac{P_p}{N_0}\urcorner + 1} < \Phi\right\} \tag{5.73}$$

Conditioned on $\urcorner$, CDF of $\gamma_{\mathcal{I}}$ is given as

$$F_{\gamma_{\mathcal{I}}|\urcorner}(\Phi|\urcorner) = \Pr\left\{\gamma_\epsilon < \Phi\left(\frac{P_p}{N_0}\urcorner + 1\right)\right\} \tag{5.74}$$

Using $F_{\gamma_{\mathcal{I}}|\urcorner}(\cdot|\cdot)$, $F_{\gamma_{\mathcal{I}}}(\cdot)$ can be obtained as

$$F_{\gamma_{\mathcal{I}}}(\Phi) = \int_0^\infty F_{\gamma_{\mathcal{I}}|\urcorner}(\Phi|x)\, f_\urcorner(x)\, dx \tag{5.75}$$

where, similar to (5.3), $f_\urcorner(y) = \frac{1}{\nu^{n_R}\Gamma(n_R)} y^{n_R-1} e^{-\frac{y}{\nu}}$. Substituting the PDF $f_\urcorner(\cdot)$ and CDF from (5.8) into (6.89) yields

$$F_{\gamma_{\mathcal{I}}}(\Phi) = 1 + \sum_{\mathcal{F}} \Delta_{\mathcal{F}} \left(\Phi\frac{P_P}{N_0}\right)^{\Xi_A-\Xi_C} \frac{e^{-\Xi_B\Phi}}{\nu^{n_R}\Gamma(n_R)} \int_0^\infty \frac{\left(x+\frac{N_0}{P_P}\right)^{\Xi_A} e^{-\frac{\Xi_B\Phi P_P}{N_0}x - \frac{x}{\nu}}}{(x+\xi_N)^{\Xi_C}} x^{n_R-1} dx \tag{5.76}$$

where $\xi_N = \frac{N_0}{P_P} + \frac{\xi}{\Phi P_P} N_0$. Making change of variable $y = x + \xi_N$, and applying binomial expansion yields

$$F_{\gamma_{\mathcal{I}}}(\Phi) = 1 + \sum_{\mathcal{F}} \sum_{i_1=0}^{\Xi_A} \sum_{i_2=0}^{n_R-1} \binom{\Xi_A}{i_1} \binom{n_R-1}{i_2} \frac{\Delta_{\mathcal{F}} e^{-\Xi_B\Phi}}{\nu^{n_R}\Gamma(n_R)} \left(\frac{\Phi P_P}{N_0}\right)^{\Xi_A-\Xi_C} \times \left(\frac{N_0}{P_P} - \xi_N\right)^{\Xi_A-i_1} (-\xi_N)^{n_R-1-i_2} e^{\xi_N\left(\frac{1}{\nu}+\frac{\Xi_B\Phi P_P}{N_0}\right)} \int_{\xi_N}^\infty y^{i_1+i_2-\Xi_C} e^{-y\left(\frac{1}{\nu}+\frac{\Xi_B\Phi P_P}{N_0}\right)} dy \tag{5.77}$$

Solving the integration in (5.77), substituting $\xi_N = \frac{N_0}{P_P} + \xi \frac{N_0}{P_P \Phi}$ and after some algebraic manipulations the CDF of the end-to-end SINR is obtained as (6.49).

Chapter 6

Performance of an Opportunistic Multi-user Cognitive Network

6.1 Introduction

In the previous chapter, the QoS in a MCS was enhanced through spatial diversity by employing multiple antennas. As was discussed in Chapter 1, in a multi-user network, spatial diversity can also be achieved by exploiting the best channels that become available due to multiple users. In this chapter, the later scenario is taken into account and performance of a multi-user underlay cognitive network is studied where the secondary user having the best channel is scheduled for transmission. In order to analyze this scheme for a practical MCS, the channel is assumed to have independent but not identical Nakagami-m fading and a the peak transmit power of the SU-Tx is assumed to be limited. In addition, the effect of interference from the PU on the SU is also considered and the performance of the opportunistic multi-user underlay cognitive network (OMU-CN) is analyzed for two scenarios; 1) OMU-CN does not experience interference from the PU (denote by OMU-CN-NI) and 2) OMU-CN experiences interference from the PU (denote by OMU-CN-WI). For both scenarios, exact

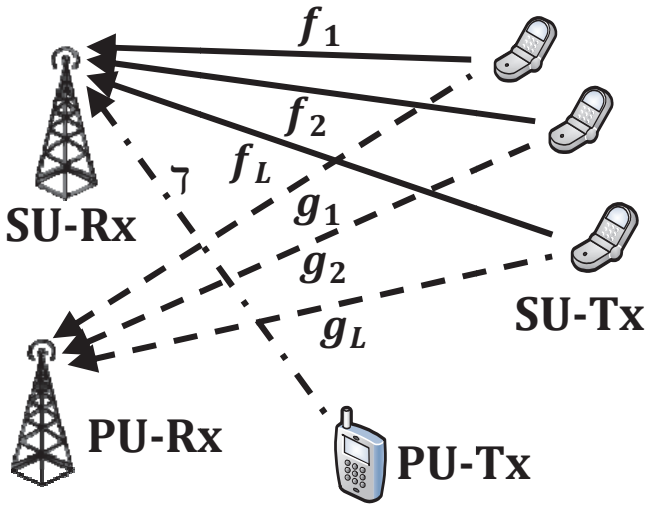

Figure 6.1: System model diagram.

closed-form expressions are obtained for the CDF of the output SNR which is then utilized to analyze the outage performance. An alternate new and simple expression for the CDF of the output SNR for the OMU-CN-NI is also derived. Using this new expression of the CDF, exact closed-form expressions are derived for the MGF of the output SNR, the SER performance and the ergodic capacity. Additionally, the performance of the OMU-CN-NI is analyzed in the asymptotic regimes. Numerical simulations are also presented to corroborate the derived analytical results. Moreover, the scheduling scheme analyzed in this chapter is compared to the hybrid scheduling scheme in [79].

6.2 System Model

Consider a spectrum sharing network as shown in Fig. 6.1, in which the primary network allows the secondary network to use the spectrum provided the interference level caused by the secondary networks is limited. The primary network consists of one transmitter, denoted by PU-Tx, and one receiver denoted by PU-Rx. The secondary

user network consists of L transmitters and one receiver denoted as SU-Rx. This scenario is analogous to an uplink system where the users want to communicate with the base station.

Let g_l denote the channel power gain of the l-th SU-Tx to the PU-Rx, f_l denote the channel power gain of the l-th SU-Tx to the SU-Rx and $\urcorner$ denote the channel power gain of the interference link from PU-Tx to the SU-Rx. The channel is assumed to have independent but not identical (i.n.i.d) Nakagami-m fading and the channel power gains are assumed to be i.n.i.d Gamma distributed. The probability density function (PDF) of a Gamma distribution with parameters $m_{a,b}$ and $\Omega_{a,b}$ is expressed as [2]

$$f_{a,b}(x) = \frac{1}{\Gamma(m_{a,b})} \left(\frac{m_{a,b}}{\Omega_{a,b}}\right)^{m_{a,b}} x^{m_{a,b}-1} \exp\left(-x\frac{m_{a,b}}{\Omega_{a,b}}\right), \tag{6.1}$$

where $a \in \{g, f\}$ and $b \in \{1, \dots L\}$ or $a = \urcorner$ and $b = 1$ and $\Gamma(\cdot)$ is the Gamma function [96, Eq. (8.310.1)]. For example, $m_{f,3}$ and $\Omega_{f,3}$ are the parameters of fading of the channel power gain from the third SU-Tx to the SU-Rx. Assuming that $m_{a,b}$ is an integer, the cumulative distribution function (CDF) can be expressed as

$$F_{a,b}(x) = \frac{\gamma\left(m_{a,b}, \frac{xm_{a,b}}{\Omega_{a,b}}\right)}{\Gamma(m_{a,b})} = 1 - \sum_{i=0}^{m_{a,b}-1} \left(\frac{m_{a,b}}{\Omega_{a,b}}\right)^{i} \frac{x^i}{i!} e^{-x\frac{m_{a,b}}{\Omega_{a,b}}}, \tag{6.2}$$

where $\gamma(\cdot,\cdot)$ denotes the lower incomplete Gamma function [96, Eq. (8.350.1)].

Given that $P_{T,l}$ is the transmit power of the l-th SU-Tx, the received signal-to-noise ratio (SNR) at the SU-Rx, Υ_l, can be expressed as

$$\Upsilon_l = \frac{P_{T,l} f_l}{N_0}. \tag{6.3}$$

As there are L SU transmitters, in order to reduce interference at the PU-Rx it is

assumed that only the SU-Tx with the maximum SNR transmits. This opportunistic transmission results in multi-user diversity and the post-scheduling/output SNR can be expressed as

$$\Upsilon = \max_{l} \left\{ P_{T,l} h_l \right\}, \tag{6.4}$$

where Υ represents the output SNR and $h_l = \frac{f_l}{N_0}$. Note that h_l is also Gamma distributed with parameters $m_{h,l} = m_{f,l}$ and $\Omega_{h,l} = \frac{\Omega_{f,l}}{N_0}$.

It can be noted that Υ depends on the power allocation policy employed at each SU-Tx. Depending on the constraints imposed by the primary network, the power allocation policy varies and each user has a different power allocation depending on the condition of its interference link and the transmission link. In the sequel, we consider an interference power constraint and a maximum transmit power constraint on the secondary user to derive the power allocation policy adopted at the SU-Tx. The interference power constraint is not present in traditional multi-user systems and thus, it leads to multi-user diversity that is different from traditional multi-user diversity. In addition, as there is limited communication among the users, so in practice the user is selected (for transmission) by a band manager that has the channel state information as well as the transmit powers of all the users, or the users feedback their power allocation information to the SU base station which then selects the user for transmission according to (6.4) [75].

Instantaneous CSI Based Power Allocation

According the peak interference power constraint, the peak interference power to the PU-Rx should be below a certain threshold Q_{pk}. This peak interference power

constraint for the l-th SU-Tx can be expressed as

$$P_S(g_l, h_l)g_l \leq Q_{pk}, \tag{6.5}$$

where $P_S(g_l, h_l)$ is the transmit power of the SU-Tx. It can be noted that the transmit power of the SU-Tx is adapted depending on the channel power gains of the network so that the interference power remains below the threshold Q_{pk}. In the worst case scenario, the transmit power of the secondary user should be chosen such that the interference level at the PU-Rx should be at most Q_{pk}. This can be expressed as

$$P_S(g_l, h_l) = \frac{Q_{pk}}{g_l}. \tag{6.6}$$

From (6.6), it can be noted that if the interference link is very poor then the power allocated by the SU-Tx is very high. Although, theoretically this results in large capacity, but in reality the SU-Tx can transmit only with limited power and has a peak power constraint i.e.

$$P_S(g_l, h_l) \leq P_{max}. \tag{6.7}$$

Thus, the constraints in (6.6) and (6.7) can be combined to obtain the power allocation policy as

$$P_{CSI,l} = \min\left\{P_{max}, \frac{Q_{pk}}{g_l}\right\}, \tag{6.8}$$

where $P_{CSI,l}$ is a short form notation of $P_S(g_l, h_l)$. It can be noted from (6.8) that P_{CSI} needs instantaneous CSI of the interference link g_l. Note that other power allocation policies can also be adopted such as the ones proposed in [104]. However, in these policies, in some channel conditions the SU is forced to stop transmission

resulting in reduced throughput. For the power allocation policy adopted in (6.8) the SUs always transmit. Moreover, only good channels are selected for transmission. In addition, the policy adopted in (6.8) leads to a tractable analysis and is thus, useful in analyzing the performance of the OMU-CN.

Substituting $P_{T,l} = P_{CSI,l}$ in (6.4), the output SNR in an OMU-CN with CSI based power allocation is

$$\Upsilon_{CSI} = \max_{l} \left\{ \min \left\{ P_{max}, \frac{Q_{pk}}{g_l} \right\} h_l \right\} = \max_{l} \left\{ \Upsilon_{CSI,l} \right\}, \tag{6.9}$$

where $\Upsilon_{CSI,l} = \min \left\{ P_{max}, \frac{Q_{pk}}{g_l} \right\} h_l$ denotes the SNR of the l-th SU-Tx. Note that the SU-Tx selection is done on the basis of output SNR and it does not take into account the interference from the PU-Tx and is thus, a sub-optimal selection scheme. However, this selection scheme has lower complexity as it does not require the CSI of the interference link from the PU-Tx, resulting in a lower overhead/feedback.

6.3 Opportunistic Multi-User Secondary Network without Interference

For the OMU-CN-NI where the SU-RX does not experience interference from the PU-Tx, the output SNR is given by Υ_{CSI} in (6.9). In order to analyze the performance of this system, the statistics (PDF and the CDF) of Υ_{CSI} are required.

6.3.1 Statistics of the Output SNR

The CDF of the output SNR for an OMU-CN-NI is given in following remark.

Remark 1. *The CDF of the output SNR for an OMU-CN-NI is given by*

$$F_{\Upsilon_{CSI}}(x) = \prod_{l=1}^{L}\left(1-\sum_{i=0}^{m_{h,l}-1}\frac{{\beta_l}^i}{i!}\left(\eta_P^i x^i e^{-\eta_P\beta_l x}F_{g,l}\left(\varrho_P\right)+\frac{x^i\Gamma\left(m_{g,l}+i,\left(\alpha_l+\frac{\beta_l}{Q_{pk}}x\right)\varrho_P\right)}{{Q_{pk}}^i{\alpha_l}^{-m_{g,l}}\Gamma(m_{g,l})\left(\alpha_l+\frac{\beta_l}{Q_{pk}}x\right)^{m_{g,l}+i}}\right)\right). \tag{6.10}$$

where $\varrho_P=\frac{Q_{pk}}{P_{max}}$, $\beta_l=\frac{m_{h,l}}{\Omega_{h,l}}$, $\alpha_l=\frac{m_{g,l}}{\Omega_{g,l}}$, $\eta_P=\frac{1}{P_{max}}$ *and* $F_{g,l}(\cdot)$ *denotes the CDF of* g_l.

Proof. See Appendix 6.6.1. □

From the CDF in (6.10), the probability of outage of an OMU-CN is obtained. However, it is difficult to obtain expressions for other interesting performance measures such as MGF, SER and ergodic capacity using the CDF in (6.10). In order to derive closed form expressions for MGF, SER and ergodic capacity, we propose a more useful alternate expression for the CDF given in Remark 2.

Remark 2. *An alternate expression of the CDF of the output SNR in* (6.10)*, which is helpful in obtaining the exact closed form expressions for the MGF, SER and ergodic capacity, is given as*

$$F_{\Upsilon_{CSI}}(x)=\sum_{\mathfrak{F}}\Delta_\kappa x^{\Xi_{i,n}^A+p}e^{-x\Xi_n^B}\left(x-\bar{\zeta}_{v_1}\right)^{-v_2}, \tag{6.11}$$

where $\Delta_\kappa=\kappa_{n,i,l}^A\kappa_{n,i,w}^B\kappa_{i,w,j}^C\kappa_{v_1,v_2}^D(\bar{\zeta},\delta,\upsilon)$, $\kappa_{n,i,l}^A=\prod_{l=1}^L(-1)^{n_l}\left(\frac{{\beta_l}^{i_l}}{i_l!}\eta_P^{i_l}F_{g,l}\left(\varrho_P\right)\right)^{n_l}m_{h,l}^{n_l-1}$, $\kappa_{n,i,w}^B=\prod_{l=1}^L\left(\frac{n_l{\alpha_l}^{m_{g,l}}}{\eta_P^{i_l}F_{g,l}(\varrho_P){Q_{pk}}^{i_l}\Gamma(m_{g,l})}\right)^{w_l}$, $\kappa_{i,w,j}^C=\prod_{l=1}^L\left(\frac{(m_{g,l}+i_l-1)!}{j_l!\varrho_P^{-j_l}e^{\alpha_l\varrho_P}}\left(\frac{\beta_l}{Q_{pk}}\right)^{j_l-m_{g,l}-i_l}\right)^{w_l}(m_{g,l}+i_l)^{w_l-1}$, $\kappa_{v_1,v_2}^D(\bar{\zeta},\delta,\upsilon)$ *can be computed recursively using* (6.75), $\Xi_{i,n}^A=\sum_{l=1}^L i_l n_l$, $\Xi_n^B=\sum_{l=1}^L\eta_P\beta_l n_l$, $\bar{\zeta}_q$ *denotes the* q*-th distinct root of* $\mathcal{G}^D(x)=\prod_{l=1}^{L+1}(x-\zeta_l)^{-\xi_{i,w,j,l}}$, $\delta_q=\sum_{o=1,\zeta_o==\bar{\zeta}_q}^L\xi_{i,w,j,o}$ *denotes the multiplicity of* $\bar{\zeta}_q$, $\zeta_l=\tau_l$ *for* $l=\{1,\dots L\}$, $\xi_{i,w,j,l}=\psi_{i,w,j,l}$ *for* $l=\{1,\dots L\}$, $\tau_l=-\frac{\alpha_l}{\beta_l}Q_{pk}$, $\psi_{i,w,j,l}=-w_l(j_l-m_{g,l}-i_l)$, $\zeta_{L+1}=-1$ *and* $\xi_{i,w,j,L+1}=1$, $\sum_{\mathfrak{F}}$

is represented using shorthand notation $\sum_{p=0}^{1}\sum_{\mathbf{n}\in\Theta_L}\sum_{\mathcal{I}}\sum_{\mathbf{w}\in\Theta_L}\sum_{\mathcal{J}}\sum_{v_1=1}^{\upsilon}\sum_{v_2=1}^{\delta_{v_1}}$, $\sum_{\mathcal{I}}$ *is short form notation of* $\sum_{i_1=0}^{m_{h,1}-1}\cdots\sum_{i_L=0}^{m_{h,L}-1}$, $\sum_{\mathcal{J}}=\sum_{j_1=0}^{m_{g,1}+i_1-1}\cdots\sum_{j_L=0}^{m_{g,L}+i_L-1}$, Θ_L *is the set of all possible* L *bit binary numbers and* n_l *is the* l*-th bit of the binary number* $\mathbf{n}\in\theta_L$ *and* w_l *is the* l*-th bit of the binary number* $\mathbf{w}\in\theta_L$.

Proof. See Appendix 6.6.2. □

The CDF in (6.11) involves multiple summations, a rational function in x and a simple exponential function and thus, can be used to obtain closed form expressions for various performance measures. For example, the moments of the output SNR are useful in characterizing the system performance and can be easily obtained from the MGF [2]. The PDF of output SNR for an OMU-CN-NI can be easily obtained by differentiating the CDF in (6.11).

6.3.2 Outage Probability

Using the CDF in (6.11), the outage performance of the OMU-CN-NI can be obtained as

$$\mathcal{O}_{\mathcal{NI}}(\Psi)=F_{\Upsilon_{\mathcal{F}}}(\Psi) \tag{6.12}$$

where $\Psi=2^{\mathcal{R}}-1$ and $\mathcal{R}$ is the transmission rate.

Asymptotic Outage Performance:

The derived expressions in (6.10), (6.11) and (6.12) do not yield much insight on outage performance with varying system parameters. Here we mention three remarks that give information regarding the outage performance in the asymptotic regimes.

Remark 3. *As the interference power threshold is relaxed, i.e. as* $Q_{pk}\to\infty$*, the*

outage probability of an OMU-CN-NI is given by

$$\mathcal{O}_{\mathcal{NI},Q}^{floor}(\Psi) = F_{\Upsilon_{CSI,Q}}^{floor}(\Psi) = \prod_{l=1}^{L}\left(1 - e^{-\Psi\eta_P\beta_l}\sum_{i=0}^{m_{h,l}-1}\frac{{\beta_l}^i}{i!}\Psi^i\eta_P^i\right). \tag{6.13}$$

Proof. In (6.10), as $Q_{pk} \to \infty$, $\Gamma\left(m_{g,l}+i, \left(\alpha_l + \frac{\beta_l}{Q_{pk}}\Psi\right)\varrho_P\right) \to 0$ and $F_{g,l}(\varrho_P) \to 1$. Replacing these function with the asymptotic values in (6.10) and doing some algebraic manipulation yields (6.13). □

From Remark 3, it can be noted that the expression in (6.13) does not include any parameter related to the primary network. Thus, when $Q_{pk} \to \infty$, the outage performance is not affected by the quality of the interference link and the secondary link is reduced to a standard point-to-point link. Furthermore, as the interference constraint is relaxed, for a fixed rate $\mathcal{R}$, the outage probability of the secondary network becomes constant. This saturation occurs due to the limited transmit power at the SU-Tx.

Remark 4. *As the limit on the transmit power of the SU-Tx is removed, i.e. as $P_{max} \to \infty$, the outage probability of an OMU-CN-NI is given by*

$$\mathcal{O}_{\mathcal{NI},P}^{floor}(\Psi) = F_{\Upsilon_{CSI,P}}^{floor}(\Psi) = \prod_{l=1}^{L}\left(1 - \sum_{i=0}^{m_{h,l}-1}\frac{\Gamma(m_{g,l}+i)}{\Gamma(m_{g,l})}\frac{1}{i!}\left(\frac{\beta_l}{\alpha_l}\frac{\Psi}{Q_{pk}}\right)^i\left(1+\frac{\beta_l}{\alpha_l}\frac{\Psi}{Q_{pk}}\right)^{-(m_{g,l}+i)}\right). \tag{6.14}$$

Proof. In (6.10), $P_{max} \to \infty$ implies $\varrho_P \to 0$, $\eta_P \to 0$, $\Gamma\left(m_{g,l}+i, \left(\alpha_l + \frac{\beta_l}{Q_{pk}}\Psi\right)\varrho_P\right) \to \Gamma(m_{g,l}+i)$ and $F_{g,l}(\varrho_P) \to 0$. Replacing these functions in (6.10) and doing some algebraic manipulation yields the constant outage probability expressed in (6.14). □

In the case when $P_{max} \to \infty$, it can be noted from (6.14) that the outage per-

formance of the secondary system is affected by the quality of the interference link unlike the case when $Q_{pk} \to \infty$. Furthermore, for a fixed rate, the outage probability saturates due to fixed Q_{pk}. It will be shown later that, for a fixed rate, even the SER and ergodic capacity saturate due to the interference constraint. This saturation is not experienced in the traditional multi-user networks as the constraint on the interference power exists mainly in a multi-user spectrum sharing network and is not so common in the traditional multi-user network. Due to this, multi-user diversity in the cognitive setting is different from that in the traditional networks.

Remark 5. *As the limit on the transmit power of the SU-Tx is removed, i.e.* $P_{max} \to \infty$*, the probability of outage of an OMU-CN-NI with a weak interference link, i.e.* $\frac{\beta_l}{\alpha_l} \to 0$*, is approximated as*

$$\mathcal{O}^{\infty}_{\mathcal{NI}}(\Psi) = F^{\infty}_{\Upsilon_{CSI}}(\Psi) = \prod_{l=1}^{L} \left(\frac{\Gamma(m_{g,l} + m_{h,l})}{\Gamma(m_{g,l})} \sum_{q=0}^{m_{h,l}-1} \frac{(-1)^{m_{h,l}-q-1}}{q!\,(m_{h,l}-q)!} \left(\frac{\Psi}{Q_{pk}} \frac{\beta_l}{\alpha_l} \right)^{m_{h,l}} \right) \tag{6.15}$$

Proof. From (6.14) one has

$$F^{floor}_{\Upsilon_{CSI,P}}(\Psi) = \prod_{l=1}^{L} \left(1 - \sum_{i=0}^{m_{h,l}-1} \frac{\Gamma(m_{g,l} + i)}{\Gamma(m_{g,l})\, i!} (z)^i (1+z)^{-(m_{g,l}+i)} \right), \tag{6.16}$$

where $z = \frac{\Psi}{Q_{pk}} \frac{\beta_l}{\alpha_l}$. $z \to 0$ when $\frac{\beta_l}{\alpha_l} \to 0$, and (6.16) can be approximated using the negative binomial expansion as

$$F^{floor}_{\Upsilon_{CSI,P}}(\Psi) = \prod_{l=1}^{L} \left(1 - \sum_{i=0}^{m_{h,l}-1} \sum_{q=0}^{\infty} \frac{\Gamma(m_{g,l} + i + q)}{\Gamma(m_{g,l})\, i! q!} (-1)^q z^{q+i} \right) \tag{6.17}$$

In (6.17), the terms of z, having powers up to $m_{h,l}-1$ cancel out and only terms having powers greater than $m_{h,l}-1$ remain. As z is very small the terms of z having powers

greater than $m_{h,l}$ are ignored. After some algebraic manipulation the asymptotic CDF in (6.15) is obtained. □

Remark 5 gives the probability of outage as the interference link approaches zero or when the secondary-to-secondary link has high power compared to the interference link. Using the concept of *generalized diversity gain*, which was introduced in [101], the generalized diversity gain of the OMU-CN-NI can be obtained. The *generalized diversity gain* is defined as

$$d_{CSI} = \lim_{\mu_l \to 0} \frac{\log\left(F^{\infty}_{\Upsilon_{CSI,P}}(x)\right)}{\log\left(\mu_l\right)}, \tag{6.18}$$

where $\mu_l = \frac{1}{\alpha_l}$. Considering that $\mu_l \to 0$, $\forall\, l$, substituting (6.15) into (6.18), it can be concluded that the generalized diversity gain for an opportunistic multi-user secondary link in the asymptotic regime is $d_{CSI} = \sum_{l=1}^{L} m_{h,l}$. Thus, this scheduling scheme achieves full diversity when the transmit power constraint is relaxed and the interference link is in a deep fade and this diversity gain increases as the number of SUs, L, increases.

6.3.3 Moment Generating Function

The exact closed form expression of the MGF of the output SNR, can be derived using (6.11) and is given by Remark 6.

Remark 6. *The MGF of the output SNR is given by*

$$\mathcal{M}_{\Upsilon_{CSI}}(s) = \sum_{\mathfrak{F}} \Delta_{\kappa} s \frac{\Gamma\left(\Xi^{A}_{i,n} + p + 1\right)}{\left(\Xi^{B}_{n} + s\right)^{\frac{\Xi^{A}_{i,n}+p-v_2+2}{2}}} \varsigma_{v_1}^{\frac{\Xi^{A}_{i,n}+p-v_2}{2}} e^{\frac{\varsigma_{v_1}}{2}(\Xi^{B}_{n}+s)} W_{\frac{-v_2-\Xi^{A}_{i,n}-p}{2}, \frac{v_2-\Xi^{A}_{i,n}-p-1}{2}}\left((\Xi^{B}_{n}+s)\varsigma_{v_1}\right), \tag{6.19}$$

where $W_{\lambda,\mu}(z)$ is the WhittakerW function defined in [96, Eq. (9.220.4)].

Proof. See Appendix 6.6.3. □

The derived MGF in (6.19) involves an exponential function and a WhittakerW function which are available in well known mathematical packages and thus, it can be easily evaluated. The n-th moment of the output SNR of an OMU-CN can be obtained by taking the n-th derivative of the MGF in (6.19) and substituting $s = 0$. The MGF can also be used to evaluate the SER performance [2].

6.3.4 Symbol Error Rate

The average symbol error rate can be obtained using the CDF of output SNR as [97]

$$\mathcal{P}_e = -\int_0^\infty \bar{P}'_e(x) F_{\Upsilon_{end}}(x) dx, \tag{6.20}$$

where $\mathcal{P}_e$ is the average symbol error rate, $\bar{P}'_e(x) = \frac{\partial P_e(\cdot)}{\partial x}$ is the derivative of the conditional error probability (CEP) $P_e(\cdot)$ and $F_{\Upsilon_{end}}(\cdot)$ denotes the CDF of the output SNR (Υ_{end}). The SER performance of the OMU-CN can be derived for various modulation formats depending on its CEP form [97].

Coherent Binary Modulations and M-PAM Modulation

The CEP for coherent binary phase-shift-keying (BPSK), coherent binary frequency-shift-keying (BFSK) and M-ary pulse amplitude modulation (M-PAM) can be represented as

$$P_{e,\mathcal{C}}(x) = a\, Q(\sqrt{bx}), \tag{6.21}$$

where $(a, b) = (1, 2)$ for BPSK, $(a, b) = (1, 1)$ for BFSK, $(a, b) = \left(2\frac{M-1}{M}, 6\frac{\log_2(M)}{M^2-1}\right)$ for M-PAM, and $Q(\cdot)$ denotes the Gaussian Q-function [94].

The unconditional SER for these modulation schemes can be found as

$$\mathcal{P}_{e,\mathcal{C},CSI} = \frac{a}{2}\sqrt{\frac{b}{2\pi}}\int_0^\infty \frac{1}{\sqrt{x}} e^{-\frac{bx}{2}} F_{\Upsilon_{CSI}}(x)dx. \tag{6.22}$$

Substituting the CDF from (6.11) into (6.22) one gets

$$\mathcal{P}_{e,\mathcal{C},CSI} = \frac{a}{2}\sqrt{\frac{b}{2\pi}}\sum_{\mathfrak{F}}\Delta_\kappa \int_0^\infty x^{\Xi^A_{i,n}+p-\frac{1}{2}} e^{-x\left(\Xi^B_n+\frac{b}{2}\right)}\left(x-\bar{\zeta}_{v_1}\right)^{-v_2} dx. \tag{6.23}$$

Similar to (6.78), applying the transformation of variable $z = x - \bar{\zeta}_{v_1}$ and solving the resulting integral using [96, Eq. (3.383.4)], $\mathcal{P}_{e,\mathcal{C}}$ is found to be given as

$$\mathcal{P}_{e,\mathcal{C},CSI} = \frac{a}{2}\sqrt{\frac{b}{2\pi}}\sum_{\mathfrak{F}}\Delta_\kappa \frac{\Gamma\left(\Xi^A_{i,n}+p+\frac{1}{2}\right)}{\left(\Xi^B_n+\frac{b}{2}\right)^{\frac{\Xi^A_{i,n}+p-v_2+\frac{3}{2}}{2}}} \varsigma_{v_1}^{\frac{\Xi^A_{i,n}+p-v_2-\frac{1}{2}}{2}} e^{\frac{\varsigma_{v_1}}{2}(\Xi^B_n+\frac{b}{2})} W_{\lambda_1,\lambda_2}\left(\left(\Xi^B_n+\frac{b}{2}\right)\varsigma_{v_1}\right), \tag{6.24}$$

where $\varsigma_{v_1} = -\bar{\zeta}_{v_1}$, $\lambda_1 = \frac{-v_2-\Xi^A_{i,n}-p+\frac{1}{2}}{2}$ and $\lambda_2 = \frac{v_2-\Xi^A_{i,n}-p-\frac{1}{2}}{2}$.

Non-Coherent Modulations

The CEP for differential binary phase-shift-keying (DBPSK) and non-coherent binary frequency-shift-keying (NCBFSK) can be represented as

$$P_{e,\mathcal{NC}}(x) = a\, e^{-bx}, \tag{6.25}$$

where $(a, b) = (0.5, 1)$ for DBPSK and $(a, b) = (0.5, 0.5)$ for NCBFSK. The unconditional SER for these modulation schemes is given as [97]

$$\mathcal{P}_{e,\mathcal{NC},CSI} = a\, b \int_0^\infty e^{-bx} F_{\Upsilon_{CSI}}(x) dx. \tag{6.26}$$

Using a similar approach as before, $\mathcal{P}_{e,\mathcal{NC}}$ can be expressed as

$$\mathcal{P}_{e,\mathcal{NC},CSI} = \\ a\, b \sum_{\mathfrak{F}} \Delta_\kappa \frac{\Gamma\left(\Xi_{i,n}^A + p + 1\right)}{(\Xi_n^B + b)^{\frac{\Xi_{i,n}^A + p - v_2 + 2}{2}}} \varsigma_{v_1}^{\frac{\Xi_{i,n}^A + p - v_2}{2}} e^{\frac{\varsigma_{v_1}}{2}(\Xi_n^B + b)} W_{\frac{-v_2 - \Xi_{i,n}^A - p}{2}, \frac{v_2 - \Xi_{i,n}^A - p - 1}{2}} \left((\Xi_n^B + b)\varsigma_{v_1}\right). \tag{6.27}$$

Quadrature Modulations

The CEP for quadrature signalling such as M-ary quadrature amplitude modulation (QAM) and coherent detected DPSK is of form

$$P_{e,\mathcal{Q}}(x) = a\, Q(\sqrt{bx}) - c\, Q^2\left(\sqrt{bx}\right), \tag{6.28}$$

where $(a, b, c) = (2, 2, 1)$ for QPSK or 4-QAM, $(a, b, c) = (2, 2, 2)$ for coherent detected DPSK and $(a, b, c) = \left(4\frac{\sqrt{M}-1}{\sqrt{M}}, 3\frac{\log_2 M}{M-1}, 4\frac{(\sqrt{M}-1)^2}{\sqrt{M}}\right)$ for M-QAM [97]. The unconditional SER for these quadrature modulations can be expressed as [97]

$$\mathcal{P}_{e,\mathcal{Q},CSI} = \frac{a}{2}\sqrt{\frac{b}{2\pi}} \int_0^\infty \frac{1}{\sqrt{x}} e^{-\frac{bx}{2}} F_{\Upsilon_{CSI}}(x) dx - c\sqrt{\frac{b}{2\pi}} \int_0^\infty \frac{1}{\sqrt{x}} e^{-\frac{bx}{2}} Q(\sqrt{bx}) F_{\Upsilon_{CSI}}(x) dx. \tag{6.29}$$

The first integral in (6.29) is the same as the integral in (6.23) where as the second integral cannot be obtained in closed form and can be approximated using the Gauss-

Laguerre formula [92] yielding

$$\mathcal{P}_{e,\mathcal{Q},CSI} \approx \mathcal{P}_{e,\mathcal{C}} - c\sqrt{\frac{b}{2\pi}} \sum_{t_1=1}^{T} \omega(x_{t_1}) e^{x_{t_1}} \frac{1}{\sqrt{x_{t_1}}} e^{-\frac{bx_{t_1}}{2}} Q(\sqrt{bx_{t_1}}) F_{\Upsilon_{CSI}}(x_{t_1}), \tag{6.30}$$

where, $\omega(x_k) = \frac{x_k}{(T+1)^2 L_{T+1}(x_k^2)}$, x_k is the k-th zero of the Laguerre polynomial $L_n(x)$ [92] and T is the number of points chosen for the Gauss-Laguerre rule. In the computer simulations, the value of T is chosen to be 16.

Asymptotic SER Performance:

The derived analytical expressions in (6.24), (6.27) and (6.30) do not yield much insight on SER performance with varying system parameters. Therefore, we discuss below the SER performance in the asymptotic regimes.

(a) SER for Coherent Modulation Schemes:

Remark 7. *As the interference power threshold is relaxed, i.e. $Q_{pk} \to \infty$, the SER of an OMU-CN-NI, employing a one-dimensional coherent modulation scheme, is given by*

$$\mathcal{P}_{e,\mathcal{C},Q}^{floor} = \frac{a}{2}\sqrt{\frac{b}{2\pi}} \sum_{\mathbf{n}\in\Theta_L} \sum_{\mathcal{I}} \kappa_Q \left(\Xi_n^B + \frac{b}{2}\right)^{-\left(\Xi_{i,n}^A + \frac{1}{2}\right)} \Gamma\left(\Xi_{i,n}^A + \frac{1}{2}\right). \tag{6.31}$$

Proof. The SER for one-dimensional coherent modulation schemes where $Q_{pk} \to \infty$, can be obtained using $F_{\Upsilon_{CSI},Q}^{floor}(\cdot)$ as

$$\mathcal{P}_{e,\mathcal{C},Q}^{floor} = \frac{a}{2}\sqrt{\frac{b}{2\pi}} \int_0^\infty \frac{1}{\sqrt{x}} e^{-\frac{b}{2}x} F_{\Upsilon_{CSI},Q}^{floor}(x)\, dx. \tag{6.32}$$

Substituting the alternate form of $F_{\Upsilon_{CSI},Q}^{floor}(\cdot)$, which is derived in Appendix 6.6.4-1, yields

$$\mathcal{P}_{e,\mathcal{C},Q}^{floor} = \frac{a}{2}\sqrt{\frac{b}{2\pi}} \sum_{\mathbf{n}\in\Theta_L} \sum_{\mathcal{I}} \kappa_Q \int_0^\infty e^{-\left(\Xi_n^B + \frac{b}{2}\right)x} x^{\Xi_{i,n}^A - \frac{1}{2}} dx. \tag{6.33}$$

Solving the integral in (6.33) we get the desired result in (6.31). □

Similar to the outage performance, at high Q_{pk}, the SER becomes constant due to the limited transmit power at the SU-Tx.

Remark 8. *As the limit on the transmit power of the SU-Tx is removed, i.e.* $P_{max} \to \infty$*, the SER of an OMU-CN-NI, employing a one-dimensional coherent modulation scheme, is given by*

$$\mathcal{P}_{e,\mathcal{C},P}^{floor} = \frac{a}{2}\sqrt{\frac{b}{2\pi}} \sum_{\mathcal{P}} \kappa_{n,i}^{P} \kappa_{v_1,v_2}^{D}(\bar{\zeta}, \delta^{P}, \upsilon) \left(\frac{b}{2}\right)^{-\frac{\Xi_{i,n}^{A}+p-v_2+\frac{3}{2}}{2}} \times \\ (\varsigma_{v_1})^{\frac{\Xi_{i,n}^{A}+p-v_2-\frac{1}{2}}{2}} \Gamma\left(\Xi_{i,n}^{A}+p+\frac{1}{2}\right) e^{\frac{b}{4}\varsigma_{v_1}} W_{\phi_1,\phi_2}\left(\frac{b}{2}\varsigma_{v_1}\right), \tag{6.34}$$

where $\phi_1 = \frac{-v_2-\Xi_{i,n}^{A}-p+\frac{1}{2}}{2}$ *and* $\phi_2 = \frac{-\Xi_{i,n}^{A}-p+v_2-\frac{1}{2}}{2}$.

Proof. Similar to (6.32), The SER for one-dimensional coherent modulation schemes where $P_{max} \to \infty$, can be obtained using $F_{\Upsilon_{CSI},P}^{floor}(\cdot)$ as

$$\mathcal{P}_{e,\mathcal{C},P}^{floor} = \frac{a}{2}\sqrt{\frac{b}{2\pi}} \int_{0}^{\infty} \frac{1}{\sqrt{x}} e^{-\frac{b}{2}x} F_{\Upsilon_{CSI},P}^{floor}(x)\, dx. \tag{6.35}$$

Substituting the alternate form of $F_{\Upsilon_{CSI},P}^{floor}(\cdot)$, which is derived in Appendix 6.6.4-2, into (6.35) and doing some algebraic manipulations yields

$$\mathcal{P}_{e,\mathcal{C},P}^{floor} = \frac{a}{2}\sqrt{\frac{b}{2\pi}} \sum_{\mathcal{P}} \kappa_{n,i}^{P} \kappa_{v_1,v_2}^{D}(\bar{\zeta}, \delta^{P}, \upsilon) \int_{0}^{\infty} e^{-\frac{b}{2}x} x^{\Xi_{i,n}^{A}+p-\frac{1}{2}} \left(x-\bar{\zeta}_{v_1}\right)^{-v_2} dx. \tag{6.36}$$

Substituting $z = x + \varsigma_{v_1}$ in (6.36), where $\varsigma_{v_1} = -\bar{\zeta}_{v_1}$, and solving the resulting integral using [96, Eq. (3.383.4)] yields the desired result in (6.34). □

Similar to the outage performance, as the peak interference power constraint is relaxed, the SER becomes constant due to the limited transmit power at the SU-Tx.

Remark 9. *As the limit on the transmit power of the SU-Tx is removed, i.e.* $P_{max} \to \infty$*, the SER of an OMU-CN-NI, employing a one-dimensional coherent modulation scheme, with a weak interference channel, i.e.* $\frac{\beta_l}{\alpha_l} \to 0$*, is approximated as*

$$\mathcal{P}_{e,\mathcal{C}}^{\infty} \approx \frac{a}{2\sqrt{\pi}} \left(\frac{b}{2}\right)^{-\sum_{l=1}^{L} m_{h,l}} \Gamma\left(\sum_{l=1}^{L} m_{h,l} + \frac{1}{2}\right) \times \prod_{l=1}^{L} \left(\left(\frac{\beta_l}{\alpha_l}\frac{1}{Q_{pk}}\right)^{m_{h,l}} \frac{\Gamma\left(m_{g,l}+m_{h,l}\right)}{\Gamma\left(m_{g,l}\right)} \sum_{q=0}^{m_{h,l}-1} \frac{(-1)^{m_{h,l}-q-1}}{q!\left(m_{h,l}-q\right)!} \right) \tag{6.37}$$

Proof. The SER performance, when $P_{max} \to \infty$ and the interference channel is weak, i.e. $\frac{\beta_l}{\alpha_l} \to 0$, can be derived using $F_{\Upsilon_{CSI}}^{\infty}(\cdot)$ as

$$\mathcal{P}_{e,\mathcal{C}}^{\infty} \approx \frac{a}{2}\sqrt{\frac{b}{2\pi}} \int_0^{\infty} \frac{1}{\sqrt{x}} e^{-\frac{b}{2}x} F_{\Upsilon_{CSI}}^{\infty}(x)\, dx \tag{6.38}$$

Substituting $F_{\Upsilon_{CSI}}^{\infty}(x)$ from (6.15) into (6.38), and doing some algebraic manipulations gives

$$\mathcal{P}_{e,\mathcal{C}}^{\infty} \approx \frac{a}{2}\sqrt{\frac{b}{2\pi}} \int_0^{\infty} e^{-\frac{b}{2}x} x^{\sum_{l=1}^{L} m_{h,l} - \frac{1}{2}} dx \times \prod_{l=1}^{L} \left(\frac{\Gamma\left(m_{g,l}+m_{h,l}\right)}{\Gamma\left(m_{g,l}\right)} \sum_{q=0}^{m_{h,l}-1} \frac{(-1)^{m_{h,l}-q-1}}{q!\left(m_{h,l}-q\right)!} \left(\frac{\beta_l}{\alpha_l}\frac{1}{Q_{pk}}\right)^{m_{h,l}} \right) \tag{6.39}$$

Solving the integral in (6.39) and doing some algebraic manipulations yields (6.37).

□

Remark 9 gives the approximate SER as the interference link approaches zero or when the secondary-to-secondary link has high power compared to the interference link. Considering that $\mu_l \to 0$, $\forall\, l$, from (6.37) it can be concluded that the SER of an OMU-CN-NI decays with an order $d_{CSI} = \sum_{l=1}^{L} m_{h,l}$ in the asymptotic regime.

(b) SER for Non-Coherent and Quadrature Modulation Schemes:

Similar to Remarks 7-9, the SER performance of an OMU-CN-NI employing one-dimensional non-coherent modulation schemes or quadrature modulation schemes can be derived in the asymptotic regime. Here, due to space limitation we just briefly mention the results.

- As the interference power threshold is relaxed, i.e. $Q_{pk} \to \infty$, the SER of an OMU-CN-NI, employing a one-dimensional non-coherent modulation scheme, becomes constant and is given by

$$\mathcal{P}_{e,\mathcal{NC},Q}^{floor} = a\, b \sum_{\mathbf{n}\in\Theta_L} \sum_{\mathcal{I}} \kappa_Q \left(\Xi_n^B + b\right)^{-\left(\Xi_{i,n}^A+1\right)} \Gamma\left(\Xi_{i,n}^A + 1\right) \tag{6.40}$$

- As the limit on the transmit power of the SU-Tx is removed, i.e. $P_{max} \to \infty$, the SER of an OMU-CN-NI, employing a one-dimensional non-coherent modulation scheme, becomes constant and is given by

$$\begin{aligned}\mathcal{P}_{e,\mathcal{NC},P}^{floor} = a\, b \sum_{\mathcal{P}} \kappa_{n,i}^P \kappa_{v_1,v_2}^D(\bar{\zeta}, \delta^P, \upsilon)\, (b)^{-\frac{\Xi_{i,n}^A+p-v_2}{2}-1} \times \\ (\varsigma_{v_1})^{\frac{\Xi_{i,n}^A+p-v_2}{2}} \Gamma\left(\Xi_{i,n}^A + p + 1\right) e^{\frac{b}{2}\varsigma_{v_1}} W_{\aleph_1,\aleph_2}\left(b\,\varsigma_{v_1}\right)\end{aligned} \tag{6.41}$$

  where $\aleph_1 = \frac{-v_2-\Xi_{i,n}^A-p}{2}$ and $\aleph_2 = \frac{-\Xi_{i,n}^A-p+v_2-1}{2}$.

- As the limit on the transmit power of the SU-Tx is removed, i.e. $P_{max} \to \infty$, the SER of an OMU-CN-NI, employing a one-dimensional non-coherent modulation

scheme, with a weak interference channel, i.e. $\frac{\beta_l}{\alpha_l} \to 0$, is approximated as

$$\mathcal{P}_{e,\mathcal{NC}}^{\infty} \approx a\, b^{-\sum_{l=1}^{L} m_{h,l}} \Gamma\left(\sum_{l=1}^{L} m_{h,l} + 1\right) \times \prod_{l=1}^{L} \left(\frac{\Gamma\left(m_{g,l} + m_{h,l}\right)}{\Gamma\left(m_{g,l}\right)} \sum_{q=0}^{m_{h,l}-1} \frac{(-1)^{m_{h,l}-q-1}}{q!\,(m_{h,l}-q)!} \left(\frac{\beta_l}{\alpha_l} \frac{1}{Q_{pk}} \right)^{m_{h,l}} \right) \tag{6.42}$$

- As the interference power threshold is relaxed, i.e. $Q_{pk} \to \infty$, the SER of an OMU-CN-NI, employing a quadrature modulation scheme, becomes constant and is given by

$$\mathcal{P}_{e,\mathcal{Q},Q}^{floor} = \mathcal{P}_{e,\mathcal{C},Q}^{floor} - c\sqrt{\frac{b}{2\pi}} \sum_{\mathbf{n}\in\Theta_L} \sum_{\mathcal{I}} \kappa_Q \frac{2^{\varkappa_1 - 1} \varkappa_3\, \Gamma\left(\varkappa_1 + \frac{1}{2}\right)}{\varkappa_1 \sqrt{\pi} (\varkappa_3^2 + \varkappa_1 \varkappa_2^2)^{\varkappa_1 + \frac{1}{2}}}\, {}_2F_1\left(1, \varkappa_1 + \frac{1}{2}; \varkappa_1 + 1; \frac{\varkappa_1 \varkappa_2^2}{\varkappa_3^2 + \varkappa_1 \varkappa_2^2}\right) \tag{6.43}$$

where $\frac{2\Xi_{i,n}^{A}+1}{2}$, $\varkappa_2^2 = \frac{2\left(\Xi_n^B + \frac{b}{2}\right)}{\left(\frac{2\Xi_{i,n}^{A}+1}{2}\right)}$ and $\varkappa_3 = \sqrt{b}$.

6.3.5 Capacity

The ergodic capacity of the OMU-CN-NI is given in Remark 10.

Remark 10. *The ergodic capacity of the OMU-CN-NI is given as*

$$C_{CSI} = -\frac{\log_2(e)}{B} \sum_{\mathfrak{C}} \Delta_{\kappa}(\Xi_n^B)^{-\frac{(\Xi_{i,n}^{A}+1)+(-v_2+1)}{2}} \times \varsigma_{v_1}^{\frac{(\Xi_{i,n}^{A}+1)+(-v_2+1)+2}{2}} \Gamma(\Xi_{i,n}^{A}+1) e^{\frac{\Xi_n^B \varsigma_{v_1}}{2}} W_{\frac{-v_2-\Xi_{i,n}^{A}}{2}, \frac{-\Xi_{i,n}^{A}+v_2-1}{2}}\left(\Xi_n^B \varsigma_{v_1}\right), \tag{6.44}$$

where $\sum_{\mathfrak{C}}$ *is the short hand notation of* $\sum_{\mathbf{n}\in\Theta_L, \mathbf{n}\neq 0} \sum_{\mathcal{I}} \sum_{\mathbf{w}\in\Theta_L} \sum_{\mathcal{J}} \sum_{v_1=1}^{v} \sum_{v_2=1}^{\delta_{v_1}}$.

Proof. See Appendix 6.6.5. □

Remark 10 gives the exact closed-form expression for ergodic capacity which can be easily evaluated as it involves the exponential function, WhittakerW function and the Gamma function which are available in well known mathematical packages. Eq. (6.44) does not yield much insight on the effect on capacity with varying system parameters. Remark 11 gives some insight by obtaining the expression for ergodic capacity in the asymptotic regime.

Remark 11. *As the interference power threshold is relaxed, i.e.* $Q_{pk} \to \infty$*, the ergodic capacity of an OMU-CN-NI, is given by*

$$\mathcal{C}_{CSI,Q}^{floor} = -\frac{\log_2(e)}{B} \sum_{\mathbf{n}\in\Theta_L,\mathbf{n}\neq 0} \sum_{\mathcal{I}} \kappa_Q e^{\Xi_n^B} \Gamma\left(\Xi_{i,n}^A + 1\right) \Gamma\left(-\Xi_{i,n}^A, \Xi_n^B\right) \tag{6.45}$$

Proof. The capacity of the OMU-CN-NI, for $Q_{pk} \to \infty$, can be obtained using $F_{\Upsilon_{CSI},Q}^{floor}(\cdot)$ as

$$\mathcal{C}_{CSI,Q}^{floor} = \frac{\log_2(e)}{B} \int_0^\infty \frac{1 - F_{\Upsilon_{CSI},Q}^{floor}(x)}{1+x} dx \tag{6.46}$$

Substituting the alternate form of $F_{\Upsilon_{CSI},Q}^{floor}(\cdot)$, which is derived in Appendix 6.6.4-1, into (6.47) gives

$$\mathcal{C}_{CSI,Q}^{floor} = -\frac{\log_2(e)}{B} \sum_{\mathbf{n}\in\Theta_L,\mathbf{n}\neq 0} \sum_{\mathcal{I}} \kappa_Q \int_0^\infty \frac{x^{\Xi_{i,n}^A} e^{-x\Xi_n^B}}{1+x} dx \tag{6.47}$$

Solving integral in (6.47) using [96, Eq. (3.383.10)] gives the desired result in (6.45).

□

From Remark 11, it can be noted that similar to the outage performance and the SER performance at high Q_{pk}, the ergodic capacity also becomes constant due to the limited transmit power at the SU-Tx.

6.4 Opportunistic Multi-User Secondary Network with Interference

In the case when the SU-Rx experiences interference from the PU-Tx, the output signal-to-noise plus interference ratio (SINR) of and OMU-NC-WI can be expressed in terms of the output SNR Υ_{CSI} as

$$\Upsilon_{\mathcal{I}} = \frac{\Upsilon_{CSI}}{P_P \daleth + 1} \tag{6.48}$$

where $\daleth$ is the power gain of the interference link from the PU-Tx and P_P denotes the transmit power of the PU-Tx.

6.4.1 Statistics of the Output SINR

The CDF expression of $\Upsilon_{\mathcal{I}}$ is given by following remark.

Remark 12. *The CDF of the Output SINR for a OMU-NC-WI can be expressed as*

$$\begin{aligned} F_{\Upsilon_{\mathcal{I}}}(\Phi) = & \sum_{\mathfrak{F}} \sum_{i_1=0}^{\Xi_{i,n}^{A}+p} \sum_{i_2=0}^{m_{\daleth,1}-1} \binom{\Xi_{i,n}^{A}+p}{i_1} \binom{m_{\daleth,1}-1}{i_2} \frac{\Delta_{\kappa}(-1)^{\Xi_{i,n}^{A}+p-i_1-i_2+m_{\daleth,1}-1}}{\Gamma(m_{\daleth,1})\left(-\bar{\zeta}_{v_1}\right)^{-\Xi_{i,n}^{A}-p+i_1}} \times \\ & \left(\frac{1}{P_P}\frac{m_{\daleth,1}}{\Omega_{\daleth,1}}\right)^{m_{\daleth,1}} \Phi^{i_1-v_2} e^{-\Xi_n^B \Phi} e^{\left(1-\frac{\bar{\zeta}_{v_1}}{\Phi}\right)\left(\frac{1}{P_P}\frac{m_{\daleth,1}}{\Omega_{\daleth,1}}+\Xi_n^B\Phi\right)} \times \\ & \left(1-\frac{\bar{\zeta}_{v_1}}{\Phi}\right)^{m_{\daleth,1}-1-i_2} \left(\frac{1}{P_P}\frac{m_{\daleth,1}}{\Omega_{\daleth,1}}+\Xi_n^B\Phi\right)^{-\varpi} \Gamma\left(\varpi, \left(\frac{1}{P_P}\frac{m_{\daleth,1}}{\Omega_{\daleth,1}}+\Xi_n^B\Phi\right)\left(1-\frac{\bar{\zeta}_{v_1}}{\Phi}\right)\right) \end{aligned} \tag{6.49}$$

where $\varpi = i_1 + i_2 - v_2 + 1$.

Proof. See Appendix 6.6.6. □

6.4.2 Performance Analysis Measures

Using the CDF in (6.49), the outage performance of the OMU-CN-WI can be obtained as

$$\mathcal{O}_{\mathcal{I}}(\Psi) = F_{\Upsilon_{\mathcal{I}}}(\Psi). \tag{6.50}$$

Similar to the analysis in the previous section, the expressions for the MGF and the SER can be obtained by substituting the CDF in (6.49), into (6.77) and (6.20), respectively, and solving the resulting integrals. However, to the best of authors knowledge closed-form solution to the resulting integrals does not exist and one has to resort to numerical integration techniques to evaluate the expressions.

6.5 Numerical Results and Discussion

In this section, some selected numerical results as well as Monte-Carlo based simulation results are presented to verify the derived analytical results. In obtaining these numerical results, $N_0 = 1$, $B = 1$, and $m_{a,b} = 2, \forall\{a, b\}$. These parameters are fixed in the simulation unless stated.

Fig. 6.2 shows the outage performance for the OMU-CN-NI. The analytical outage performance is plotted using (6.12). It can be observed that the outage probability reduces as the interference constraint is relaxed. Furthermore, the outage probability decreases as the number of users increases. The figure also shows the effect of varying the peak power constraint. At high Q_{pk}, the power allocated using (6.8) is fixed to P_{max} and thus the outage performance becomes constant depending on the value of P_{max}. (6.13) is used to plot the outage probability when $Q_{pk} \to \infty$ and it shows the outage probability at which the performance saturates. Note that for $L > 2$ the asymptotic performance ($Q_{pk} \to \infty$) for $P_{max} = 10$ dB cannot be observed in the Fig.

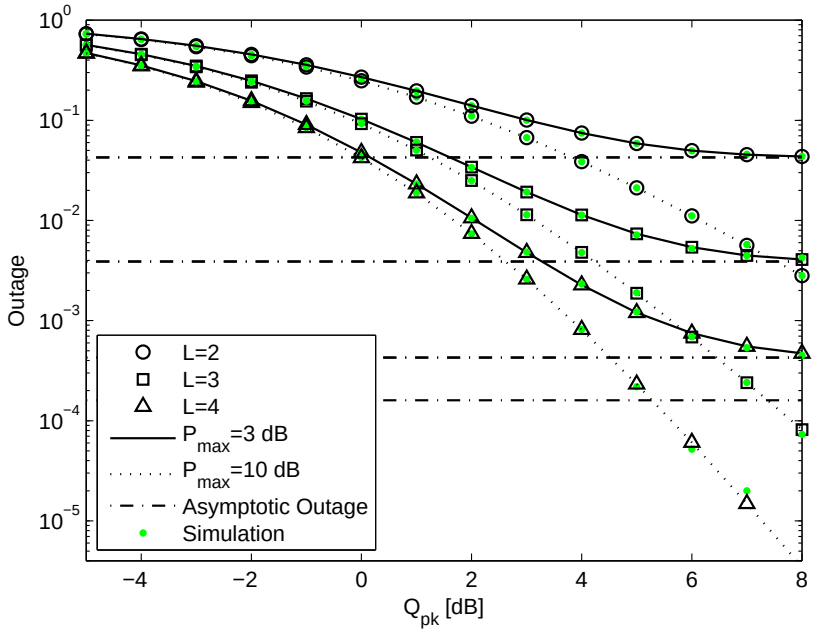

Figure 6.2: Probability of outage of an OMU-CN-NI where $x = 1$, $\Omega_{g,l} = \{1, 2, 3, 4\}$[dB], $\Omega_{h,l} = \{2, 1, 6, 5\}$[dB], and $l = 2, \ldots 4$.

6.2 as it is much below 10^{-5}.

The SER performances of QPSK and BDPSK for the OMU-CN-NI are shown in Fig. 6.3. The curves for QPSK are plotted using (6.30) where $(a, b, c) = (2, 2, 1)$. Similarly the curves for BDPSK are generated using (6.27) where $(a, b) = (0.5, 1)$. It can be observed that the SER reduces as the peak interference power constraint is relaxed. It can also be observed that as the number of users increases the SER reduces. Again one can observe that at high Q_{pk}, the SER becomes constant depending on the values of P_{max}. (6.40) and (6.43) are used to plot the asymptotic SER (where $Q_{pk} \to \infty$) for BDPSK and QPSK, respectively. Note that for $L = 4$ the asymptotic performance (where $Q_{pk} \to \infty$) for $P_{max} = 10$ dB cannot be observed in the Fig. 6.3 as it is much below 10^{-4}.

Fig. 6.4 shows the ergodic capacity of the OMU-CN-NI. The ergodic capacity is plotted using (6.44). It can be observed that the capacity increases as the interference

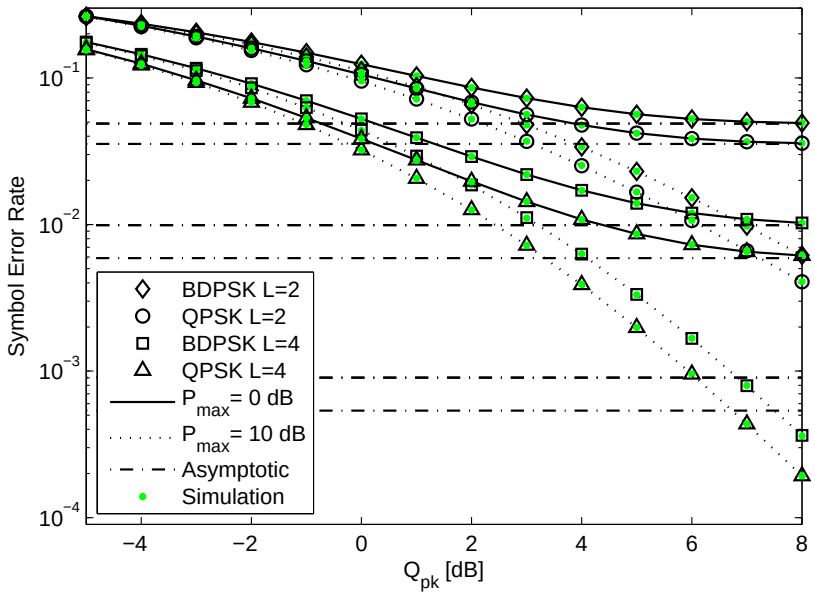

Figure 6.3: Symbol error rate performance of an OMU-CN-NI where $\Omega_{g,l} = \{1, 2, 3, 4\}$[dB], $\Omega_{h,l} = \{2, 1, 6, 5\}$[dB], and $l = 2, \ldots 4$.

constraint is relaxed. Furthermore, the capacity increases as the number of users increases from $L = 2$ to $L = 4$. Increasing P_{max}, increases the capacity, however, the capacity saturates at high Q_{pk} depending on the value of P_{max}. (6.45) is used to plot the asymptotic ergodic capacity (where $Q_{pk} \to \infty$). In all the previous figures, it can be observed that the derived expressions are exact and match well with the computer based Monte-Carlo simulations.

Fig. 6.5 show the outage performance of the OMU-CN-NI as a function of ratio of channel parameters α_l and β_l at high P_{max}. Similarly, Fig. 6.6 and Fig. 6.7 show the SER performance of BPSK modulation and DBPSK modulation schemes, respectively, as a function of ratio of channel parameters α_l and β_l at high P_{max}. In generating the curves for these figures, $m_{g,l} = 1, \forall\, l$ and the users channels are considered to be i.i.d. It can be observed that as $\frac{\alpha_l}{\beta_l}$ increases the outage probability and the SER reduces. Similarly, the outage probability and SER reduces with increasing the

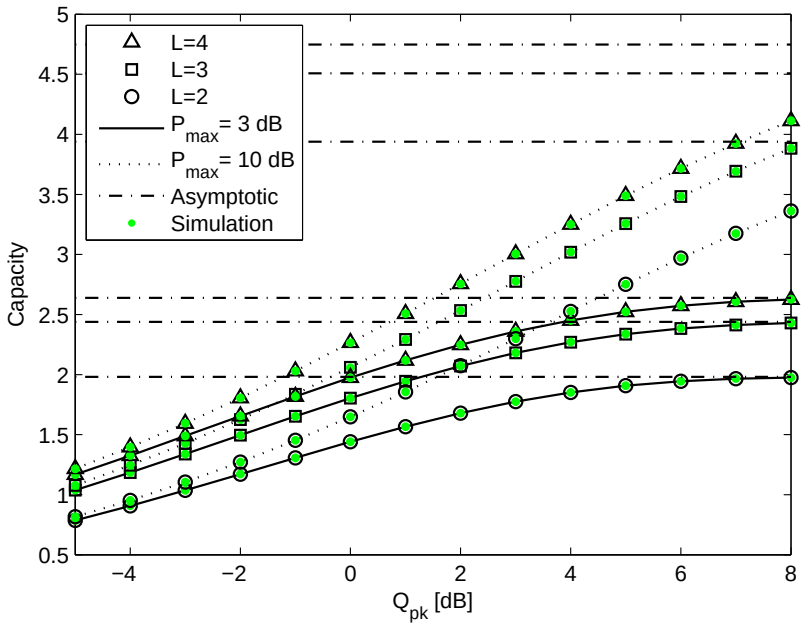

Figure 6.4: Ergodic capacity of an OMU-CN-NI where $\Omega_{g,l} = \{1, 2, 3, 4\}$[dB], $\Omega_{h,l} = \{2, 1, 6, 5\}$[dB], and $l = 2, \ldots 4$.

number of users L. Furthermore, as the channel parameter $m_{h,l}$ increases, the performance improves because it impacts the diversity order as was explained previously. The diversity order of the system with $(L, m_{h,l}) = (2, 3)$ matches the diversity order of the system with $(L, m_{h,l}) = (3, 2)$ as for both system have same $d_{CSI} = \sum_{l=1}^{L} m_{h,l}$. However, the system with $(L, m_{h,l}) = (3, 2)$ gives better performance due to higher coding gain. The asymptotic outage and SER performance is plotted using (6.15), (6.37) and (6.42), respectively.

For an OMU-CN-NI, Fig. 6.8 shows the comparison of the multiuser scheduling scheme analyzed in this chapter, denoted as "max scheduling" scheme, with the hybrid scheduling scheme proposed in [79]. The hybrid scheduling scheme in [79] chose multiple SUs for transmission and thus resulted in improved throughput. However, as we select only a single SU for transmission, thus, we compare the hybrid scheduling scheme with single SU selection. We can observe from Fig. 6.8 that the max

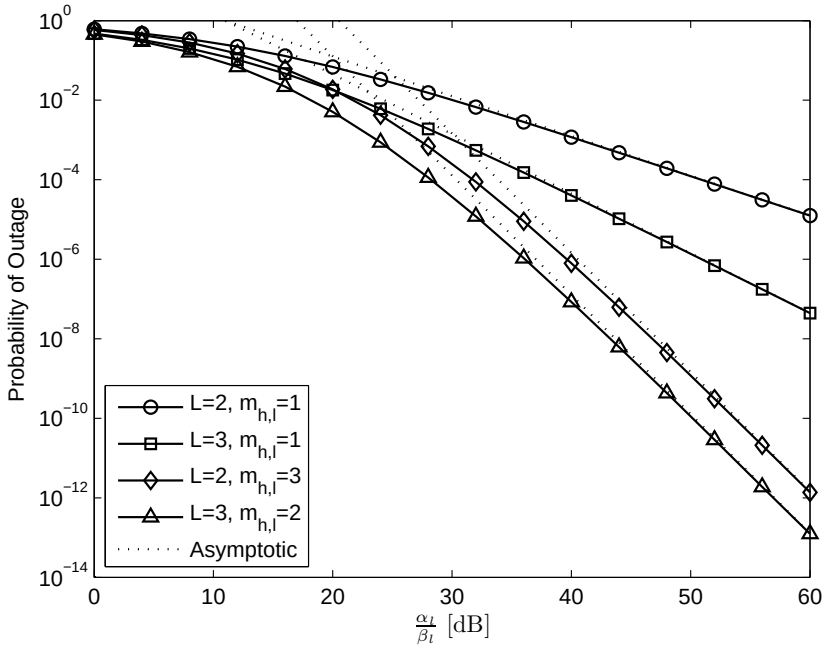

Figure 6.5: Probability of outage of an OMU-CN-NI in the asymptotic regime i.e. $P_{max} \to \infty$.

scheduling scheme has higher ergodic capacity compared to the hybrid scheduling scheme. The reason for the lower capacity of the hybrid scheduling scheme results from the pre-selecting a subset of SUs based on the interference link only. It is quite possible that the SU with a poor interference link also has a poor transmission link or sometimes no SU is selected as none of the SU satisfies the interference constraint. However, in the max scheduling scheme, the selection procedure considers the forward transmission link and a SU is always selected for transmission. In addition, it can be observed in Fig. 6.8 that, for the hybrid scheduling scheme, at low values of Q_{pk}, increasing transmit power of the SUs results in lower capacity which is not the case for the max scheduling scheme. This happens because the number of SUs selected in the initial subset decreases. However at large Q_{pk}, increasing transmit power increases the capacity and follows a normal trend.

The outage performance of a OMU-CN-WI is shown in Fig. 6.9. The curves

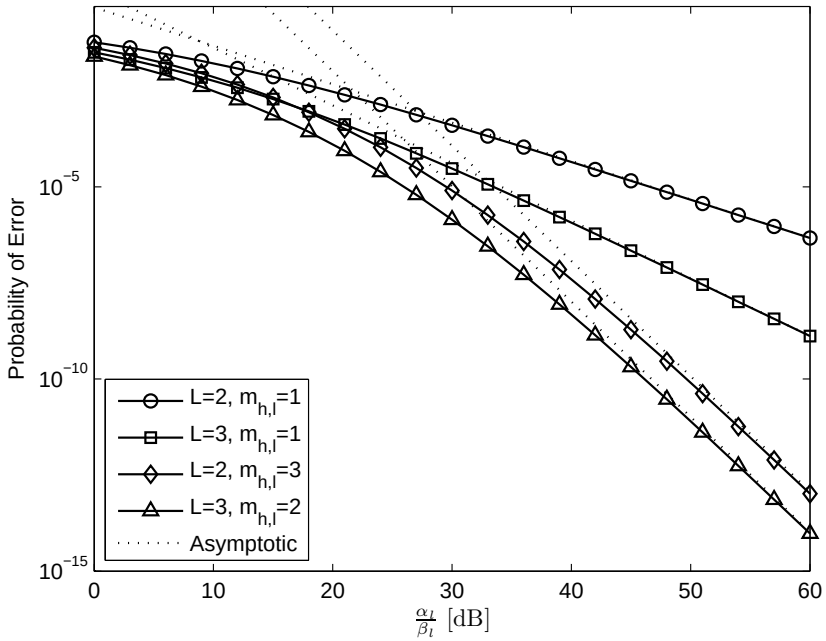

Figure 6.6: Symbol error rate performance of an OMU-CN-NI in the asymptotic regime, i.e. $P_{max} \to \infty$, for BPSK modulation.

for probability of outage are generated using (6.49). In the simulations, we have considered the case where the PU-Tx transmits with the maximum available power i.e. P_{max} i.e. $P_P = P_{max}$. It can be observed that interference from the primary network results in severe degradation in performance of the secondary network and that the outage probability of the OMU-CN-WI increases as the interference power from the PU-Tx increases. However, the outage performance can be improved by increasing the number of secondary users. It can also be observed that increasing the maximum transmit power P_{max} does not always improve the secondary network performance. This happens because the PU-Rx interference constraint limits the transmit power of the SU-Tx, where as the interference power from the PU-Tx increases with increasing P_{max}. However, when the PU-Rx interference constraint is relaxed (Q is large), increasing P_{max} improves the outage performance.

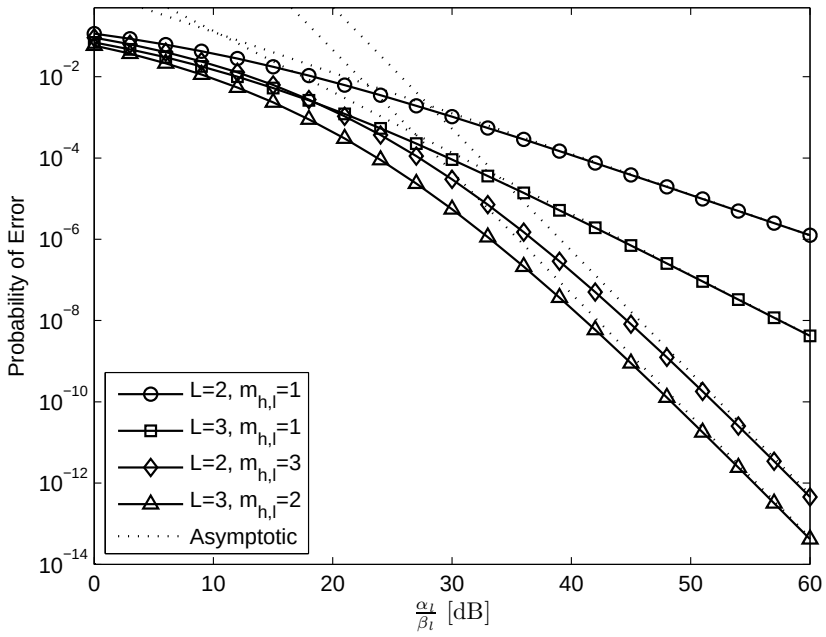

Figure 6.7: Symbol error rate performance of an OMU-CN-NI in the asymptotic regime, i.e. $P_{max} \to \infty$, for BDPSK modulation.

6.6 Appendix

6.6.1 CDF of Output SNR

As the channels are assumed to be independent, therefore the CDF of Υ_{CSI}, $F_{\Upsilon_{CSI}}(\cdot)$, is given by

$$F_{\Upsilon_{CSI}}(x) = \prod_{l=1}^{L} F_{\Upsilon_{CSI,l}}(x), \tag{6.51}$$

where $F_{\Upsilon_{CSI,l}}(\cdot)$ denotes the CDF of $\Upsilon_{CSI,l}$ and can be expressed as

$$F_{\Upsilon_{CSI,l}}(x) = Pr\left\{ \min\left\{P_{max}, \frac{Q_{pk}}{g_l}\right\} h_l < x \right\}. \tag{6.52}$$

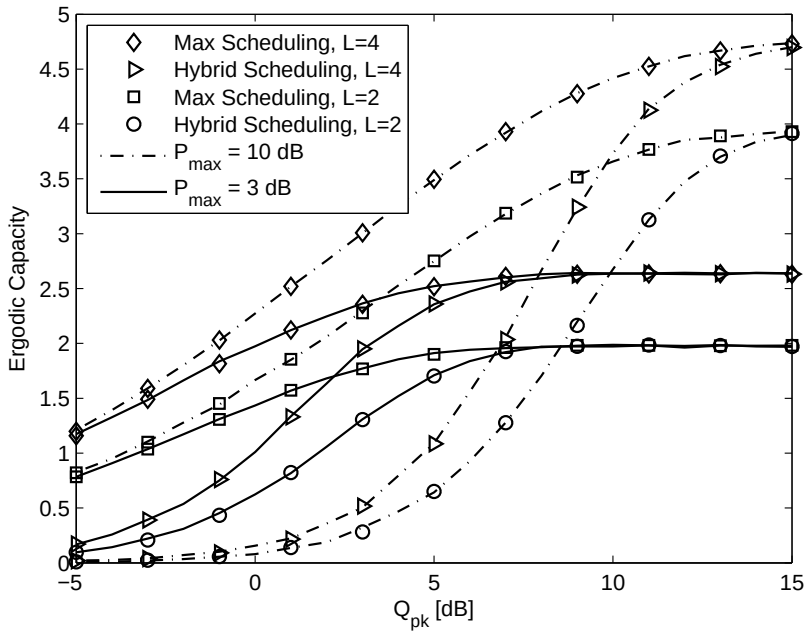

Figure 6.8: Comparison between ergodic capacity of maximum output SNR based scheduling scheme with the hybrid scheduling scheme, where $\Omega_{g,l} = \{1, 2, 3, 4\}$[dB], $\Omega_{h,l} = \{2, 1, 6, 5\}$[dB], and $l = 2, \ldots 4$.

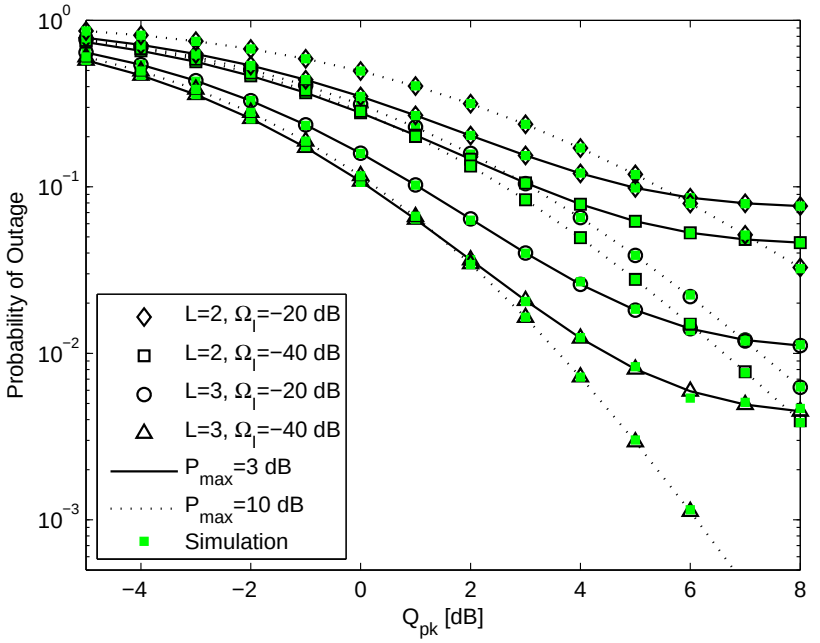

Figure 6.9: Probability of outage of an OMU-CN-WI where $x = 1$, $m_{\neg,1} = 1$, $\Omega_I = \Omega_{\neg,1}$, $\Omega_{g,l} = \{1, 2, 3, 4\}$[dB], $\Omega_{h,l} = \{2, 1, 6, 5\}$[dB], and $l = 2, \ldots 3$.

Conditioned on g_l, $F_{\Upsilon_{CSI,l}}(\cdot)$ can be expressed as

$$F_{\Upsilon_{CSI,l|g_l}}(x) = \begin{cases} Pr\Big\{P_{max}h_l < x\Big\} & \text{if } g_l \leq \frac{Q_{pk}}{P_{max}} \\ Pr\Big\{Q_{pk}\frac{h_l}{g_l} < x\Big\} & \text{if } g_l > \frac{Q_{pk}}{P_{max}} \end{cases} = \begin{cases} F_{h,l}\left(\frac{1}{P_{max}}x\right) & \text{if } g_l \leq \frac{Q_{pk}}{P_{max}} \\ F_{h,l}\left(\frac{g_l}{Q_{pk}}x\right) & \text{if } g_l > \frac{Q_{pk}}{P_{max}} \end{cases}, \tag{6.53}$$

where $F_{h,l}(\cdot)$ denotes the CDF of h_l. The unconditional CDF can be obtained by averaging $F_{\Upsilon_{CSI,l|g_l}}(\cdot)$ over the PDF of g_l as

$$F_{\Upsilon_{CSI,l}}(x) = \int_0^{\frac{Q_{pk}}{P_{max}}} F_{h_l}\left(\frac{1}{P_{max}}x\right) f_{g,l}(g)dg + \int_{\frac{Q_{pk}}{P_{max}}}^{\infty} F_{h_l}\left(\frac{g}{Q_{pk}}x\right) f_{g,l}(g)dg, \tag{6.54}$$

where $f_{g,l}(g)$ denotes the PDF of g_l. Substituting CDF and PDF expressions for the Nakagami-m case,

$$\begin{aligned} F_{\Upsilon_{CSI,l}}(x) = &\int_0^{\varrho_P} \left(1 - \sum_{i=0}^{m_{h,l}-1} \frac{{\beta_l}^i \eta_P^i}{i!} x^i e^{-\eta_P \beta_l x}\right) \left(\frac{{\alpha_l}^{m_{g,l}}}{\Gamma(m_{g,l})} g^{m_{g,l}-1} e^{-g\alpha_l}\right) dg \\ &+ \int_{\varrho_P}^{\infty} \left(1 - \sum_{i=0}^{m_{h,l}-1} \frac{{\beta_l}^i}{i!{Q_{pk}}^i} g^i x^i e^{-\frac{\beta_l}{Q_{pk}}xg}\right) \left(\frac{{\alpha_l}^{m_{g,l}}}{\Gamma(m_{g,l})} g^{m_{g,l}-1} e^{-g\alpha_l}\right) dg, \end{aligned} \tag{6.55}$$

where $\varrho_P = \frac{Q_{pk}}{P_{max}}$, $\beta_l = \frac{m_{h,l}}{\Omega_{h,l}}$, $\alpha_l = \frac{m_{g,l}}{\Omega_{g,l}}$, $\eta_P = \frac{1}{P_{max}}$ and $F_{g,l}(\cdot)$ denotes the CDF of g_l. $F_{\Upsilon_{CSI,l}}(x)$ in (6.55) can be expressed as

$$\begin{aligned} &F_{\Upsilon_{CSI,l}}(x) = \\ &\int_0^{\varrho_P} \frac{{\alpha_l}^{m_{g,l}}}{\Gamma(m_{g,l})} g^{m_{g,l}-1} e^{-g\alpha_l} dg - \sum_{i=0}^{m_{h,l}-1} \frac{{\beta_l}^i \eta_P^i}{i!} x^i e^{-\eta_P \beta_l x} \int_0^{\varrho_P} \frac{{\alpha_l}^{m_{g,l}}}{\Gamma(m_{g,l})} g^{m_{g,l}-1} e^{-g\alpha_l} dg \\ &+ \int_{\varrho_P}^{\infty} \frac{{\alpha_l}^{m_{g,l}}}{\Gamma(m_{g,l})} g^{m_{g,l}-1} e^{-g\alpha_l} dg - \int_{\varrho_P}^{\infty} \sum_{i=0}^{m_{h,l}-1} \frac{{\beta_l}^i}{i!{Q_{pk}}^i} g^i x^i e^{-\frac{\beta_l}{Q_{pk}}xg} \frac{{\alpha_l}^{m_{g,l}}}{\Gamma(m_{g,l})} g^{m_{g,l}-1} e^{-g\alpha_l} dg. \end{aligned} \tag{6.56}$$

After solving the integral, combining the summations and doing some simplifications the CDF of the received SNR from the l-th SU-Tx is given as

$$F_{\Upsilon_{CSI,l}}(x) = 1 - \sum_{i=0}^{m_{h,l}-1} \frac{{\beta_l}^i}{i!} \left(\eta_P^i x^i e^{-\eta_P \beta_l x} F_{g,l}\left(\varrho_P\right) + \frac{x^i \Gamma\left(m_{g,l}+i, \left(\alpha_l + \frac{\beta_l}{Q_{pk}} x\right) \varrho_P\right)}{{Q_{pk}}^i {\alpha_l}^{-m_{g,l}} \Gamma(m_{g,l}) \left(\alpha_l + \frac{\beta_l}{Q_{pk}} x\right)^{m_{g,l}+i}} \right). \tag{6.57}$$

Substituting (6.57) into (6.51), the CDF of output SNR is given by (6.10).

6.6.2 Alternative Representation of CDF of the Output SNR

In this section, an alternative representation of the CDF is derived which helps to obtain closed form expressions for the SER and capacity. The CDF in (6.10) can be expressed as

$$F_{\Upsilon_{CSI}}(x) = \prod_{l=1}^{L} \left(1 - \mathcal{G}_l^A(x)\right), \tag{6.58}$$

where

$$\mathcal{G}_l^A(x) = \left(\sum_{i=0}^{m_{h,l}-1} \frac{{\beta_l}^i}{i!} \left(\eta_P^i x^i e^{-\eta_P \beta_l x} F_{g,l}\left(\varrho_P\right) + \frac{x^i \Gamma\left(m_{g,l}+i, \left(\alpha_l + \frac{\beta_l}{Q_{pk}} x\right) \varrho_P\right)}{{Q_{pk}}^i {\alpha_l}^{-m_{g,l}} \Gamma(m_{g,l}) \left(\alpha_l + \frac{\beta_l}{Q_{pk}} x\right)^{m_{g,l}+i}} \right) \right).$$

Using [99, Eq. (9)], the CDF $F_{\Upsilon_{CSI}}(\cdot)$ can be expressed as

$$F_{\Upsilon_{CSI}}(x) = \sum_{\mathbf{n} \in \Theta_L} \prod_{l=1}^{L} (-1)^{n_l} \left(\mathcal{G}_l^A(x)\right)^{n_l}, \tag{6.59}$$

where Θ_L is the set of all possible L bit binary numbers and n_l is the l-th bit of the binary number $\mathbf{n} \in \theta_L$. As $n_l \in \{0,1\}$, $\left(\mathcal{G}_l^A(x)\right)^{n_l}$ can be expressed as

$$\begin{aligned}\left(\mathcal{G}_l^A(x)\right)^{n_l} = \sum_{i=0}^{m_{h,l}-1} \left(\frac{{\beta_l}^i}{i!}\eta_P^i F_{g,l}\left(\varrho_P\right)\right)^{n_l} m_{h,l}^{n_l-1} x^{in_l} e^{-\eta_P\beta_l n_l x} \times \\ \left(1 + \frac{n_l {\alpha_l}^{m_{g,l}} e^{\eta_P\beta_l x}\Gamma\left(m_{g,l}+i, \left(\alpha_l + \frac{\beta_l}{Q_{pk}}x\right)\varrho_P\right)}{\eta_P^i F_{g,l}\left(\varrho_P\right) {Q_{pk}}^i \Gamma(m_{g,l}) \left(\alpha_l + \frac{\beta_l}{Q_{pk}}x\right)^{m_{g,l}+i}}\right).\end{aligned} \tag{6.60}$$

Using (6.60), $\mathcal{G}_l^B(x) = \prod_{l=1}^{L}(-1)^{n_l}\left(\mathcal{G}_l^A(x)\right)^{n_l}$ can be expressed as

$$\begin{aligned}\mathcal{G}_l^B(x) = \prod_{l=1}^{L}(-1)^{n_l} \sum_{i=0}^{m_{h,l}-1} \left(\frac{{\beta_l}^i}{i!}\eta_P^i F_{g,l}\left(\varrho_P\right)\right)^{n_l} m_{h,l}^{n_l-1} x^{in_l} e^{-\eta_P\beta_l n_l x} \times \\ \left(1 + \frac{n_l {\alpha_l}^{m_{g,l}} e^{\eta_P\beta_l x}\Gamma\left(m_{g,l}+i, \left(\alpha_l + \frac{\beta_l}{Q_{pk}}x\right)\varrho_P\right)}{\eta_P^i F_{g,l}\left(\varrho_P\right) {Q_{pk}}^i \Gamma(m_{g,l}) \left(\alpha_l + \frac{\beta_l}{Q_{pk}}x\right)^{m_{g,l}+i}}\right).\end{aligned} \tag{6.61}$$

Changing the product of sum into sum of products one obtains

$$\begin{aligned}\mathcal{G}_l^B(x) = \sum_{i_1=0}^{m_{h,1}-1} \cdots \sum_{i_L=0}^{m_{h,L}-1} \kappa_{n,i,l}^A \times \\ \prod_{l=1}^{L} x^{i_l n_l} e^{-\eta_P\beta_l n_l x} \left(1 + \frac{n_l {\alpha_l}^{m_{g,l}} e^{\eta_P\beta_l x}\Gamma\left(m_{g,l}+i_l, \left(\alpha_l + \frac{\beta_l}{Q_{pk}}x\right)\varrho_P\right)}{\eta_P^{i_l} F_{g,l}\left(\varrho_P\right) {Q_{pk}}^{i_l} \Gamma(m_{g,l}) \left(\alpha_l + \frac{\beta_l}{Q_{pk}}x\right)^{m_{g,l}+i_l}}\right),\end{aligned} \tag{6.62}$$

which can be expressed as

$$\mathcal{G}_l^B(x) = \sum_{\mathcal{I}} \kappa_{n,i,l}^A x^{\Xi_{i,n}^A} e^{-x\Xi_n^B} \prod_{l=1}^{L} \left(1 + \frac{n_l {\alpha_l}^{m_{g,l}} e^{\eta_P\beta_l x}\Gamma\left(m_{g,l}+i_l, \left(\alpha_l + \frac{\beta_l}{Q_{pk}}x\right)\varrho_P\right)}{\eta_P^{i_l} F_{g,l}\left(\varrho_P\right) {Q_{pk}}^{i_l} \Gamma(m_{g,l}) \left(\alpha_l + \frac{\beta_l}{Q_{pk}}x\right)^{m_{g,l}+i_l}}\right), \tag{6.63}$$

where $\kappa_{n,i,l}^A = \prod_{l=1}^{L}(-1)^{n_l}\left(\frac{{\beta_l}^{i_l}}{i_l!}\eta_P^{i_l} F_{g,l}\left(\varrho_P\right)\right)^{n_l} m_{h,l}^{n_l-1}$, $\Xi_{i,n}^A = \sum_{l=1}^{L} i_l n_l$, $\Xi_n^B = \sum_{l=1}^{L}\eta_P\beta_l n_l$ and $\sum_{\mathcal{I}}$ is short form notation of $\sum_{i_1=0}^{m_{h,1}-1}\ldots\sum_{i_L=0}^{m_{h,L}-1}$. Substituting (6.63) in (6.59)

one obtains

$$F_{\Upsilon_{CSI}}(x) = \sum_{\mathbf{n}\in\Theta_L} \sum_{\mathcal{I}} \kappa^A_{n,i,l} x^{\Xi^A_{i,n}} e^{-x\Xi^B_n} \mathcal{G}^C(x), \tag{6.64}$$

where $\mathcal{G}^C(x)$ is given as

$$\mathcal{G}^C(x) = \prod_{l=1}^{L} \left(1 + \frac{n_l {\alpha_l}^{m_{g,l}} e^{\eta_P \beta_l x} \Gamma\left(m_{g,l} + i_l, \left(\alpha_l + \frac{\beta_l}{Q_{pk}} x\right) \varrho_P\right)}{\eta_P^{i_l} F_{g,l}\left(\varrho_P\right) {Q_{pk}}^{i_l} \Gamma(m_{g,l}) \left(\alpha_l + \frac{\beta_l}{Q_{pk}} x\right)^{m_{g,l}+i_l}} \right). \tag{6.65}$$

Using [99, Eq. (9)], $\mathcal{G}^C(x)$ can be expressed as

$$\mathcal{G}^C(x) = \sum_{\mathbf{w}\in\Theta_L} \prod_{l=1}^{L} \left(\frac{n_l {\alpha_l}^{m_{g,l}} e^{\eta_P \beta_l x} \Gamma\left(m_{g,l} + i_l, \left(\alpha_l + \frac{\beta_l}{Q_{pk}} x\right) \varrho_P\right)}{\eta_P^{i_l} F_{g,l}\left(\varrho_P\right) {Q_{pk}}^{i_l} \Gamma(m_{g,l}) \left(\alpha_l + \frac{\beta_l}{Q_{pk}} x\right)^{m_{g,l}+i_l}} \right)^{w_l}, \tag{6.66}$$

where w_l is the l-th bit of the binary number $\mathbf{w} \in \theta_L$. Using [96, Eq. (8.352.2)], $\mathcal{G}^C(x)$ can be expressed as

$$\begin{aligned} \mathcal{G}^C(x) = & \sum_{\mathbf{w}\in\Theta_L} \kappa^B_{n,i,w} \times \\ & \prod_{l=1}^{L} \left(\sum_{j=0}^{m_{g,l}+i_l-1} \frac{(m_{g,l}+i_l-1)!}{j! \varrho_P^{-j} e^{\alpha_l \varrho_P}} \left(\frac{\beta_l}{Q_{pk}}\right)^{j-m_{g,l}-i_l} \left(x + \left(\frac{\alpha_l}{\beta_l} Q_{pk}\right)\right)^{j-m_{g,l}-i_l} \right)^{w_l}, \end{aligned} \tag{6.67}$$

where $\kappa^B_{n,i,w} = \prod_{l=1}^{L} \left(\frac{n_l {\alpha_l}^{m_{g,l}}}{\eta_P^{i_l} F_{g,l}(\varrho_P) {Q_{pk}}^{i_l} \Gamma(m_{g,l})} \right)^{w_l}$. As $w_l \in \{0,1\}$, $\mathcal{G}^C(x)$ can be expressed as

$$\mathcal{G}^C(x) = \sum_{\mathbf{w}\in\Theta_L} \kappa^B_{n,i,w} \times \prod_{l=1}^{L} \sum_{j=0}^{m_{g,l}+i_l-1} \left(\frac{(m_{g,l}+i_l-1)!}{j! \varrho_P^{-j} e^{\alpha_l \varrho_P}} \left(\frac{\beta_l}{Q_{pk}} \right)^{j-m_{g,l}-i_l} \right)^{w_l} (m_{g,l}+i_l)^{w_l-1} \left(x + \left(\frac{\alpha_l}{\beta_l} Q_{pk} \right) \right)^{w_l(j-m_{g,l}-i_l)} . \tag{6.68}$$

Changing the product of sum into sum of products one obtains

$$\mathcal{G}^C(x) = \sum_{\mathbf{w}\in\Theta_L} \kappa^B_{n,i,w} \sum_{\mathcal{J}} \kappa^C_{i,w,j} \prod_{l=1}^{L} (x-\tau_l)^{-\psi_{i,w,j,l}} , \tag{6.69}$$

where $\sum_{\mathcal{J}} = \sum_{j_1=0}^{m_{g,1}+i_1-1} \cdots \sum_{j_L=0}^{m_{g,L}+i_L-1}$, $\tau_l = -\frac{\alpha_l}{\beta_l} Q_{pk}$, $\psi_{i,w,j,l} = -w_l(j_l - m_{g,l} - i_l)$ and $\kappa^C_{i,w,j} = \prod_{l=1}^{L} \left(\frac{(m_{g,l}+i_l-1)!}{j_l! \varrho_P^{-j_l} e^{\alpha_l \varrho_P}} \left(\frac{\beta_l}{Q_{pk}} \right)^{j_l-m_{g,l}-i_l} \right)^{w_l} (m_{g,l}+i_l)^{w_l-1}$. Substituting (6.69) into (6.64), the CDF of output SNR is given as

$$F_{\Upsilon_{CSI}}(x) = \sum_{\mathbf{n}\in\Theta_L} \sum_{\mathcal{I}} \sum_{\mathbf{w}\in\Theta_L} \sum_{\mathcal{J}} \kappa^A_{n,i,l} \kappa^B_{n,i,w} \kappa^C_{i,w,j} x^{\Xi^A_{i,n}} e^{-x\Xi^B_n} \prod_{l=1}^{L} (x-\tau_l)^{-\psi_{i,w,j,l}} , \tag{6.70}$$

Note that in (6.70), if $\mathbf{w} = 0$, i.e. the all zero vector, then $\psi_{i,w,j,l} = 0$ and $\prod_{l=1}^{L} (x-\tau_l)^{-\psi_{i,w,j,l}} = 1$ and therefore $F_{\Upsilon_{CSI}}(x)$ can be expressed as

$$F_{\Upsilon_{CSI}}(x) = \begin{cases} \sum_{\mathbf{n}\in\Theta_L} \sum_{\mathcal{I}} \sum_{\mathbf{w}\in\Theta_L} \sum_{\mathcal{J}} \kappa^A_{n,i,l} \kappa^B_{n,i,w} \kappa^C_{i,w,j} x^{\Xi^A_{i,n}} e^{-x\Xi^B_n} & ,\mathbf{w} = 0 \\ \sum_{\mathbf{n}\in\Theta_L} \sum_{\mathcal{I}} \sum_{\mathbf{w}\in\Theta_L} \sum_{\mathcal{J}} \kappa^A_{n,i,l} \kappa^B_{n,i,w} \kappa^C_{i,w,j} x^{\Xi^A_{i,n}} e^{-x\Xi^B_n} \prod_{l=1}^{L} (x-\tau_l)^{-\psi_{i,w,j,l}} & ,\mathbf{w} \neq 0 \end{cases} \tag{6.71}$$

In order to evaluate the expressions for moment-generating function (MGF) and SER, both these cases need to be treated separately. However, they can be combined by multiplying and dividing by $1+x$. This multiplication will make sure that the product term will exist even when $\mathbf{w}=0$. After multiplying and dividing by $1+x$ one gets

$$F_{\Upsilon_{CSI}}(x)=\sum_{p=0}^{1}\sum_{\mathbf{n}\in\Theta_L}\sum_{\mathcal{I}}\sum_{\mathbf{w}\in\Theta_L}\sum_{\mathcal{J}}\kappa_{n,i,l}^{A}\kappa_{n,i,w}^{B}\kappa_{i,w,j}^{C}x^{\Xi_{i,n}^{A}+p}e^{-x\Xi_{n}^{B}}\prod_{l=1}^{L+1}\left(x-\zeta_l\right)^{-\xi_{i,w,j,l}}, \tag{6.72}$$

where $\zeta_l=\tau_l$ for $l=\{1,\dots L\}$, $\xi_{i,w,j,l}=\psi_{i,w,j,l}$ for $l=\{1,\dots L\}$, $\zeta_{L+1}=-1$ and $\xi_{i,w,j,L+1}=1$. Let $\mathcal{G}^{D}(x)=\prod_{l=1}^{L+1}\left(x-\zeta_l\right)^{-\xi_{i,w,j,l}}$. It can be noted that ζ_l are not distinct $\forall\ l$. Assuming that there are υ distinct ζ_l and $\upsilon\leq L+1$, $\mathcal{G}^{D}(x)$ can be expressed as

$$\mathcal{G}^{D}(x)=\prod_{q=1}^{\upsilon}\left(x-\bar{\zeta}_q\right)^{-\delta_q}, \tag{6.73}$$

where $\bar{\zeta}_q$ denotes the q-th distinct root of $\mathcal{G}^{D}(x)$ and $\delta_q=\sum_{o=1,\zeta_o==\bar{\zeta}_q}^{L}\xi_{i,w,j,o}$ denotes the multiplicity of $\bar{\zeta}_q$. Thus, $\mathcal{G}^{D}(x)$ can be expressed using partial fraction expansion as [103, Eq. (2)]

$$\mathcal{G}^{D}(x)=\sum_{v_1=1}^{\upsilon}\sum_{v_2=1}^{\delta_{v_1}}\kappa_{v_1,v_2}^{D}(\bar{\zeta},\delta,\upsilon)\left(x-\bar{\zeta}_{v_1}\right)^{-v_2}, \tag{6.74}$$

where $\kappa_{v_1,v_2}^{D}(\bar{\zeta},\delta,\upsilon)$ can be computed recursively as

$$\kappa_{v_1,v_2}^{D}(\bar{\zeta},\delta,\upsilon)=\begin{cases}\prod_{q=1,q\neq v_1}^{\upsilon}\left(\bar{\zeta}_{v_1}-\bar{\zeta}_q\right)^{-\delta_q} & ,v_2=\delta_i\\ \sum_{q=1}^{\delta_{v_1}-v_2}\frac{\kappa_{v_1,v_2+q}^{D}(-1)^q}{\delta_{v_1}-v_2}\times & \\ \sum_{p=1,p\neq v_1}^{\upsilon}\frac{\delta_p}{\left(\bar{\zeta}_{v_1}-\bar{\zeta}_p\right)^{-q}} & ,v_2=\delta_{v_1}-1,\dots 1.\end{cases} \tag{6.75}$$

Finally, by substituting (6.74) into (6.70), $F_{\Upsilon_{CSI}}(x)$ is obtained as

$$F_{\Upsilon_{CSI}}(x) = \sum_{p=0}^{1} \sum_{\mathbf{n}\in\Theta_L} \sum_{\mathcal{I}} \sum_{\mathbf{w}\in\Theta_L} \sum_{\mathcal{J}} \sum_{v_1=1}^{\upsilon} \sum_{v_2=1}^{\delta_{v_1}} \kappa^A_{n,i,l}\kappa^B_{n,i,w}\kappa^C_{i,w,j}\kappa^D_{v_1,v_2}(\bar{\zeta},\delta,\upsilon) x^{\Xi^A_{i,n}+p} e^{-x\Xi^B_n} \left(x-\bar{\zeta}_{v_1}\right)^{-v_2}. \tag{6.76}$$

$F_{\Upsilon_{CSI}}(x)$ can be expressed simply as (6.11), where $\Delta_\kappa = \kappa^A_{n,i,l}\kappa^B_{n,i,w}\kappa^C_{i,w,j}\kappa^D_{v_1,v_2}(\bar{\zeta},\delta,\upsilon)$ and $\sum_{p=0}^{1}\sum_{\mathbf{n}\in\Theta_L}\sum_{\mathcal{I}}\sum_{\mathbf{w}\in\Theta_L}\sum_{\mathcal{J}}\sum_{v_1=1}^{\upsilon}\sum_{v_2=1}^{\delta_{v_1}}$ is represented using shorthand notation $\sum_{\mathfrak{F}}$.

6.6.3 Moment Generating Function

The MGF of the output SNR can be found using the CDF of Υ_{CSI} as [99, Eq. (18)]

$$\mathcal{M}_{\Upsilon_{CSI}}(s) = s\int_0^\infty e^{-sx} F_{\Upsilon_{CSI}(x)} dx. \tag{6.77}$$

Substituting (6.11) into (6.77) one obtains

$$\mathcal{M}_{\Upsilon_{CSI}}(s) = \sum_{\mathfrak{F}} \Delta_\kappa s \int_0^\infty x^{\Xi^A_{i,n}+p} e^{-x(\Xi^B_n+s)} \left(x-\bar{\zeta}_{v_1}\right)^{-v_2} dx. \tag{6.78}$$

By making transformation of variable $z = x - \bar{\zeta}_{v_1}$ and using [96, Eq. (3.383.4)] the MGF is given in (6.19), where $\varsigma_{v_1} = -\bar{\zeta}_{v_1}$ and $W_{\lambda,\mu}(z)$ is the WhittakerW function defined in [96, Eq. (9.220.4)].

6.6.4 Alternate representations of Asymptotic Outage Expressions

1. Alternate representation of $F^{floor}_{\Upsilon_{CSI},Q}(x)$

$$F^{floor}_{\Upsilon_{CSI},Q}(x) = \sum_{\mathbf{n}\in\Theta_L}\sum_{\mathcal{I}} \kappa_Q x^{\Xi^A_{i,n}} e^{-x\Xi^B_n} \tag{6.79}$$

where $\kappa_Q = \prod_{l=1}^{L}(-1)^{n_l}\frac{(\beta_l\eta_P)^{n_l i_l}}{(i_l!)^{n_l}} m_{h,l}^{n_l-1}$, $\Xi^A_{i,n} = \sum_{l=1}^{L} n_l i_l$ and $\Xi^B_n = \eta_P \sum_{l=1}^{L} n_l\beta_l$.

2. Alternate representation of $F^{floor}_{\Upsilon_{CSI},P}(x)$

$F^{floor}_{\Upsilon_{CSI},P}(x)$ can be represented as

$$F^{floor}_{\Upsilon_{CSI},P}(x) = \sum_{p=0}^{1}\sum_{\mathbf{n}\in\Theta_L}\sum_{\mathcal{I}} \kappa^P_{n,i} x^{\Xi^A_{i,n}+p}\prod_{l=1}^{L+1}(x-\zeta_l)^{-\xi^P_{n,i,l}} \tag{6.80}$$

where $\kappa^P_{n,i} = \prod_{l=1}^{L}(-1)^{n_l}\left(\frac{\Gamma(m_{g,l}+i_l)}{\Gamma(m_{g,l})i_l!}\right)^{n_l} m_{h,l}^{n_l-1}\left(\frac{\beta_l}{\alpha_l}\frac{1}{Q_{pk}}\right)^{-n_l m_{g,l}}$, $\psi^P_{n,i,l} = n_l(m_{g,l}+i_l)$, $\Xi^A_{i,n} = \sum_{l=1}^{L} n_l i_l$, $\xi^P_{n,i,l} = \psi^P_{n,i,l}$, for $l = \{1,...L\}$and $\xi^P_{n,i,L+1} = 1$. Using partial fractions

$$F^{floor}_{\Upsilon_{CSI},P}(x) = \sum_{\mathcal{P}} \kappa^P_{n,i}\kappa^D_{v_1,v_2}(\bar{\zeta},\delta^P,\upsilon) x^{\Xi^A_{i,n}+p}\left(x-\bar{\zeta}_{v_1}\right)^{-v_2} \tag{6.81}$$

where $\sum_{\mathcal{P}}$ denotes $\sum_{p=0}^{1}\sum_{\mathbf{n}\in\Theta_L}\sum_{\mathcal{I}}\sum_{v_1=1}^{\upsilon}\sum_{v_2=1}^{\delta^P_{v_1}}$ and $\delta^P_q = \sum_{o=1,\zeta_o==\bar{\zeta}_q}^{L}\xi^P_{n,i,l}$.

The proofs follow similar steps as outlined in Appendix 6.6.1 and are omitted here due to space limitation.

6.6.5 Ergodic Capacity of OMU-CN-NI

The capacity of the OMU-CN-NI can be found using the CDF of Υ_{CSI} as

$$C_{CSI} = \frac{\log_2(e)}{B} \int_0^\infty \ln(1+x)\, f_{\Upsilon_{CSI}}(x) dx = \frac{\log_2(e)}{B} \int_0^\infty \frac{1 - F_{\Upsilon_{CSI}(x)}}{(x+1)} dx. \quad (6.82)$$

The CDF in (6.70) can be represented as

$$F_{\Upsilon_{CSI}}(x) = 1 + \sum_{\mathbf{n}\in\Theta_L, \mathbf{n}\neq 0} \sum_{\mathcal{I}} \sum_{\mathbf{w}\in\Theta_L} \sum_{\mathcal{J}} \kappa^A_{n,i,l} \kappa^B_{n,i,w} \kappa^C_{i,w,j} x^{\Xi^A_{i,n}} e^{-x\Xi^B_n} \prod_{l=1}^{L} (x-\tau_l)^{-\psi_{i,w,j,l}}, \quad (6.83)$$

Substituting (6.83) into (6.82) the capacity can be expressed as

$$C_{CSI} = -\frac{\log_2(e)}{B} \times \int_0^\infty \frac{\sum_{\mathbf{n}\in\Theta_L, \mathbf{n}\neq 0} \sum_{\mathcal{I}} \sum_{\mathbf{w}\in\Theta_L} \sum_{\mathcal{J}} \kappa^A_{n,i,l} \kappa^B_{n,i,w} \kappa^C_{i,w,j} x^{\Xi^A_{i,n}} e^{-x\Xi^B_n} \prod_{l=1}^{L} (x-\tau_l)^{-\psi_{i,w,j,l}}}{(x+1)} dx. \quad (6.84)$$

By incorporating the denominator term $(x+1)$ inside of the product one obtains

$$C_{CSI} = -\frac{\log_2(e)}{B} \times \sum_{\mathbf{n}\in\Theta_L, \mathbf{n}\neq 0} \sum_{\mathcal{I}} \sum_{\mathbf{w}\in\Theta_L} \sum_{\mathcal{J}} \kappa^A_{n,i,l} \kappa^B_{n,i,w} \kappa^C_{i,w,j} \int_0^\infty x^{\Xi^A_{i,n}} e^{-x\Xi^B_n} \prod_{l=1}^{L+1} (x-\zeta_l)^{-\xi_{i,w,j,l}} dx. \quad (6.85)$$

Using partial fractions (6.86) can be expressed as

$$C_{CSI} = -\frac{\log_2(e)}{B} \times \sum_{\mathbf{n}\in\Theta_L, \mathbf{n}\neq 0} \sum_{\mathcal{I}} \sum_{\mathbf{w}\in\Theta_L} \sum_{\mathcal{J}} \sum_{v_1=1}^{\upsilon} \sum_{v_2=1}^{\delta_{v_1}} \kappa^A_{n,i,l} \kappa^B_{n,i,w} \kappa^C_{i,w,j} \kappa^D_{v_1,v_2}(\zeta,\delta,\upsilon) \int_0^\infty x^{\Xi^A_{i,n}} e^{-x\Xi^B_n} \left(x-\bar{\zeta}_{v_1}\right)^{-v_2} dx. \quad (6.86)$$

Applying transformation of variable $z = x - \bar{\zeta}_{v_1}$ and solving the resulting integral and using [96, Eq. (3.383.4)], one obtains (6.44), where $\sum_{\mathfrak{C}}$ is the short hand notation of $\sum_{\mathbf{n}\in\Theta_L,\mathbf{n}\neq 0}\sum_{\mathcal{I}}\sum_{\mathbf{w}\in\Theta_L}\sum_{\mathcal{J}}\sum_{v_1=1}^{v}\sum_{v_2=1}^{\delta_{v_1}}$.

6.6.6 CDF of the Output SINR

The CDF of $\Upsilon_{\mathcal{I}}$ is given as

$$F_{\Upsilon_{\mathcal{I}}}(\Phi) = \Pr\{\Upsilon_{\mathcal{I}} < \Phi\} = \Pr\left\{\frac{\Upsilon_{CSI}}{P_p \daleth + 1} < \Phi\right\} \tag{6.87}$$

Conditioned on $\daleth$, CDF of $\Upsilon_{\mathcal{I}}$ is given as

$$F_{\Upsilon_{\mathcal{I}}|\daleth}(\Phi|\daleth) = \Pr\{\Upsilon_{CSI} < \Phi(P_p \daleth + 1)\} \tag{6.88}$$

Using $F_{\Upsilon_{\mathcal{I}}|\daleth}(\cdot|\cdot)$, $F_{\Upsilon_{\mathcal{I}}}(\cdot)$ can be obtained as

$$F_{\Upsilon_{\mathcal{I}}}(\Phi) = \int_0^{\infty} F_{\Upsilon_{\mathcal{I}}|\daleth}(\Phi|x)\, f_{\daleth}(x)\, dx \tag{6.89}$$

where, $f_{\daleth}(\cdot)$ is the PDF of $\daleth$. Substituting the PDF $f_{\daleth}(\cdot)$ and CDF from (6.11) into (6.89) yields

$$\begin{aligned} F_{\Upsilon_{\mathcal{I}}}(\Phi) = \sum_{\mathfrak{F}} \Delta_{\kappa} (\Phi P_P)^{\Xi_{i,n}^{A}+p-v_2} e^{-\Xi_n^B \Phi} \frac{1}{\Gamma(m_{\daleth,1})} \left(\frac{m_{\daleth,1}}{\Omega_{\daleth,1}}\right)^{m_{\daleth,1}} \times \\ \int_0^{\infty} \frac{\left(x+\frac{1}{P_P}\right)^{\Xi_{i,n}^{A}+p} e^{-\Xi_n^B \Phi P_P x}}{(x+\xi_N)^{v_2}} x^{m_{\daleth,1}-1} e^{-x\frac{m_{\daleth,1}}{\Omega_{\daleth,1}}} dx \end{aligned} \tag{6.90}$$

where $\xi_N = \frac{1}{P_P} - \frac{\bar{\zeta}_{v_1}}{\Phi P_P}$. Making change of variable $y = x + \xi_N$, and applying binomial expansion yields

$$F_{\Upsilon_{\mathcal{I}}}(\Phi) = \sum_{\mathfrak{F}} \sum_{i_1=0}^{\Xi^A_{i,n}+p} \sum_{i_2=0}^{m_{\urcorner,1}-1} \binom{\Xi^A_{i,n}+p}{i_1} \binom{m_{\urcorner,1}-1}{i_2} \frac{\Delta_\kappa e^{-\Xi^B_n \Phi}}{\left(\frac{\Omega_{\urcorner,1}}{m_{\urcorner,1}}\right)^{m_{\urcorner,1}} \Gamma(m_{\urcorner,1})} (\Phi P_P)^{\Xi^A_{i,n}+p-v_2} \times$$
$$(-\xi_N)^{m_{\urcorner,1}-1-i_2} \left(\frac{1}{P_P} - \xi_N\right)^{\Xi^A_{i,n}+p-i_1} e^{\xi_N\left(\frac{m_{\urcorner,1}}{\Omega_{\urcorner,1}} + \Xi^B_n \Phi P_P\right)} \int_{\xi_N}^{\infty} y^{i_1+i_2-v_2} e^{-y\left(\frac{m_{\urcorner,1}}{\Omega_{\urcorner,1}} + \Xi^B_n \Phi P_P\right)} dy \tag{6.91}$$

Solving the integration, substituting $\xi_N = \frac{1}{P_P} - \frac{\bar{\zeta}_{v_1}}{P_P \Phi}$ and after some algebraic manipulations the CDF of the output SINR is obtained as (6.49).

Chapter 7

Conclusion and Future Work

7.1 Summary

This dissertation contributes towards making cooperative and cognitive radio networks more feasible by considering realistic scenarios. In real world systems, the communicating nodes only possess imperfect CSI. In view of this practical scenario, novel coherent, non-coherent and half-coherent receivers for amplify-and-forward relaying in the presence of imperfect CSI were proposed. New receiver metrics were derived for each case. In case of coherent receiver, new metrics have been proposed that do not perform channel estimation at the destination and use the pilot signal directly for decoding. It has been shown that the receivers using DCE perform better than the receivers using CCE when infinite bit quantization is assumed. Also, the receivers with and without channel distribution perform essentially the same in the case of balanced links. The receivers with channel distribution using DCE perform better than the receivers without channel distribution if the source-relay link is very good, while if the destination links are very good, they perform approximately the same. However, for both those cases, they have similar performances in the case of CCE. Furthermore, it was shown that utilizing decision history in the receivers improves

performances greatly at the cost of little additional complexity and by weighting the decision history optimally, the performance of the receivers can be further improved. In addition, novel non-coherent and half-coherent receivers have been proposed for the case when the receiver has either no CSI or partial CSI i.e. CSI of either the source-relay link or the relay-destination link is available. It has been shown for a Rician fading channel, that the non-coherent and half-coherent receivers give better performance compared to the conventional energy detector based receiver.

Due to the time varying nature of the wireless channel, the CSI available at the communicating nodes can become outdated and again in this case the nodes do not possess perfect CSI resulting in performance degradation. In this dissertation, the impact of outdated CSI on the performance of a two-way relay network employing max-min relay selection is characterized and expressions for the outage probability, moment generating function and symbol error rate are derived for a Rayleigh faded channel. Numerical simulation results show that the diversity is lost due to outdated CSI. Furthermore, relay location was also taken into consideration and it was shown that the performance can be improved by placing the relay closer to the source whose channel is more outdated.

Transmit antenna selection (which has lower complexity and can be implemented with lower cost) was proposed to improve the performance of MIMO cognitive radio systems. The transmitter was assumed to have limited peak transmit power. The performance of this scheme was analyzed for two scenarios; the secondary network experiences and/or does not experience interference from the primary network and expressions characterizing the outage probability performance of the MCS-TM-NI and the MCS-TM-WI were obtained in closed-form. Furthermore, closed-form expressions were obtained for MGF, SER performance and ergodic capacity of the MCS-TM-NI. In addition, the outage and SER performance of MCS-TM-NI was analyzed for

asymptotic regimes and it is shown that the MCS-TM-NI achieves a generalized diversity order equal to the product of number or transmit and receive antenna.

A user scheduling scheme, which exploits the multiple channels available in a multi-user cognitive network, was also proposed to improve the QoS of the cognitive network. The secondary user with the best output SNR was selected for transmission. In conformance with realistic scenarios, the transmitter was assumed to have limited peak transmit power and the channel was modeled using independent but not identically distributed Nakagami-m fading model. Exact closed form expressions for the outage performance, MGF of the output SNR, SER performance, and the ergodic capacity were obtained and the performance of this scheme was also analyzed in the asymptotic regimes where it is shown that when the interference link is poor, and there is no constraint on the transmit power, this scheduling scheme achieves maximum generalized diversity gain. Furthermore, it is shown that this scheduling scheme achieves higher capacity compared to the hybrid scheduling scheme. Additionally, the impact of interference from the primary network on the performance of the OMU-CN was also considered and exact closed-form expression for the outage probability performance was obtained.

7.2 Future Directions

In order to make cooperative and cognitive radio systems more practical, the contributions in this dissertation can be extended into multiple directions. Some of them are discussed below.

7.2.1 Receiver Design for Cognitive Radio Systems

There has been very little or no research on receivers structures for underlay cognitive radio networks. Due to the interference constraint, the power allocation in cognitive radio transmitters is random and thus, traditional receivers structure will give sub-optimal performance. Based on the on the maximum averaged likelihood (MAL) methods [28, 31], using the distribution of the channels, power allocation and the noise, receivers can be derived which give better SER performance. Similar to the receivers obtained in Chapter 2, these receivers will be more practical as they do not require channel estimation and use pilots directly for decoding.

7.2.2 Transmit Antenna Selection in Cognitive Radio Systems Based on Imperfect CSI

In this dissertation, it was assumed that the cognitive transmitter/receiver pair has knowledge of exact CSI based on which a single antenna was selected. However, as discussed previously, in practical systems the CSI available at the nodes is imperfect due to estimation errors or due to outdatedness. The impact of imperfect CSI on the performance of TAS in cognitive radio networks needs to be studied and can be a good next step towards implementable cognitive radio systems.

REFERENCES

[1] A. Goldsmith, *Wireless Communications*. Cambridge. UK: Cambridge Univ. Press, 2005.

[2] M. K. Simon and M. S. Alouini, *Digital Communication over Fading Channels*, 2nd ed. Hoboken, New Jersey. USA: John Wiley & Sons, Inc., 2005.

[3] Federal Communications Commission and others, "Facilitating opportunities for flexible, efficient, and reliable spectrum use employing cognitive radio technologies," *ET Docket*, no. 03-108, 2003.

[4] L. Zheng and D. N. C. Tse, "Diversity and multiplexing: A fundamental tradeoff in multiple-antenna channels," *IEEE Transactions on Information Theory*, vol. 49, no. 5, pp. 1073–1096, May 2003.

[5] J. Proakis and M. Salehi, *Digital Communications*, 5th ed. McGraw-Hill, 2008.

[6] S. Alamouti, "A simple transmit diversity technique for wireless communications," *IEEE Journal on Selected Areas in Communications*, vol. 16, no. 8, pp. 1451 –1458, Oct. 1998.

[7] H. Jafarkhani, *Space-Time Coding: Theory and Practice*. Cambridge. UK: Academics, 2005.

[8] A. Molisch and M. Win, "MIMO systems with antenna selection," *IEEE Microwave Mag.*, vol. 5, no. 1, pp. 46–56, Mar. 2004.

[9] R. Pabst, B. Walke, D. Schultz, P. Herhold, H. Yanikomeroglu, S. Mukherjee, H. Viswanathan, M. Lott, W. Zirwas, M. Dohler, H. Aghvami, D. Falconer, and G. Fettweis, "Relay-based deployment concepts for wireless and mobile

broadband radio," *IEEE Communications Magazine*, vol. 42, no. 9, pp. 80–89, Sep. 2004.

[10] J. Laneman and G. Wornell, "Distributed space-time-coded protocols for exploiting cooperative diversity in wireless networks," *IEEE Transactions on Information Theory*, vol. 49, no. 10, pp. 2415–2425, Oct. 2003.

[11] A. Sendonaris, E. Erkip, and B. Aazhang, "User cooperation diversity-Parts I and II," *IEEE Transactions on Communications*, vol. 51, no. 11, pp. 1927–1948, Nov. 2003.

[12] I. P802.16j, "IEEE standard for local and metropolitan area networks, part 16: Air interface for fixed and mobile broadband wireless access systems: Multihop relay specification," vol. P802.16j/D3, Feb. 2008.

[13] Y. Jing and B. Hassibi, "Distributed space-time-coded protocols for exploiting cooperative diversity in wireless networks," *IEEE Transactions on Wireless Communications*, vol. 5, no. 12, pp. 3524–3536, Dec. 2006.

[14] J. N. Laneman, D. N. C. Tse, and G. W. Wornell, "Cooperative diversity in wireless networks: Efficient protocols and outage behavior," *IEEE Transactions on Information Theory*, vol. 50, no. 11, pp. 3062–3080, Dec. 2004.

[15] P. Popovski and H. Yomo, "Wireless network coding by amplify-and-forward for bi-directional traffic flows," *IEEE Communications Letters*, vol. 11, no. 1, pp. 16–18, Jan. 2007.

[16] J. Mitola III and G. Maguire Jr, "Cognitive radio: Making software radios more personal," *IEEE Personal Communications Magazine*, vol. 6, no. 4, pp. 13–18, Aug. 1999.

[17] S. Haykin, "Cognitive radio: Brain-empowered wireless communications," vol. 23, no. 21, pp. 201–220, Feb. 2005.

[18] I. Akyildiz, W. Lee, M. Vuran, and S. Mohanty, "NeXt generation/dynamic spectrum access/cognitive radio wireless networks: A survey," *Computer Networks*, vol. 50, no. 13, pp. 2127–2159, Jul. 2006.

[19] A. Ghasemi and E. Sousa, "Spectrum sensing in cognitive radio networks: Requirements, challenges and design trade-offs," *IEEE Communications Magazine*, vol. 46, no. 4, pp. 32–39, Apr. 2008.

[20] T. Yucek and H. Arslan, "A survey of spectrum sensing algorithms for cognitive radio applications," *IEEE Communications Surveys and Tutorials*, vol. 11, no. 1, pp. 116–130, First Quarter 2009.

[21] I. F. Akyildiz, B. F. Lo, and R. Balakrishnan, "Cooperative spectrum sensing in cognitive radio networks: A survey," *Elsevier Journal of Physical Communication*, vol. 4, no. 1, pp. 40–62, 2011.

[22] S. Sanayei and A. Nosratinia, "Antenna selection in MIMO systems," *IEEE Communications Magazine*, vol. 42, no. 10, pp. 68–73, Oct. 2004.

[23] S. Thoen, L. Van der Perre, B. Gyselinckx, and M. Engels, "Performance analysis of combined transmit-SC/receive-MRC," vol. 49, no. 1, pp. 5–8, Jan. 2001.

[24] R. Knopp and P. Humblet, "Information capacity and power control in single-cell multiuser communications," in *Proc. IEEE International Conference on Communications (ICC 1995), Seattle, USA*, Jun., 1995.

[25] D. Tse, "Optimal power allocation over parallel Gaussian broadcast channels," in *Proc. IEEE International Symposium on Information Theory (ISIT 1997), Ulm, Germany*, Jun., 1997.

[26] P. Viswanath, D. Tse, and R. Laroia, "Opportunistic beamforming using dumb antennas," *IEEE Transactions on Information Theory*, vol. 48, no. 6, pp. 1277–1294, Jun. 2002.

[27] L. Yang and M.-S. Alouini, "Performance analysis of multiuser selection diversity," *IEEE Transactions on Vehicular Technology*, vol. 55, no. 6, pp. 1848–1861, Nov. 2006.

[28] G. Taricco and E. Biglieri, "Space-time decoding with imperfect channel estimation," *IEEE Transactions on Wireless Communications*, vol. 4, no. 4, pp. 1874 – 1888, Jul. 2005.

[29] G. Taricco and G. Coluccia, "Optimum receiver design for correlated rician fading MIMO channels with pilot-aided detection," *IEEE Journal on Selected Areas in Communications*, vol. 25, no. 7, pp. 1311 –1321, Sep. 2007.

[30] Y. Chen and N. Beaulieu, "Optimum pilot symbol assisted modulation," *IEEE Transactions on Communications*, vol. 55, no. 8, pp. 1536 –1546, Aug. 2007.

[31] ——, "Maximum likelihood receivers for space-time coded MIMO systems with Gaussian estimation errors," *IEEE Transactions on Communications*, vol. 57, no. 6, pp. 1712 –1720, Jun. 2009.

[32] D. Chen and J. Laneman, "Cooperative diversity for wireless fading channels without channel state information," in *Proc. IEEE 38th Asilomar Conference on Signals, Systems, and Computers (ASILOMAR 2004), Pacific Grove, CA, USA*, Nov. 07-Nov. 11 2004, pp. 1307 – 1312.

[33] M. Uysal and H. Mheidat, "Maximum-likelihood detection for distributed space-time block coding," in *Proc. IEEE Vehicular Technology Conference (VTC-Fall 2004), Los Angeles, CA, USA*, Sep. 2004, pp. 2419 – 2423.

[34] R. Annavajjala, P. Cosman, and L. Milstein, "On the performance of optimum noncoherent amplify-and-forward reception for cooperative diversity," in *Proc. IEEE Military Communications Conference MILCOM 2005, Atlantic City, USA*, Oct. 2005.

[35] H. Mheidat and M. Uysal, "Non-coherent and mismatched-coherent receivers for distributed STBCs with amplify-and-forward relaying," *IEEE Transactions on Wireless Communications*, vol. 6, no. 11, pp. 4060 –4070, Nov. 2007.

[36] Y. Zhu, P.-Y. Kam, and Y. Xin, "Non-coherent detection for amplify-and-forward relay systems in a Rayleigh fading environment," in *Proc. IEEE Global Telecommunications Conference (GLOBECOM 2007), Washington, DC, USA*, Nov. 26-Nov. 30 2007, pp. 1658 –1662.

[37] G. Farhadi and N. Beaulieu, "A low complexity receiver for noncoherent amplify-and-forward cooperative systems," *IEEE Transactions on Communications*, vol. 58, no. 9, pp. 2499 –2504, Sep. 2010.

[38] M. Souryal, "Non-coherent amplify-and-forward generalized likelihood ratio test receiver," *IEEE Transactions on Wireless Communications*, vol. 9, no. 7, pp. 2320–2327, July 2010.

[39] M. Ju and I. Kim, "Error probabilities of noncoherent and coherent FSK in the presence of frequency and phase offsets for two-hop relay networks," *IEEE Transactions on Communications*, vol. 57, no. 8, pp. 2244–2250, Aug. 2009.

[40] C. Patel and G. Stuber, "Channel estimation for amplify and forward relay based cooperation diversity systems," *IEEE Transactions on Communications*, vol. 6, no. 6, pp. 2348 –2356, Jun. 2007.

[41] B. Gedik and M. Uysal, "Impact of imperfect channel estimation on the performance of amplify-and-forward relaying," *IEEE Transactions on Wireless Communications*, vol. 8, no. 3, pp. 1468 –1479, Mar. 2009.

[42] P. Liu and I. Kim, "Optimum/sub-optimum detectors for multi-branch dual-hop amplify-and-forward cooperative diversity networks with limited CSI," *IEEE Transactions on Wireless Communications*, vol. 9, no. 1, pp. 78–85, Jan. 2010.

[43] B. Gedik and M. Uysal, "Two channel estimation methods for amplify-and-forward relay networks," in *Proc. IEEE 21st Canadian Conference on Electrical and Computer Engineering (CCECE 2008), Ontario, Canada*, May 4-7 2008, pp. 615 – 618.

[44] O. Amin, B. Gedik, and M. Uysal, "Channel estimation for amplify-and-forward relaying: Cascaded against disintegrated estimators," *IET Communications*, vol. 4, no. 10, pp. 1207 –1216, Jul. 2010.

[45] A. Bletsas, A. Khisti, D. Reed, and A. Lippman, "A simple cooperative diversity method based on network path selection," *IEEE Journal on Selected Areas in Communications*, vol. 24, no. 3, pp. 659–672, Mar. 2006.

[46] Y. Zhao, R. Adve, and T.-J. Lim, "Improving amplify-and-forward relay networks: optimal power allocation versus selection," *IEEE Transactions on Wireless Communications*, vol. 6, no. 8, pp. 3114–3123, Aug. 2007.

[47] A. Ibrahim, A. K. Sadek, W. Su, and K. J. R. Liu, "Cooperative communications with relay-selection: When to cooperate and whom to cooperate with?" *IEEE Transactions on Wireless Communications*, vol. 7, no. 7, pp. 2814–2827, Jul. 2008.

[48] I. Krikidis, "Relay selection for two-way relay channels with MABC DF: A diversity perspective," *IEEE Transactions on Vehicular Technology*, vol. 59, no. 9, pp. 4620–4628, Nov. 2010.

[49] Y. Jing, "A relay selection scheme for two-way amplify-and-forward relay networks," in *Proc. IEEE International Conference on Wireless Communications and Signal Processing (WCSP 2009), Nanjing, China*, Nov. 2009.

[50] L. Song, "Relay selection for two-way relaying with amplify-and-forward protocols," *IEEE Transactions on Vehicular Technology*, vol. 60, no. 4, pp. 1954–1959, May 2011.

[51] S. Atapattu, Y. Jing, H. Jiang, and C. Tellambura, "Relay selection schemes and performance analysis approximations for two-way networks," *IEEE Transactions on Communications*, vol. 61, no. 3, pp. 987–998, Mar. 2013.

[52] Q. F. Zhou, Y. Li, F. C. Lau, and B. Vucetic, "Decode-and-forward two-way relaying with network coding and opportunistic relay selection," *IEEE Transactions on Communications*, vol. 58, no. 11, pp. 3070–3076, Nov. 2010.

[53] Y. Li, R. H. Louie, and B. Vucetic, "Relay selection with network coding in two-way relay channels," *IEEE Transactions on Vehicular Technology*, vol. 59, no. 9, pp. 4489–4499, Nov. 2010.

[54] J. L. Vicario, A. Bel, J. A. Lopez-Salcedo, and G. Seco, "Opportunistic relay selection with outdated CSI: Outage probability and diversity analysis," *IEEE Transactions on Wireless Communications*, vol. 8, no. 6, pp. 2872–2876, Jun. 2009.

[55] M. Torabi, D. Haccoun, and J.-F. Frigon, "Impact of outdated relay selection on the capacity of AF opportunistic relaying systems with adaptive transmission

over non-identically distributed links," *IEEE Transactions on Wireless Communications*, vol. 10, no. 11, pp. 3626–3631, Nov. 2011.

[56] M. Seyfi, S. Muhaidat, and J. Liang, "Performance analysis of relay selection with feedback delay and channel estimation errors," *IEEE Signal Processing Letters*, vol. 18, no. 1, pp. 67–70, Jan. 2011.

[57] M. Soysa, H. A. Suraweera, C. Tellambura, and H. K. Garg, "Partial and opportunistic relay selection with outdated channel estimates," *IEEE Transactions on Communications*, vol. 60, no. 3, pp. 840–850, Mar. 2012.

[58] D. S. Michalopoulos, H. A. Suraweera, G. K. Karagiannidis, and R. Schober, "Amplify-and-forward relay selection with outdated channel estimates," *IEEE Transactions on Communications*, vol. 60, no. 5, pp. 1278–1290, May 2012.

[59] L. Fan, X. Lei, R. Hu, and W. Seah, "Outdated relay selection in two-way relay network," *IEEE Transactions on Vehicular Technology*, To appear. 2013.

[60] H. Cui, R. Zhang, L. Song, and B. Jiao, "Performance analysis of bidirectional relay selection with imperfect channel state information," *http://arxiv.org/abs/1112.2374*, Dec. 2011.

[61] Z. Chen, J. Yuan, and B. Vucetic, "Analysis of transmit antenna selection/maximal-ratio combining in Rayleigh fading channels," *IEEE Transactions on Vehicular Technology*, vol. 54, no. 4, pp. 1312–1321, Jul. 2005.

[62] J. Tang and X. Zhang, "Transmit selection diversity with maximal-ratio combining for multicarrier DS-CDMA wireless networks over Nakagami-m fading channels," *IEEE Journal on Selected Areas in Communications*, vol. 24, no. 1, pp. 104–112, Jan. 2006.

[63] S. Meraji, "Performance analysis of transmit antenna selection in Nakagami-m fading channels," *Wireless Personal Communications*, vol. 43, no. 2, pp. 327–333, Oct. 2007.

[64] Z. Chen, Z. Chi, Y. Li, and B. Vucetic, "Error performance of maximal-ratio combining with transmit antenna selection in flat Nakagami-m fading channels,"

IEEE Transactions on Wireless Communications, vol. 8, no. 1, pp. 424–431, Jan. 2009.

[65] B.-Y. Wang and W.-X. Zheng, "Ber performance of transmitter antenna selection/receiver-MRC over arbitrarily correlated fading channels," *IEEE Transactions on Vehicular Technology*, vol. 58, no. 6, pp. 3088–3092, Jul. 2009.

[66] J. Romero-Jerez and A. Goldsmith, "Performance of multichannel reception with transmit antenna selection in arbitrarily distributed Nagakami fading channels," *IEEE Transactions on Wireless Communications*, vol. 8, no. 4, pp. 2006–2013, Apr. 2009.

[67] L. Zhang and L. J. Cimini Jr., "Hop-by-hop routing strategy for multihop decode-and-forward cooperative networks," in *Proc. IEEE Wireless Communications and Networking Conference (WCNC 2008), Las Vegas, Nevada, USA*, Mar. 31 - Apr. 3 2008, pp. 576 –581.

[68] R. Duan, M. Elmusrati, R.Jantti, and R. Virrankoski, "Capacity for spectrum sharing cognitive radios with MRC diversity at the secondary receiver under asymmetric fading," in *Proc. IEEE Global Telecommunications Conference (GLOBECOM 2010), Miami, FL, USA*, Dec. 2010.

[69] R. Duan, R.Jantti, M. Elmusrati, and R. Virrankoski, "Capacity for spectrum sharing cognitive radios with MRC diversity and imperfect channel information from primary user," in *Proc. IEEE Global Telecommunications Conference (GLOBECOM 2010), Miami, FL, USA*, Dec. 2010.

[70] D. Li, "Performance analysis of MRC diversity for cognitive radio systems," *IEEE Transactions on Vehicular Technology*, vol. 61, no. 2, pp. 849–853, Feb. 2012.

[71] V. Blagojevic and P. Ivanis, "Ergodic capacity of spectrum sharing cognitive radio with MRC diversity and Nakagami fading," in *Proc. IEEE Wireless Communications and Networking Conference (WCNC 2012), Paris, France.*, Apr. 2012.

[72] Asaduzzaman and H. Kong, "Ergodic and outage capacity of interference temperature-limited cognitive radio multi-input multi-output channel," *IET Communications*, vol. 5, no. 5, pp. 652–659, May 2011.

[73] H. Wang, J. Lee, S. Kim, and D. Hong, "Capacity enhancement of secondary links through spatial diversity in spectrum sharing," *IEEE Transactions on Wireless Communications*, vol. 9, no. 2, pp. 494–499, Feb. 2010.

[74] V. Blagojevic and P. Ivanis, "Ergodic capacity for TAS/MRC spectrum sharing cognitive radio," *IEEE Communications Letters*, vol. 16, no. 3, pp. 321–323, Mar. 2012.

[75] T. Ban, W. Choi, B. Jung, and D. Sung, "Multi-user diversity in a spectrum sharing system," *IEEE Transactions on Wireless Communications*, vol. 8, no. 1, pp. 102–106, Jan. 2009.

[76] S. Ekin, F. Yilmaz, H. Celebi, K. A. Qaraqe, M.-S. Alouini, and E. Serpedin, "Capacity limits of spectrum-sharing systems over hyper-fading channels," *Wireless Communications and Mobile Computing*, vol. 12, no. 16, pp. 1471–1480, Nov. 2012.

[77] D. Li, "On the capacity of cognitive broadcast channels with opportunistic scheduling," *Wireless Communications and Mobile Computing*, DOI: 10.1002/wcm.1108, 2011.

[78] R. Zhang and Y. Liang, "Investigation on multiuser diversity in spectrum sharing based cognitive radio networks," *IEEE Communications Letters*, vol. 14, no. 2, pp. 133–135, Feb. 2010.

[79] Y. Li and A. Nosratinia, "Hybrid opportunistic scheduling in cognitive radio networks," *IEEE Transactions on Wireless Communications*, vol. 11, no. 1, pp. 328 –337, Jan. 2012.

[80] H. Wang, J. Lee, S. Kim, and D. Hong, "Capacity of secondary users exploiting multispectrum and multiuser diversity in spectrum-sharing environments," *IEEE Transactions on Vehicular Technology*, vol. 59, no. 2, pp. 1030 –1036, Feb. 2010.

[81] A. Tajer and X. Wang, "Multiuser diversity gain in cognitive networks," *IEEE/ACM Transactions on Networking*, vol. 18, no. 6, pp. 1766 –1779, Dec. 2010.

[82] R. Nabar, H. Bolcskei, and F. Kneubuhler, "Fading relay channels: Performance limits and space-time signal design," *IEEE Journal on Selected Areas in Communications*, vol. 22, no. 6, pp. 1099 – 1109, Aug. 2004.

[83] M. Uysal and O. Canpolat, "On the distributed space-time signal design for a large number of relay terminals," in *Proc. IEEE Wireless Communications and Networking Conference (WCNC 2005), New Orleans, LA, USA*, vol. 2, Mar. 2005, pp. 990 – 994.

[84] J. He and P. Kam, "Cooperative spacetime block coding with amplify-and-forward strategy: Exact bit error probability and adaptive forwarding schemes," *Elsevier Journal of Physical Communication*, vol. 1, no. 3, pp. 209 – 220, Sep. 2008.

[85] M. Taghiyar, S. Muhaidat, and J. Liang, "On pilot-symbol-assisted cooperative systems with cascaded Rayleigh and Rayleigh fading channels with imperfect CSI," *Journal of Selected Areas in Telecommunications (JSAT)*, vol. 1, pp. 24–31, Nov. 2010.

[86] H. Muhaidat, M. Uysal, and R. Adve, "Pilot-symbol-assisted detection scheme for distributed orthogonal space-time block coding," *IEEE Transactions on Wireless Communications*, vol. 8, no. 3, pp. 1057 –1061, Mar. 2009.

[87] M. Malkawi and K. Il-Min, "Hard/soft detection with limited CSI for multi-hop systems," *IEEE Transactions on Wireless Communications*, vol. 8, no. 7, pp. 3435 –3441, Jul. 2009.

[88] B. Gedik, O. Amin, and M. Uysal, "Power allocation for cooperative systems with training-aided channel estimation," *IEEE Transactions on Wireless Communications*, vol. 8, no. 9, pp. 4773–4783, Sep. 2009.

[89] S. M. Kay, *Fundamentals of Statistical Signal Processing, Volume 1: Estimation Theory*, 1st ed. Prentice Hall, 1998.

[90] Y. Chen and N. Beaulieu, "Maximum likelihood estimation of SNR using digitally modulated signals," *IEEE Transactions on Wireless Communications*, vol. 6, no. 1, pp. 210–219, Jan. 2007.

[91] D. Pauluzzi and N. Beaulieu, "A comparison of SNR estimation techniques for the AWGN channel," *IEEE Transactions on Communications*, vol. 48, no. 10, pp. 1681–1691, Oct. 2000.

[92] M. Abramowitz and I. A. Stegun, *Handbook of Mathematical Functions with Formulas, Graphs, and Mathematical Tables*, 9th ed. New York, USA: Dover Publications, 1972.

[93] F. Khan, Y. Chen, and M. Alouini, "Novel coherent receivers for AF distributed STBC using disintegrated channel estimation," in *Proc. IEEE Vehicular Technology Conference (VTC-Spring 2011), Budapest, Hungary*, May 15-May 18 2011, pp. 1 – 5.

[94] M. K. Simon, *Probability Distributions Involving Gaussian Random Variables: A Handbook for Engineers and Scientists*, 1st ed. Netherlands: Springer, 2002.

[95] Q. Zhang, "Outage probability of cellular mobile radio in the presence of multiple nakagami interferers with arbitrary fading parameters," *IEEE Transactions on Vehicular Technology*, vol. 44, no. 3, pp. 661–667, Aug. 1995.

[96] I. S. Gradshteyn and I. M. Ryzhik, *Table of Integrals, Series, and Products*, 5th ed. Academic Press, 1994.

[97] Y. Chen and C. Tellambura, "Distribution functions of selection combiner output in equally correlated Rayleigh, Rician, and Nakagami-m fading channel," *IEEE Transactions on Communications*, vol. 52, no. 11, pp. 1948–1956, Nov. 2004.

[98] Wolfram Functions, *http://functions.wolfram.com/*, 2012.

[99] F. Yilmaz, A. Yilmaz, M.-S. Alouini, and O. Kucur, "Transmit antenna selection based on shadowing side information," in *Proc. IEEE Vehicular Technology Conference (VTC-Spring 2011), Budapest, Hungary*, May, 2011.

[100] A. Annamalai, R. Palat, and J. Matyjas, "Estimating ergodic capacity of cooperative analog relaying under different adaptive source transmission techniques," in *Proc. IEEE Sarnoff Symposium (Sarnoff 2010), Princeton, NJ, USA*, Apr., 2010.

[101] Y. Zou, J. Zhu, B. Zheng, and Y. Yao, "An adaptive cooperation diversity scheme with best-relay selection in cognitive radio networks," *IEEE Transactions on Signal Processing*, vol. 58, no. 10, pp. 5438–5445, Oct. 2010.

[102] F. Yilmaz and M.-S. Alouini, "Novel asymptotic results on the high-order statistics of the channel capacity over generalized fading channels," in *Proc. IEEE International Workshop on Signal Processing Advances in Wireless Communications (SPAWC 2012), Izmir-Cesme, Turkey*, Jun., 2012.

[103] G. Herjólfsson, A. Hauksdóttir, and S. Sigurdsson, "Closed form expressions of linear continuous-and discrete-time filter responses," in *Proc. IEEE 7th Nordic Signal Processing Symposium (NORSIG 2006), Reykjavik, Iceland*, Jun., 2006.

[104] L. Musavian and S. Aissa, "Capacity and power allocation for spectrum-sharing communications in fading channels," *IEEE Transactions on Wireless Communications*, vol. 8, no. 1, pp. 148–156, Jan. 2009.

Chapter 8

Accepted/Submitted Papers

Journal Papers

- **F. A. Khan**, K. Tourki, M. -S. Alouini and K. A. Qaraqe, "Performance analysis of a power limited spectrum sharing system with TAS/MRC," Submitted to *IEEE Transactions on Signal Processing*.

- **F. A. Khan**, K. Tourki, M. -S. Alouini and K. A. Qaraqe, "Performance of an opportunistic multi-user cognitive network in Nakagami fading," Submitted to *IEEE Transactions on Vehicular Technology*.

- **F. A. Khan**, Y. Chen and M. -S. Alouini, "Novel non-coherent and half-coherent receivers for amplify and forward relaying," Submitted to *Wiley Journal on Wireless Communications and Mobile Computing*.

- **F. A. Khan**, K. Tourki, M. -S. Alouini and K. A. Qaraqe, "Performance analysis of an opportunistic multi-user underlay cognitive network with multiple primary users," Submitted to *Wiley Journal on Wireless Communications and Mobile Computing*.

- K. Tourki, **F. A. Khan**, M. -S. Alouini, H-.C. Yang and K. A. Qaraqe, "Exact performance analysis of MIMO cognitive radio system using transmit antenna

selection," To appear in *IEEE Journal on Selected Areas in Communications - Cognitive Radio Series (Nov 2013 Issue).*

- **F. A. Khan**, K. Tourki, M. -S. Alouini and K. A. Qaraqe, "Delay performance of a broadcast spectrum sharing network in Nakagami-m fading,"To appear in *IEEE Transactions on Vehicular Technology.*

- F. Yilmaz, **F. A. Khan** and M. -S. Alouini, "Performance of amplify-and-forward multihop transmission over relay clusters with different routing strategies," To appear in *International Journal of Autonomous and Adaptive Systems (IJAACS).*

- Y. Chen, M. -S. Alouini, L. Tang and **F. A. Khan**, "Analytical evaluation of adaptive-modulation-based opportunistic cognitive radio in Nakagami-m fading channels," *IEEE Transactions on Vehicular Technology*, vol.61, no.7, pp. 3294-3300, Sep. 2012.

- **F. A. Khan**, Y. Chen and M. -S. Alouini, "Novel receivers for AF relaying with distributed STBC using cascaded and disintegrated channel estimation," *IEEE Transactions on Wireless Communications*, vol.11, no.4, pp.1370-1379, Apr. 2012.

Conference Papers

- **F. A. Khan**, K. Tourki, M. -S. Alouini and K. A. Qaraqe, "Performance of an opportunistic multi-user cognitive network with multiple primary users," Submitted to Proc. of IEEE Wireless Communications and Networking Conference (WCNC 2014), Istanbul, Turkey, Apr. 2014.

- **F. A. Khan**, M. Debbah, K. Tourki and M. -S. Alouini, "Performance of fading multi-user diversity for underlay cognitive networks," in Proc. of IEEE

International Conference on Acoustics, Speech, and Signal Processing (ICASSP 2013), Vancouver, Canada, May 2013.

- **F. A. Khan**, K. Tourki, M. -S. Alouini and K. A. Qaraqe, "Outage and SER performance of spectrum sharing system with TAS/MRC under transmit power constraint," in Proc. of the Fifth Workshop on Cooperative and Cognitive Networks (CoCoNet5) in conjunction with IEEE international Conference on Communications (ICC 2013), Budapest, Hungary, Jun. 2013.

- **F. A. Khan**, K. Tourki, M. -S. Alouini and K. A. Qaraqe, "Outage and SER performance of an opportunistic multi-user underlay cognitive network," in Proc. of IEEE Symposium on New Frontiers in Dynamic Spectrum Access Networks (DySPAN 2012 Poster Session), Bellevue, WA, USA, Oct. 2012. (**Received Best Poster Award**)

- **F. A. Khan**, K. Tourki, M. -S. Alouini and K. A. Qaraqe, "Delay analysis of a point-to-multipoint spectrum sharing network with CSI based power allocation," in Proc. of IEEE Symposium on New Frontiers in Dynamic Spectrum Access Networks (DySPAN 2012), Bellevue, WA, USA, Oct. 2012.

- **F. A. Khan**, Y. Chen and M. -S. Alouini, "Novel half coherent receivers for amplify and forward relaying," in Proc. of IEEE International Workshop on Signal Processing Advances in Wireless Communications (SPAWC 2012), Cesme, Turkey, Jun. 2012.

- **F. A. Khan**, F. Yilmaz and M. -S. Alouini, "Generalized routing protocols for multihop relay networks," in Proc. of International Wireless Communications and Mobile Computing Conference (IWCMC 2011), Istanbul, Turkey, Jul. 2011.

- **F. A. Khan**, Y. Chen and M. -S. Alouini, "Superior coherent receivers for AF relaying with distributed Alamouti code, in Proc. of IEEE Vehicular Technology Conference (VTC-Fall 2011), San Francisco, CA, USA, Sep. 2011.

- **F. A. Khan**, Y. Chen and M. -S. Alouini, "Novel coherent receivers for AF distributed STBC using disintegrated channel estimation," in Proc. of IEEE Vehicular Technology Conference (VTC-Spring 2011), Budapest, Hungary, May 2011.